PALAEO-GEOTHERMAL ACTIVITY IN BASALTIC LAVAS OF LOWER CARBONIFEROUS AGE IN THE MIDLAND VALLEY OF SCOTLAND

Michael McDonald

A Thesis Submitted for the Degree of PhD
at the
University of St Andrews

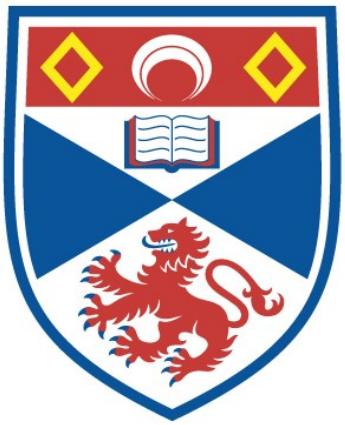

1992

PALAEO-GEOTHERMAL ACTIVITY IN BASALTIC LAVAS OF LOWER CARBONIFEROUS AGE IN THE WESTERN MIDLAND VALLEY OF SCOTLAND

Michael M°Donald

Thesis presented in partial fulfilment of the

Degree of Doctor of Philosophy.

July 1991.

ProQuest LLC.
789 East Eisenhower Parkway
P.O. Box 1346
Ann Arbor, MI 48106 – 1346

THESIS DECLARATION

I Michael McDonald herby certify that this thesis has been composed by myself, that it is a record of my own work, and that it has not been accepted in partial or complete fulfilment of any other degree or professional qualification.

Signed..... On..19th July 1991...

I was admitted to the Faculty of Science of the University of St. Andrews under Ordinance General Number 12 on Oct...1988... and as a candidate for the degree of Ph.D. on Oct...1989...

Signed..... On..19th July...1991...

I hereby certify that the candidate has fulfilled the conditions of the Resolution and Regulations appropriate to the degree of Ph.D.

Signed..... On..July 10th 1991

COPYRIGHT

Unrestricted

In submitting this thesis to the University of St. Andrews I understand that I am giving permission for it to be made available for use in accordance with the regulations of the University Library for the time being in force, subject to any copyright vested in the work not being affected thereby. I also understand that the title and abstract will be published, and that a copy of the work may be made and supplied to any bona fide library or research worker.

ACKNOWLEDGEMENTS

I would like to start by thanking everyone who has shown an interest in this project. (all two of them). In particular, I would like to thank Grahame Oliver for his supervision, notably in the field, occasionally from fields afar. It was his thoughtful, directed critical comments and general bad language which provided the necessary impetus for a prompt finish; an object lesson in "the running of a tight ship". Also, more importantly, it was he who was partly responsible for the re-launch of my cricket career. Mention must also be made of Dr Peter Bowden for a variety of useful suggestions and endless cross comparisons with a certain country located in Southern Africa (beginning with K for those who might not know). A big thanks must also go to Dr Tony Fallick at SURRC for his thoughtful suggestions and supervision, without which this project would not have been possible. Also, the technical advice of staff at SURRC was invaluable. I would also like to thank everyone at Delft Geotechnics UK for being so accommodating.

The technical advice of staff at St. Andrews University Geology Dept. is also gratefully acknowledged. I would particularly like to thank Jim Allen, Richard Batchelor, Angus Calder (slapped it!), Donald Herd (larger tops-now!), Judy Kinnaird and Andy Mackie (your sections will be ready next Tuesday).

I would also like to acknowledge the following young doctors who made the nightmare a little more bearable, namely, Knight Dix, Edward Errington, David Trubshaw, Kieth Seedhouse, Drs. Andrew Paterson and Timothy Yarr, not forgetting Essex Man (suffice is to say "it's not my round"). The Disciples of Clive Clark, Messars Seedhouse and Yarr, both of whom wished they played Daiwa are thanked for golfing entertainment.

Finally, I would like to thank my folks for bailing me out on occasions when "the bank that likes to say yes", said no. NERC is thanked for financial support.

ABSTRACT

Post-extrusive hydrothermal alteration within basaltic lavas has been examined with special reference to the Lower Carboniferous Clyde Plateau Basalts of the Midland Valley of Scotland. Within this province several steep-sided, narrowly constrained zones of intense water-rock interaction have been located and examined. It is thought that these zones, or metadomains, developed where hydrothermal fluids exploited permeability contrasts within the volcanic pile and as such they represent foci for geothermal fluids which advected through the lavas.

In the field metadomains are often manifest as areas of intense alteration and hydrofracting of the host basalts. Characteristic alteration mineralogies are often hydrous and typically include evolved phyllosilicate assemblages, prehnite, analcime and calcite. Petrography reveals that prehnite and analcime are always paragentetically earlier than calcite across the whole of the lavas. Also, metadomain development was accompanied by significant elemental mobility within the host basalts; Si, Ti, Fe, Mn, Mg, Ca, Na and K all exhibit varying degrees of mobility, whilst Sr, Rb, Cu and Zn display extreme mobility. Furthermore, metadomain basalts have higher volatile contents than there unaltered counterparts.

Fluids present during metadomain development typically were Ca^{2+}, Na^{+}, Cl^{-} dominated brines which exhibited both a wide range in salinity (approximately 0 to 25 equiv. wt. % NaCl) and temperatures (approximately 50°C to 300°C). As the development of metadomains proceeded it appears that the fluid present was a hybrid formed from the interaction and mixing of a low temperature, low salinity fluid which was ultimately of surface origin and a higher temperature brine derived from the underlying sediments. The presence of minor amounts of hydrocarbon material within the fluids testified to the involvement of organic rich sequences within the underlying Inverclyde Group sediments. These fluids also record a number of physical processes which are observed within currently active geothermal systems such as mixing and boiling indicative of near surface conditions. Such processes appeared to be largely responsible for controlling the gas content of the fluids.

Combined fluid inclusion and stable isotopic analysis of alteration phases (specifically analcime and calcite) has been used to determine fluid origins and evolution during metadomain development. Fluids present during the precipitation of analcime appears to have originated as a surface derived fluid which interacted (isotopically and chemically) with reactive, carbonate rich sediments, possibly the underlying Inverclyde Group.

Fluids present during calcite precipitation can be separated into two distinct groups; a low to intermediate (c. 90 to 200°C) surface derived fluid and a higher temperature fluid which also appears to have interacted with reactive sediments. Carbon isotopic results confirm that organic derived material interacted with these fluids. Uniformity in carbon isotopic compositions suggests that the carbon reservoir was active prior to calcite precipitation.

As geothermal activity waned calcite precipitation still continued whilst fluid temperatures decreased due to convective cooling of the lava pile. During this stage it appears that fluids were dominantly of surficial origin.

CONTENTS PAGE

FRONTISPIECE : THE CAMPSIES AS VIEWED FROM THE SOUTHWEST

The landscape is dominated by the effects of the Campsie Fault which has a downthrow of approximately 900 metres to the south. In the background the Campsie block consists of a sequence of lavas which form part of the Clyde Plateau Lavas, occupying a major part of the Lower Carboniferous succession around the Clyde Estuary. Towards the top of the plateau it is possible to observe individual lava flows, whilst to the extreme left the prominent hills, Dumgoyne and Dumfoyne, which are volcanic vents, near contemporaneous with the lavas. Occupying the mid-ground is an 18 hole, par 72 golf course (note clubhouse to extreme left), beneath which there are sediments belonging to the Calciferous Sandstone and Carboniferous Limestone Series.

locality.

1.2 Techniques used

A variety of techniques have been used to address the aims outlined in the previous section. The first four chapters of this thesis are concerned with the characterisation of the metadomains following an integrated study using petrographic, XRD, microprobe and XRF analysis. The following two chapters present and discuss the results of a combined fluid inclusion and stable isotopic analysis of alteration minerals from the metadomains (analcime and calcite). The final chapter then presents a synthesis of all the work carried out.

1.3 Regional setting

A general account of the regional geology of the Midland Valley is given by Cameron and Stephenson (1985). For detailed accounts of the petrology and petrogenesis of the Clyde Plateau Lavas (hereafter referred to as the Clyde Lavas) the reader is referred to Whyte and MacDonald (1974), MacDonald (1975) and Craig (1983). A detailed account of the lithostratigraphy of the region is given by Paterson and Hall (1983), whilst reviews of the deeper geology of the region can be found in Bamford (1979) and Upton et al. (1983). Since MacDonald (1973) gives a brief account of minor, localised alteration phenomena within the Campsie Fells, the subject has not attracted extensive attention until the study of Evans (1987).

The Clyde Lavas form a major igneous province within the Midland Valley and are Dinantian in age, ranging from approximately 350 to 320 Ma. They are found outcropping in the western Midland Valley, surrounding much of the area to the north, west and south of Glasgow where they form the Campsie Fells, Kilpatrick Hills and Renfrewshire Hills respectively (see Figure 1.1). Structurally, they consist of several fault bounded blocks, each with distinctive petrological characteristics and reach thicknesses of up to 900 metres in

places. Borehole information demonstrates that they extend eastwards and overlap with the western extension of the Bathgate Volcanics. Cameron and Stephenson (1985) estimate that the original extent of the Clyde Lavas may have been up to 3 000 km^2.

The lavas constitute a major component of the Dinantian Calciferous Sandstone Measures within the western Midland Valley and have been assigned to the base of the Strathclyde Group by Paterson and Hall (1983) which is directly overlain by fluviodeltaic sediments of the Lower Limestone Group. The volcanic sequences which constitute the Clyde Lavas overlie rocks ranging in age from Upper Devonian to Lower Carboniferous suggesting a period of uplift prior to eruption.

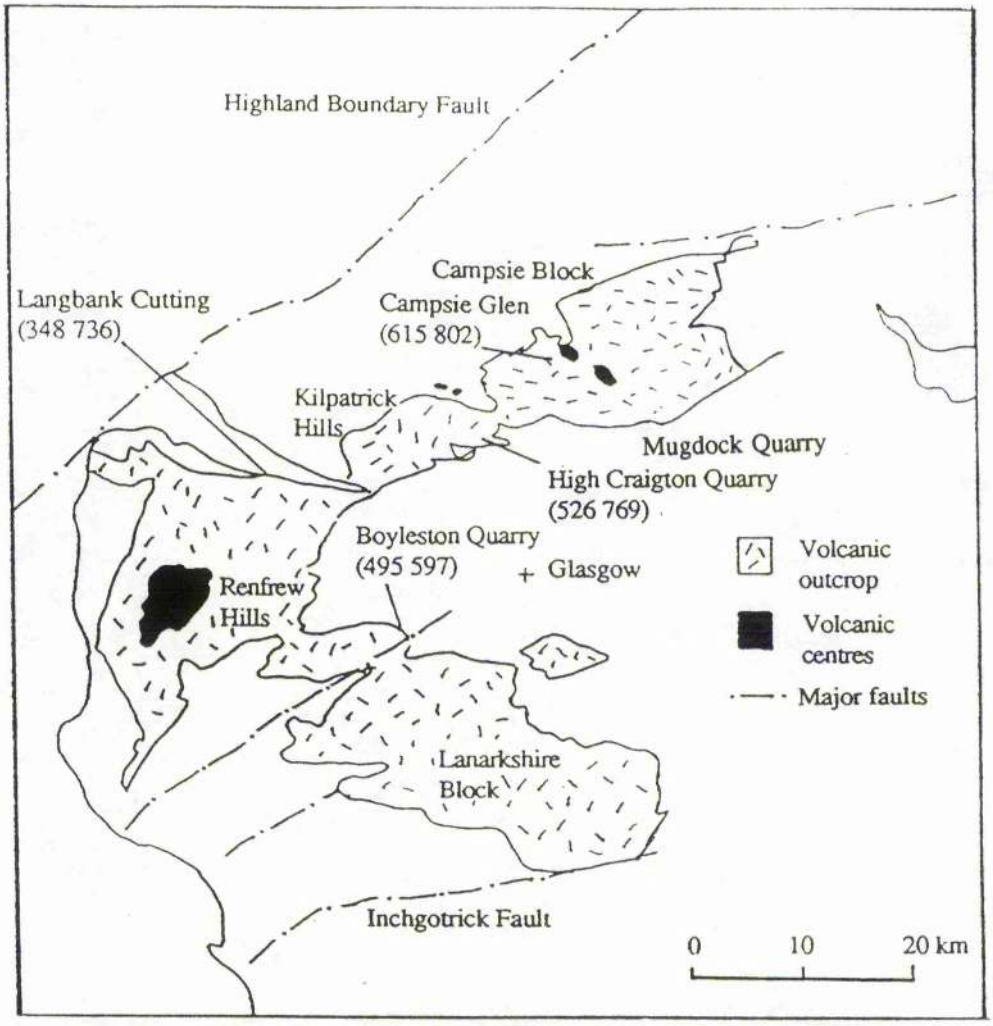

Figure 1.1 Sketch map showing outcrop of the Clyde Plateau Lavas and associated features (after Cameron and Stephenson, 1985). Also shown are metadomain localities described in this study (after Evans, 1987)

Plate 1.1. Prehnite development at Boyleston Quarry. Prehnite is most commonly found within the reddened, oxidised flow top of the lowest flow exposed at Boyleston (see Plate 1.4). It is frequently pale green and mammilary, occurring mainly within amygdales and vein networks which do not exhibit hydrofracturing. This example can be found at the northeastern periphery of the quarry (see Plate 1.4).

Plate 1.2. Prehnite vein from Boyleston Quarry. This sample is collected from the locality shown above. Note the porous and highly altered nature of the host basalt and also the green staining upon some surfaces which is due to the presence of copper within the vein.

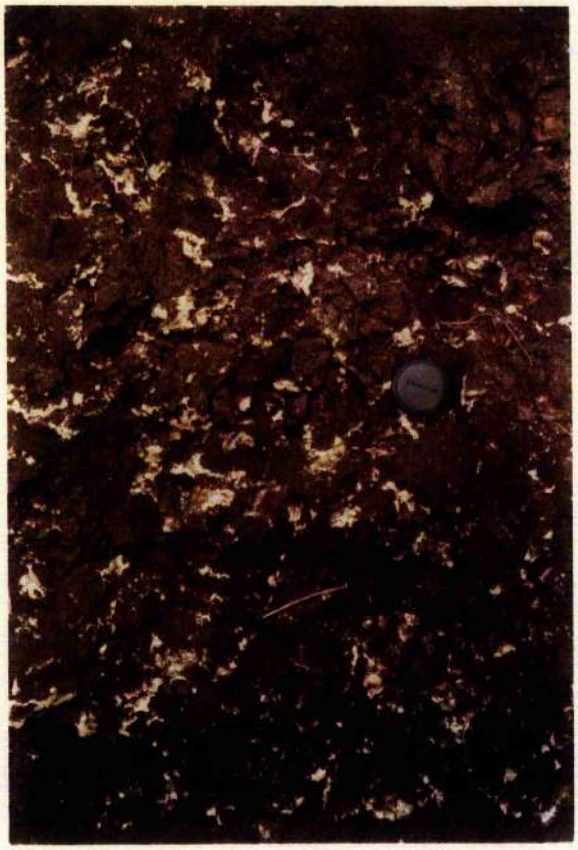

Plate 1.3. Hydrofractured analcime vein from Boyleston Quarry. Analcime is frequently found within the middle flow where it forms large hydrofractured vein networks. It is commonly found as white or pink, well formed icosi-tetrahedra. Also, note the angularity of the encapsulated basalt fragments suggesting transport of detached material over small distances. There is a change from matrix to clast supported conditions downwards indicating that fragments settled through the hydrothermal fluid following initial fracturing.

Plate 1.4. Boundary between lower and main flow, Boyleston Quarry. This locality is found within the northeastern corner of the quarry and provides a vertical section through a metadomain whilst also demonstrating the undulatory and sharp nature of the contact between flows. The lower flow is extensively altered, oxidised and impregnated by prehnite and minor, later calcite. The middle (main) flow is grey on fresh surfaces, is relatively unaltered, but has undergone extensive hydraulic fracturing. Analcime is abundant within veins together with minor calcite. The boundary between analcime and prehnite dominated conditions is coincident with the flow boundary.

Plate 1.5. Metadomain intersecting volcaniclastic wedge. This metadomain develops within the main lava flow at Boyleston Quarry and is readily identified because of intense veining and hydrofracturing of the host basalt. It can be seen that the volcaniclastic wedge immediately above the main lava flow is intersected by the metadomain as shown by bleeching of the sediment due to the precipitation of light coloured alteation minerals. Also, it can be seen that the uppermost lava flow within the quarry is not affected by metadomain activity.

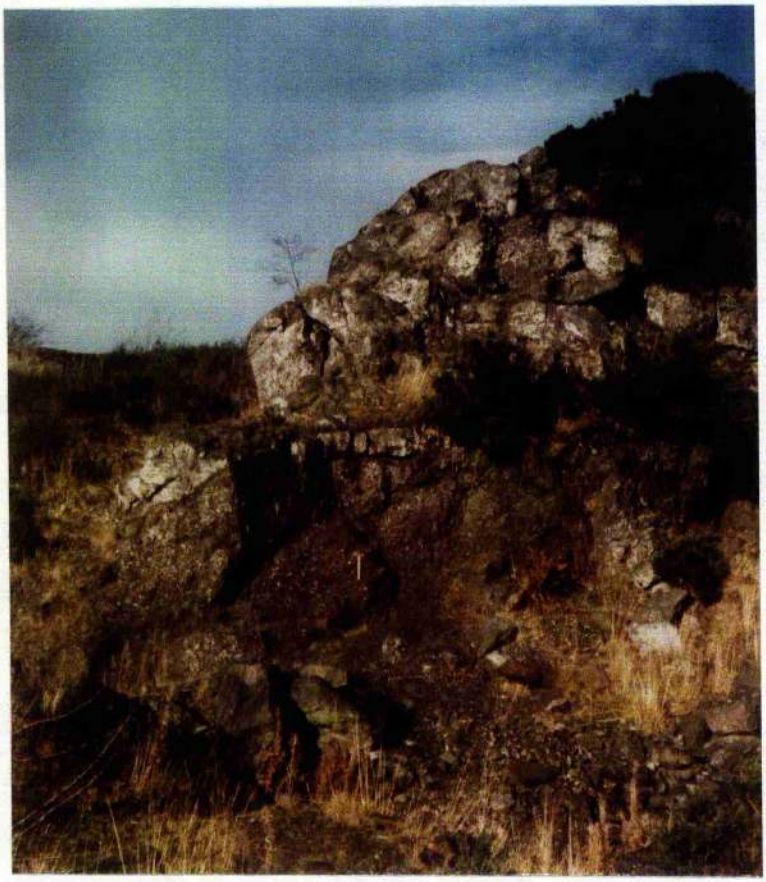

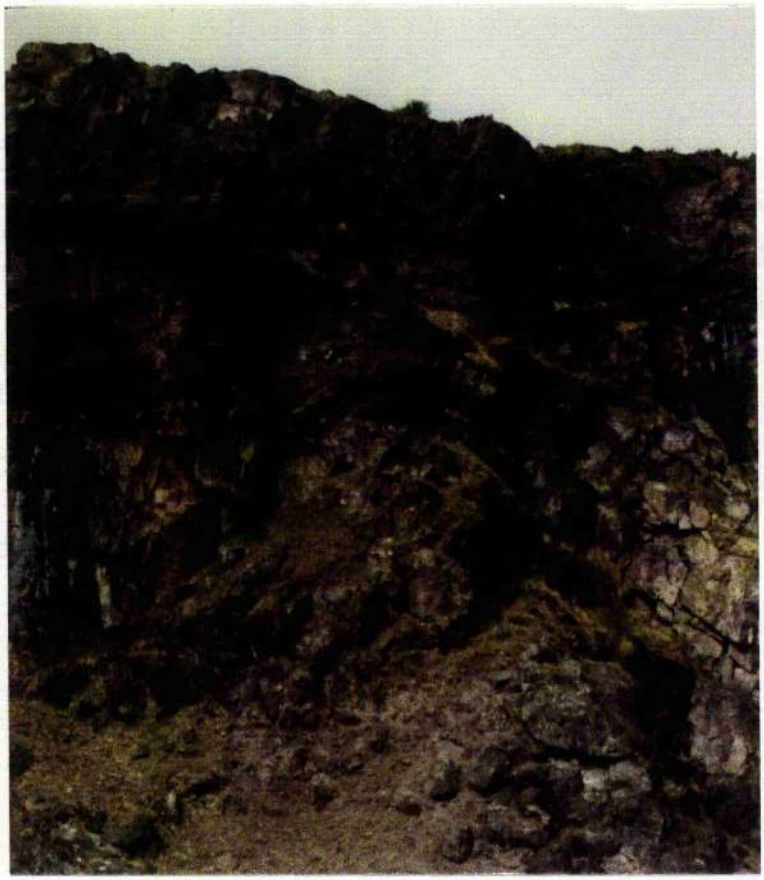

Directly underlying the lavas around the Clyde Estuary are sediments of the Inverclyde Group comprising the Clyde Sandstone Formation, Ballagan Formation and Kinnesswood Formation. Inverclyde Group sediments typically consist of cementstones and sandstones, characterised by beds and nodules of limestone in association with silty mudstone formations containing thin dolomite horizons. Around the base of the Campsie Fells the Ballagan Formation is well exposed and consists of grey, silty mudstones with numerous dolomitic horizons. This formation is thought to vary in thickness, reaching a maximum of approximately 400 metres and has been interpreted as having been deposited under marginal marine conditions subjected to periodic desiccation.

Chemically most of the Clyde Lavas are basalts with subordinate trachytes and have been classified on the basis of phenocryst type and proportion by MacGregor (1928). Towards the base of the sequence volcanic detritus, ashes and tuffs are common whilst oxidised flow tops and boles are found throughout the sequence and are indicative of eruption in a sub-aerial environment. In the Northern Clyde Plateau there is abundant evidence for the existence of eruptive centres with lava flows cut by agglomerate filled vents and small cylindrical plugs often displaying marked columnar jointing. Heavy brecciation and metasomatism are often associated with these features. For example, Meikle Bin within the Campsie Fells consists of trachytic agglomerate which has undergone extensive metasomatism by CO_2 enriched fluids (MacDonald, 1973). Combined geophysical and field evidence (Craig, 1980) suggests that a large caldera, underlain by an intrusive complex was centred upon this area.

1.4 Field relationships

Evans (1987) identified several key localities where metadomain activity had occurred at widely spaced points across the Clyde Lavas. These localities have acted as the basis of this investigation and are shown on Figure 1.1 together with grid references (The reader is referred to O.S. Landranger 1: 50 000 Series, Sheets 63 and 64). A total of five metadomain

localities were examined, of these special attention was given to two at Boyleston Quarry (within the Renfrew Hills) and High Craigton Quarry (within the Kilpatrick Hills).

1.4.1 Boyleston Quarry

This locality lies within the Fereneze Hills, northwest of Barrhead and is reached by travelling along the B774 towards Paisley. It is renowned for providing museum quality specimens of both analcime and prehnite, native copper and rarely thomsonite which were first described in detail by Heddle (1897).

Within the quarry three lava flows are exposed, though only the uppermost part of the lowest flow is observed. The middle flow is seen in the main quarry face and is separated from the thinner uppermost flow by a thick (approximately 5 metre) wedge of reddish brown volcaniclastic sediment. Metadomain development occurs within the lowest and middle flows, and is generally most intense at the boundary between these two flows. The most recent description of the alteration phenomena is given by Hall et al. (1989) and the reader is referred to Bluck (1973) for a detailed description of the alteration minerals. The relevant features of the alteration phenomena are given in Figure 1.2 and Plates 1.1, 1.2, 1.3 and 1.4. However, within the context of this project the important consideration is depth , and by inference timing of metadomain alteration. Is metadomain development a near surface process occurring as the lava was erupted as advocated by Hall et al. (1989), or did development occur after considerable quantities of lava had been deposited above those flows now exposed at Boyleston?

Two pieces of evidence can be used to examine this problem:

1. The first comes from the relationship between the metadomains and the volcaniclastic wedge which overlies the main flow in the quarry. Plate 1.5 appears to show that the wedge is cross-cut by a sub-vertical metadomain at its eastern margin as shown by a bleaching of the sediment, due to the development of alteration phases such as carbonate. It can also be seen that the uppermost flow within the quarry does not appear to be cross cut by this

hydrothermal fluids were forced to migrate laterally as the upper lava acted as an impermeable barrier to fluid transport. Furthermore, if metadomain activity was a near surface phenomena then disturbance of the individual beds by the ascending hydrothermal fluid within the wedge might be expected prior to consolidation of the sediment.

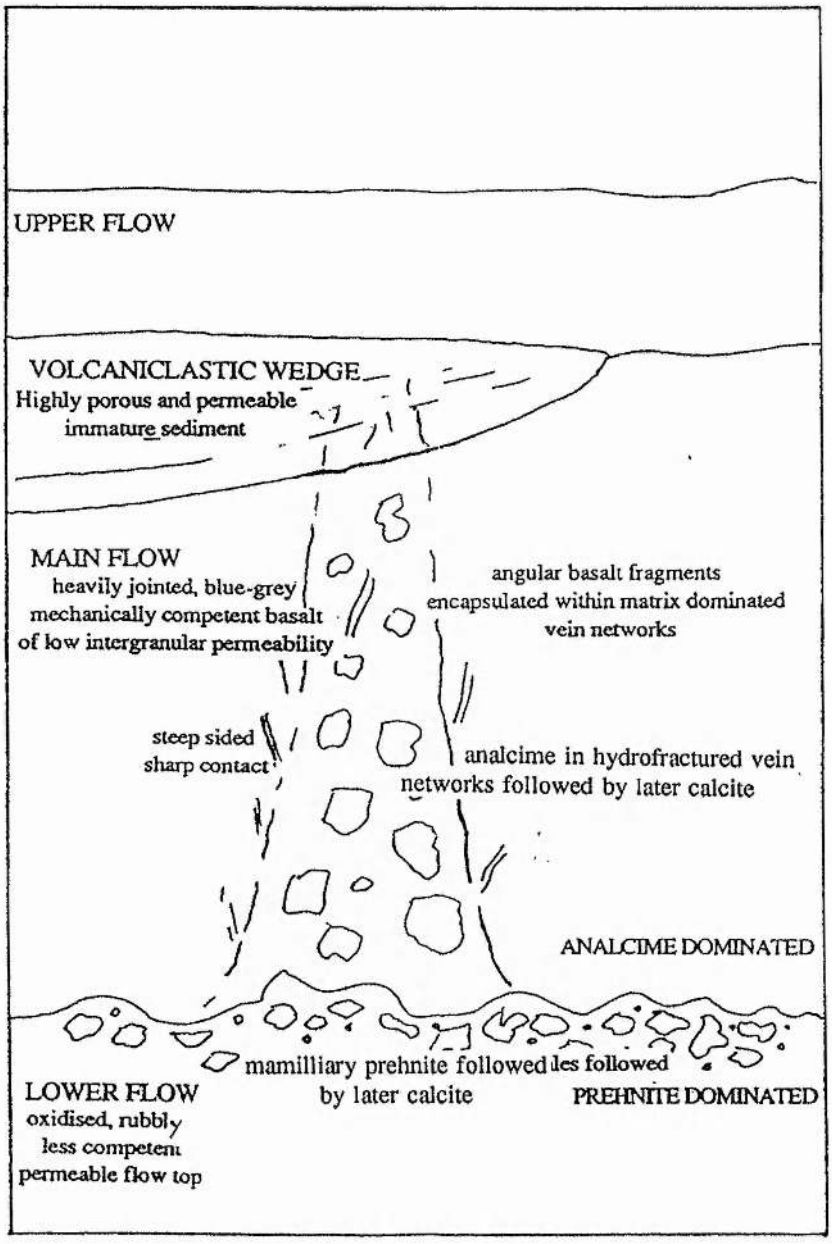

Figure 1.2. Cartoon illustrating salient features of metadomain alteration at Boyleston.

It can be seen from Plate 1.5 that this is clearly not the case.

2. Where metadomain development occurs within the more competent middle flow a commonly observed feature is intense hydraulic fracturing of the host basalt. This feature is illustrated in Plate 1.3. Hydrothermal eruption products are reported from both extinct and active geothermal systems worldwide. A summary of the salient features of these phenomena is given by Nelson and Giles (1985). Within fossilised systems these authors report that "eruption products are frequently eroded away"....."one is likely instead to encounter steep-walled eruption vents from which fragmented material is partially ejected". Also, they point out that these features "are commonly steep walled, irregular in shape and can be either sharp or gradational through several metres of dense rock". It can be seen from Plate 1.3 that the fragments of basalt within the veins observed at Boyleston are angular suggesting transport over short distances and that the vein network is matrix supported suggesting localised transport in a fluid medium.

Phillips (1972) and Norton (1984) point out that hydrofracturing of rock only occurs where fluid pressures exceed the sum of lithostatic confining pressure plus rock strength and therefore fracturing and brecciation can only occur in overpressured environments, that is, those in which the geothermal fluid pressure exceeds its hydrostatic boiling pressure. However, pressure measurements below currently active geothermal systems (Nelson and Giles, 1985) indicate fluid pressures much less than lithostatic indicating that overpressured fluids only exist for very short periods of time. Sibson (1975) suggests that possible mechanisms for overpressuring include influxes of magmatic heat and/or volatiles into a localised region.

Clearly, hydraulic fracturing at Boyleston has been on a reduced scale relative to documented examples. The transition from hydraulic fracturing to hydrothermal eruption is largely a function of the available energy within the geothermal system.

Based on the scenario for metadomain development at Boyleston forwarded by Hall et al. (1989) it might be expected that the degree and intensity of hydrofracturing would be greater because under small lithostatic pressures hydrothermal fluids would be able to break

through to the surface perhaps producing eruption deposits.

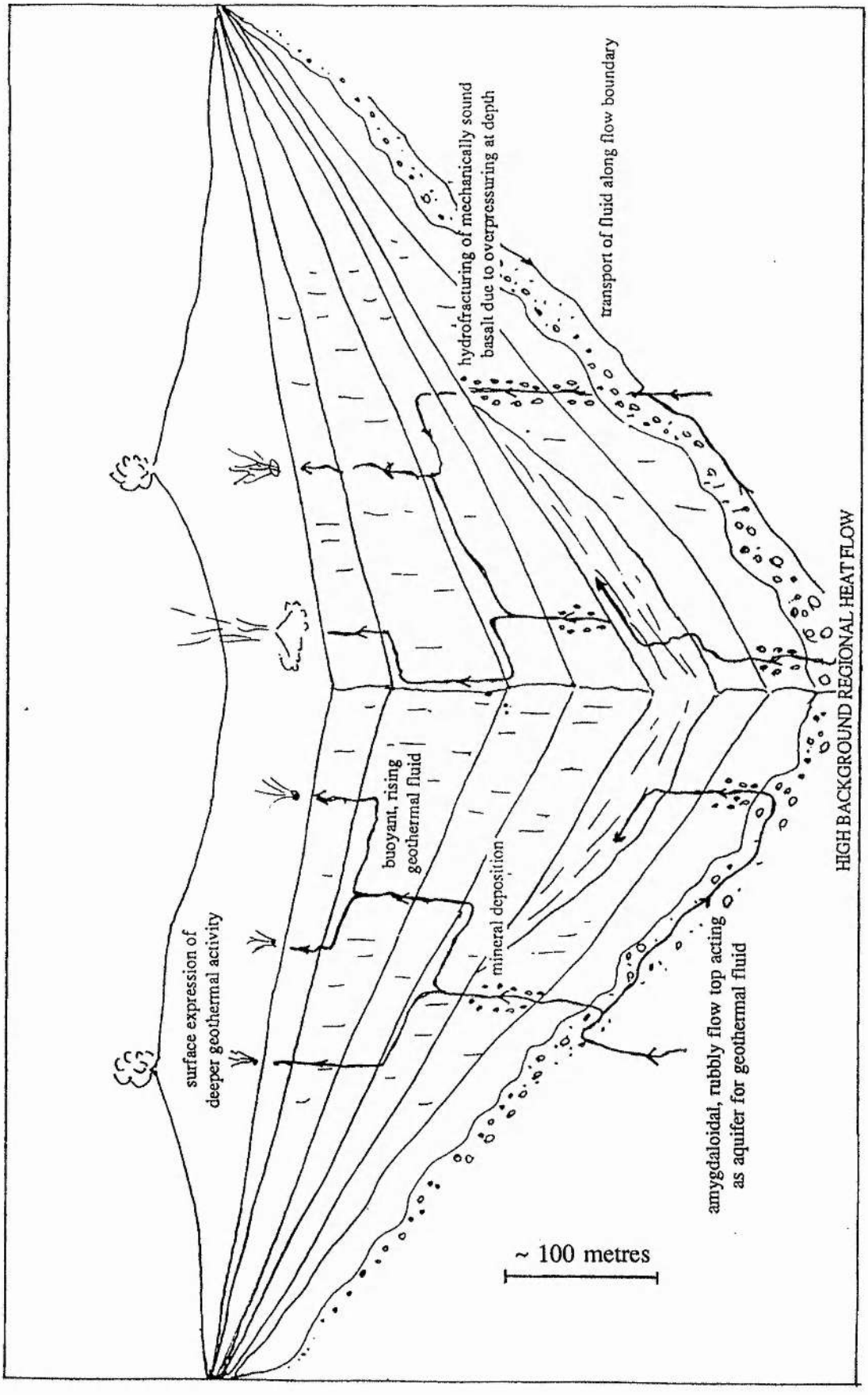

Figure 1.3 A cartoon illustrating a possible mechanism for metadomain development

Based on the two pieces of evidence discussed above it is proposed that metadomain development at Boyleston did not occur immediately after the main lava was erupted as implied by Hall et al. (1989). It is more likely that development occurred after lithostatic pressures were sufficiently large enough to prevent development of hydrothermal eruption products. Figure 1.3 presents a possible mechanism for metadomain development involving the metadomains acting as feeders to geothermal activity at higher levels within the lavas.

1.4.2 High Craigton Quarry

This quarry is located on the eastern flank of the Kilpatrick Hills approximately two kilometres north of Milngavnie along the A 809. Locally, the geology within the quarry is complex as it is located within macro-porphyritic olivine basalts of Markle Type (MacGregor, 1928) which are intruded by a plug of extremely resistant Dunsapie basalt located along the northern margin of the main quarry face (Appendix 2.1). Unfortunately quarrying has removed the contact between the two basalt types. Lying adjacent to the plug, but overlying the Markle basalt along the western margin of the quarry face is a large lahar deposit, the contact between the plug and lahar being faulted. The lahar is both matrix and clast supported, texturally immature and contains sub-rounded clasts up to several metres across. This contact is shown in Plate 1.6 whilst part of the plug is shown in Plate 1.7. The whole sequence is then overlain be a sequence of lava flows consisting of Markle Type which can then be traced westwards across the Kilpatrick Hills.

Alteration is manifest in a variety of forms, the most common alteration phases being clear or cloudy calcite, or massive white or pink analcime (prehnite is absent). It has occurred at the faulted contact between the plug and adjacent lahar, and also at flow boundaries within Markle basalts overlying the present level of the quarry. Within plug basalt immediately below the fault there is minor hydrofracturing of the host lithology on a much smaller scale than that seen at Boyleston. Again, basalt fragments are angular (see Plate 1.8) suggesting transport over small distances. Within the matrix of the lahar alteration is quite different as

Plate 1.6 Northwest face of quarry at High Craigton. Metadomain development occurs primarily within the lahar (centre) where the matrix is extensively altered and mechanically unsound. The lahar is separated from the plug basalt (far right) by a fault (marked) dipping approximately 60 ^{0} to the south. Also, the lavas above the lahar can be seen (upper midground). The total length of this section is approximately 100 metres.

Plate 1.7. Plug basalt at High Craigton Quarry. The plug basalt lying adjacent to the lahar is readily identifiable because it is often extremely resistant, forming promontories and often displays spectacular columnar jointing as shown in this plate. This particular example can be found at the northern margin of the quarry.

Plate 1.8. Hydraulic fracturing of plug basalt adjacent to fault at High Craigton. As with examples at Boyleston Quarry the basalt fragments within the vein network are angular indicating transport within a fluid medium over short distances. Also, note the change from matrix to clast supported conditions across the vein indicating settling of fragments after initial transport. In this case the vein mineral is analcime which consists of individual crystals forming a large interlocking mass.

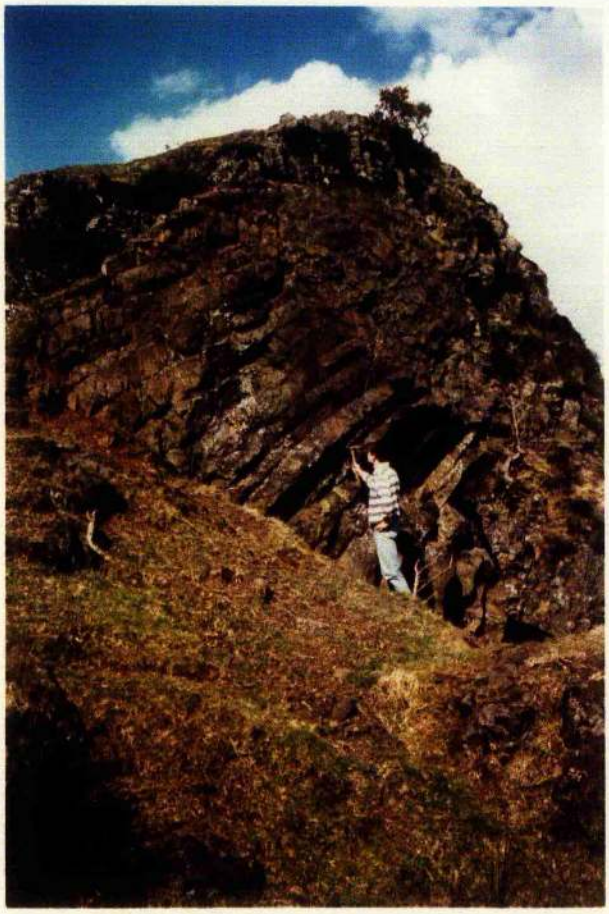

Plate 1.9. Metadomain development within lahar. In this case it can be seen that alteration of the lahar has been much more pervasive owing to the highly permeable nature of the matrix. It is accompanied by a complete loss of mechanical integrity together with deposition of large amounts of carbonate rich material within pore spaces.

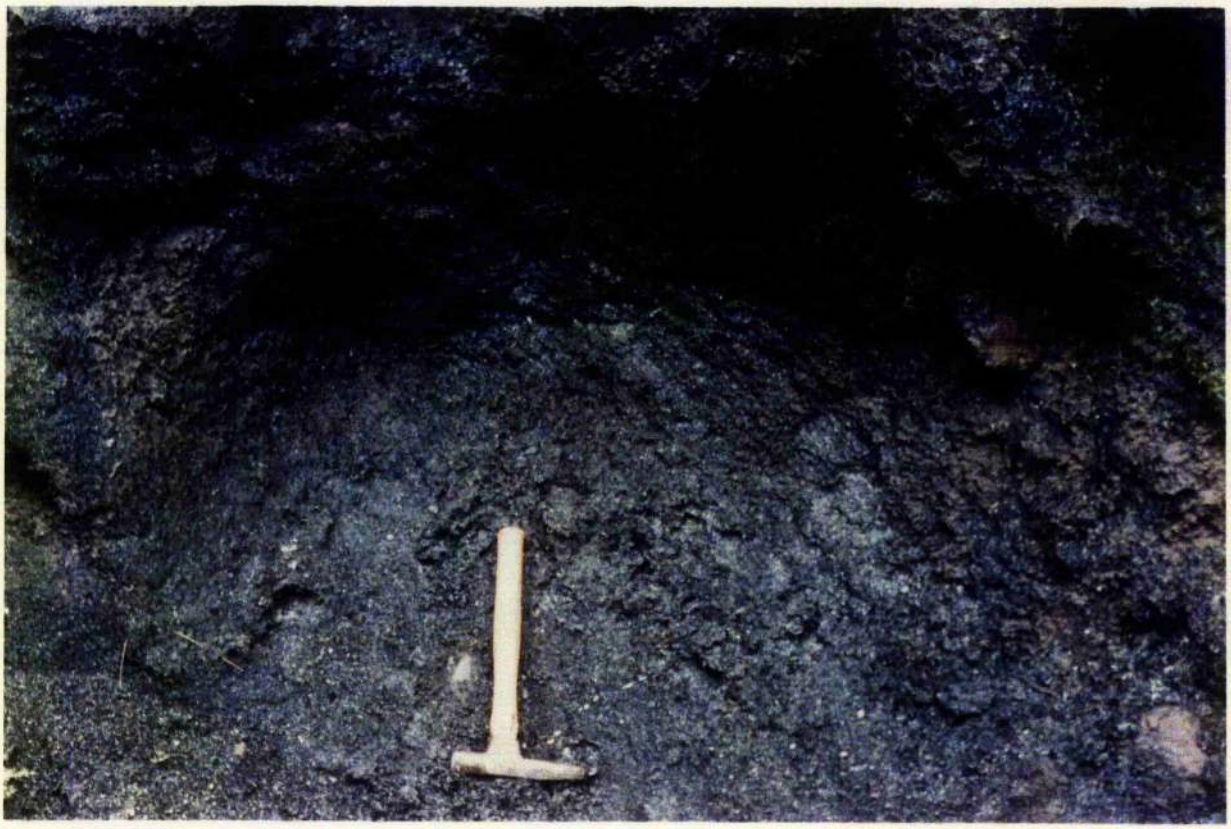

alteration fluids have clearly permeated the whole deposit with development of small calcite grains within pore spaces (see Plate 1.9). Also, within vesicular clasts there is precipitation of calcite. Towards the fault there is a complete loss of mechanical integrity within the lahar. Alteration minerals can also be found between flows above the quarry where they are deposited within amygdales and cavities. It appears that permeability contrasts have played an important part in the development of the metadomain at High Craigton as the fault between the plug basalt and lahar has acted as a focus for fluid transport. Once this had occurred, fluid was then able to permeate the lahar owing to the highly porous and permeable nature of its matrix. Periodic increases in fluid pressure would have resulted in the development of small hydrofractured vein networks within the basalt immediately below the fault.

1.4.3 Other localities

Metadomains at Langbank Cutting and Campsie Glen are similar in that they are laterally confined, developing along flow boundaries which provided high permeability pathways through the lavas. Both are often accompanied by a loss of mechanical strength manifest either as complete degradation of the groundmass material or restricted hydraulic fracturing of basalt. Bleaching of the host lithology is common at both localities. Massive white, or occasionally pink analcime followed by calcite is the dominant alteration mineralogy occurring within veins, amygdales and cavities. Prehnite is only found in minor quantities.

1. Langbank Cutting

This locality is found along an east-west trending road-cut parallel to the A8, several kilometres to the east of Port Glasgow. Metadomain development occurs within Markle basalt (see Chapter 2) at the boundary between two thick (>15 metres) lava flows. This boundary dips at approximately 20° to the west and is distinctive in that the upper margin of the lower flow is typically reddened suggesting a period of weathering prior to eruption of the upper flow. Also, the volume percent of amygdales within this flow reaches up to 50 % within 1

metre of its upper margin. These amygdales are often infilled by both analcime and calcite with minor amounts of pale green prehnite. Away from the upper boundary of the lower flow the volume percent of plagioclase phenocrysts increases. These are frequently altered and friable. In places the basalt is highly friable within the immediate vicinity of the flow boundary.

At either end of the cutting, thick (approximately 5 metre), NE-SW trending basic dykes are found crosscutting both lava flows. Jointing is well developed within these dykes and there is no evidence of there having been affected by the fluids which were responsible for metadomain development. If these dykes were Dinantian in age and supplied lavas stratigraphically above those seen at Langbank the inference is that metadomain activity was occurring concurrently with basalt eruption. Therefore, it is tentatively suggested that metadomain activity occurred before burial metamorphism of the lavas, relatively early in the post-eruptive history of the lavas contrary to the view expressed by Evans (1987). However, these dykes may be of Westphalian or Stephanian age and related to the swarm of dykes emplaced along NE-SW fractures which developed across the Midland Vallley during this time.

2. Campsie Glen

This locality is mentioned in Bluck (1973) and is found in a small abandoned quarry which overlooks the B 822, approximately 200 metres south west of Jamie Wright's Well (see Appendix 3.2). The metadomain is found at the eastern end of the quarry and is located at the margin between two flow units as shown in Figure 1.4.

Bluck (1973) suggests that the two flow units may represent overlapping tongues of the same flow. This flow is the eighteenth in the succession exposed at Campsie Glen and is distinctive in that it contains unusually large phenocrysts, many of which exceed 2 cm in length. Also, along the boundary between the two flow units the lava is vesicular. Alteration of feldspars is a commonly observed feature, many being friable and creamy yellow in colour. Within the metadomain, which is approximately 1 metre wide, the basalt also takes on a creamy colour and is characterised by a complete loss of mechanical integrity.

MacDonald (1973) notes similar alteration phenomena within the immediate area and suggests that this is due to "intense carbon dioxide metasomatism" within the lavas. Analcime is not seen at this locality and calcite occurrence within veins and amygdales is relatively restricted.

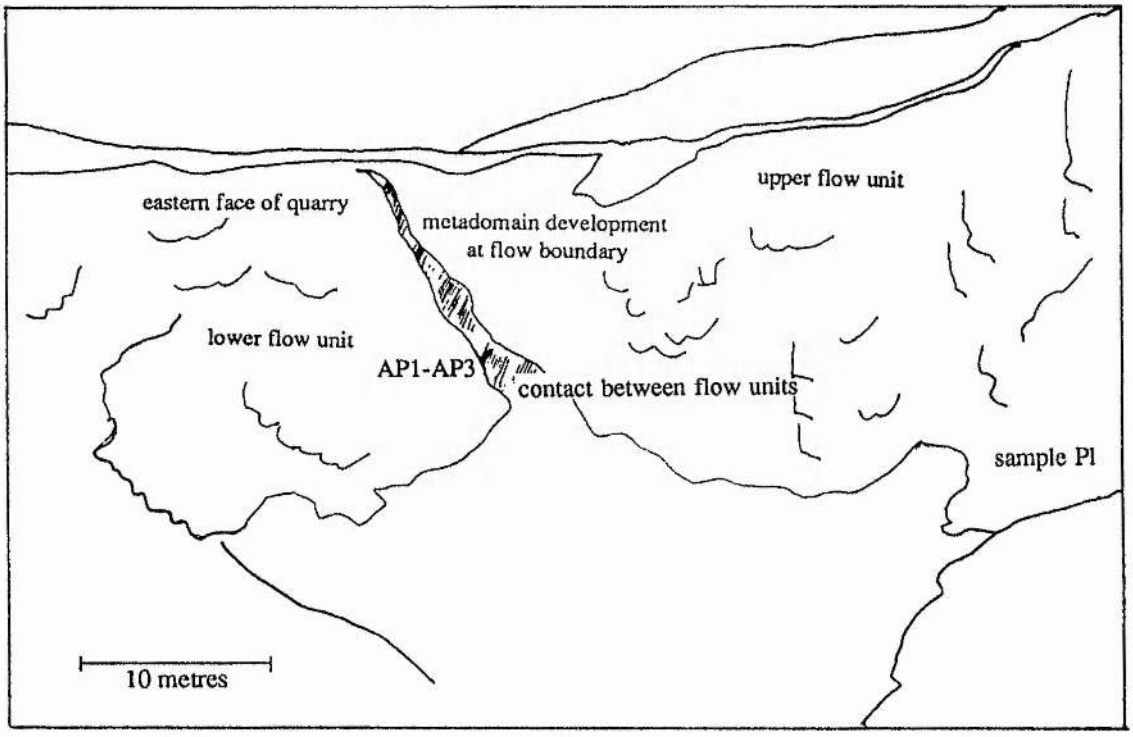

Figure 1.4 Sketch section of metadomain locality at Campsie Glen

1.4.4 Mugdock Quarry

This is a large abandoned quarry found to the north of Mugdock Village (559 769) located approximately three kilometres south of the Campsie Fells within the quartz-calcite zone of Evans (1987). Within the quarry the basalt is macroporphyritic, containing plagioclase phenocrysts (Markle Type) and altered olivine. In certain areas vesicles and fissures within the lavas are infilled by polycrystalline quartz and sparry calcite, though the two are never found juxtaposed. It is assumed that these minerals have developed during burial metamorphism of the lavas and the purpose of studying this locality is to provide a contrast

with those minerals present within the metadomains. This is expanded upon in Chapter 5.

1.5 Conclusions

1. Development of metadomains or alteration zones would have proceeded wherever permeability contrasts existed within the host lavas and were subsequently exploited by circulating geothermal fluids. A variety of geothermal phenomena appear to provide possible pathways for fluid migration including vesicular and rubbly boles, flow boundaries, lithological contrasts and fault zones.

2. Alteration is manifest in a variety of forms which are a function of the permeability structure of the material through which the fluid is transported. For example, basalt flows with low intergranular permeability appear to have been susceptible to hydraulic fracturing and veining whilst such features are not seen in lithologies of higher permeability such as volcaniclastic deposits or lahars. In these deposits alteration is often of a more pervasive nature.

3. Loss of mechanical strength accompanied by colour changes within the rock matrix often delimit the extent of metadomains. Boundaries between host rock and metadomains are frequently sharp and steep, most metadomains being sub-vertical and laterally confined. Characteristic alteration minerals include analcime, prehnite and calcite.

CHAPTER 2 PETROGRAPHY

2.1 Introduction

Detailed petrographic examination of samples from metadomains has been carried out in order to address the following:

1. To what extent are relic igneous assemblages affected by the hydrothermal fluid? This may indicate whether these minerals acted as "sources" or "sinks" for dissolved species within the hydrothermal fluid.
2. To establish the metadomain assemblages from a range of localities.
3. To compare metadomain assemblages with those found within modern geothermal systems. This can then be used to give a general indication of the nature of the fluid phase which was present during metadomain activity.

In order to establish any relationship between hydrothermal paragenesis and host rock composition it is necessary to provide a classification scheme for differing basalt types. The classification used in this study is that used by MacGregor (1928) which was originally defined for basic igneous rocks of Carboniferous and Permian age from the Midland Valley of Scotland. This scheme is presented below in Table 2.1.

BASALT TYPE MacGregor (1928)	**PHENOCRYSTS**	**CHEMICAL CLASSIFICATION** McDonald (1977)
Macroporphyritic (phenocrysts >2mm)		
MARKLE	plag+/-ol+/-opx+/-Fe oxide	plag+/-ol+/-Fe oxides-phyric basalts, basaltic hawaiites or hawaiites.
DUNSAPIE	plag+/-ol+/-opx+/-Fe oxide	ol-cpx-plag oxides-phyric basaltic hawaiites or ol-cpx-plag-phyric basalts.

	PHENOCRYSTS	CHEMICAL CLASSIFICATION McDonald (1977)
Macroporphyritic (phenocrysts >2mm)		
CRAIGLOCKHART	ol+opx	Ankaramite
Microporphyritic (phenocrysts <2mm)		
JEDBURGH	plag+/-ol, Fe-Ti oxide	plag+/-ol+/-Fe oxides phyric (basaltic) hawaiites (occasionally basalt).
DALMENY	ol+/-cpx, plag	ol+/-cpx phyric basalt.
HILLHOUSE	ol+opx	ol+/-cpx-phyric basalt (rarely basanite).

Table 2.1 Classification of basic igneous rocks from the Midland Valley of Scotland (MacGregor, 1928)

2.2 Petrography

This section describes the general petrographic features of both primary igneous phases and secondary hydrothermal phases, together with associated alteration phenomena, which characterise the metadomain basalts. Approximately 75 thin sections were used as part of this study and were collected both within and outside the metadomains. Details are given in Appendix 2.1.

2.2.1 Primary igneous features

1.Plagioclase Feldspar

This is quantitatively the most important igneous phase forming up to 70 % of some sections by volume. It is present in all samples, occasionally as phenocrysts and always as groundmass microlites which frequently show flow alignment. Occasionally

glomeroporphyritic textures are observed, with preservation of primary igneous zoning features. Routine compositional determinations of feldspar phenocrysts from metadomains, using both optical and microprobe techniques indicates compositions ranging from approximately An_{5-40} (albite to andesine). MacDonald et al. (1977) indicate that plagioclase phenocryst composition ranges from An_{40-60} within "fresh lava" from the Campsie Fells. This implies that metadomain alteration has involved a degree of albitisation of primary feldspar. This is further supported by refractive index determination upon groundmass plagioclase microlites from samples both within and outside of metadomains which are extensively albitised. Detrital feldspars (both phenocrysts and microlites) found within volcaniclastic sediment at Boyleston Quarry collected from outside the range of influence of the metadomain also display this type of alteration. This has important consequences regarding the timing of this widespread hydrothermal event since it implies that alteration occurred soon after initial eruption of the lavas.

The degree of alteration exhibited by plagioclase phenocrysts is highly variable, both within individual localities and thin sections. Alteration is manifest in a variety of forms, but most common is the partial or total replacement of original grains by phyllosilicates or carbonate. Within such grains the phyllosilicate commonly appears dull brown or green and the host grain takes on a cloudy appearance. It is commonly observed that phyllosilicates within feldspars cross cut areas of albitisation together with fine grained carbonate suggesting that they developed after albitisation. XRD analysis (Chapter 3) shows that there is a range in phyllosilicate compositions within the lavas, the dominant species being mixed layer chlorite-smectite. Development of phyllosilicates along cracks within individual grains is also a common feature, even within less altered samples. Grain margins are often highly irregular and indurated suggesting partial dissolution of the feldspar by the invading hydrothermal fluid (see Plate 2.1). This effect is most apparent within groundmass microlites together with disappearance of twin planes again suggesting widespread alteration.

A range of alteration products can be seen within individual localities. Generally, at localities north of the Clyde, replacement of feldspar by carbonate is common whilst to the

south albite, phyllosilicates and analcime dominate. For example, at Langbank Cutting, analcime development within feldspar is most striking (this is discussed in a later section), whilst at Campsie Glen and the surrounding region there is widespread replacement and pseudomorphing of feldspar phenocrysts by fine grained carbonate.

2. Augite

This is a rare phase within metadomain basalts and occurs both as euhedral phenocrysts and groundmass clots. It is also found as a detrital phase within volcaniclastic sediment. Slight pleochroism in light brown to buff colours suggests a titanaugite composition, which is a characteristic of the alkali-olivine basalts of the Clyde Lavas (MacDonald, 1977).

The occurrence of this phase is remarkable since it appears to have undergone very little decomposition. This is the case both within basalts showing varying degrees of alteration and also within highly permeable volcaniclastic sediment at Boyleston Quarry where it is found as large detrital grains and also as subhedral phenocrysts within highly altered basaltic clasts. There is little evidence of textural reworking of augite grains within the volcaniclastic horizon at Boyleston, suggesting a local derivation. Plate 2.4 illustrates the occurrence of fresh detrital grains within volcaniclastic sediment at Boyleston.

3. Olivine

Olivine is a rare phase and occurs as pseudomorphed subhedral phenocysts within the lavas. Alteration of this phase is ubiquitous with partial or total pseudomorphing of the individual grain, the common alteration products being a complex mixture of clay minerals and opaque oxides. The phyllosilicate phase is commonly pale to dark green within such grains (see Plate 2.2). Textural interrelationships between the various alteration products are often highly complex suggesting a protracted history of replacement interspersed with periods of dissolution of the alteration mineralogy. It is common to observe red-brown opaques concentrated around grain margins and cracks.

4. Palagonite

The former presence of glass is inferred from the existence of near isotropic dark

yellow to brown coloured palagonite. This is frequently associated with vesicular basalt, such as that found at Langbank Cutting. Within the palagonite it is possible to identify small plagioclase phenocrysts. Also it is found that opaque oxides are concentrated around the margins of the palagonite mass. Staudigel and Hart (1983) indicate that titanium in glass is retained within residual Fe-Ti oxides, or as alteration intensity increases within sphene. Both are observed to varying extents within palagonite from metadomains and indicate varying degrees of alteration. However, there is no systematic variation in the proportion of these two phases within metadomains though sphene is only found where there is a high density of opaques. Cann (1983) indicates that basaltic glass is transformed into a range of phases during palagonization including mixed layer chlorite-smectite and analcime, the former being more common in this study.

2.2.2 Alteration phases

The characteristic occurrence and textures of the main alteration minerals is presented below. In the following section their occurrence is compared with other geothermal systems and their interelationships are then discussed more fully.

1.Phyllosilicates

Fine grained phyllosilicates are ubiquitous throughout the Clyde Lavas and quantitatively constitute a major alteration product, both within and outside the metadomains. They are found pseudomorphing and replacing igneous phases, particularly plagioclase and to a lesser extent olivine (see Plate 2.2). They are also found within replacing groundmass, microveins and fractures and infill both pore spaces and vesicles where they commonly exhibit concentric zoning of dark (fine) and light (coarse) bands.When they are found in vesicles associated with other alteration phases (eg.calcite) they always are found around the margins indicating an early formation. Colours range from colourless to greenish brown. XRD analysis (see Chapter 3) indicates that randomly interlayered chlorite-smectite is ubiquitous both within and outside metadomains whilst discrete phases such as chlorite are restricted to

metadomains.

2. Calcite

This is a common alteration mineral found throughout the lavas, both within and outside metadomains. It is found as a partial replacement of primary plagioclase together with secondary phyllosilicates as shown in Plate 2.1, and occasionally as irregular grains within the groundmass of some samples. It is most commonly seen within veins, fractures and amygdales within the metadomains where grains are often interlocked, frequently euhedral and are occasionally centimetre sized as seen in Plate 2.3. In all circumstances the calcite is colourless and XRD analysis shows that there is no dolomitic component.

When calcite is found within the vein or amygdale environment it is always paragenetically late. It can be seen overgrowing other amygdale minerals such as analcime and prehnite (Plates 2.5 and 2.7). Also, it is seen overgrowing zeolite minerals within metadomains as seen in Plate 2.9.

Cathodoluminescence shows that calcites collected across the lavas show a dull orange luminescence indicating the presence of Mn^{2+}. However, there is no zonation or variation in luminescence within individual veins, or samples suggesting that fluid conditions were relatively constant during calcite formation.

3. Analcime

This is a common alteration phase within metadomains though is rarely seen outside. It is occasionally seen as a partial replacement mineral of feldspar and glass, though more commonly as discrete clear crystals showing weak birefringence within veins and amygdales. Occasionally, lamellar twining is observed. Within such environments it is often massive or forms interlocking idiomorphic crystals as shown in Plate 2.5. Paragenetically it is always earlier formed than vein / amygdale calcite but appears to be coeval with calcite which replaces feldspar phenocrysts. It is very rarely seen in direct association with prehnite. Plate 2.10 shows one exception to this rule where it appears that analcime is overgrown by prehnite.

4. Prehnite

This phase occurs only within metadomains where it can form spectacular radiating aggregates as shown in Plates 2.5 and 2.6. In thin section prehnite is characterised by spectacular radiating overgrowths within veins and amygdales and displays second order interference colours though it is normally colourless or pale yellow in ordinary light. It is always paragenetically earlier than calcite which can be seen growing on some samples as shown in Plate 2.7.

Prehnite and analcime are always the dominant vein / amygdale minerals within metadomains. However, within any one locality they are rarely seen in association with one another i.e. co-precipitated within the same vein. At Boyleston Quarry it is found that prehnite occurs mainly within interconnected amygdales and veins whilst analcime is commonly found within closed pore spaces and isolated veins. The transition from prehnite to analcime dominated conditions can often occur over distances of tens of centimetres in the field (see Chapter 1). Also it is noted that prehnite is restricted to the oxidised flow top of the lower flow at this locality as described in Chapter 1.

5. Opaque oxides

These consist of either opaque Fe-Ti oxides as confirmed by probe analysis or as dull red hematite which it is believed is a residual product of intense sub-aerial weathering. As previously mentioned these phases are commonly found as a residual alteration product of palagonite their presence indicating intense alteration (Staudigel and Hart, 1983).

Within the metadomains, opaque Fe-Ti oxides frequently appear as small irregular to sub-regular blades which are thought to be pseudomorphs of olivine as shown in Plate 2.8. Alternatively they appear as small, interstitial irregular masses forming a large proportion of the groundmass. They are often a patchy red-brown colour and may be associated with phyllosilicate. There is often concentration of opaques around the margins of amygdales and pore spaces.

6. Natrolite-Thomsonite

These undersaturated zeolites are relatively rare and restricted to veins and amygdales

Plate 2.1. Altered plagioclase phenocryst. In this case there is almost total replacement by carbonate which is also seen within a vein lined by phyllosilicate to the extreme left. Also, note replacement along fractures and grain margins by fine grained phyllosilicates (brown to pale geen) together with induration of phenocryst margins suggesting invasion of hydrothermal fluid. There is also widespread replacement of groundmass material by phyllosilicates (especially feldspar microlites) and carbonate.

Sample No. AP3. Contact between ovelapping flows in quarry at Jamie Wright's Well, Campsie Glen.

Plate 2.2. Replacement of olivine by phyllosilicates within Craiglockhart basalt. In this case there is total replacement of olivine by pale brown phyllosilicate (mixed layer chlorite-smectite). Pale green phyllosilicates are seen within the groundmass suggesting that the composition of the pre-cursor phase exerts a degree of influence upon phyllosilcate composition. Also, there is total albitisation of feldspar microlites within this section. Note that there appears to be heterogeneity within phyllosilicates found within vessicles as shown by alternating dark and light bands.

Sample No. HC5. Base of western face of quarry, High Craigton.

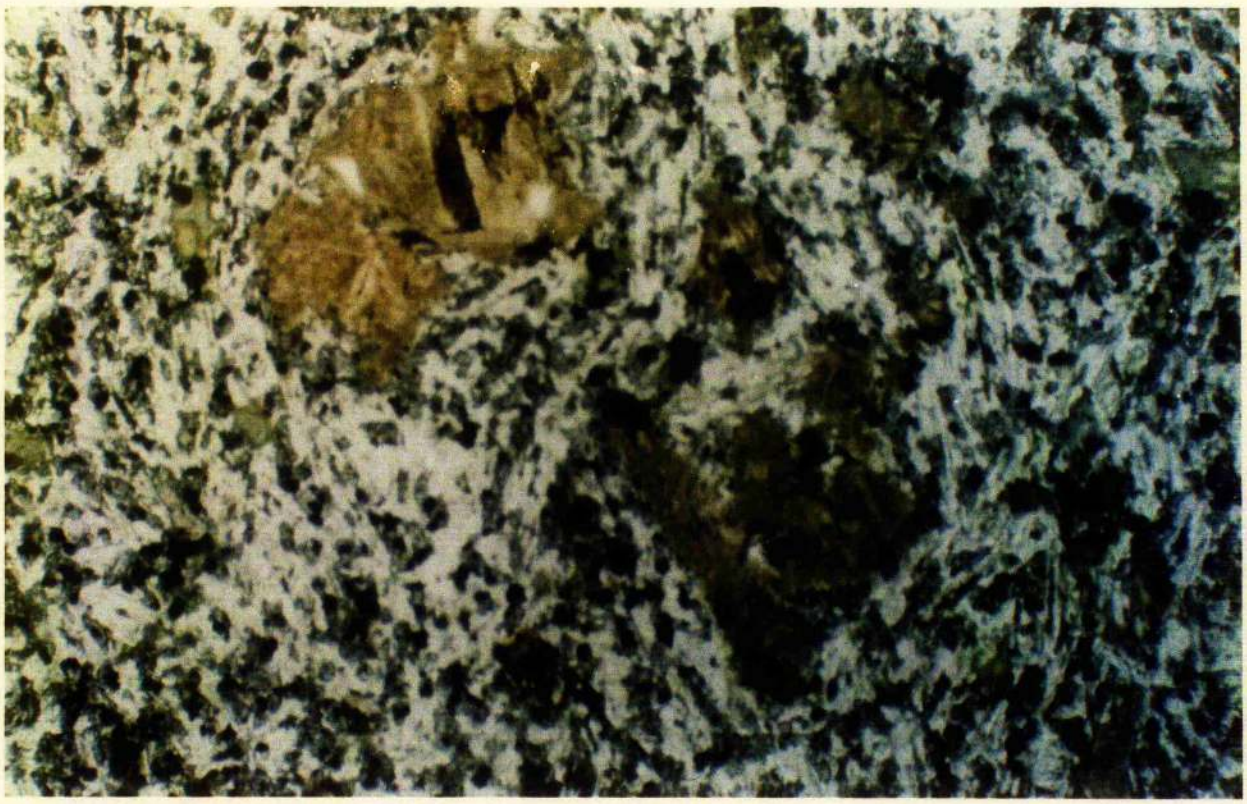

Plate 2.3. Hydrofractured calcite vein from metadomain. Here calcite forms an interlocking network within a large vein containing angular fragments of glassy basalt. It can be seen that this vein is matrix (calcite) supported suggesting transport in a fluidised medium. This vein sample was collected within a holocrystalline lava flow though the encapsulated basalt fragments are clearly glassy. This suggests that the vein forming fluid transported the basalt fragments over a distance of several metres.

Sample No. LB7. Langbank Cutting. Located at boundary between lava flows, towards western margin of outcrop.

Plate 2.4. Volcaniclastic sediment from Boyleston Quarry. This sediment is both texturally and compositionally immature, possessing high porosity and permeability. Sub-angular, detrital, relatively unaltered pyroxenes are clearly visible within this sample and suggest a local derivation. Several hundred metres to the west of this locality there is abundant augite rich Dunsapie basalt. Also, note that the detrital basalt clasts are highly altered suggesting that the parental basalt had undergone extensive, widespread alteration prior to sediment formation. Also, note the presence of thin carbonate stringers around some grain margins.

Sample No. BS. Block of volcaniclastic sediment found towards northwest face of Boyleston Quarry.

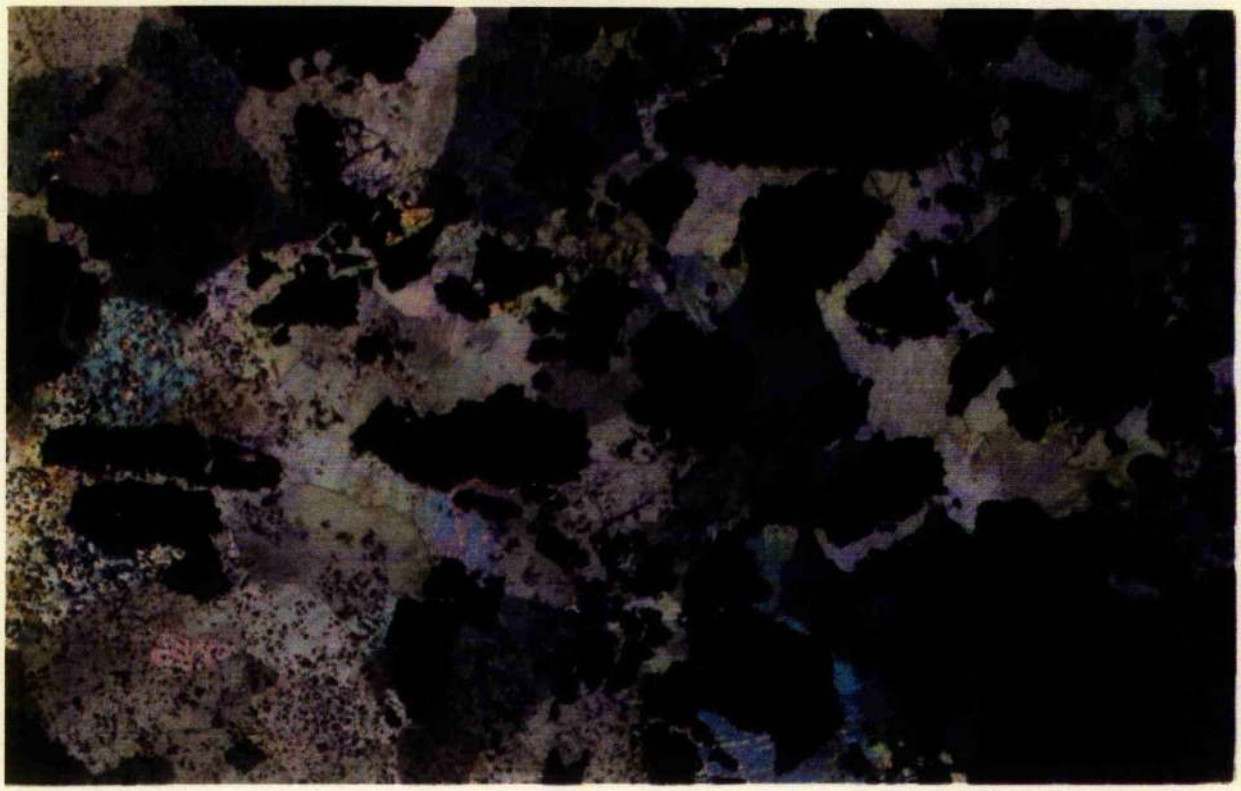

Plate 2.5. Spectacular prehnite. This sample is taken from Boyleston Quarry and shows typical radiating clusters within vein and amygdale networks. Most samples show maximum birefringence up to second order yellow. Also, many samples are faint yellow in ordinary light indicating Fe-rich compositions.

Sample No. B4. Taken from oxidised lower flow exposed in northeastern margin of Boyleston Quarry (see Plate 1.4), approximately 1 metre below the contact with the middle flow.

Plate 2.6. Calcite after prehnite. A large prehnite vein from Boyleston Quarry within which there has been later precipitation of calcite as shown by individual calcite grains crosscutting prehnite grain boundaries. Again note that prehnite forms radiating clusters and that calcite does not form at the expense of prehnite.

Sample No. B2. Taken from the same locality as B4, though from 2 metres below contact with overlying middle flow.

Plate 2.7. Fe-Ti oxides. This section shows pseudomorphing of olivines by Fe-Ti oxides within Dunsapie basalt. Note that there is concentration of opaques around grain margins whilst there is extensive albitisation and replacement by carbonate of groundmass microlites. *Sample No. AP2. Quarry in Flow No. 18, at contact between overlapping flows, Jamie Wright's Well, Campsie Glen.*

Plate 2.8 Thomsonite within amygdale. Thomsonite (a burial metamorphic index mineral, Evans, 1987) is overgrown by calcite within this amygdale. Thomsonite characteristically exhibits a radiating habit though displays lower birefringence than prehnite.
Sample No. C8. Boyleston Quarry. Collected approximately 3 metres above contact between lower and middle flows in northeastern margin of quarry (see Plate 1.4).

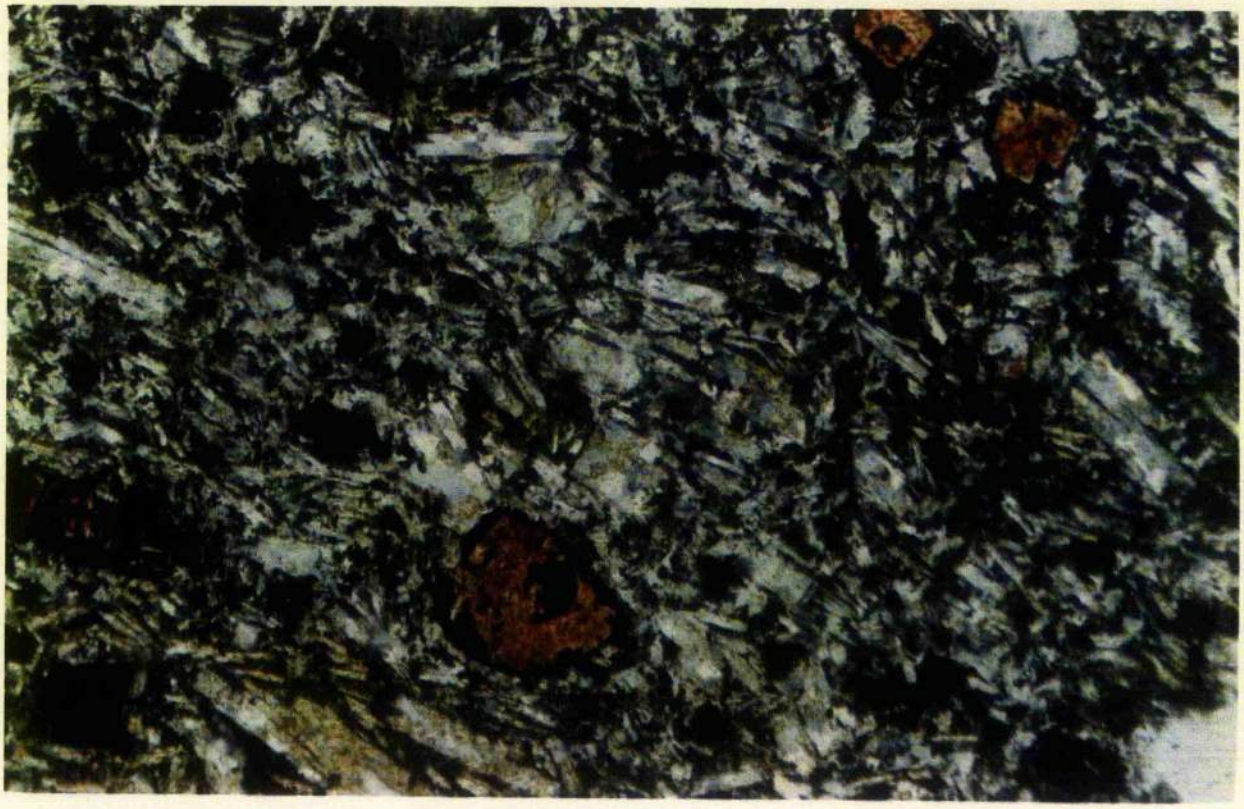

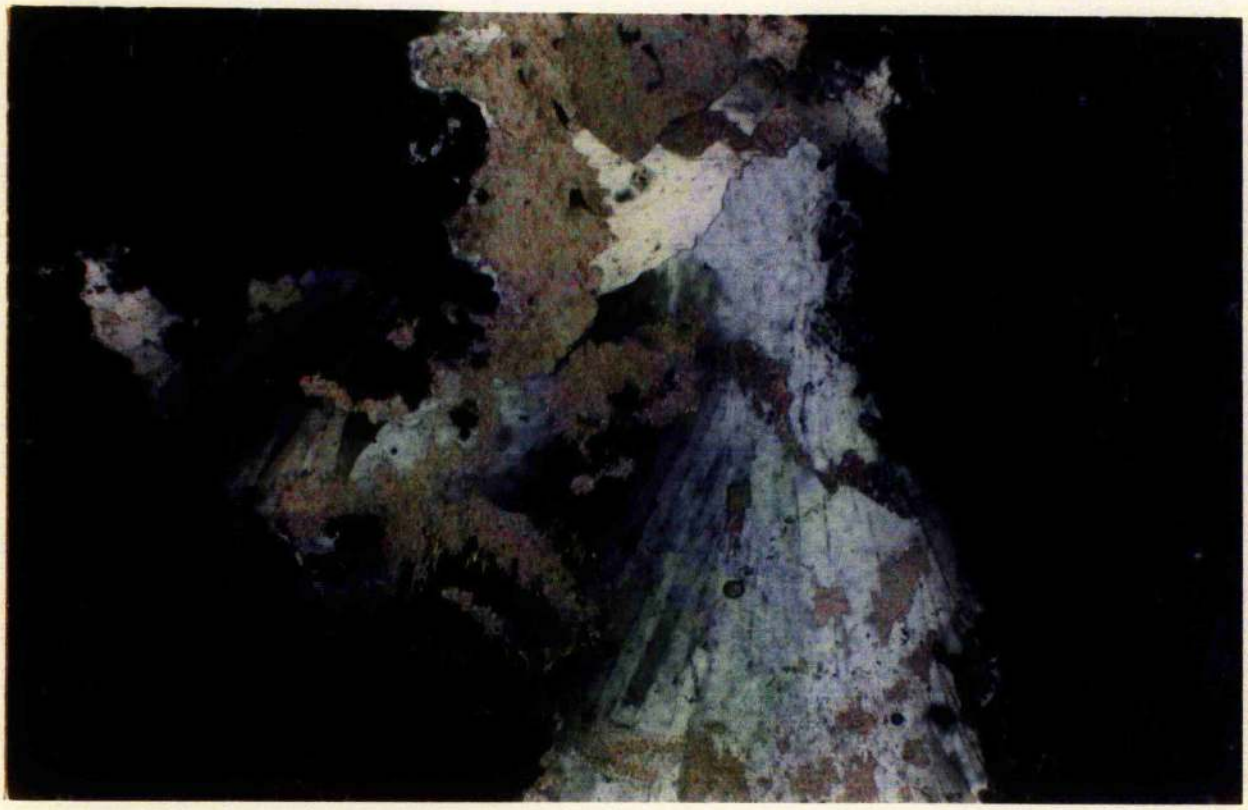

within the metadomains. Typically they are colourless, show grey to pale yellow interference colours and are of very low relief. At Boyleston Quarry and Langbank Cutting they are seen growing as small tabular or sheath-like radiating aggregates. As with analcime and prehnite these zeolites are often overgrown by calcite as shown in Plate 2.9. However, Plate 2.12 clearly indicate that they overgrow those phases which characterise metadomain alteration.

The study of Evans (1987) indicates that thomsonite and natrolite are burial metamorphic index minerals within the Renfrewshire Block unlike prehnite and analcime which are clearly related to metadomain activity. Therefore, it appears that calcite precipitation continued throughout both the geothermal (as represented by metadomain development) and burial metamorphic history of the lavas.

7. Clinozoisite-Epidote

This series is present only in accessory amounts and occurs both within and outside of the metadomains. Clinozoisite is found mainly outside the metadomains where it is an interstitial phase, commonly with a lath shaped form. Typically it is colourless and shows weak grey to yellow interference colours. Epidote however is colourless to faint pale yellow, the colour being patchily distributed and it is more widespread within the metadomains. Colouring is generally attributed to a relatively high Fe^{3+} content (Deer et al., 1965).

2.3 Variations within metadomains

Within individual metadomains there is often heterogeneity as evidenced by variations in the intensity of alteration, variations in alteration phase ratios, variations in vein characteristics etc. In general it is inherent primary volcanological features which exert a major influence in the extent of the alteration. Two examples of this heterogeneity are given below.

1. Langbank Cutting

Here metadomain development occurs at the boundary between two sub-horizontal lava

flows as illustrated in Chapter 1. There is a general decrease in the intensity of alteration away from the flow boundary. Petrographic observations reveal that heterogeneity is manifest in a variety of forms:

a) There is an overall decrease in the volume percent of amygdales away from the flow boundary. This ranges from up to 70% at the flow boundary to less than 5% 15 metres below the boundary. Also, maximum amygdale diameter decreases downwards from 2 mm to less than 0.5 mm over the same distance interval.

b) The volume percent of plagioclase phenocrysts increases from less than 5% to 50% downwards, away from the flow boundary.

c) There is a progressive decrease in the abundance of the three main phases which characterise metadomain alteration (analcite, calcite and prehnite in order of relative abundance) downwards, whilst the proportion of thomsonite increases.

d) There is a progressive decrease in pseudomorphing of plagioclase phenocrysts by analcime away from the flow boundary.

2. Boyleston Quarry

Metadomain development at this locality occurs across flow boundaries as shown in Chapter 1. In particular, they are commonly observed crosscutting the boundary between the lowest oxidised, weathered flow top and the overlying flow which forms the main section of the quarry face. In thin section it is clear that the volume percent of amygdales within the upper flow progressively decreases to less than 5% at a distance of 0.5 metres from the flow boundary. Within this zone analcime is the dominant alteration mineralogy occurring within closed amygdales. However, whilst analcime is still dominant above this zone it occurs predominantly within hydrofractured vein networks which ramify up to a vertical distance of approximately 10 metres and range in thickness from millimetres to tens of centimetres. Within this zone the bulk of the lava is much less altered, with only incipient alteration of groundmass feldspar microlites.

Within the lower lava, prehnite is the dominant alteration mineral where it forms spectacular radiating clusters, both within veins and amygdales (see Plate 2.6). The transition

Plate 2.9. Calcite vein dissecting plagioclase phenocryst. This vein forms part of a hydrofractured network within a metadomain. Note that there has been extensive replacement of the feldspar by albite and carbonate prior to vein development.
Sample No. LB6. Langbank Cutting. This sample is collected from the western margin of the metadomain outcrop at Langbank, within the upper lava flow.

Plate 2.10. Prehnite and analcime within amygdale. Within this section analcime (clear) is found around the margin of the amygdale whilst prehnite (displaying a range of second order interference colours) is found towards the centre. It appears that prehnite is overgrowing analcime within this sample. These two minerals are rarely found in contact with one another.
Sample No. B5. Boyleston Quarry. This sample is taken approximately 0.2 metres below the contact between the lower and middle flows at the northeastern margin of the quarry (see Plate 1.4).

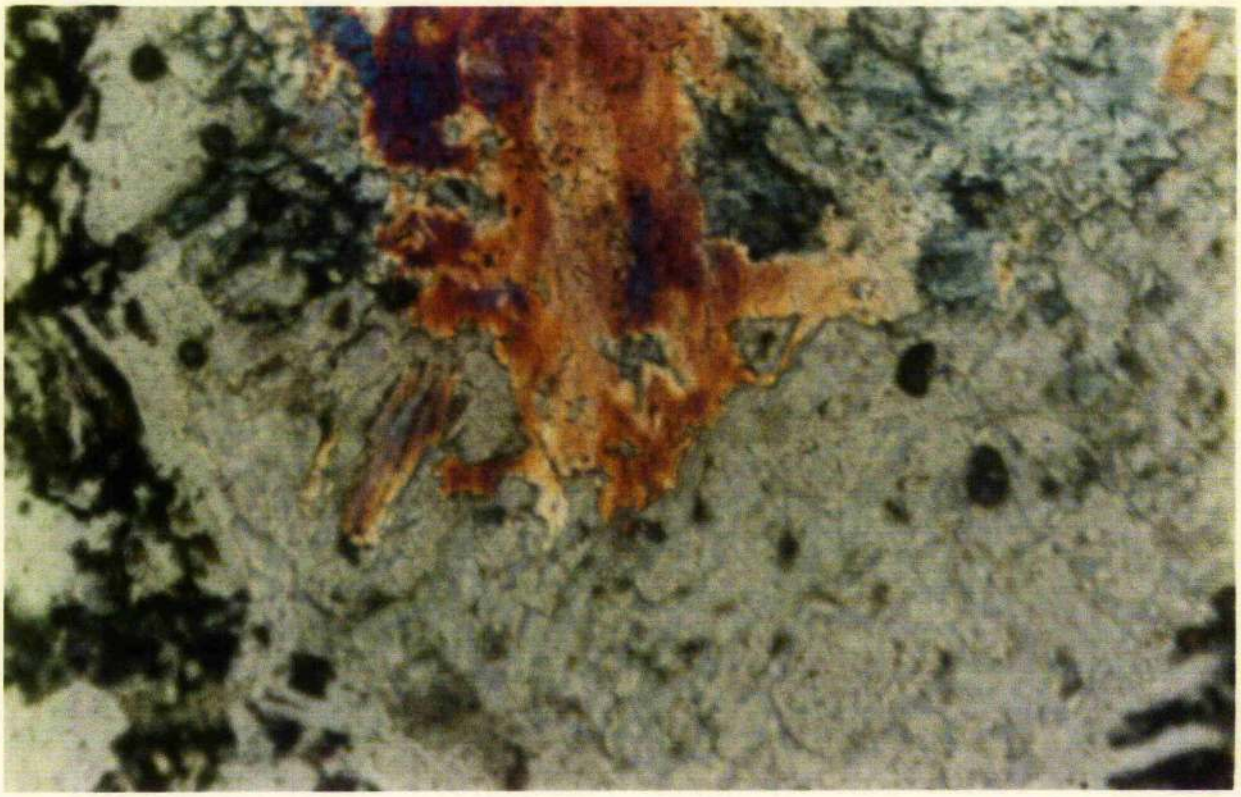

Plate 2.11. Thomsonite overgrowing analcime. In this section metadomain analcime (showing very low birefringence) forms a massive interlocking network within a large vein and is overgrown by tabular, radiating thomsonite (a burial metamorphic index mineral) needles. *Sample No. LA2. Langbank Cutting. Located at the western margin of the cutting, within the lower lava flow.*

Plate 2.12.Thomsonite and calcite overgrowing analcime. In this section both thomsonite and calcite overgrow analcime. The margin between the single large calcite grain and the thomsonite bundle is highly irregular. It appears that calcite is paragenetically later as shown by disappearance of individual thomsonite needles under the calcite grain. This suggests that carbonate deposition has been occurring throughout the post-extrusive history of the lavas. *Sample No. LA2. Langbank Cutting.*

from prehnite to analcime dominated mineralogies occurs over a distance of 0.2 metres and is coincident with the boundary between lava flows.

2.4 Discussion

2.4.1 Vein textures and paragenetic sequence

A common characteristic of metadomain alteration is the development of intense hydrofractured veins as discussed in Chapter 1. Using the thin section evidence presented in Section 2.2 it is possible to establish a paragenetic sequence and to establish a temporal relationship between metadomain activity and burial metamorphism as illustrated in Figure 2.1. Using this approach it is possible to recognise three distinct alteration episodes:

1. Early widespread alteration

This stage is characterised by the widespread alteration of groundmass material and the palagonisation of volcanic glass to varying degrees. It affected lava both within and outside metadomains. Studies of active ocean floor hydrothermal circulation (eg. Cann, 1983) shows that this process commences soon after basalt eruption. However, the presence of numerous boles and volcaniclastic horizons within the Clyde Lavas (such as those exposed at Boyleston Quarry) is indicative of a sub-areal eruptive environment and Francis (1983) indicates that full marine conditions did not exist within the Glasgow area until the close of Calciferous Sandstone times. Also, variable degrees of alteration are exhibited within the sections studied ranging from relatively fresh to totally altered. These observations suggest that meteoric water as opposed to seawater was largely responsible for producing this style of alteration. Minerals which characterise this style in the Clyde Lavas include (in order of abundance) mixed layer chlorite-smectite, analcime, calcite, albite and epidote-clinozoisite.

Samples which showed only this type of alteration were used to define the starting compositions of basalt prior to metadomain alteration. This is discussed fully in Chapter 4, which focuses upon chemical mobility associated with metadomain development.

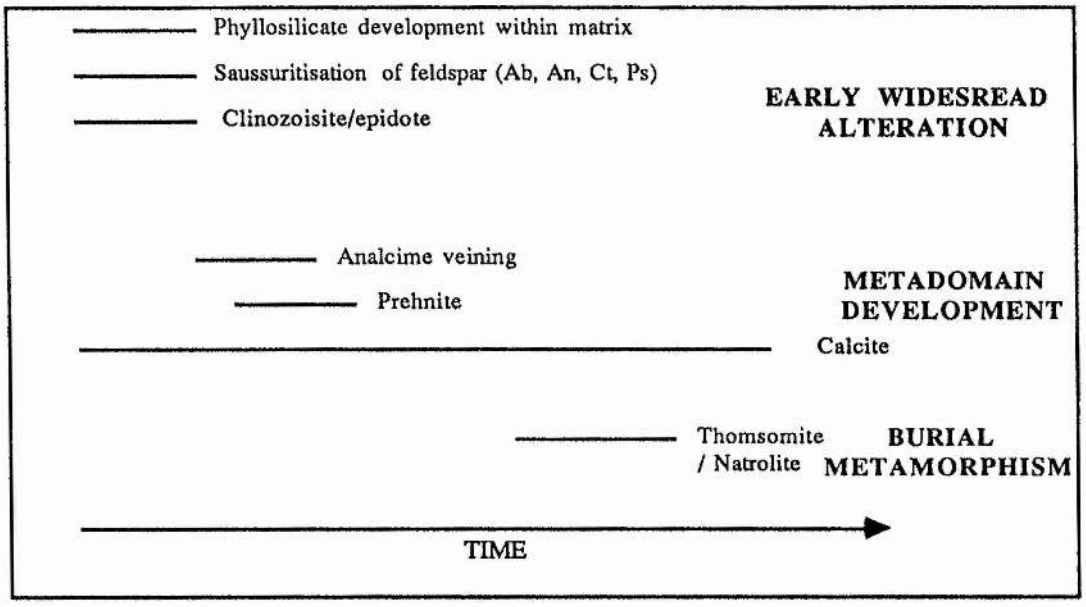

Figure 2.2 Paragenetic sequence as deduced from textural relationships within metadomain veins

(Ab = albite, An = analcime, Ct = carbonate, Ps = phyllosilicate)

2. Metadomain alteration

This stage is characterised by the intense hydraulic fracturing and veining of basalt caused by the advection of hydrothermal fluids which exploited permeability contrasts within the basalt (see Chapter 1). The presence of fragments of basalt within hydrofractured veins which show the characteristic features of Stage 1 clearly indicates that this metadomain alteration occurred after early, widespread alteration. This feature is illustrated in Plate 2.3. Also, it is possible to observe carbonate rich veins which dissect plagioclase phenocrysts which have undergone earlier alteration as shown in Plate 2.10. Minerals which characterise this stage include (in order of abundance) analcime, calcite and prehnite. Also, there is a change in the nature of the phyllosilicate phase within the metadomains as shown by the development of chlorite from mixed-layer phases. This process is discussed in full in Chapter 3. It is suggested that both prehnite and analcime were formed before calcite as shown in Plates 2.5 and 2.7. The relationship between prehnite and analcime is less clear since the two are rarely found in contact with one another. Plate 2.11 shows prehnite occupying the centre of an amygdale which is lined by analcime. This suggests that prehnite was precipitated slightly later than analcime. However, closer examination of the contact between the two

minerals clearly shows fragments of analcime which are in optical continuity with the main analcime mass and which appear to grow upon prehnite suggesting the reverse situation to be true.

3.Burial metamorphism

For a detailed account of this phase in the post-eruptive evolution of the Clyde Lavas the reader is referred to Evans (1987). In the context of this discussion, thin section evidence presented in Plate 2.12, namely the growth of index minerals which characterise burial metamorphism within the area (such as thomsonite) upon minerals which characterise metadomain alteration (analcime) indicates that burial metamorphism followed metadomain alteration.

2.4.2 Equilibrium

Metadomains within the Clyde Lavas are characterised by the assemblage phyllosilicate + calcite +/- analcime +/- prehnite +/- epidote-clinozoisite. These minerals described above are common in low grade basalt sequences worldwide. In order to provide information on the immediate physical and chemical environment within metadomains it is necessary to establish the extent to which mineralogical equilibrium has been achieved. This is because reaction rates are reduced due to relatively low temperatures and therefore equilibrium between the various phases is not always achieved. The scale over which equilibrium exists within low grade metabasites has been the subject of much debate. Nakajima et al. (1977) believe that equilibrium exists over the area of a single thin section whilst Kawachi (1975) argues that only minerals in direct contact can be assumed to have reached equilibrium. For the metadomain vein environment this would include only analcime-calcite and prehnite-calcite pairs. Liou et al. (1985) stress that low variance buffered assemblages are of significance when considering the question of equilibrium. What is clear from proceeding sections is that there is marked heterogeneity within individual metadomains which exists down to the thin section scale (evidenced for example by the varying degrees

of feldspar alteration over a single section) suggesting buffering has not occurred to any significant extent. However, evidence in Chapter 3 indicates that phyllosilicates within the metadomains represent an overall evolutionary sequence as early formed material partially equilibrated as metadomain development proceeded. This suggests that the basalts have attempted to equilibrate with the alteration fluids.

2.4.3 Fluid temperatures

Kristmannsdottir (1983), following a study of alteration products within drillcores taken from areas of geothermal activity in Iceland, notes the following:

1. Calcite is common at all depths up to a temperature of 270 °C.
2. No correlation between prehnite occurrence and rock temperature was established. However, Henley and Ellis (1983) in a review of aluminosilicate paragenesis in geothermal systems note that prehnite is found only in systems where temperatures exceed 200 °C. Bowers and Taylor (1987) following a study which models water-rock interaction predict that prehnite is present at temperatures between 200 and 250 °C during seawater-basalt interaction.
3. Epidote group minerals occur sporadically between 200 to 260 °C, though are relatively unimportant until temperatures exceed 260 °C. However, Liou et al. (1985) showed that epidote with X_{Fe} less than 0.3 (ie. iron rich) was stable at temperatures less than approximately 160 °C within the model basaltic system.
4. Zeolites are common at below 100°C and are replaced by laumontite above this temperature. Within olivine tholeiites thomsonite and mesolite-scolecite predominate over mordenite, heulandite and stilbite.

Campbell and Fyfe (1965) and Thompson (1971) demonstrate that the formation of analcime via the reaction

albite + water = analcime + quartz

is independent of pressure at P_{H2O} less than 2kb: the reaction temperature is constant at 180 to 190 °C. Iijiama (1978) also showed that Na^+ concentration in the hydrothermal fluid also

controls the albite to analcime reaction temperature such that at Na concentrations of approximately 10^3 ppm (corresponding to weakly alkaline geothermal waters) reaction temperature is decreased by approximately 20 °C.

Therefore, it is suggested that temperatures within the metadomain fluids based on observed mineral assemblages ranged from approximately 150 to 250 °C. The lack of either actinolite or epidote-andradite assemblages indicates that temperatures within the metadomains never exceeded 300 °C (Ellis, 1983). Furthermore, the lack of pumpellyite-laumontite bearing assemblages suggests temperatures never exceeded approximately 230 °C based on the data of Liou et al. (1985). This would place metamorphism intermediate between the zeolite and prehnite-pumpellyite / prehnite-actinolite facies as defined by Liou et al. (1985). The presence of natrolite-thomsonite growing upon characteristic metadomain minerals (such as calcite) suggests fluid temperatures had decreased significantly during burial metamorphism.

2.4.4 Fluid chemistry

The pervasive nature of the alteration as evidenced by the widespread alteration of groundmass plagioclase suggests that water / rock ratios were relatively high and therefore fluid chemistry will have exerted an important control on secondary mineral paragenesis. Spooner and Fyfe (1973) suggest that the circulation of large volumes of water of surface origin through basalts implies a correspondingly large oxygen flux. Relic igneous Fe-Ti oxides are present within most sections but $f\,O_2$ is not likely to have been controlled by magnetite-hematite buffering since water flow rates were high (see Chapter 1) and reaction rates were low because of low fluid temperatures. The lack of any secondary sulphides and sulphates within the metadomains also suggests high fluid $f\,O_2$. Also, the presence of native copper as stringers within metadomains at Boyleston Quarry (Hall et al., 1989) can be used to estimate Eh using the data of Pollard et al. (1990) who, following a study of basic copper chlorides, suggest native copper is stable at Eh ranging from 0 to 0.22 volts (mildly oxidising) and pH less than 8.

The presence of abundant secondary Ca-aluminosilicates minerals within veins (prehnite, calcite and minor clinozoisite-epidote) testifies to the mobility of the cations (Ca, Al and to a lesser extent Fe) within the hydrothermal fluid. Also, Thompson (1971) points out that the composition of prehnite (ideally $Ca_2Al_2Si_3O_{10}(OH)_2$) requires there to be an excess of Ca within the fluid phase. Many experimental studies, such as that by Mottl (1983) confirms the transfer of Ca to the fluid phase during basalt-water interaction. Furthermore, the dominance of Ca bearing zeolites over Na and K bearing zeolites within the later burial metamorphic zones defined by Evans (1987) suggests the broad-scale transport of Ca enriched fluids during this period.

Calcite is a ubiquitous alteration phase throughout the metadomains and is a paragenetically late metadomain mineral. Within hydrothermal fluids the solubility of calcite increases with decreasing temperature and decreases with decreasing pressure (Zheng, 1990). Therefore, calcite cannot be deposited from the fluid by simple cooling under closed system conditions. If a fluid cools adiabatically (i.e. boils) carbonate is likely to precipitate because CO_2 is partitioned into the vapour phase which affects the following equilibrium;

$$CaCO_3 + CO_2 + H_2O = Ca^{2+} + 2HCO_3^-.$$

However, fluid inclusion evidence presented in Chapter 5 suggests that fluid boiling was not a widely occurring process during metadomain activity though calcite is ubiquitous throughout the metadomains. Cooling which tends to move a solution towards a state of calcite undersaturation is generally offset by partitioning of CO_2 into the vapour (Fournier, 1985). Therefore, it is more likely that CO_2 was lost gradually from fluids which were open to the surface but were not at a temperature high enough to cause boiling.

Giggenbach (1981) suggests that CO_2 concentrations within geothermal fluids are controlled by reactions of the type

$$\text{plagioclase} + CO_2 = \text{phyllosilicate} + \text{calcite}$$

An estimate of CO_2 concentration within the fluid comes from Browne and Ellis (1971) following a study of fluid chemistry and alteration mineralogy at the Ohaki-Broadlands area of New Zealand. They suggest that for systems such as the Clyde Lava metadomains where

zoisite and wairakite (the Ca analogue of analcime) are absent that CO_2 concentrations are approximately 1.0 mol/kg geothermal fluid. It is noted that the abundance of Ca bearing aluminosilicates within metadomains is much greater than paragenetically later calcite suggesting that aCa in the hydrothermal fluid decreased as the metadomains evolved.

The coexistence of calcite and Ca-aluminosilicates within hydrothermal systems has been the topic of debate (eg. Thompson, 1971) because in the presence of CO_2 reactions of the following type can occur

$$\text{prehnite} + \text{silica} + CO_2 + H_2O = \text{laumontite} + \text{calcite}.$$

However, within the Clyde Lava metadomains calcite is never seen replacing earlier formed phases. Also, earlier formed metadomain minerals such as prehnite or analcime are rarely seen in a state of decomposition. This suggests that these phases had became metastable with respect to the fluids which were present during calcite formation, possibly because of an overall reduction in fluid temperatures as the lava pile cooled via groundwater convection.

2.5 Conclusions

Petrographic examination has identified three separate hydrothermal events within the Clyde Lavas:

a) Stage 1: Early widespread alteration

This stage involved the widespread alteration of the lavas soon after eruption and involved replacement of primary igneous phases to varying degrees (notably plagioclase feldspar) with mixed layer chlorite-smectite, analcime, calcite, albite, epidote-clinozoisite and concentration of residual Fe-Ti oxides.

b) Stage 2 : Metadomain alteration

This stage is characterised by the development of metadomains in very localised regions of high permeability such as faults, lithological contrasts and flow boundaries. This phase is often accompanied by intense veining and hydrobrecciation of the host basalt. Minerals which characterise this stage include analcime, calcite and prehnite. Also, there is a change

in the nature of the phyllosilicate phase accompanying this stage which is discussed fully in Chapter 3. Within individual metadomains there is often marked heterogeneity in the intensity of the alteration.

c) Stage 3 : Burial metamorphism

This stage is characterised by the development of a range of zeolites (occasionally seen growing upon metadomain minerals) as discussed by Evans (1987).

Comparison of alteration minerals developed within the Clyde Lava metadomains with those reported in other geothermal areas suggest fluid temperatures varied between 150 to 250°C. The presence of abundant secondary Ca-aluminosilicsates within veins (prehnite, calcite and minor clinozoisite-epidote) indicates mobility of Ca,Si,Al and Fe within the hydrothermal fluid.

CHAPTER 3 PHYLLOSILICATE PARAGENESIS

3.1 Introduction

The widespread alteration of oceanic basalts by seawater observed in ocean floor basalts and hydrothermal alteration affecting present day continental geothermal areas can be likened to the situation within the Clyde Lavas. In each case pervasive fluid advection results in the formation of a series of secondary mineralogies and metadomain phyllosilicates derived from igneous precursors.

Phyllosilicates are ubiquitous throughout the Clyde Lavas and quantitatively constitute a major alteration product, both within and outside the metadomains. They are found pseudomorphing and replacing igneous phases, within microviens and fractures, and infilling both pore spaces and vesicles where they commonly exhibit concentric zoning of dark (fine) and light (coarse) bands (see Chapter 2).

Phyllosilicates such as smectite, interlayered chlorite-smectite and chlorite are abundant in a variety of low grade and geothermal environments where metabasites are present (eg. Bettison and Schiffman, 1988, Cann, 1979, Kristmannsdottir, 1979). These studies show that within such environments phyllosilicate mineralogy and composition has been closely correlated with measured temperatures and are also sensitive indicators of changes in other factors which influence alteration mineralogy such as permeability and fluid chemistry. As such, phyllosilicates provide an opportunity to establish and assess how conditions within and outside the metadomains may have varied during the alteration process, a topic which is central to the aims of this project. Also, if differences exist then this may have consequences for the development of geothermal activity within the lavas. In order to address the above issues an approach which integrates both X-ray diffraction and microprobe analysis is adopted.

3.2 Qualitative Identification of Phyllosilicates by X-Ray Diffraction Analysis

In order to establish the exact nature of the phyllosilicates present diffractograms were obtained for air dried, glycolated and heated samples. Details of sample preparation and treatments are given in Appendix 3.1. A summary of the main diffraction characteristics of the quantitatively important "pure" mineral species found within the lavas (chlorite, illite, kaolinite) is given below in Table 4.1.

Mineral name	Layer type	Characteristic reflections of air dried sample	Glycolation	Heat treatment to 500 °C
Chlorite	2:1	14 Å (001)* 7 Å (002) 4.7 Å (003) 3.5 Å (004)	No effect	001 shifts to high angle side
Illite **	2:1	10 Å (001) a-sym. on low angle side	No effect	Sharpening of 10 Å peak
Kaolinite (ordered)	1:1	7.15 Å (001) sharp 3.58 Å (002) sharp	No effect	Collapse at 550 °C

* the exact position and intensity of the various reflections varies as a function of the nature of the cations occupying octahedral and tetrahedral positions (Thorez, 1976).

** illite can be further classified on the basis of the characteristics of the 10 Å peak upon glycolation. For example, expansion of the shoulder on the low angle side of this peak is characteristic of illite with montmorillonite behavour (I_M). Conversely, contraction of this shoulder is a characteristic of illite with vermiculite behavour (I_V). These varieties are not to be confused with mixed layer clays discussed below (Thorez, 1976).

Table 4.1 Main characteristics of main reflections of "pure" phyllosilicate phases.

In addition to pure clay minerals interstratified or mixed layer species also occur within metabasites (eg.Bettison and Schiffman, 1988). These species are characterised by the combination and interstratification of two or more different mineral types. Within the Clyde lavas it is these which are most frequently found throughout and include both regular and randomly interlayered chlorite-smectite and, less commonly, chlorite-vermiculite.

X-Ray analysis also provides a way of differentiating between:

1. Regularly interstratified minerals; those composed of identical layers separated by two regularly alternating interlayer species.

2. Randomly interstratified minerals; those composed of identical or differing layers, separated by differing interlayers showing no repetition.

Kirsch (1974) notes that the relative intensities of the 14 Å and 7 Å reflections can be used to identify the nature of the interlayer species; thus I 7 Å > I 14 Å is indicative of chlorite alone; I 14-15 Å >> I 7 Å indicates interstratified chlorite-smectite and I 14-15 Å > I 7 Å indicates interstratified chlorite-vermiculite (where I = intensity). The latter two species can be further distinguished in their response to glycol saturation.

3.2.1 Recognition of regular and randomly interstratified minerals

1. Regularly interstratified species; stacking is perfectly ordered, the d-spacing of the mixed layer superlattice being expressed by;

$$d_{(001)\ AB} = d_{(001)\ A} + d_{(001)\ B}$$

where AB = mixed layer species (eg. chlorite-montmorillonite)

" A = pure mineral species (eg. chlorite)

" B = pure mineral species (eg. montmorillonite).

Recognition of these species is based upon the fact that they possess an integral series of orders with a superlattice spacing at dÅ derived from the sum of the d-spacings of the component clays. Also, there is an integral series of sharp, well defined reflections possesing well defined d-spacings not corresponding to those of simple clay minerals. In the case of regularly interstratified minerals single mineral names are often given. For example, corrensite is the name assigned to regularly layered chlorite-smectite. The (001) superlattice spacing of any mixed layer species falls outside the detection range of the Phillips PW1049 diffractometer. Therefore, identification is based largely on the behaviour of the 002 reflection at 14-15 Å.

2. Randomly interstratified species; as mentioned above regularly stratified minerals show

single reflections at characteristic d-spacings owing to "fusion" of the two closest reflections from minerals A and B, the new reflection having an intermediate d-spacing. This phenomena is termed a point effect by Thorez (1976). Randomly stratified minerals do not show this effect.

In certain zones of the X-ray pattern, where the original reflections from A and B are located a new, ill defined reflection appears. Typically this new reflection, or diffraction plateau, will be large at its base and flat topped, its limits being set by the d-spacings of the component minerals.

3.3 Results of X-Ray Diffraction

Approximately 70 smears were analysed as part of this study, samples having been selected from a range of localities. The results of this study are tabulated fully in Appendix 3.2.

1. Chlorite. This phase is restricted in occurrence and is not found outside the metadomains. It is identified primarily by the 001 peak at 14.2 Å which occurs as a shoulder on the main 002 mixed layer reflection as shown in Figure 3.2. This peak remains unaffected upon glycolation, though its intensity may change following heat treatment to 550° C.

2. Illite. This phase is rare and is restricted to some metadomain localities (eg. at Boyleston Quarry). Glycolation induces a very minor peak shift implying minor illite-smectite interlayering. In most cases however there is negligible collapse indicating a discrete illite phase. Sharpening of the 10 Å peak following heat treatment is seen, indicative of illite showing vermiculite behavour (Thorez, 1976). This is not to be confused with true mixed layer behaviour.

3. Kaolinite. This phase is rare and restricted to metadomains, being found only in Campsie Glen. It is characterised by two very strong reflections at 7 Å and 3.5 Å as shown in Figure 3.1. These peaks remain unaffected following HCl treatment, though are destroyed upon heating to 550° C. The significance of this phase will be dealt with below.

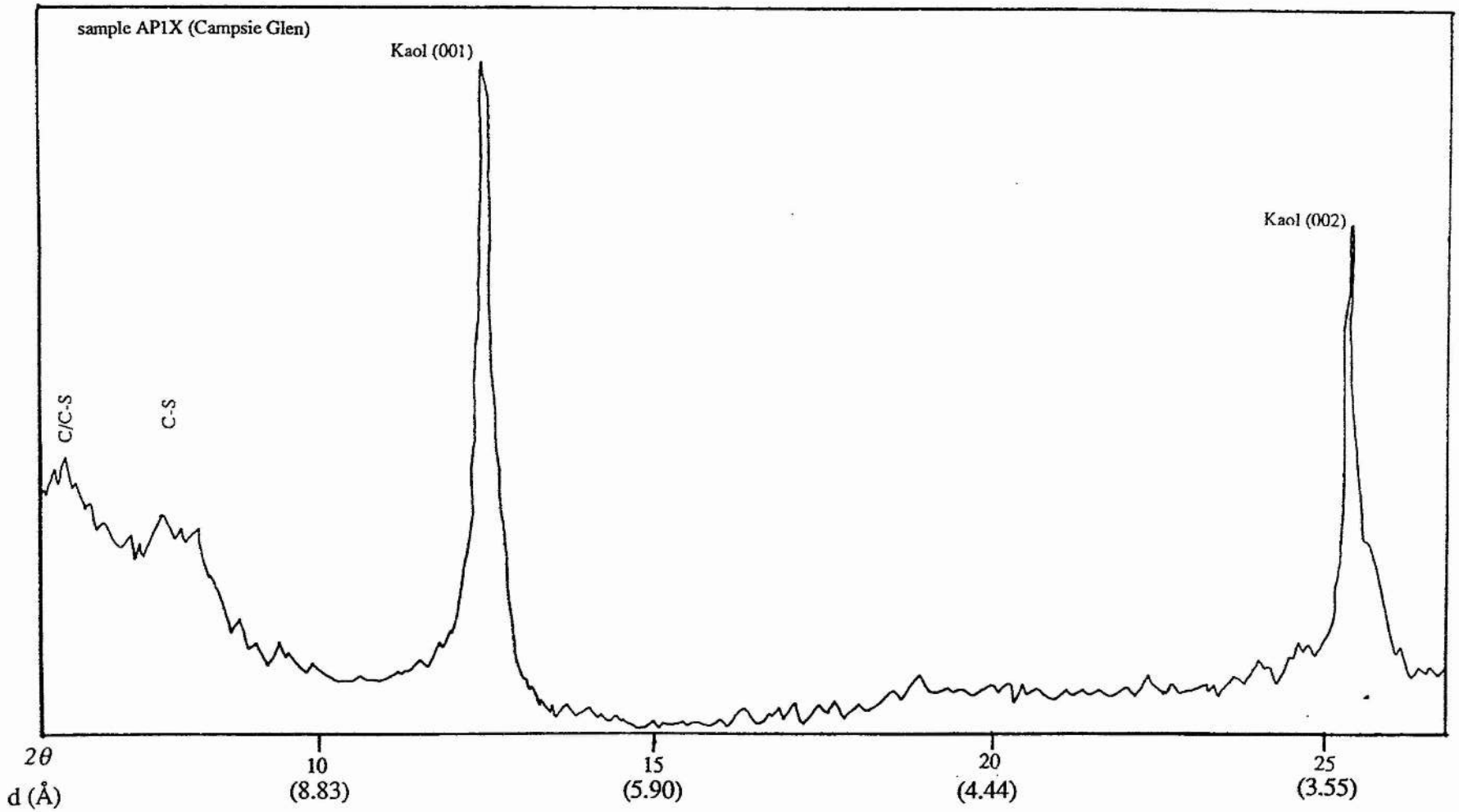

Figure 3.1 Diffractogram for air dried kaolinite

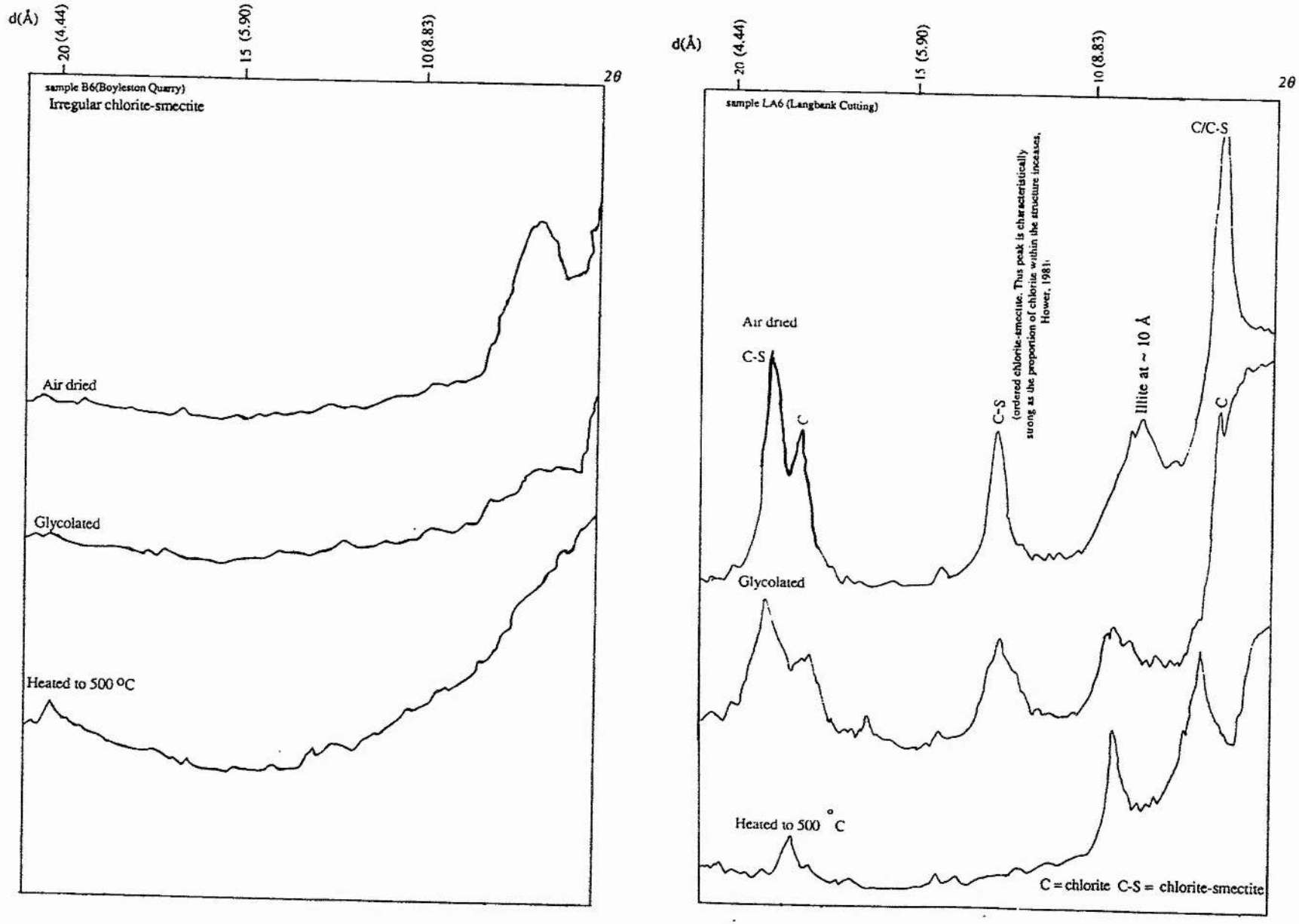

Figure 3.2 Diffractograms for irregular and regular chlorite/ smectite. Also shown are characteristic peaks for chlorite and illite

4. Interstratified chlorite-smectite. Both regular and irregular varieties have been identified in this study. With the exception of one locality (Langbank) irregular chlorite-smectite occurs throughout the lavas; regular chlorite-smectite occurs only within the metadomains. Both are absent where kaolinite is the dominant phyllosilicate.

Regular chlorite-smectite is characterised by an integral series of sharp, well defined reflections at 14.4 Å (002), 7.1 Å (003) and 4.7 Å (004). This is illustrated in Figure 3.2. Typically, the 002 reflection at 14.4 Å shows the strongest intensity and corresponds to a superlattice spacing of 28.8 Å. Hauff (1981) reports values between 28 and 30 Å for chlorite-smectite in the air dried state.

Glycolation induces an expansion of the (002) reflection to 15.2 Å, together with development of a shoulder on the high angle side. There is marked collapse of the remaining reflections following this treatment. Heating to 550 °C leads to collapse, broadening and partial recorrecting to 13.5 Å of the (002) reflection together with the disappearance of all other reflections.

Irregular chlorite-smectite is characterised by a strong, though broad and ill defined (002) reflection at approximately 14 Å such as that reported by Wilson and Bain (1970). Glycolation leads to further broadening and collapse with the apex located at approximately 15.5 Å. A diffractogram for irregular chlorite-smectite is shown on Figure 3.2.

Liou et al. (1985) provide a means of distinguishing between chlorite and interstratified chlorite-smectite based on the X-ray diffraction characteristics of the basal spacings under dry conditions upon glycolation. Following glycolation of mixed-layer chlorite-smectites initially possessing d_{100} (dry) values of ~ 14-15 Å an expansion to 14-16 Å occurs. This behaviour is not seen in chlorite. For this study, dry d_{100} chlorite-smectite values range from approximately 13.4-14.7 Å. These values increase to a maximum of 15.7 Å following glycolation. The degree of expansion obviously increases with the increase in expandable components. This is illustrated in Figure 3.3.

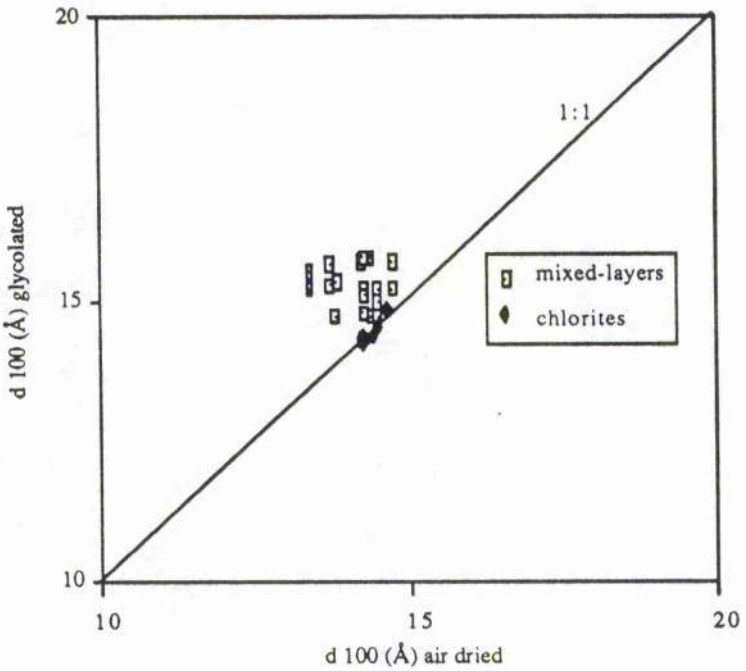

Figure 3.3 Change in phyllosilicate d spacings following glycolation

5. Chlorite-vermiculite. This is a rare phase, regular and irregular varieties occurring sporadically within metadomains. Typically, this phase possesses a strong to medium (002) reflection at 14.4 Å with integral harmonics at 7.1 Å (003) and 4.7 Å (004), similar to those reported by Sarkisyan and Kotelnikov (1972) for the air dried state. Glycolation has little or no effect; heating to 550 °C induces sharpening of the 002 reflection, together with a shift to 13.5 Å and loss of the remaining reflections.

3.4. Discussion

From the preceeding discussion, the following two points emerge:

1. Randomly interstratified chlorite-smectite is present throughout the lavas and also occurs within metadomains. A discrete smectite phase such as saponite, which was reported by Hall et.al. (1989) within these lavas, was not found.

2. Within metadomains there are a variety of phases, both mixed layer varieties and discrete phases are found. The former includes mixed layer chlorite-smectite and chlorite-vermiculite,

the latter includes chlorite, illite and occasionally kaolinite. These discrete phases are *not* seen outside the metadomains.

There now exists a wide body of data (Thompson, 1983) indicating that during the initial stages of basalt alteration, shortly after eruption, smectite is the dominant phyllosilicate phase. Alt et al. (1986) report successive stages of alteration within sea floor basalts to a depth of 400 metres in which a range of secondary mineralogies develop. Phyllosilicate phases which are found include both saponite (Mg rich smectite) and nontronite (Fe rich smectite). At depths greater than 500 metres there is sporadic chlorite. Alteration is attributed to repeated interaction with seawater derived solutions which are progressively modified as interaction proceeds.

Modelling of basalt-seawater interaction by Bowers and Taylor (1987) indicated that both temperature and reaction path progress (a measure of the degree of interaction) are important controls on the alteration mineralogy. At temperatures well below 200 °C, in the early stages of interaction, abundant smectites (eg. saponite and nontronite) form. As both temperature and reaction progress increase, then chlorite develops. Typically, temperatures range from 200 to 250 °C, whilst progress, measured in terms of grams basalt dissolved in 1 kg seawater, equals approximately 220g kg^{-1}.

Mottl (1983), in a review of experimental results of basalt-seawater interaction notes that a characteristic of the process is the complete removal of Mg^{2+} from seawater solutions at temperatures of approximately 150 °C. The net result of this process is the precipitation of Mg-smectites such as saponite. Cann (1979) and Thompson (1983) label basalts which undergo alteration at temperatures below approximately 100 °C as belonging to the Brownstone facies. Such basalts are characterised by the palagonitization of glass and partial replacement of igneous pre-cursors by smectites.

As alteration proceeds, then there is a fundamental change in the observed alteration mineralogy. Kristmannsdottir (1979) notes that for Icelandic basalts interlayering of smectite commences at approximately 200 °C, gradual transformation of chlorite occuring between 200-240 °C. Mixed-layer clays of chlorite and smectite are dominant within this temperature

range. Bettison and Schiffman (1988) note that this transition within the Point Sal Ophiolites roughly parallels the transition from prehnite-pumpellyite to prehnite-actinolite facies defined by Liou et al. (1987) on the basis of calc-silicate mineral assemblages. However, Cann (1979) suggests that the top of the zeolite facies is marked by the disappearance of all mixed layer phases.

Iijima (1978) noted the occurrence of a 14-15 Å mixed-layer phase, together with chlorite at temperatures as low as 100 °C (at depths of 1 700-3 500 metres) within marine volcaniclastics in Japan. Furthermore, Viereck (1982) following a study of alteration minerals within a tuff-basalt sequence on Iceland, described the occurrence of a Si-rich chlorite which was replaced by an Al-rich chlorite at temperatures significantly lower than 200 °C. When compared to basalt sequences these two studies indicate the importance of permeability on alteration mineralogy, supporting the evidence from experimental and modelling studies that reaction progress as well as temperature is also an important variable in determining obseved alteration mineralogy.

From the previous discussion it is now possible to consider the situation within the Clyde Lavas. It was earlier stated that mixed-layer clays are found throughout the lavas, both within and outside metadomains, whilst "pure" species occur only within. Furthermore, smectite, a product of early, low temperature alteration, documented in many studies, is absent. Therefore, it is unlikely that the phyllosilicate assemblages found within the Clyde Lavas were formed immediately after eruption of the lavas following interaction with cool surface waters. It is much more likely that they represent the products of a process of fluid-rock interaction which lead to the progressive transformation of an earlier smectite phase.

It is unlikely that the assemblages seen within the metadomains represent a very early metastable assemblage developed exclusively during burial. If this were the case the development of phyllosilicates with a uniform compositions might be expected both within and outside metasdomains owing to uniformity of fluid compositions during burial. This is not observed. Therefore, the inference is that metadomain development did not occur immediately following eruption but some time after, possibly contemporaneous with burial

metamorphism; the presence of "pure" species representing the acme of a transition through less ordered mixed-layer species ultimately leading to the formation of chlorite. Regular and random mixed-layer chlorite-smectites occur as intermediate products of the continuous transformation of smectite to chlorite. This change has been documented by several studies such as that by Iijima and Matsumoto (1982) and Curtis et al. (1985) for phyllosilicates within the sedimentary environment undergoing deep burial diagenesis.

Given that fluid temperatures within metadomains (deduced from fluid inclusion studies; see Chapter 5) do not differ radically from those outside as concluded by Evans (1987) then it is suggested that temperature may assume secondary importance in controlling development of alteration phases. This issue is further addressed in the following sections.

Kaolinite appears to have been the stable phyllosilicate phase within hydrothermal fluids present within the Campsie Glen metadomain. This suggests that the metadomain may represent a buried zone of acid alteration. Inflow of oxygenated water might oxidise any sulphide which was present leading to acidic conditions. However, there is abundant carbonate also present at this locality suggesting that low pH conditions did not exist. Alternatively, studies such as that by Browne and Ellis (1971) suggest that kaolinite is the stable phyllosilicate phase in situations where both Mg, Na and Ca concentrations are low in the hydrothermal fluid, such as the Ohaki-Broadlands geothermal field.

3.5. Compositional Variations in Phyllosilicates

Having established both the mineralogy and distribution of the main phases it now becomes necessary to characterise compositional variations within the phyllosilicates using wavelength dispersive microprobe analysis.

Samples were selected from Campsie Glen (NS 616 803) which provided a 400 metre section through the lavas. Care was taken to collect from a range of lava types in order to assess what influence rock compositions might exert on phyllosilicate chemistry. In addition, samples were taken from a metadomain locality within this section to assess what influence

metadomain fluids exerted on phyllosilicate chemistry; clearly X-ray diffraction analysis indicates that fundamental differences do exist.

Analyses were carried out using a JEOL JCXA-733 electron probe microanalyser. Approximately 100 analyses were performed on a total of 10 sections. Full experimental details together with results are given in Appendix 3.2.

There are several limitations to the above technique. All iron is recorded as ferrous, though Cathelineau and Nieva (1985) report that numerous studies indicate that the trivalent iron content in chlorites is less that 5 % of the total iron content. More serious is the possibility that minerals such as hematite become attached to clay plates leading to variations in Fe : Mg : Al ratios as reported by Curtis et. al. (1984). Furthermore, because of the fine grained and porous nature of the phyllosilicates it is often difficult to direct the beam (~1-2 μm in diameter) onto the grain to be analysed leading to interaction with, and contamination with adjacent grains. Given these difficulties it has proved possible to analyse a sufficient number of grains allowing for certain patterns to emerge. These are discussed below.

3.6 Chemical composition of the phyllosilicates

3.6.1 General characteristics

Phyllosilicate compositional data is expressed in Figure 3.4 and is given in terms of total iron against silicon following the classification of Hey (1954). Cationic values were calculated on the basis of 28 oxygens. The diagram also shows a range in phyllosilicate compositions recorded from other low grade metabasites together with an independent set of data from the Clyde Lavas obtained by Evans (1987)

Clearly most interlayered phyllosilicates fall within the pycnochlorite and diabantite field, whilst chlorite plots within the ripidolite field. This of course does not imply that these names should be applied to the Clyde Lava mixed-layer phyllosilicates. Chlorites from a range of studies also plot within this field (see diagram for details), though they are generally

depleted in iron relative to samples from the Clyde Lavas.

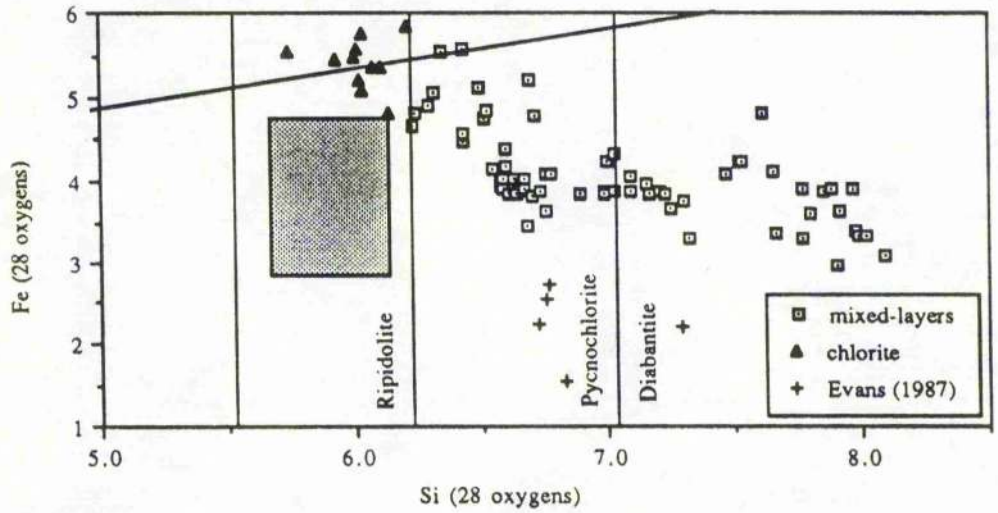

Figure 3.4 Compositional variation in phyllosilicates expressed in terms of Fe vs. Si after Hey (1954). Also shown (stippled region) are ranges in phyllosilicate compositions from studies by Evarts and Schiffman (1983) and Bevins and Merriman (1988)

Furthermore, there is an overall weak negative correlation between silica and iron, chlorites tending to be enriched in the latter element. Velde (1977) has demonstrated that during co-formation of mixed-layer chlorite/smectite and chlorite that Mg is preferentially incorporated into the former phase whilst the reverse has shown to be true for Fe.

Mafic phyllosilicates from other low temperature, low pressure, hydrothermal environments document the transition from interlayer species to discrete chlorite as occurring within the range of 6.25-5.95 cations per 28 oxygens (eg. Bettison and Schiffman, 1988). Reference to Figure 3.4 indicates that the transition occurs at approximately 6.2 Si cations for the Clyde Lava phyllosilicates. Evans (1987) noted a trend of decreasing iron content with increased metamorphic grade for phyllosilicates collected from analcime, heulandite and stilbite zones, attributing this to a decreased Fe availability with depth.

Calcium contents of chlorites are consistently below 0.1 cations per 28 oxygens, as this phase can accommodate only a limited amount of Ca into its structure. Bettison and Schiffman (1988) confirm, using X-ray diffraction analysis, that phases with greater than 0.1 cations / 28 oxygens contain a discrete smectite component. Mixed-layer species show a wide

range in calcium content (.01-.29 cations per 28 oxygens).

If it is assumed that the regularly interlayered phase is 1:1 chlorite-smectite then structural formula should ideally be calculated on the basis of 1/2 unit cell chlorite + 1/2 unit cell smectite. In this case the total octahedral cations should be 9 if both chlorite and smectite are trioctahedral, or 7.5 if one of the layers is dioctahedral. As an example, the total octahedral cations in sample CG 7 is 9.22, which approximates to the ideal 9. Therefore, both the chlorite and smectite layers are nearly trioctahedral. The smectite component is therefore most likely to be saponite. This may account for the Mg rich nature of certain samples.

Finally, it is noted that there is a much greater range of data for the interlayer species relative to chlorite. Furthermore, within-grain variations in composition are greater for the mixed-layer phases. Bevins and Merriman (1988) suggest that uniformity of compositions within the area of a single thin section indicates an approach towards equilibrium. On the basis of the evidence cited here it is suggested that chlorite represents an approach towards equilibrium, promoting the transition from less ordered mixed-layer species through to ordered chlorite. Since the transition is seen to occur only within metadomains temperature may not be the dominant factor controlling phyllosilicate evolution since fluid inclusion evidence (see Chapter 5) indicates that temperatures within and outside metadomains are not significantly different.

3.6.2. Temperature-composition relationships

Cathelineau and Nieva (1985) following a study of hydrothermal chlorites conclude that tetrahedral charge is positively correlated with estimated formation temperatures, whilst for the octahedral vacancy (VAC = (6 - Al^{VI} - (Mg^{VI} + Fe^{VI}) based on half structural formula) the reverse is true. Subsequent studies, such as that by Jahren and Aagaard (1989) show that this is the case. Figure 3.5 presents the change in these two paramaters with depth within the lava pile. It can be seen that there is no systematic depth related change in

composition.

Therefore, it appears that there was an insufficient vertical temperature differential through approximately 400 metres of lava to bring about any systematic change in aluminium site occupancy. However, it is noteworthy that phyllosilicates from the metadomain locality are characterised by high Al^{VI} and low to intermediate VAC values suggesting that temperatures within these localities were higher. Table 4.2 presents a correlation matrix for the whole data set showing the interrelationships between the principal cations within the phyllosilicates.

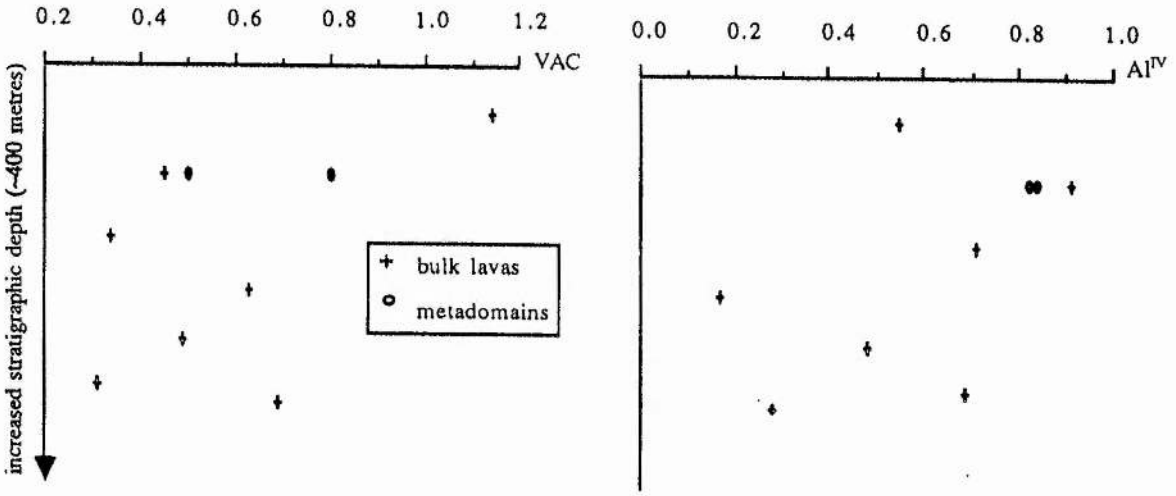

Figure 3.5. Variation in mean octahedral vacancy and tetrahedral aluminium with depth for phyllosilicates from Campsie Glen

	Al^{IV}	Al^{VI}	Fe^{VI}	Mg^{VI}	VAC
Si^{IV}	-0.97(-1.00)	0.38 (0.31)	-0.73(-0.64)	-0.15(0.01)	0.76(0.81)
Al^{IV}		-0.39(-0.31)	0.70(0.64)	0.17(-0.01)	-0.76(-0.81)
Al^{VI}			0.17(-0.31)	-0.8(-0.68)	-0.74(0.8)
Fe^{VI}				0.26(-0.46)	-0.48(-0.48)
Mg^{VI}					-0.64(-0.41)

Table 4.2. Correlation matrix (values are expressed as Pearson's r) of the major chemical variables within the Clyde Lava Phyllosilicates

(numbers in brackets refer to data obtained by Cathelineau and Nieva (1985), for chlorites from the Los Azufres geothermal system)

There are several points which emerge from the above table:

1. Al^{IV} is negatively correlated with Si^{4+} and the octahedral vacancy. There is also a strong positive correlation with Fe^{VI}.

2. The octahedral vacancy is strongly correlated with Si^{4+} and Al^{VI}.

3. There is almost no correlation between Mg^{VI} and Fe^{VI}.

In other words, "evolved" phyllosilicates are characterised by high Al^{IV}, Fe^{VI}, low Si^{4+}, Mg^{VI} and Al^{VI}. Also, analysis of Table 4.1 shows that phyllosilicates (chlorites) from the metadomain locality are characterised by high Al^{IV}, low Mg^{VI}, Al^{VI}, Si^{4+} and CaO, ie. they possess most of the features characteristic of evolved phyllosilicates.

Figure 3.6 is a plot of Al^{IV} against VAC for all phyllosilicates from Campsie Glen. Also shown on this diagram is a line derived from Cathelineau and Nieva (1985) showing estimated formation temperatures, based on variations in Al^{IV} content and octahedral site occupancy. It is immediately apparent that there is a large scatter of data points throughout the phyllosilicate population, some (including metadomain chlorites) showing higher

octahedral vacancy values than expected. The reverse was found to be the case for sedimentary chlorites in the study of Jahren and Aagaard (1989). Chlorites appear to have formed at approximately 170-220 °C, though there is a degree of overlap with some mixed layers.

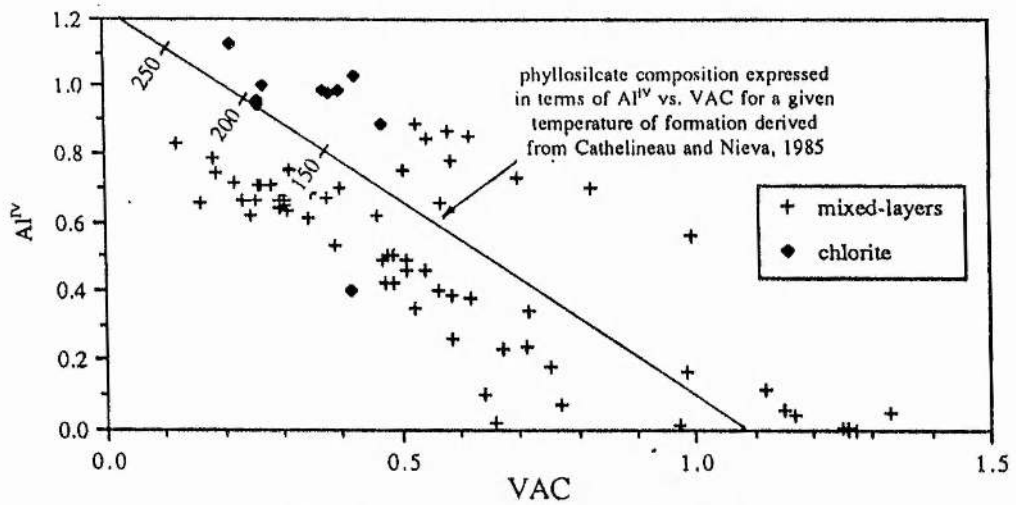

Figure 3.6. Tetrahedral aluminium vs. octahedral vacancy for phyllosilcates from Campsie Glen

This would place alteration in the upper zeolite facies, consistent with the work of Evans (1987). Kristmannsdottir (1979) records the transition from a phyllosilicate assemblage dominated by mixed-layer species to one which in chlorite is quantitatively important as occurring at between 200-240 °C within Icelandic basalts. This is also marked by the formation of wairakite at the expense of other zeolites and sporadic appearance of epidote. These features have been recorded within the Clyde metadomain localities (see Chapter 2).

The above analysis suggests that temperatures within the metadomains were significantly higher than those outside. This has important consequences; if metadomain development was contemporaneous with burial metamorphism, as was suggested in section 3.4, why was there a contrast in estimated fluid temperatures? It was earlier implied that temperature assumed a secondary role in controlling phyllosilicate paragenesis. This requires further consideration.

It was indicated in previous chapters that metadomains owe their existence and distribution because of permeability contrasts within the lava pile. They developed as alteration fluids exploited high permeability pathways inherited from primary volcanological features such as flow horizons. Heat loss by the fluid to its surroundings might be low in these high flow zones; in certain instances, as the fluid rises, it would expand and boil adiabatically; boiling is recorded within some fluid inclusion populations from metadomains north of the Clyde (see Chapter 5). Within the bulk of the lavas permeabilities are relatively low, fluid flow is reduced, and as a consequence the fluid loses heat to its surroundings and cools. Therefore, fluid temperature might have a bearing on phyllosilicate composition. More importantly, contrasts in fluid temperatures might be controlled by permeability contrasts within the basalts.

3.6.3. The influence of basalt chemistry on phyllosilicate compositions

In order to address whether whole rock chemistry has any influence on phyllosilicate composition, XRF analysis was performed on lava samples for which microprobe data was available. The details of XRF analysis are given in Chapter 4. Table 4.3 presents correlation coefficients determined by comparing mean phyllosilicate compositions with whole rock chemical analyses for several major oxides (SiO_2, Al_2O_3, total iron, MgO, CaO, and Na_2O).

Oxide	Pearson's r
SiO_2	0.57
Al_2O_3	-0.37
Total Fe	0.89
MgO	0.53
CaO	0.72
Na_2O	-0.37

Table 4.3. Relationships between major oxide compositions for whole rock and phyllosilicates within lavas from Campsie Glen

There is a poor correlation for Al_2O_3 and Na_2O; for SiO_2 and MgO the correlation is moderate, but is stronger for CaO and total iron. Cathelineau and Nieva (1985) established that a strong positive correlation exists between iron and magnesium in hydrothermal chlorites and their host rocks. Bevins and Merriman (1988) also noted this relationship within metadolerites metamorphosed to prehnite-pumpellyite facies. However, in this study the relationship is not so simple since magnesium shows only a weak correlation whilst for iron the correlation is very strong.

It appears that the composition of the phyllosilicates is controlled by the host rock in terms of CaO, FeO and, to a lesser extent MgO. This in turn suggests that the composition of the hydrothermal fluid is controlled locally by the host basalt. This has been found to be the case both within the geothermal environment (Cathelineau and Nieva,1985) and within the deep diagenetic environment (Jahren and Aagaard, 1989). The latter authors suggest that, in general, chlorites within such environments are in equilibrium with fluids possessing very low Fe (II) concentrations, the chlorites attempting to scavenge all available Fe (II). The presence of hematite within these lavas suggests that oxygen fugacity was high. This is further

supported by the observation that the smectite component within the clays is likely to be saponite. A possible explanation for the relatively poor correlation coefficient obtained for Mg may reflect competition from other Mg rich alteration phases forming within the lavas concurrently with the phyllosilicates. For example, locally there is widespread development of carbonates; MacDonald (1973) identifies ankerite as being quantitatively important.

3.7 Conclusions

1. A range of phyllosilicates, developed during hydrothermal alteration of the Clyde Lavas has been identified. They are similar to those reported throughout a range of low grade metamorphic and hydrothermal environments where basic igneous rocks are present. Their widespread distribution within the lavas testifies to the pervasive nature of the metamorphic / hydrothermal event. Compositional data suggests that fluid temperatures reached a maximum of approximately 220 °C. This estimate is consistent with the study made by Evans (1987) based on silicate paragenesis.

2. The distribution and composition of the phyllosilicates is controlled indirectly by permeability variations within the lavas. This is demonstrated in high permeability metadomains which are characterised by more evolved phyllosilicate assemblages.

3. It is concluded that the phyllosilicates observed within the lavas represent an overall evolutionary sequence as early formed material partially equilibrated, to differing degrees, to changes in external conditions as development of the lava pile proceeded.

CHAPTER 4 WHOLE ROCK GEOCHEMISTRY

4.1 Introduction

The development of hydrous phases (eg. analcime) within the metadomains as discussed in Chapter 2 requires that the basalts have interacted with a hydrothermal fluid. Such a process is likely to have a profound effect on the bulk chemical composition of the basalts as decomposition of primary phases and precipitation of secondary phases will lead to a redistribution of elements within the basalts. Such processes are reported in a number of classical studies within a range of basaltic lavas which were subject to periods of low grade metamorphism and hydrothermal interaction (eg. Wood et al., 1976, Cann, 1979, Seyfried and Bishcoff, 1977).

The following study has several aims:

1. To establish which elements have behaved conservatively and which have behaved in a mobile manor during metadomain activity.
2. To quantify elemental fluxes during metadomain activity.
3. To establish any relationships between elemental behaviour and hydrothermal fluid conditions.

2.1 Methodology

2.1.1 Recognition of element mobility

Several studies (eg. Pearce and Cann, 1973, Wood et al., 1976, Winchester and Floyd, 1977) indicate that certain trace elements (eg. Y, Zr, Ti) remain immobile during the weathering, diagenesis and low grade metamorphism of basaltic lavas. However, more recent studies such as those by Walsh (1983) and Luc et al.(1989) have clearly demonstrated that this is not always the case. Walsh (1983) suggests that normally immobile elements such Ti,

Hf, Sc and REE are susceptible to significant degrees of post-crystallisation mobility in the presence of a CO_2 rich vapour phase via formation of carbonate complexes. Also, Luc et al. (1989) demonstrate enrichment in Ti, Zr, Ni, Co, Zn, Y, Nb, Hf and REE within Proterozoic metabasites which have undergone both laterisation and later granulite facies metamorphism. Therefore, it is necessary to establish the extent to which trace elements have behaved conservatively during the alteration of the Clyde Lavas. In order to assess elemental behaviour during metadomain activity major and trace element compositions have been determined for selected samples using Philips PW 1450/20 and PW 1212 sequential spectrometers. Samples were selected from three metadomain localities at Boyleston Quarry, Langbank Cutting and Campsie Glen, the purpose being to collect material which was representative of both the individual metadomain and the local host basalt. Details of sample locations are given in Appendix 2.1 whilst chemical analysis are reported in Appendix 4.1. Also, data from Evans (1987) has been incorporated which includes basalts collected from burial metamorphic zones within the Clyde Lavas. Unfortunately, the precise location of these samples was not given.

Figure 4.1 (a) is a binary plot of Y against Zr for samples taken from the Clyde Lavas using data obtained during this study and also that of Evans (1987). It can be seen that this data set defines a broad linear array which projects towards the origin indicating that elemental ratios are preserved even though absolute concentrations may have changed. Pearsons's r for this data set is +0.97 indicating coherence. Coherence between elemental pairs such as Y and Zr is normally taken to indicate that these elements remain relatively immobile during low grade metamorphism (Pearce and Cann, 1973). This is supported by chemical analyses of hydrothermal fluids reported by Cann (1979) which show that such fluids have characteristically low concentrations of elements such as Zr, Nb, Ta etc. The exact position of points on this diagram is a function of:

1. Initial elemental concentrations prior to alteration of the basalts.
2. Dilution or concentration effects due to addition or subtraction of other components during alteration.
3. Machine accuracy and precision (quoted in Appendix 4.1).

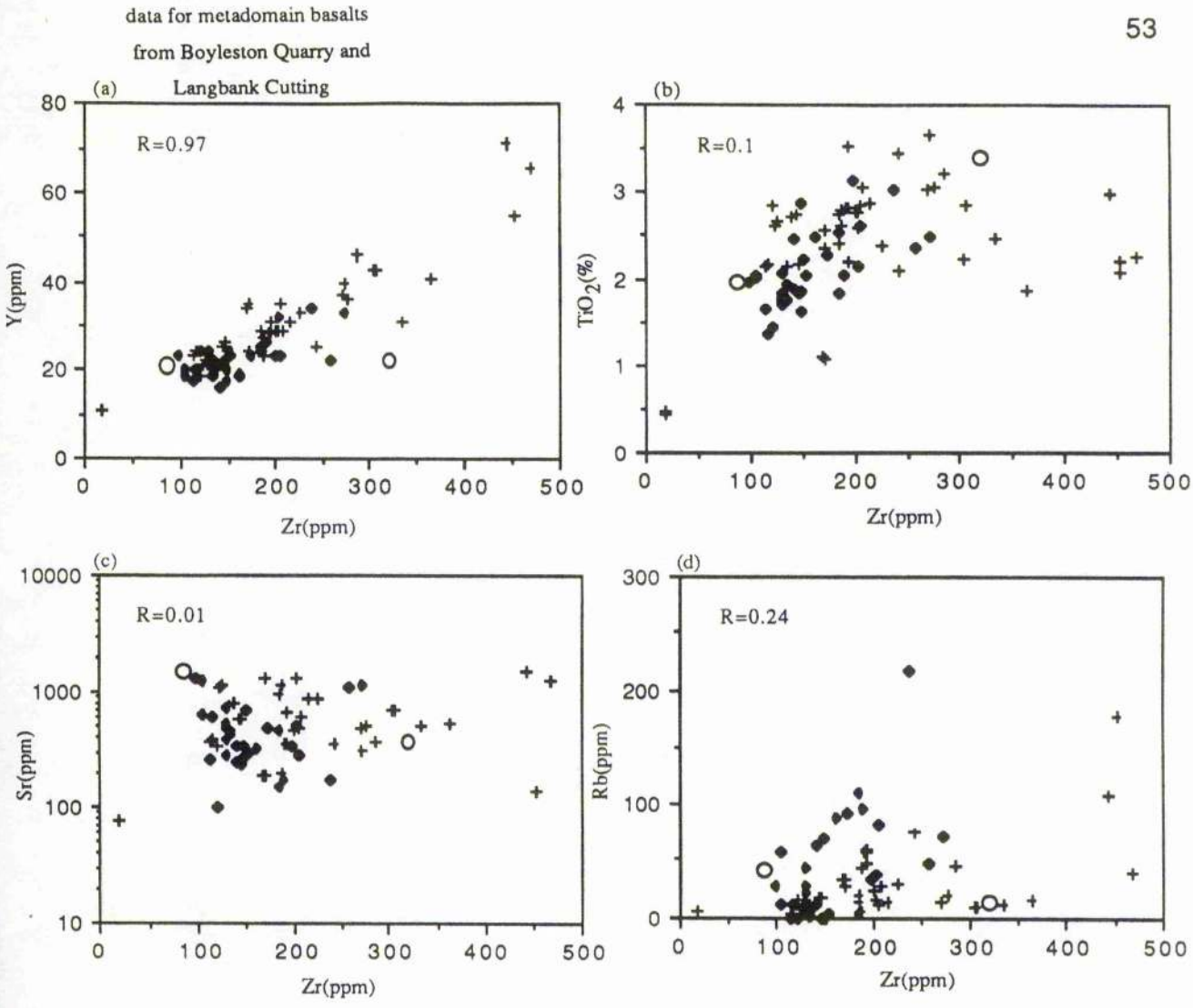

Figure 4.1 Binary diagrams showing variation in Y,Ti,Sr and Rb against Zr. Values for Pearson's r are given. Crosses are from Evans (1987), diamonds are for metadomain material, circles are for material collected outside of metadomain areas.

Figures 4.1(b), 4.1(c) and 4.1(d) are binary plots of Ti against Zr, Sr against Zr and Rb against Zr respectively. The scatter shown by both Sr and Rb, and to a lesser extent Ti is thought to be due to these elements being mobile during alteration. Also, it can be seen that there is significant enrichment in both Sr and Rb; Pearce (1982) reports mean values of Sr = 428 ppm and Rb = 23 ppm for calc-alkali basalts. Thompson (1983) notes that during the

oxidation and hydration of basalts following seawater interaction there is ubiquitous uptake of Rb and Sr. Also Wood et al. (1976) noted that Icelandic basalts within higher grade zeolite zones were enriched in Sr thought to be supplied by seawater.

Given that Zr and Y appear to have behaved conservatively during alteration it is possible to assess the behavour of selected major elements by plotting either one of these trace elements (arbitrarily Zr) against the major element in question. This approach is shown in Figure 4.2 which also gives values of Pearson's r for each pair. It can be seen that all of the major elements selected (Si, Al, Fe^{3+}, Mn, Mg, Ca, Na and K) show broad scatters with no clearly defined trends observable suggesting that all have been mobile during alteration. A knowledge of the composition of the initial and final states is not enough in itself to calculate elemental flux into or out of the system ie. it is not sufficient to quantify changes in basalt chemistry as being equal to the differences in major oxide weight percents. This approach assumes that the overall volume of the rock has remained constant during the hydrothermal episode.

Preservation of primary igneous textures within basalts from metadomains (see Chapter 2) argues for constant volume during alteration. However, Cann (1979) demonstrated that if serpentinisation of peridotites occurred without volume change the quantities of water involved were orders of magnitude greater than that necessary for the formation of the serpentine minerals themselves. This was despite good textural evidence for the constant volume assumption. Widespread hydrofracturing of basalt within the metadomains from the Clyde Lavas suggests that a volume change accompanying alteration may have occurred. Also, reactions which may have been occurring during metadomain activity of the type

$$NaAlSi_3O_8 + H_2O = NaAlSi_2O_6.\ H_2O + SiO_2$$

(albite + water = analcime + silica)

have large positve volume changes for the forward reaction (Thompson, 1971). Many metasomatic processes involve large positive volume changes. For example, serpentisation of oceanic crust by seawater can involve volume increases of up to 40% (Cann, 1979) whilst Whitford et al. (1986) reports a net volume expansion of 50% within volcanogenic sulphide

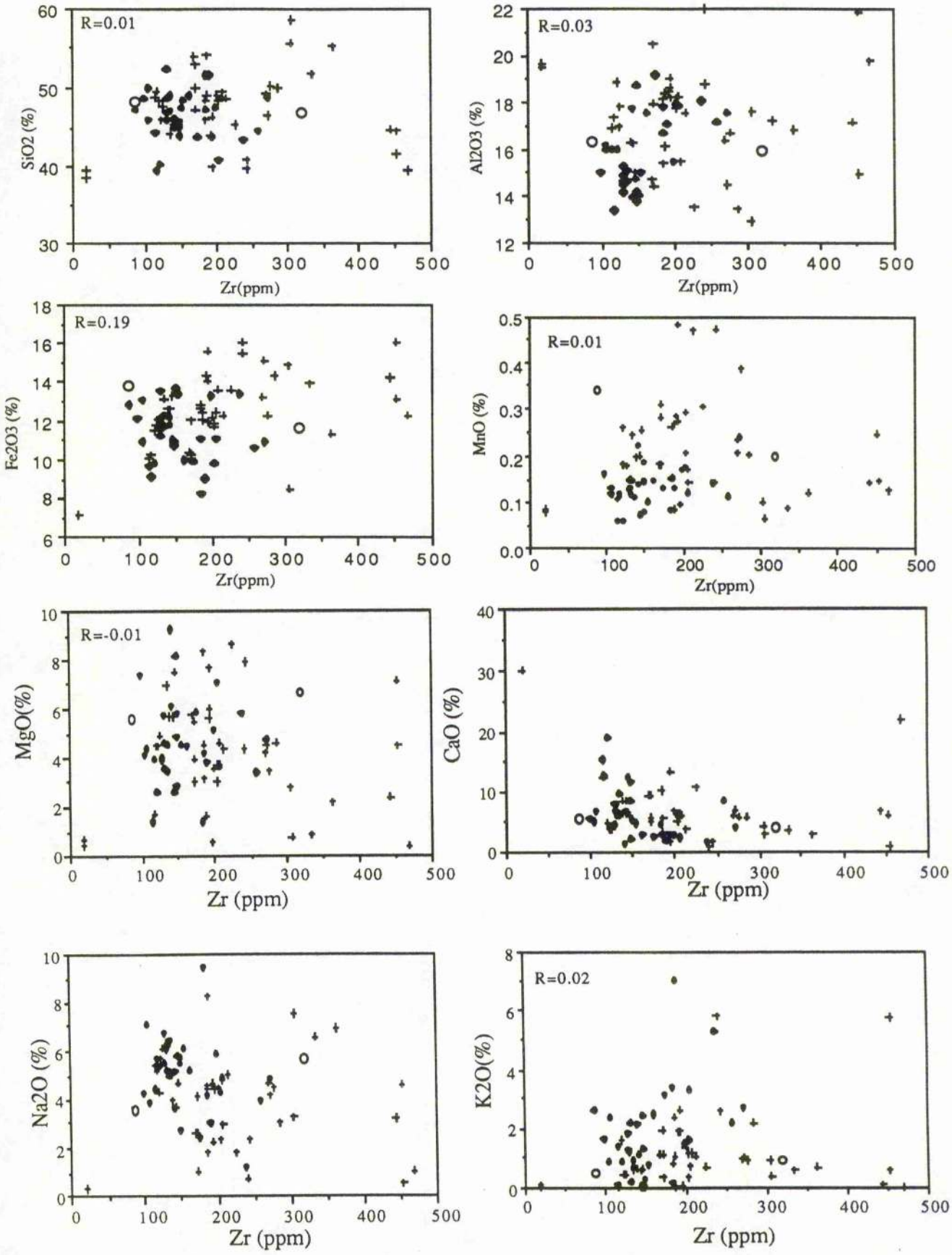

Figure 4.2 Variation in major oxide contents against Zr (ornament as for Figure 4.1)

deposits in Tasmania. Therfore, the preservation of igneous textures alone is insufficient to justify constant volume during alteration.

2.1.2 Modelling metasomatic processes; the isocon diagram

Grant (1986) provides a simple graphical method which allows for solution of equations for mass or volume changes during metasomatic processes, after Gresens (1966). The basis of Gresens arguement is that some components remain immobile during the alteration process, and if they can be identified, they can be used to establish any volume change which has taken place. Relative gains and losses of other components can then be calculated assuming that the volume change is a factor common to the behaviour of all components. That is, the alteration is pervasive which is justified in the case of the Clyde Lava metadomains based upon thin section evidence presented in Chapter 2.

In order to determine relative gains and losses of constituents during alteration, representative samples of basalt both outside and within the metadomains are selected. Analyses are then compared to one another for each individual locality by using the "isocon method" devised by Grant (1986). This technique provides a simple, direct means of determining changes in mass, volume and concentration within equivalent units during metadomain alteration. It should be borne in mind that samples of basalt taken from outside the metadomain will be, in fact altered, since they have been subject to both early and burial metamorphism (Evans, 1987). However, since we are concerned only with changes accompanying metadomain alteration, this approach is justified. The technique involves the establishment of a reference line corresponding to zero concentration change which is termed an isocon. The isocon then represents a graphical solution to Gresens equation (1966) for zero concentration change. The isocon may be established on the immobility of one component (eg. Zr), a group of components, or upon constancy of volume or mass. Once the isocon is established then the determination of any chemical gains or losses relative to the concentration of the precursor lithology can be readily determined graphically by the amount of

displacement away from the reference isocon.

Grant (1986) provides a series of equations which can be used to define the isocon as follows:

1. If constant volume is assumed during alteration

$$C^A = (\rho^O / \rho^A)C^O$$

where C^A = elemental concentration after alteration

" C^O = elemental concentration prior to alteration

" ρ^O and ρ^A = bulk densities before and after alteration respectively.

2. If constant mass is assumed during alteration

$$C^A = C^O$$

In the general case (M^A/M^O) is determined from the best fit isocon where M = mass of sample.

For a given element (eg Zr) whose mass does not change during alteration the equation of the isocon is given as

$C^A = (C^A_{Zr}/C^O_{Zr})C^O$

where C^O_{Zr} and C^A_{Zr} represent the concentration of Zr prior to, and after alteration.

4.3 Results

Mean chemical compositions for selected elements are presented in Table 4.1 for metadomain localities at Boyleston Quarry, Langbank Cutting and Campsie Glen as discussed in Chapter 1. Full sample details are given in Appendix 4.1.

	Boyleston Quarry		**Langbank Cutting**		**Campsie Glen**	
Element	Basalt outside metadomain	Metadomain basalt	Basalt outside metadomain	Metadomain basalt	Basalt outside metadomain	Metadomain basalt
	n=1	n=19	n=1	n=13	n=1	n=3
SiO_2	48.2	46.7	46.8	46.5	46.9	47.5
TiO_2	1.97	1.83	3.41	2.48	3.08	2.68

	Boyleston Quarry		Langbank Cutting		Campsie Glen	
Al_2O_3	16.29	14.80	15.94	17.56	15.72	13.92
Fe_2O_3	13.82	11.63	11.64	10.38	15.74	15.70
MnO	0.34	0.12	0.20	0.15	0.13	0.16
MgO	5.55	4.23	6.69	5.15	1.89	2.42
CaO	5.58	8.59	4.19	3.39	5.59	5.24
Na_2O	3.6	5.6	5.7	4.3	3.5	1.2
K_2O	0.5	1.0	0.9	2.9	0.4	1.0
P_2O_3	0.28	0.29	0.62	0.37	0.54	0.4
F.Loss	3.6	5.2	4.8	6.2	4.6	9.06
Tot.	99.73	99.99	100.95	99.83	98.49	99.28
Sr	1510	477	103	99	447	50
Rb	42	12	14	80	9	20
Cu	5	69	n.d.	n.d.	n.d.	n.d.
Zn	80	75	283	215	53	65
Y	21	21	22	25	30	29
Zr	87	126	319	194	243	222
Bulk * density (kgm^{-3})	2 940	2 460	2 740	2 440	2 840	2 460

Table 4.1 Mean chemical analysis of selected elements from basalts of the Clyde Lavas

(major elements in oxide weight percents, trace elements in ppm)

* Bulk densities were determined using a Jolly Balance as described by Battey (1981). This method involves the use of solid blocks of basalt. During sampling, care was taken to ensure that the material collected provided a realistic a view of the metadomain as possible. Therefore, samples which were veined with characteristic metadomain material were also included within the study. However, care was taken to ensure that amygdaloidal material containing voids was excluded.

Isocon diagrams for the three localities are presented in Figure 4.3. These are prepared by plotting the weight percent of major oxides and pertinent trace elements (in ppm), of the

metadomains to be examined.

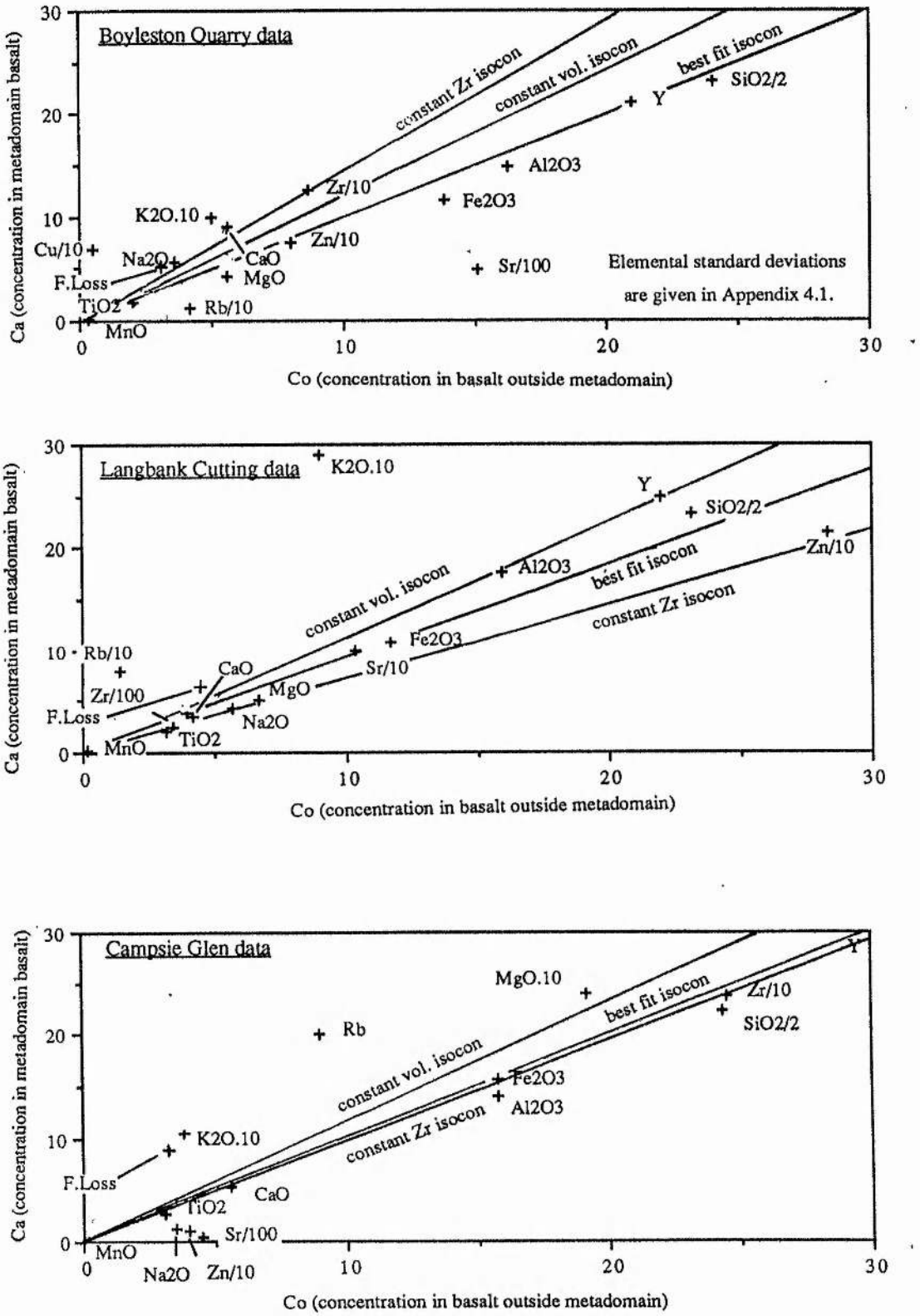

Figure 4.3 Isocon diagrams for metadomains within the Clyde Lavas (major oxides in wt. %, trace elements in ppm)

In these diagrams the data are scaled for ease of reading, thus SiO_2 is presented as 0.5 SiO_2 etc. Grant (1986) shows this approach to be mathematically valid. Isocons for constant mass, volume and Zr are then generated and compared to the isocon which best fits the plotted major oxides as determined by least squares analysis. Choice of this reference isocon then fixes the compositional, mass and volume changes to be interpreted from each data set. Those elements which plot below the reference isocon are interpreted as having been lost to the hydrothermal fluid, and those which lie above are interpreted as having been gained by the basalt. Table 4.2 lists the volume change for each locality and the fractional gain and loss of each component relative to the amount in the original rock (Grant, 1986). Clearly, those elements showing only minor losses or gains generally approximate the reference isocon. From the table the following points emerge:

1. All the major oxides, except Fe_2O_3, Al_2O_3 and SiO_2 exhibit substantial changes in concentration during metadomain alteration. Only TiO_2 (an element normally considered to be immobile) exhibits systematic loss at all three localities.

Element	Boyleston Quarry	Langbank Cutting	Campsie Glen
SiO_2	-0.03	0.12	-0.03
TiO_2	-0.06	-0.19	-0.10
Al_2O_3	-0.07	0.22	-0.10
Fe_2O_3	-0.08	0.00	0.04
MnO	-0.68	-0.25	0.23
MgO	-0.12	-0.16	0.30
CaO	0.50	-0.10	-0.07
Na_2O	0.51	-0.15	-0.66
K_2O	1.05	1.75	1.50
F.Loss	0.30	0.28	1.10
Sr	-0.66	0.28	-0.81
Rb	-1.91	7.80	1.23
Cu	2.74	n.d.	n.d.
Zn	-0.06	-0.20	0.23

Element	Boyleston Quarry	Langbank Cutting	Campsie Glen
Y	0.12	0.25	0.00
Zr	0.55	-0.10	-0.03
Mass	0.03	0.11	0.05
Volume	0.22	0.20	0.16

Table 4.2 Concentration, mass and volume changes expressed in percent for metadomains within the Clyde Lavas

2. The alkali metal oxides exhibit significant mobility, showing both gains and loss from metadomain localities. It is noteworthy that Na_2O is uptaken within metadomains at Boyleston Quarry whilst it is lost from metadomain basalts at other localities. A mineralogical expression of this may be the widespread development of analcime at the former locality.

3. Sr, Rb and Cu exhibit extreme mobility. It is noteworthy that K and Rb, which are geochemically similar, show extreme mobility. Y and Zr also exhibit a degree of mobility.

4. In all cases there is a significant increase in the total volatile content (F.Loss) accompanying alteration.

5. Alteration is always accompanied by small,non systematic changes in mass and more significant increases in volume.

2.3 Discussion

2.3.1. Choice of reference isocon

It can be seen in Figure 4.3 that the major oxides which are used to define the reference isocon such as Al_2O_3, Fe_2O_3, SiO_2, TiO_2 etc. form a broad linear array which trends towards the origin. Grant (1986) suggests that the elements forming such an array may be considered to be immobile and thus used to define the isocon. This may mean that there has

been little mass transfer of components used to define the isocon or that the concentration of one component relative to that of another has not changed, ie. they have not decoupled geochemically. For the case of elements such as K and Rb which are geochemically similar and as such are likely to have been mobilised together then their potential for defining an isocon is limited. However, the elements cited above are geochemically dissimilar and therefore are unlikely to have been mobilised simultaneously and can be used to define the isocon.

Earlier in this chapter it was suggested that both Zr and Y were immobile based on the observation that they formed a well defined linear array when compared upon a binary plot. It can be seen from Figure 4.3 (a) that at Boyleston Quarry, if Zr were used to define the reference isocon then there would be a loss of all elements excluding K and Rb. Also, this would be accompanied by a decrease in the volatile content of the metadomain basalt together with large decreases in both mass and volume. Several lines of geological evidence suggest that this is unlikely. For example, the development of hydrous and volatile rich phases within metadomains (eg, prehnite, analcime, calcite etc.) would necessitate the influx of volatiles. Also, it seems unlikely that the development of large quantities of analcime within metadomains at Boyleston Quarry could have occurred without influx of Na. Therefore, the earlier conclusion that elements such as Zr and Y are immobile requires clarification. The linear array of data points observed on a binary plot of Zr against Y, as shown on Figure 4.1 (a) indicates that these elements do not decouple geochemically during metadomain alteration ie.the ratio Y/Zr remains fixed. However, the absolute concentration of these elements within the metadomain basalts may change due to dilution or concentration of other components during the alteration process.

2.3.2. Implications for fluid-rock interaction

Mottl (1983), in a review of hydrothermal processes at seafloor spreading centres notes that as reaction between basalt and seawater proceeds there is a tendency for the hydrothermal

solution to approach equilibrium with the secondary phases which precipitate. The extent to which equilibrium is approached is a function of;

a) the reaction rates for dissolution of primary phases and precipitation of secondary phases, and

b) the flow rate of the solution through the rock.

This also applies to the chemical species which participate with the dissolution / precipitation reactions.

Mottl (1983) and Thompson (1983) note that the most characteristic feature of basalt-seawater interaction at elevated temperatures (ie. those greater than 150 °C) is the rapid removal of Mg^{2+} from the hydrothermal solution into the rock; at water-rock ratios up to 50 basalt has the capacity to remove all Mg from the fluid. This is manifest as high Mg ocean floor metabasalts containing Mg bearing alteration phases. In the case of the Clyde Lavas it is apparent from Table 4.2 that Mg concentrations have changed significantly during metadomain activity. Although Mg has clearly been mobilised there has been both loss and gain of this element by the basalt. As Bowers and Taylor (1987) point out metabasites which are enriched in Mg typically contain chlorite. Therefore, it might be expected that the metadomain basalts which are depleted in Mg might not contain chlorite. However, it has been demonstrated in Chapter 3 that chlorite occurs within all of the metadomains examined. One possible explanation for the variable behaviour may be that the invading hydrothermal solution was undersaturated with respect to Mg. Data from Thompson (1983) shows that seawater is enriched in Mg with respect to intracontinental waters (by up to three orders of magnitude). This would suggest that the hydrothermal fluid present during metadomain development was unlikely to have been wholly seawater.

It has been shown earlier that all of the major oxides excluding SiO_2 and Fe_2O_3 exhibit varying changes in concentration. In an extensive review of low temperature (less than 150 °C) alteration of oceanic basalts Mottl (1983) notes that oxidation and hydration is ubiquitous. This stage is characterised by uptake of K and Rb and is accompanied by loss of Ca, Si and Mg from the basalt. At temperatures greater than 150 °C, Thompson demonstrates that there

is loss of Si, Ca, K, Mn, Sr, Rb, Cu and Zn from rocks of basaltic composition but gain of H_2O with Mg replacing Ca on a 1:1 molar basis. Metadomain development within the Clyde Lavas is characterised by large increases in the Rb and K content of the basalts which is a characteristic of lower temperature alteration. However, it has been shown that the behaviour of Mg within the metadomain basalts is variable (ie. there is both loss and gain) possibly indicating that hydrothermal fluid temperatures have varied around 150 °C during metadomain activity.

Mottl (1983) notes that the heavy metals Fe, Mn, Zn and Cu are leached from the basalt into solution during basalt-seawater interaction, their concentrations being controlled by the combined effects of temperature, pressure and pH. Clearly, the large changes in the concentration of Mn, Zn and Cu between metadomain basalt and protolith observed within the Clyde Lavas testifies to their mobility. Seyfried and Mottl (1982) demonstrated that at water-rock ratios greater than 50 then these three elements are almost completely leached from the basalt. Concentrations of these elements both within and outside the metadomains are sufficiently high to suggest that water-rock ratios were well below this value.

Finally, studies of ocean floor alteration, including that of Thompson (1983) show that the major stages of chemical fluxing within basalts occurs within 10 million years of their formation with palagonite formation and phylloslicate development occurring within the first 3 million years.

4.4 Conclusions

1. Using binary diagrams it has been possible to determine elemental mobility during metadomain activity. Elemental pairs which behave conservatively, i.e.those elements which do not decouple geochemically during metadomain alteration form linear arrays on such plots. The linear array of data points observed on a binary plot of Zr against Y indicates conservative behaviour. However, the absolute concentration of these elements within the metadomain basalts may change due to removal or addition of other components during the

alteration process. Plots of Zr against major oxides (Si, Ti, Al, Fe^{3+}, Mn, Mg, Ca, Na and K) show variable degrees of scatter indicating mobility of these elements during metadomain activity.

2. Using the isocon method of Grant (1986) it has been possible to assess the geochemical changes accompanying metadomain activity. In all cases this stage is characterised by small increases in mass and more significant increases in volume. Also, there is always an increase in volatile content (F.Loss). All of the major oxides, except Fe_2O_3 and SiO_2 exhibit substantial changes in concentration during metadomain alteration with the alkali metal oxides showing both gain and loss from metadomain localities. Sr, Rb and Cu and Zn exhibit extreme mobility. It is noteworthy that Rb and K, which are geochemically similar, show extreme mobility.

3. Previous studies of geochemical changes accompanying basalt-seawater interaction show that there is significant elemental mobility during this process. At temperatures above 150 °C gain of Mg is the most characteristic feature of this process. However, at only one locality within the Clyde Lavas does this appear to have occurred. Also, metadomain development is often characterised by large increases in the Rb and K content of the basalts, a characteristic of lower temperature (less than 150 °C) alteration. This suggests that fluid temperatures have varied about 150 °C during metadomain activity.

CHAPTER 5 FLUID INCLUSION ANALYSIS

5.1 Introduction

Fluid inclusion studies provide a way of obtaining a relatively large amount of quantitative and semi-quantitative information regarding the physiochemical state of the fluids present during metadomain development. For the purpose of this study calcite and analcime were selected for study, primarily because they are quantitatively the most important alteration phases. Also, it has been established (see Chapter 2) that analcite is formed prior to calcite within the metadomains. Therefore, the potential exists to assess how the alteration fluids may have evolved during metadomain development. Wafers were made for prehnite rich areas, though no fluid inclusions were found within this mineral, in contrast to the study of Evans (1987).

To complement the study, bulk fluid extraction analysis has also been made in order to measure the actual concentrations and relative proportions of phases present in the alteration fluids. Immediately below, there is a discussion of the methodology followed by a presentation of results from the metadomain localities.

5.2 Methodology

1. Equipment

Microthermometric analysis was carried out on 50-100μm doubly polished wafers using a Linkham TH600 heating/freezing stage. This consists of a temperature controlled chamber designed to operate between -180 to 600 °C at a maximum resolution of 0.1 °C. Shepherd et al. (1985) report accuracies of +/- 0.05 °C below 0 °C, and +/-0.5 °C above 100 °C. Accurate calibration was achieved using high purity organic compounds of known melting point. Heating rates were variable, generally less than 10 °C $min.^{-1}$, though these were reduced to approximately 1 °C $min.^{-1}$ near phase transformations. Finally, all measurements were

repeated in order to ensure precision.

2. Post-entrapment modification

It is important to assess the extent to which inclusions may have changed following their original entrapment within a mineral grain. Failure to do so may result in incorrect interpretation of results. These changes can occur either isochemically, in which case the process is termed necking down, or with loss (or more rarely gain) of material from the inclusion. This latter process is termed leakage.

a. Necking down. Irregularly shaped inclusions have a tendency to adopt negative or spheroidal morphologies with time via internal solution and reprecipitation along the cavity walls. Large inclusions also have a tendency to split into several smaller, more regular inclusions. If these processes occur prior to nucleation of the vapour phase, then liquid to vapour ratios are preserved. However, if this occurs as the inclusion cools, the daughter inclusions develop variable phase ratios. Such a population may be misinterpreted as representing trapping of a heterogeneous fluid characterised by a wide range in homogenisation temperatures. Necked inclusions are readily identified since they often possess long, irregular tails which may interconnect with other inclusions.

b. Leakage. This is a particularly serious problem in this study since calcites are prone to leakage along well developed cleavage planes. Variable phase ratios are often an indication that leakage has occurred. If the process occurs rapidly the process is termed decrepitation and is often recognised by the presence of star shaped clusters of inclusions. Such an array may testify to a later thermal overprint which caused rupture of original inclusions.

3. Origin of Inclusions

Calcite is prone to disolution and reprecipitation over a wide range of fluid temperatures and chemistries. Therefore, for the purpose of this study it is particularly important to be able to distinguish between separate generations of fluids. In order to establish the precise nature of an inclusion assemblage it is necessary to identify separate populations within one wafer. Traditionally, inclusions are classified as being either primary, secondary or pseudosecondary (Shepherd et al.,1985).

Primary inclusions are identified as those which are found; a) growing parallel to crystal growth faces; b) randomly distributed; c) isolated (separated by distances greater than 5 times the mean inclusion diameter). Also, they are often relatively large.

Secondary inclusions are found in planar arrays along healed fractures and possess thin flat morphologies. Shepherd et al. (1985) classify pseudosecondary inclusions as those possessing the characteristics of secondary inclusions, but as occcurring along fractures which are terminated by a growth zone. Finally, having identified a distinct population of inclusions within a wafer, it is often possible to recognise further generations within that population using crosscutting relationships.

5.3 Results

Microthermometric results from each locality are presented and discussed separately below. Full results are given in Appendix 5.1.

5.3.1 Inclusion types

Material was selected from veins and amygdales both within and outside metadomains, approximately 40 wafers were analysed as part of this study. Detailed descriptions of the samples used are given in Appendix 6.1. Overall inclusion abundance was generally high and a variety of inclusion types were found. The classification scheme used in this study is essentially that of Shepherd et al. (1985), a similar one was used by Evans (1987). The following types were observed; monophase liquid, monophase vapour, liquid rich (2 phase), vapour rich (2 phase) and multiphase solid (3 phase). The main features of these types are given in Table 5.1 below.

By far the most abundant type were L+V inclusions. Bodnar et al. (1985) point out that fluid inclusions from epithermal and geothermal systems worldwide are dominantly 2 phases at room temperature consisting of a low salinity aqueous fluid and vapour bubble.

Inclusion type	Degree of fill (F)	Example	Abundance
monophase liquid (L)	1.00		common
monophase vapour (V)	1.00		rare
liquid rich, 2phase (L+V)	0.95-0.80		very common
vapour rich, 2phase (V+L)	0.70-0.50		very rare
multiphase solid (S+L+V)	variable		very rare

Table 5.1. Classification scheme for fluid inclusions from metadomains within basalts from the Clyde Lavas

In addition to the inclusions described above, a number of darker, possible hydrocarbon inclusions were found, especially within analcime. These will be discussed separately.

5.3.2 Temperatures of interest

All microthermometric measurements were made during the heating (melting) cycle to allow for the effects of supercooling. Measurements were made at sub-ambient temperatures, followed by a systematic progression to higher temperatures. There are a range of temperatures which are recorded for inclusions from the Clyde Lavas.

a) *Temperature of first ice melting* ($T_{fm\ ice}$)

This corresponds to the eutectic temperature of the salt-water system. It is invariant and is diagnostic of the cationic composition of the aqueous fluid.

b) *Temperature of final ice melting* ($T_{m\ ice}$)

The invarient fusion temperature of ice is 0.015 °C and this temperature is depressed

by the addition of salts to the aqueous fluid. The degree of depression is directly proportional to the amount of salt present therefore $T_{m\ ice}$ can be used to estimate the salinity of the aqueous fluid (Clynne and Potter, 1977). Normally, this value is reported as equivalent weight percent NaCl, since NaCl is the most abundant salt in natural systems. Hedenquist and Henley (1985 a) give a mean salinity of approximately 4 wt.% NaCl for seawater recharged geothermal brines, whilst evolved continental brines can have much higher salinities.

c) *Homogenisation temperature (T_h)*

The temperature of homogenisation indicates the point at which the inclusion fluid leaves the two phase boundary and moves into the single phase field of the appropriate chemical system. If it is assumed that the inclusion fluid was trapped as a single phase, then the formation conditions of the inclusion must lie along an isochore (constant density line) from this point in P-T space. As a result the measured temperature of homogenisation is a minimum estimate of true trapping temperature.

In this study homogenisation was nearly always observed by gradual disappearance of the vapour bubble. In special circumstances homogenisation is marked either by disappearance of the liquid phase, or gradual fading of the liquid vapour meniscus. The former results when the density of the fluid is less than approximately 0.3 g cm^{-3} and is observed within some wafers from the Clyde Lavas. Inclusions exhibiting such behaviour are often evidence that a fluid has boiled, especially when found with liquid rich populations which homogenise over a similar temperature interval.

d) *Vapour rich, 2 phase inclusions*

As stated in the above table carbon dioxide-water immiscible inclusions were occasionally seen at High Craigton Quarry. Two further temperatures can be recorded for such inclusions; the temperature of CO_2 fusion (Tm_{CO2}) and the homogenisation temperature of the CO_2 rich phase. The temperature of CO_2 fusion is a measure of the purity of the phase. Pure CO_2 melts at -56.6 °C, the triple point of CO_2. Addition of other gaseous phases, such as methane, nitrogen, hydrogen suphide, results in depression of this triple point. Homogenisation of the CO_2 phase represents only partial homogenisation of the inclusion

leaving a coexisting aqueous liquid and CO_2 fluid. The temperature and mode of homogenisation is a function of CO_2 density. In this study all homogenisations were to the liquid phase.

5.3.3 Boyleston Quarry

Calcite and analcime were collected from a variety of sites within the quarry. In order to compare calcite hosted inclusions in analcime and prehnite rich areas samples were taken from a mound along the north face of the quarry which provided a full section through a metadomain. This locality is illustrated in Figure 5.1. Calcite is always paragenetically late (see Chapter 2). The aim of this study is twofold:

1. To compare results with those of Hall et. al. (1989); these authors suggest that both a low (c. 85 ^{o}C) and high temperature (>100 ^{o}C) fluid were present during basalt alteration. This may be a real observation, or is perhaps due to a sampling bias.
2. To compare fluid compositions where analcime and prehnite are the dominant alteration phases.

a) Calcite

Quantitatively, there are two dominant inclusion types, overall inclusion abundance generally being good.

1) *Liquid and vapour inclusions.* These ranged in size from 10 to 50 μm, ranging in shape from negative to irregular. Most of these inclusions can be classified as primary using the above criteria. There is minor necking of some samples, degrees of fill (F) ranging from approximately 0.8 to 0.95.

2) *Liquid only inclusions.* These inclusions range in size from 5 to 30 μm, and generally are arranged in flat or tabular arrays which commonly cross grain boundaries. As such, they satisfy secondary criteria. Yermakov (1965) determined the upper formation temperature of liquid filled monophase inclusions to be 70 °C.

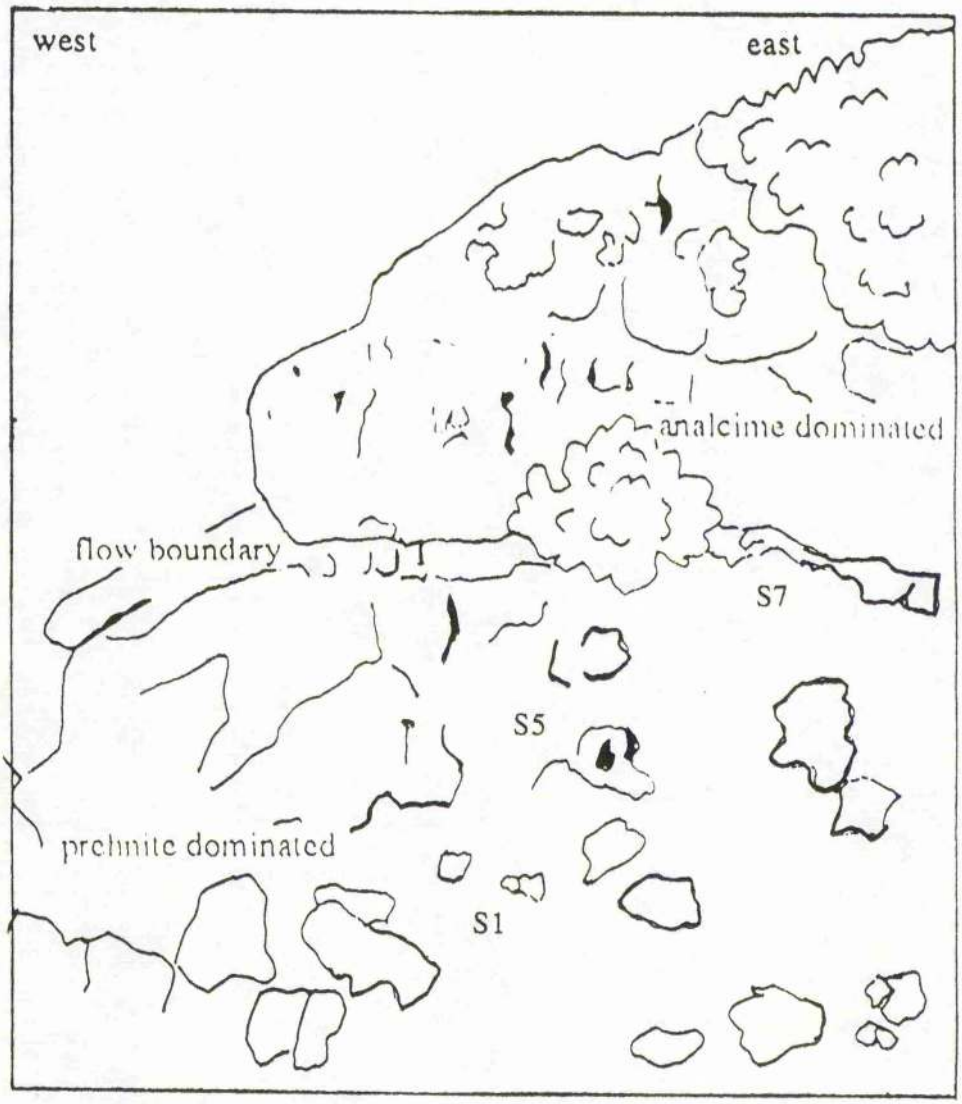

Figure 5.1. Sketch section showing me adomain locality at northeastern periphery of Boyleston Quarry. The prehnite rich area was extensively sampled for fluid inclusion material during the study.

In marked contrast to the study of Hall et al. (1989), no vapour dominated, or vapour + liquid + solid inclusions were seen. It is these inclusions which Hall et al. use to infer boiling of the hydrothermal fluid. This has important consequences regarding the origin of the metadomains at Boyleston, since one of the main pieces of evidence favouring a near surface environment, cited by the above authors is the recognition of boiling assemblages. Minor hydrocarbon (?) inclusions were also found, though only in very small quantities. These are discussed more fully in following sections.

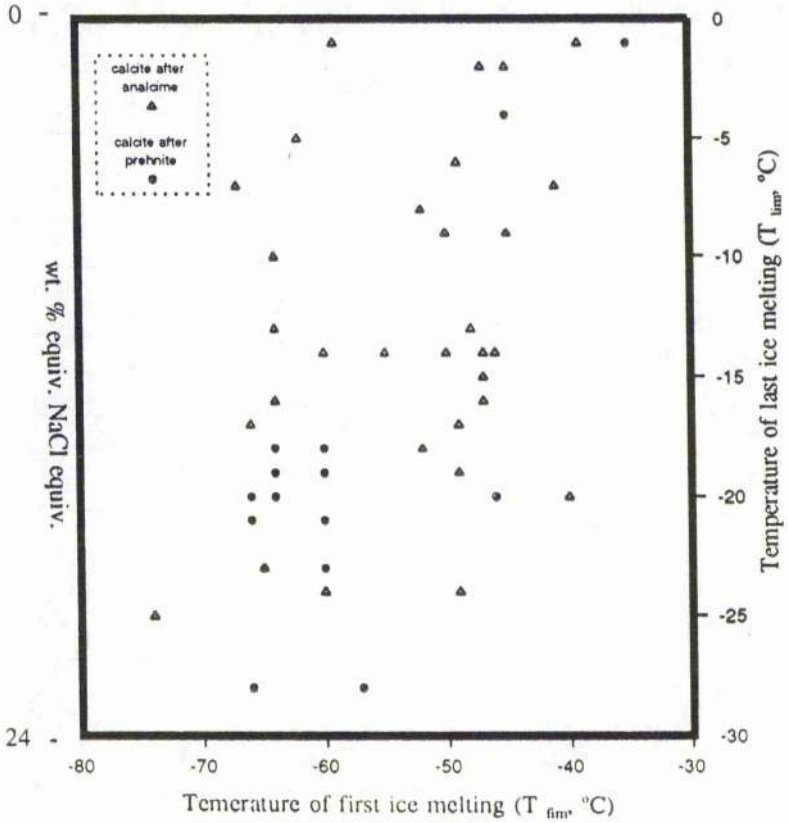

Figure 5.2. T_{lim} vs. T_{fim} for primary, 2 phase inclusions within calcite from Boyleston Quarry (for all paired measurements)

Both type 1 and 2 inclusions take on a brown, grainy appearance on freezing, though no hydrohalites were observed. Eutectic temperatures range from both prehnite and analcime

dominated areas range from approximately -35 to -75 °C (see Figure 5.2). Type 2 inclusions have eutectic temperatures ranging from -45 to -65 °C. Data quoted by Shepherd et al. (1985) show that salt water systems dominated by Na, Ca and Mg carbonates possess eutectic temperatures ranging from approximately -23 to -55 °C. Also, Shepherd et al. (1985) indicate that the development of a brown colouration during freezing is due to the formation of a $CaCl_2$ hydrate indicating the presence of Ca.

The study of Hall et al. (1989) also noted very low eutectic values for inclusions within calcite and suggested that this was due to the presence of a H_2O-KCl-$CuCl_2$ species with a eutectic temperature of -65 °C. They also note that traces of copper were detected during SEM-EDS analysis of opened inclusions. Banks (1987) also notes very low eutectic temperatures for fluids associated with base metal mineralisation at Tynagh. Hein et al. (1990) record very low eutectic temperatures ranging between -40 to -60 °C for fluorite hosted inclusions from the Southern Alps. SEM-EDS analysis confirmed the presence of Na, Ca and Cl as the main constituants of this fluid. Field evidence (see Chapter 2) shows that native copper is generally associated with prehnite rich areas.

Gross salinities ranged from 0 to 26 weight % NaCl. Samson and Banks (1988) also note high salinity inclusions from calcite hosted inclusions within Dinantian base metal deposits in the Southern Uplands. Figure 5.2 indicates that for calcite associated with prehnite, mean salinities are lower.

Figure 5.3 illustrates the range in homogenisation temperatures for Type 1 inclusions. It can be seen that there is a wide range in homogenisation temperature, ranging from approximately 50 to 250 °C, with a mean of approximately 140 °C. Homogenisation is always to the liquid state. Also, it can be seen that there are strong modes at approximately 140 and 180 °C. Such patterns are often cited as evidence of the existence of two separate fluids which have mixed. However, Figure 5.4 shows the predicted Gaussian probability density function (pdf) together with the observed population distribution for this data set. Clearly the observed data closely follows that which is expected. Therefore it is unlikely that the obseved fluid inclusion population was derived from mixing of two end member fluids with contrasting

temperatures.

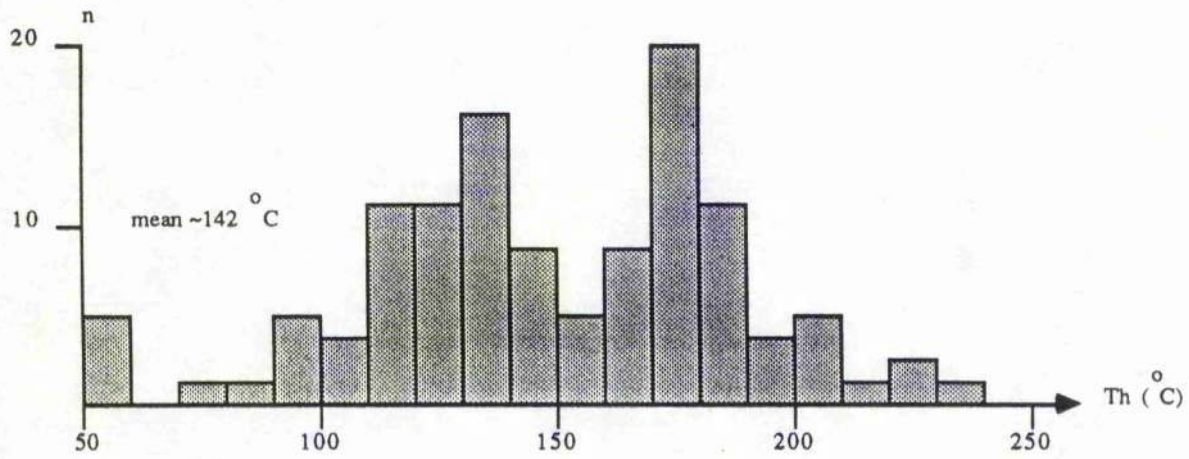

Figure 5.3. Homogenisation temperature histogram for liquid dominated, calcite hosted, primary inclusions from Boyleston

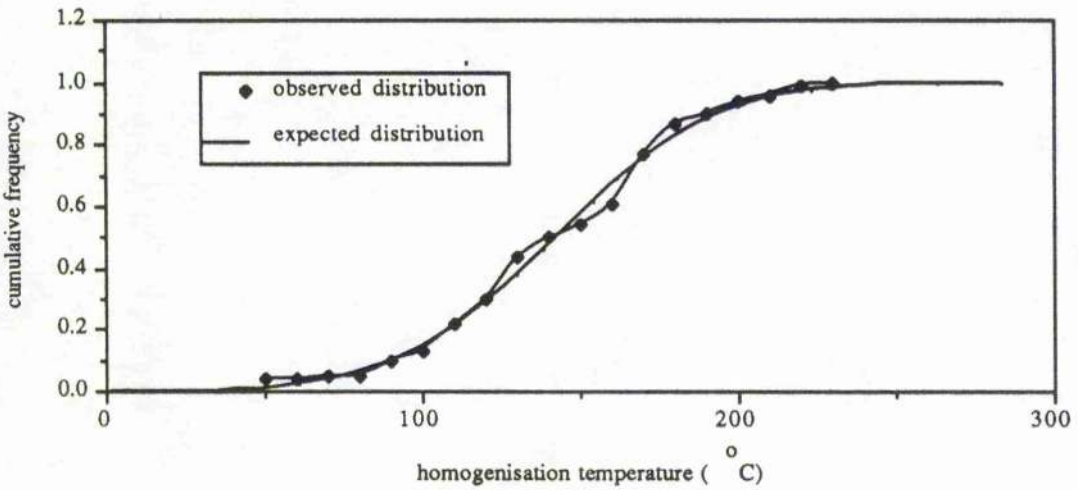

Figure 5.4 Expected and observed homogenisation temperature distributions for primary, two phase (L+V) inclusions from Boyleston Quarry

b) Analcime

There are two main inclusion types within analcime, overall inclusion abundance generally being poor.

1) *Liquid and vapour inclusions.* These inclusions generally satisfy primary criteria (see above), though some show a minor degree of decrepitation. They are thin walled, ranging in morphology from highly irregular to sub-regular. Sizes range from 10 to 100 μm, degrees of fill ranging from 0.85 to 0.95. An example of these inclusions is given in Figure 5.5.

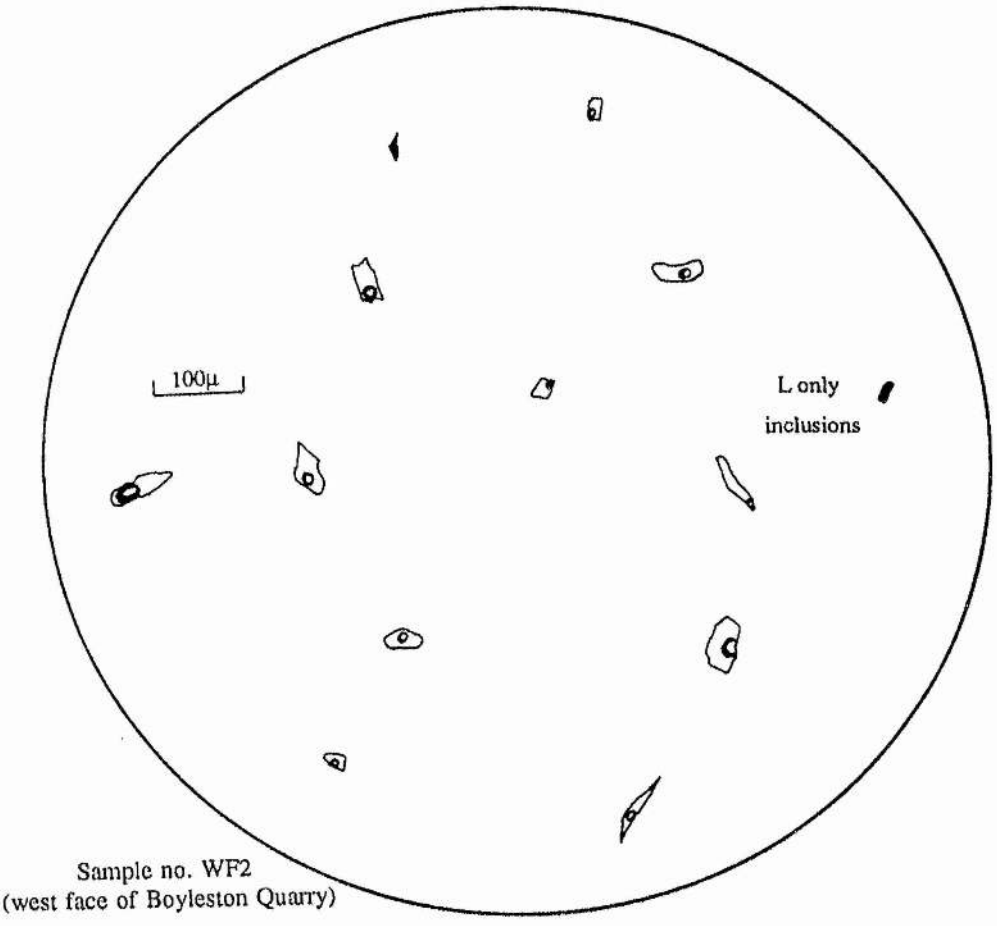

Figure 5.5 Hand sketch of L+V and L only primary inclusions at room temperature from analcime at Boyleston Quarry

Upon freezing these inclusions take on a brown, grainy appearance, as did Type 1 inclusions in calcite, again suggesting the presence of Ca. Mean eutectic temperature is approximately -21 °C, with a standard deviation of 2.3 °C. Data from Shepherd et al. (1985) indicates that H_2O-NaCl-$NaHCO_3$ salt-water systems have eutectic temperatures over this range. Hall et al.(1989) recorded eutectic temperatures between -21 to -34 °C for inlusions

within analcime. Ice hydrates were not observed in this study. Tm ice ranged from -1 to 0 °C indicating a very dilute aqueous fluid. This was also found to be the case in the study made by Hall et al..

Figure 5.6 shows the range in homogenisation temperature for inclusions within analcime. It can be seen that there is a relatively restricted temperature range, with a strong mode between 180 and 220 °C. Mean homogenisation temperature is 203 °C, in contrast to Hall's study (145 °C).

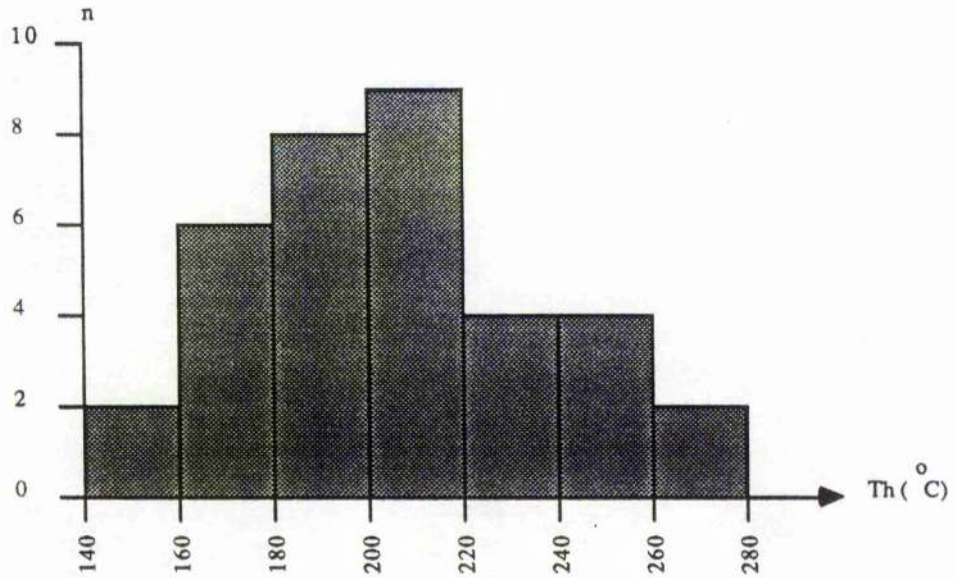

Figure 5.6 Homogenisation temperature histogram for primary, liquid dominated inclusions from analcime, Boyleston Quarry

2) *Hydrocarbon inclusions*. These are relatively abundant in certain wafers and are often found in close proximity to cracks and grain margins. They are typically highly irregular, and are up to 500 μm in size. The core of these inclusions is generally opaque, whilst the margins appear light brown or pale yellow. No aqueous phase is seen in association with these inclusions. Progressive heating of these inclusions causes a colour change around the margins, which take on a dark brown or orange hue. This colour change commences at approximately 230 °C, prior to which the marginal areas become diffuse, and is not reversible on cooling to room temperature. The effects of stepwise heating are shown in Plate 5.1.

Plate 5.1. Hydrocarbon material within analcime. Hydrocarbon rich material is typically found within large (> 200 μm) clusters which are mainly concentrated around fractures and fissures within the host grain. The plate shows the effects of stepwise heating from 25°C (lower photograph) to 230 °C (upper photograph) at a heating rate of 5 °C $min.^{-1}$. It can be seen that a colour change occurs as the hydrocarbon changes from a light brown to a darker reddish-brown colour. This colour change is not reversible upon cooling. Also, at temperatures above 150 °C there is often limited migration of material along grain boundaries and intergranular fissures.

Sample No. WF2, Boyleston Quarry. This sample is taken from the middle lava flow within the quarry, at the base of the western face, approximately 100 metres from the northern margin.

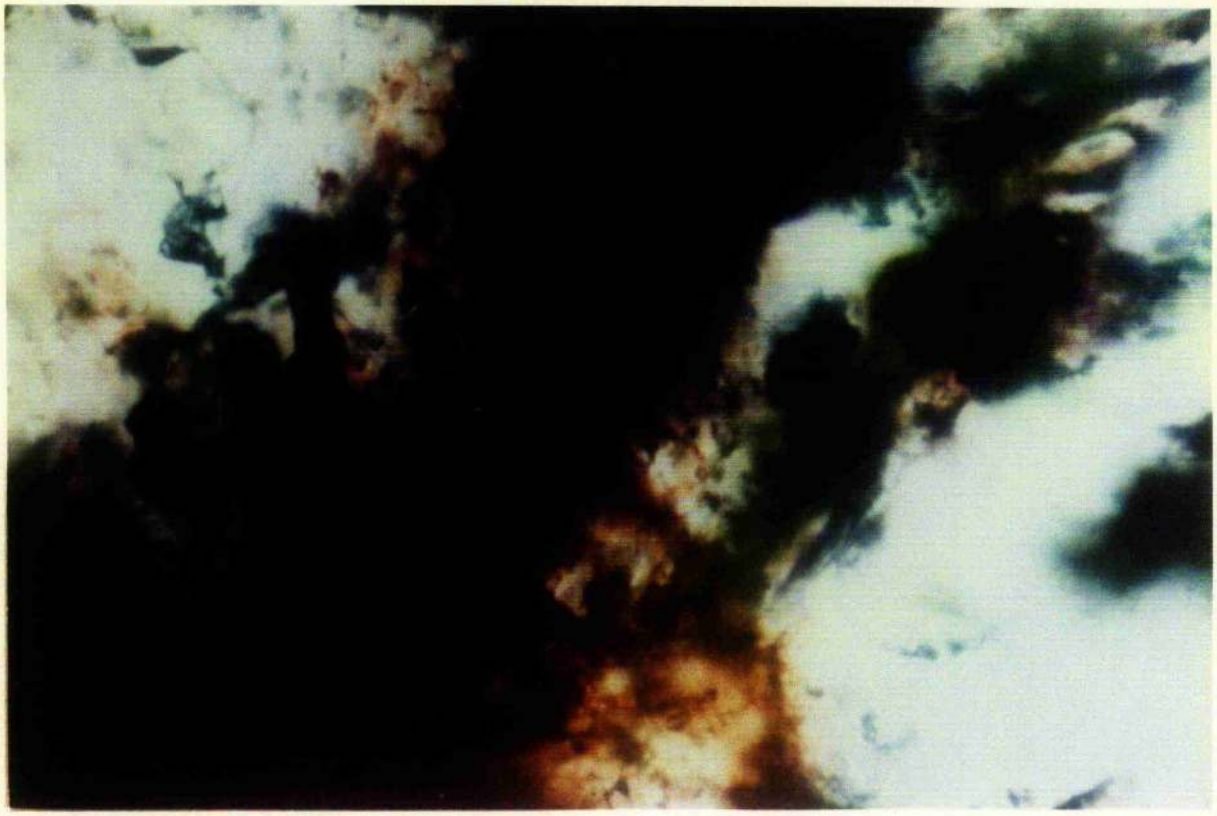

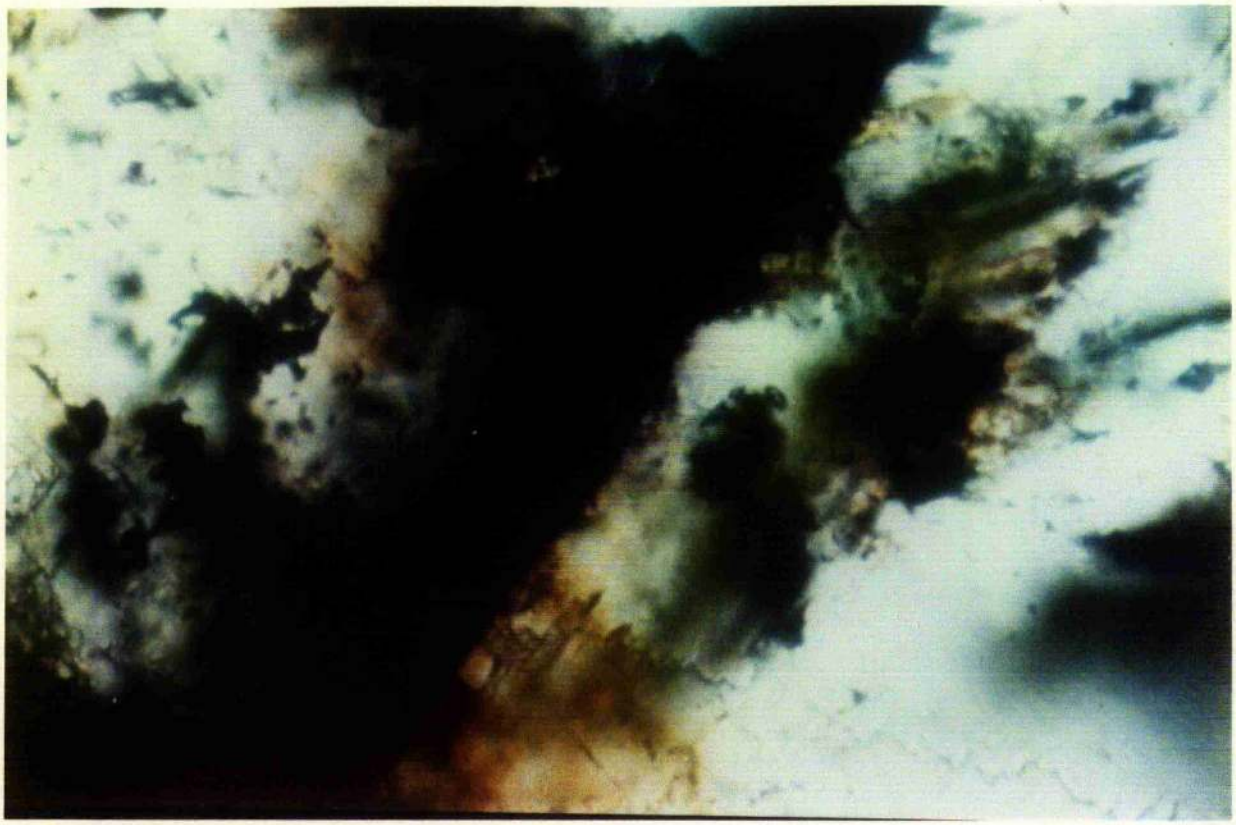

5.3.4 Discussion

Clearly Type 1 primary inclusions within calcite exhibit a wide range in salinity. One possible cause might be boiling with resultant concentration of salts within the residual fluid fraction. Hall et al.(1989) advocate boiling as a possible cause for the widespread brecciation of the lava seen at Boyleston, yet they did not report the presence of low salinity inclusions within calcite in their study which would represent condensates from the boiling process. Also, in this study phase ratios are relatively constant, and homogenisation is always to the liquid state. Therefore, the conclusion is that if boiling did occur, it was on a very limited scale, and was not sufficient to cause either the observed salinity variations or widespread brecciation.

One possible mechanism which could account for salinity variations is the mixing of fluids with contrasting salinity. Samson and Banks (1988) suggest that saline (19-30 equiv. wt.% NaCl), low temperature (c.150 °C) fluids from the Southern Uplands are simply modified meteoric fluids which have interacted with halite bearing Dinantian sedimentary successions. Figure 5.7 below shows the composition of fluids from Type 1 inclusions expressed in terms of salinity and temperature.

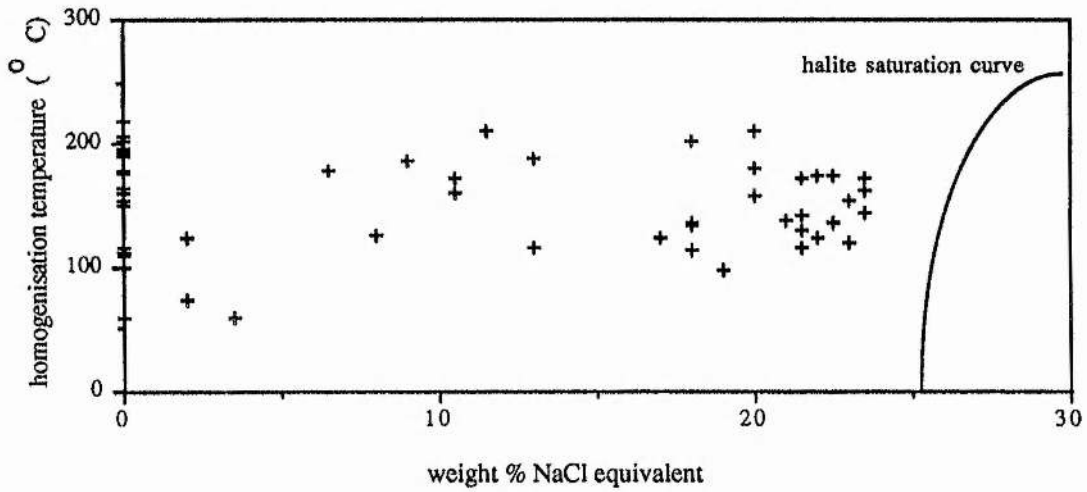

Figure 5.7. All paired temperature-salinity measurements for primary, two phase, calcite hosted inclusions from Boyleston Quarry

It can be seen that there is a broad horizontal scatter in fluid compositon. Such a trend can be interpreted as near-isothermal mixing of fluids of contrasting salinity. The Dinantian Inverclyde Group underlie the Clyde Lavas and contain the Ballagan Formation (Browne,1980). This formation consists of silty mudstones with numerous thin beds of dolomitic limestone, and is thought to have been deposited under marginal marine conditions, "subject to periodic desiccation and salinity fluctuations" (Paterson and Hall, 1986). These beds may have acted as the source of dissolved salts, in particular Ca.

Fluids which were present during the formation of analcime are characteristically of very low salinity, bicarbonate dominated, organic rich and of higher temperature than those which were present during calcite formation. The first two features suggest that this fluid may represent a surface derived fluid, possibly groundwater, since seawater would be expected to be of slightly higher salinity and chloride dominated. One possible source for the organics might be organic rich mudstones within the underlying Ballagan Formation. Hydrocarbons may have been mobilised and transported by groundwaters during baking by the overlying lavas. The effects of the lava and associated intrusives on the sediments is seen at the base of Campsie Glen where recrystallisation of carbonate enriched sediment is a common feature. This is essentially in keeping with the model proposed by Hall et al. (1989).

The fact that the fluid present during the formation of analcime was of relatively high temperature testifies to an overall progressive cooling within the metadomains at Boyleston Quarry with time. Also, liquid only secondary inclusions within calcite indicate that advection of low temperaure fluids continued after initial formation of calcite.

Minor variations in fluid temperatures and compositions can be explained by considering field evidence. It was shown earlier that in material collected from a metadomain along the north face of the quarry (see Figure 5.1), where prehnite was the dominant alteration phase salinities were high within the later calcites, the reverse being true for analcime dominated zones. Also fluid temperatures are slightly higher as shown in figure 5.8. Prehnite occurs only within the oxidised, vesicular flow top, whilst analcime is restricted to the main overlying lava. The sharp contact of the underlying lava also marks the

mineralogical change.

It is sugested that within the lower lava, fluid residence time is relatively long, leading to loss of heat to the surroundings. However, in the overlying main lava, because overall permeability is much reduced, fluid residence time is shortened, fluid and basalt only coming into contact during catastrophic surges when the lava is brecciated. This would mean reduced heat loss, and little time for interaction and exchange with the host basalt. Hall et al. (1989) suggest fluid compositional variations are due to interaction of the fluid with pre-existing analcime and prehnite.

5.3.5 High Craigton Quarry

Calcite samples were collected from the main west face of the quarry, both from viens within and below the lahar. In addition, samples were also taken several hundred metres to the west within Upper High Craigton Quarry within lavas which are stratigraphically higher than those present in the main quarry. A variety of inclusion types were encountered in this investigation.

1) *Type 1 (Liquid and vapour inclusions)*

These inclusions were amongst the most common encountered and generally satisfied primary criteria, as laid out above. Morphologies range from sub-regular to negative, sizes from 10 to 70 µm. Degress of fill ranged from 0.9 to 0.95, homogenisation always being to the liquid state. The inclusions took on a brown grainy appearance upon freezing below -50 °C.

Eutectic temperatures ranged from -40 to -70 °C, with a very strong mode between -60 to -70 °C. These values are similar to those obtained from Boyleston Quarry. Data from Shepherd et al. (1985) indicates that the H_2O-NaCl-$CaCl_2$ system has the lowest eutectic temperature of the common salt-water systems at -55 °C. Hall et al. (1989) report Li-salt systems with very low eutectics (-75 to -80 °C), though there is no evidence of there being a Li-enriched horizon within the area. Also copper, in the form of stringers and grains is

absent from this locality.

There are wide variations in salinity within this population of inclusions, which appear to be controlled in part by stratigraphic height (see discussion below). Gross salinities range from 26 to 0 equiv. weight % NaCl. For samples taken from beneath the lahar, salinities range from approximately 11 to 26 equiv. weight % NaCl, with a mean of 18.3. Samples above and within the lahar have salinities ranging from 0 to 23 equiv. weight %NaCl. However, this population is characteristically bimodal, with strong modes at 0 and 20 equiv. weight %NaCl. This is illustrated in Figure 5.8 below.

Homogenisation temperatures vary from between c. 50 to 200 °C. Again, the population distribution appears to be controlled by stratigraphic height as shown in Figure 5.8. Samples beneath the lahar show a modal value between 150-170 °C, whilst those within and above show a symmetrical distribution, with a mode lying between 110-130 °C.

2) *Type 2 (Monophase liquid inclusions)*

These inclusions are common throughout, and satisfy secondary criteria as they are frequently found as trails within healed fractures, or cross cutting grain boundaries. Furthermore, it is often possible to observe multiple generations of these inclusions. Most inclusions are < 10 μm in size and possess tabular morphologies. Occasionally, it is possible to observe minute vapour bubbles within these inclusions, which move around at high speed. No measurements are possible on these inclusions.

Isolated, large (10-50μm), dark, sub-regular, monophase inclusions are occasionally observed interspersed amongst primary Type 1 inclusions, and are not genetically related to Type 2 monophase populations. Again, no measurements are possible on these inclusions.

3) *Type 3 (Vapour rich, 2 phase inclusions)*

These inclusions are rare, and possess many of the features of Type 1 inclusions; also satisfying primary criteria. They differ in that they are characterised by low degrees of fill (0.5 to 0.7) and always homogenise to the vapour state. Eutectic temperatures within these inclusions are difficult to observe, though they have relatively high salinities, ranging from 15 to 21 equiv. weight %NaCl.

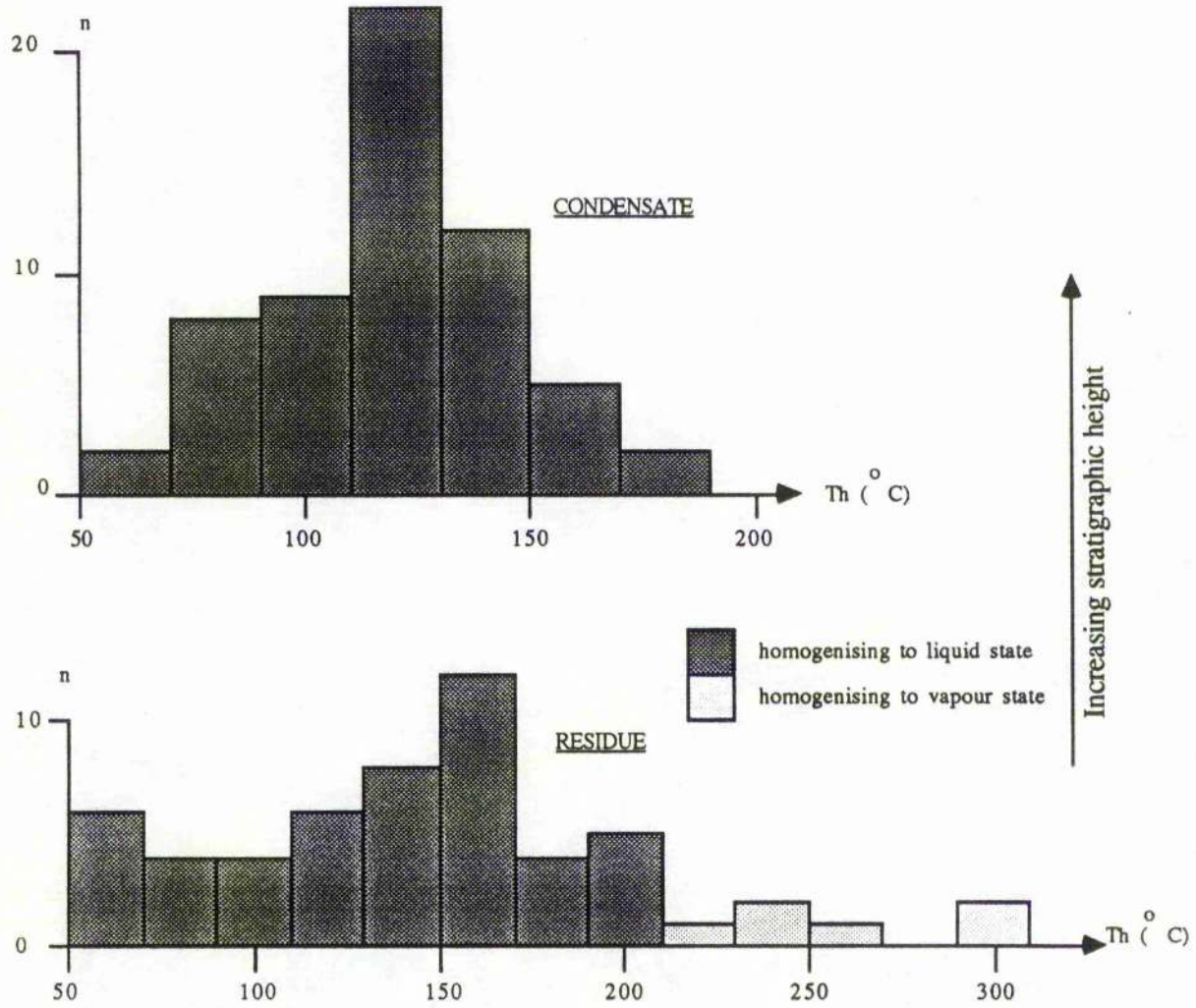

Figure 5.8 Variation in homogenisation temperatures between calcite hosted primary inclusions collected from the base and the top of the quarry floor at High Craigton

Upon cooling a double bubble appears in some instances suggesting the presence of a CO_2 rich vapour. Upon reheating, final CO_2 melting temperatures were not observed, even for samples held well below the CO_2 triple point. Rehomogenisation was always to the vapour phase and occurred between 12 and 26 °C. Data from Shepherd et al. (1985) indicates that the density of this CO_2 rich phase is very low, between 0.3 and 0.15 gcm^{-3}.

4) Type 4 (Liquid + vapour + solid inclusions)

These were only seen in one sample, located beneath the lahar. The solid phase is cubic in shape and is most probably halite. Dissolution temperatures were not obseved.

5.3.6 Discussion

The presence of primary, liquid and vapour rich (Types 1 and 3) inclusions in close proximity to one another indicates that fluid boiling, a commonly reported feature of geothermal systems, occurred at High Craigton. This may have occurred as ascending fluids infiltrated the highly permeable lahar as shown in Figure 5.9. As the process continued the residual liquid phase became increasingly saline as water boiled off; Type 4 inclusions are found at the base of the quarry. Also, salinities are highest within this area. In comparison, the escaping vapour phase possessed a very low salt concentration (in extreme cases this would be zero). Type 1 inclusions found at higher levels within and above the main quarry show bimodal salinity variations, the strongest mode occurring at 0 to 1 equiv. weight %NaCl. The relative scarcity of vapour rich inclusions suggests that either there was only very limited boiling (this would explain why vapour rich inclusions have relatively high salinities) or that the system was "flooded" by liquid water which in turn suggests that the system was located below the local water table.

Further evidence in support of fluid boiling is the presence of CO_2 rich (Type 3) inclusions within calcites collected from the lahar. This is because during fluid boiling gases such as N_2 and CH_4 and, to a lesser extent CO_2 are partitioned into the vapour phase. Giggenbach (1981) expresses this partitioning behaviour, for single stage separation, in terms of a gas distribution coefficient (B), given as:

Concentration of gas in vapour / Concentration of gas in liquid.

For CO_2 this is given as; log B CO_2=4.7593-0.01092T (T in °C). Values for B range from 3.66 at 100 °C, to 1.48 at 300 °C. Therefore, CO_2 is most strongly partitioned when a fluid is boiled and cooled, for example by mixing with groundwater.

If the fluid at High Craigton was boiling it is possible to estimate the depth of

trapping, assuming that the system was open to the surface i.e. assuming hydrostatic conditions.

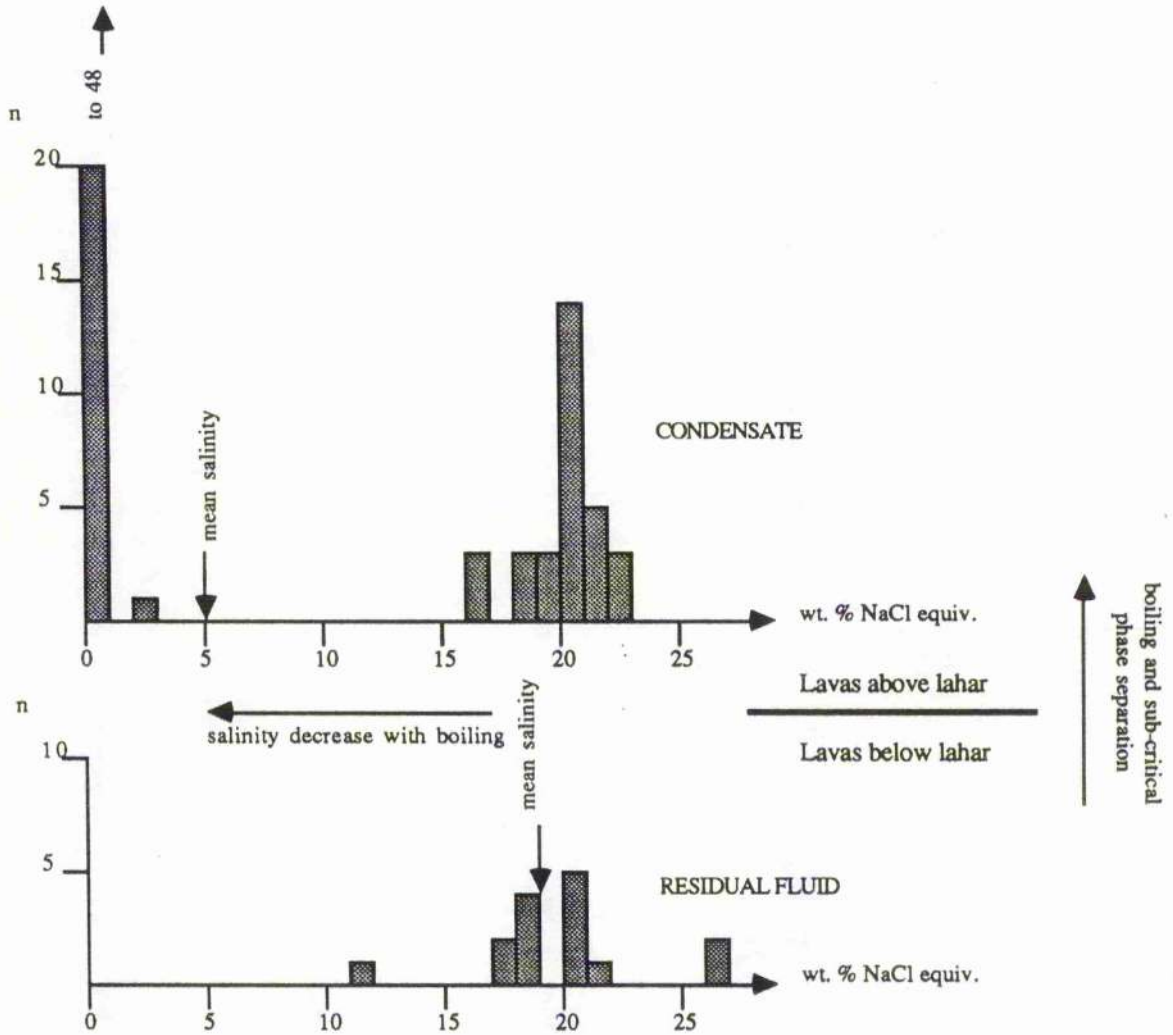

Figure 5.9 Salinity variations with stratigraphic height for primary, calcite hosted inclusions from High Craigton Quarry

If it is assumed that cooler groundwater was entering the system from above then the intergrated density of the overall fluid column is increased and as such the estimate of trapping depth is overestimated slightly. Using the data of Haas (1971), reported in Shepherd et al. (1985) it is possible to arrive at a range in depth estimates. This is achieved by assuming an overall mean fluid salinity of 5 equiv. wt. % NaCl, and a range in

homogenisation temperatures for Type 1 inclusions ranging from 100 to 250 °C. These values lead to depth estimates ranging from less than 50 metres to 450 metres. This finding has important consequences regaring the timing of metadomain activity; the depth estimates above suggest that geothermal activity was contemporaneous with volcanism, and occurred before burial by the overlying Strathclyde Group sequences.

5.3.7 Enthalpy-chloride relationships

It is possible to further address the relationships between fluids of differing temperature and composition at High Craigton Quarry by making use of an enthalpy-chloride diagram. Such studies by Truesdall and Fournier (1976) have proved useful in evaluating fluid evoluion in geothermal areas. Because both ethalpy and chloride are additive quantities, then trajectories for boiling and mixing are straight lines on such plots. Further details of the technique can be found in Fournier (1979) and Fournier (1981).

For example, single stage steam loss, a process which is likely to have occurred at High Craigton can be represented by straight lines radial to the composition and enthalpy of steam. This is illustrated in Figure 5.10 below. Given the composition and temperature (and hence enthalpy using tables in Henley et al., 1985) of the residual fluid found at the base of the quarry (18.3 equiv. wt. % NaCl and mean temperature of approximately 160 °C) it is possible to determine the composition of the fluid prior to boiling, assuming single stage separation occurred at approximately 190 °C. This is possible since this composition must lie along line A-B at point C. It can be seen from the diagram that this fluid composition is approximately 14.8 equiv. wt. % NaCl. Henley (1985) suggests that seawater recharged geothermal systems have maximum salinities of approximately 4.5 equiv. wt. % NaCl. High salinity fluids from inclusions from mid-ocean ridge environments have been reported by Cowan and Cann (1988) and also Kelley and Delaney (1987). In both instances high salinities are thought to be due to supercritical 2 phase separation of seawater. It is unlikely that fluids from the Clyde Lavas ever experienced such temperatures exceeding the critical point of

water (374 °C).

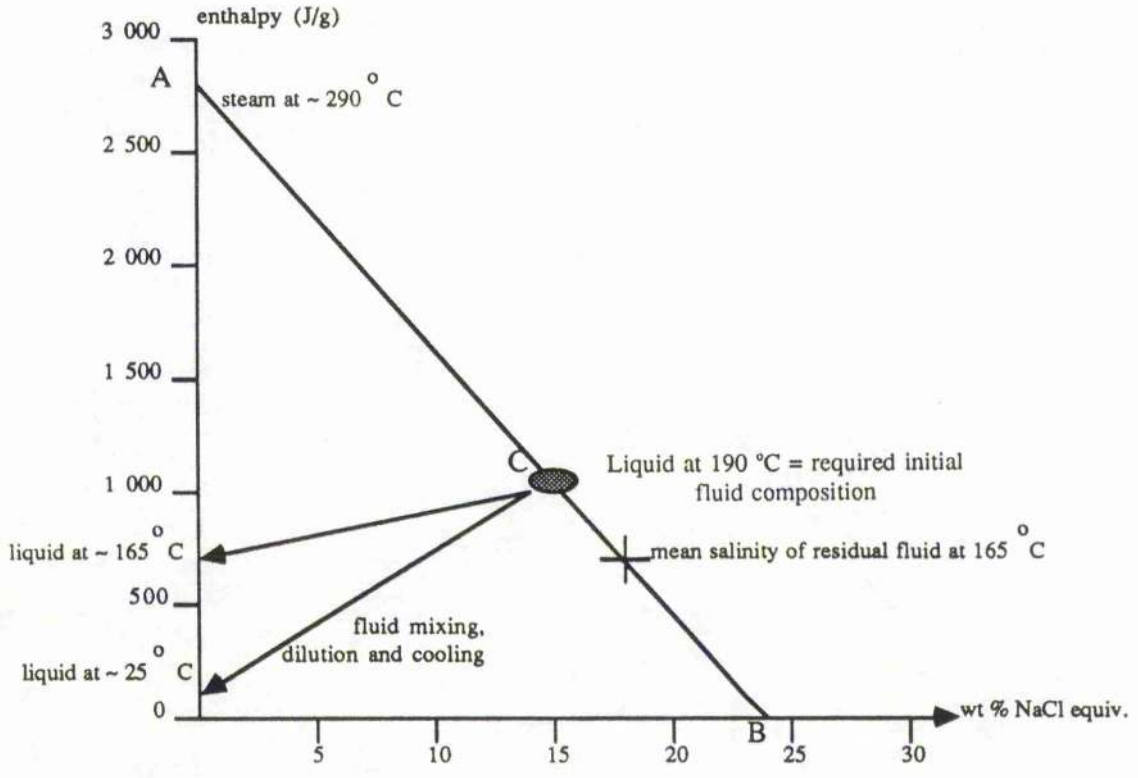

Figure 5.10 Enthalpy-chloride diagram showing possible evolutionary pathways for fluids present during metadomain formation at High Craigton

Therefore, the fluid found at High Craigton is likely to have represented an evolved continental brine, derived from surrounding sedimentary successions.

Compositional data from fluid inclusion measurements indicates that overall mean salinity at High Craigton was approximately 6 equiv. wt. % NaCl. This suggests that mixing occurred between the brine and a fluid of lower salinity, possibly a fluid of surface origin, given that a large number of Type 1 inclusions have very low (<2 equiv. wt. % NaCl) salinity. Also, given that homogenisation temperatures for these inclusions range from approimately 120 to 200 °C, it is possible to calculate the temperature of the surface derived fluid as shown. It can be seen from the diagram that temperatures ranged from approximately 25 °C to 160 °C. In order for surface derived fluid to reach such temperatures it is neccesary either that the fluid resided in reservoirs at intermediate to high temperatures for relatively long periods of time, or that the mass flow rates were relatively low. Chemical equilibration

with the surrounding rocks might be expected if the former were true, though this does not appear to be the case since fluid salinity is extremely low and within the system is extremely varied. Therefore, it is concluded that mass flow rates were low. Fournier (1979) gives a value of 117 kg/minute for flow in a conduit of circular cross section, within a shallow (less than 500 metres in depth) system where fluids are cooling adiabatically. For comparison, Cann and Strens (1982) calculate mass flow rates of $6 * 10^4$ kg/minute for a black smoker vent of unit cross section, corresponding to a linear flow rate of 1 ms^{-1}within these vents. Sams and Thomas-Betts (1988) calculated that at shallow depths (<500 metres), maximum mass flow rates of $2.45*10^{-5}$ kg/minute for convective fluid flow around the Cornubian batholith.

5.3.8 Langbank Cutting

Calcite samples were collcted from above and below the flow boundary. The overall quality and abundance of inclusions at this locality was generally poor. Variable phase ratios and high homogenisation temperatures indicate that some leakage has occurred in these samples. Furthermore, fracture density is high in these samples. However, it has been possible to obtain some information on the nature of the fluid phase at this locality. There is a restricted range in inclusion types found here.

1)*Type 1 (Liquid and vapour inclusions)*

These inclusions vary in size from 5 to 50 μm, and range in morphology from negative to highly irregular. They satisfy both primary and secondary criteria, phase ratios for the primary inclusions ranging from 0.7 to 0.95, whilst secondary inclusions show a much more restricted range >0.95. Homogenisation for both primary and secondary inclusions is always to the liquid state. Upon freezing below -60 °C, the inclusions become grainy and brown in colour. Because of their small size, no freezing measurements were possible for secondary inclusions. Ice hydrates were not observed. In common with other localities, eutectic temperatures were very low, T*fm ice* ranging from -72 to -35 °C, with a mean value of -61

°C. Again, copper is absent suggesting that the H_2O-KCl-$CuCl_2$ system does not exert a major influence on eutectic temperatures across the lava outcrop, as suggested by Hall et al. (1989). Salinities, as determined from freezing point depression varied widely, though not systematically at this locality. Estimates ranged from 0 to 23 equiv. wt. % NaCl.

Homogenisation temperatures for primary inclusions ranged from approximately 80 to 180 °C as shown in Figure 5.11.

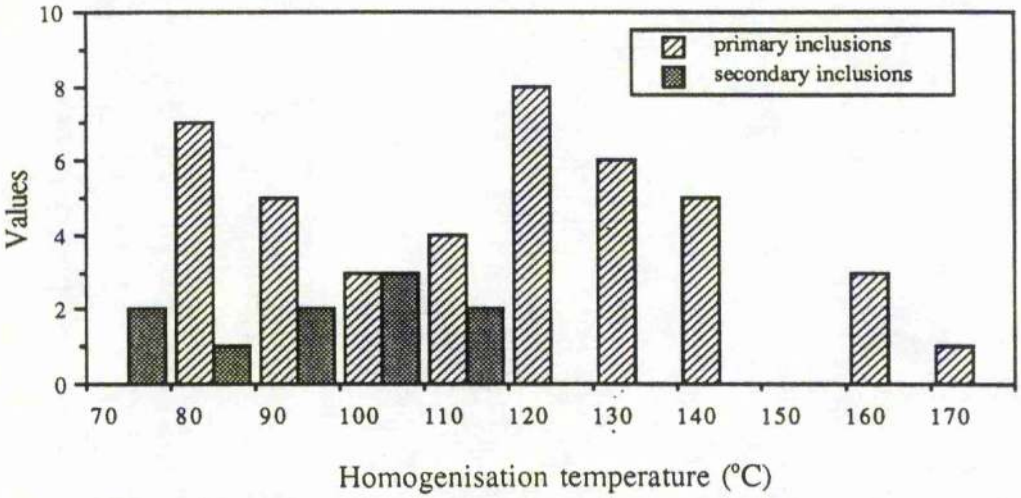

Figure 5.11. Histogram showing range in homogenisation temperature for primary and secondary inclusions from Langbank Cutting

It can also be seen from this diagram that there is a wide spread of data with no well developed mode. Homogenisation temperatures for secondary inclusions are generally lower, ranging from approximately 70 to 120 °C.

2) *Type 2 (Monophase liquid inclusions)*

These inclusions are very common throughout, and satisfy secondary criteria as they are frequently found as trails within healed fractures or cross cutting grain boundaries. They are found in close association with secondary, 2 phase inclusions.

Most inclusions are less than 10 μm in size and possess tabular, or negative morphologies. No measurements are possible on these inclusions. Their presence, together with those found at other localities testifies to the widespread existence of a low temperature fluid, present after the main phase of geothermal fluid advection across the whole lava field.

5.3.9 Discussion

Since leakage is generally associated with the movement of fluid out of the individual inclusion rather than filling by a later fluid, the effect on salinity might be expected to be minimal. It can therefore be concluded that the wide range in salinity reported here is a feature of the fluid present during geothermal activity.

Since there is no evidence of boiling at this locality, one possible mechanism which could account for wide salinity variations is mixing of fluids of contrasting salinity. Because there appears to be a strong bimodal distribution of salinities, this suggests that the end-member fluids did not equilibrate chemically with one another. Density is a possible cause of this "unmixing behavour", though there is no salinity stratification in vertical sections across the lava. Furthermore, Type 1 inclusions of contrasting salinity are frequently found juxtaposed to one another in single samples. Fluids with salinity values upwards of 20 equiv. wt. % NaCl are likely to represent "evolved continetal brines", as dicussed in section 5.3.6 above.

Homogenisation temperatures for Type 1 inclusions are within a similar range to those found at other localities. If it is assumed that these metadomains do provide a cross section through the lava pile, then the conclusion is that fluid advection during geothermal activity was relatively high i.e. fluid residence times were relatively low, therefore conductive cooling losses were low, hence ascent of fluids was near adiabatic.

5.4 Mugdock Quarry

As discussed in Chapter One this locality lies within the quartz-calcite burial metamorphic zone defined by Evans (1987). The purpose of studying fluid inclusion material from this locality is to provide an independent assessment of fluid conditions during burial metamorphism of the lavas. This is achieved by studying fluid inclusion wafers prepared from

polycrystalline quartz which is found infilling vesicles within the lava. Unfortunately, it proved impossible to prepare calcite wafers using samples collected at this locality.

The question which arises is; could the low temperature secondary fluids which are found within calcites from all the above localities represent a later stage fluid which was present during burial metamorphism of the lavas? If so, then the inference is that metadomain development (recorded within primary inclusion populations from metadomain localities) occurred prior to burial metamorphism of the lava pile by overlying sediments. This view is contrary to that expressed by Evans (1987), who favoured a model in which the metadomains developed after burial. The results of this study are discussed below. There are two inclusion types;

1) *Type 1 (Liquid and vapour inclusions).* These inclusions are quantitatively most important and generally satisfy primary criteria. They range in size from 5 to 30 μm and generally possess irregular morphologies. Phase ratios are tightly constrained and are always greater than 0.9. Homogenisation is always to the liquid state.

Eutectic temperatures were difficult to record and were reported for only a few inclusions. Temperatures ranged from -35 to -25 °C. Data from Shepherd et al. (1985) indicates that H_2O-$MgCl_2$ dominated systems have eutectic temperatures within this range. Salinity values, based on freezing point depression indicate that the fluid was relatively dilute, with maximum salinity less than 4 equiv. wt. % NaCl (see Appendix 5.1).

Homogenisation temperatures ranged between approximately 60 and 150 °C, with a strong modal value between 80 and 110 °C. This is illustrated in Figure 5.12. These are within the range of those reported for secondary inclusions from calcites at Langbank Cutting.

2) *Type 2 (Monophase liquid inclusions)*

Large clusters of these inclusions are found along grain boundaries and cross cutting individual quartz grains. They are extremely small (<10 μm) and no measurements are possible.

Evans (1987) suggests that fluids present as burial metamorphism were of high salinity, and were subsequently diluted by less saline seawater or groundwater as burial

proceeded. If this is the case then the fluid at Mugdock Quarry represents such a late stage fluid, possibly seawater, or evolved groundwater.

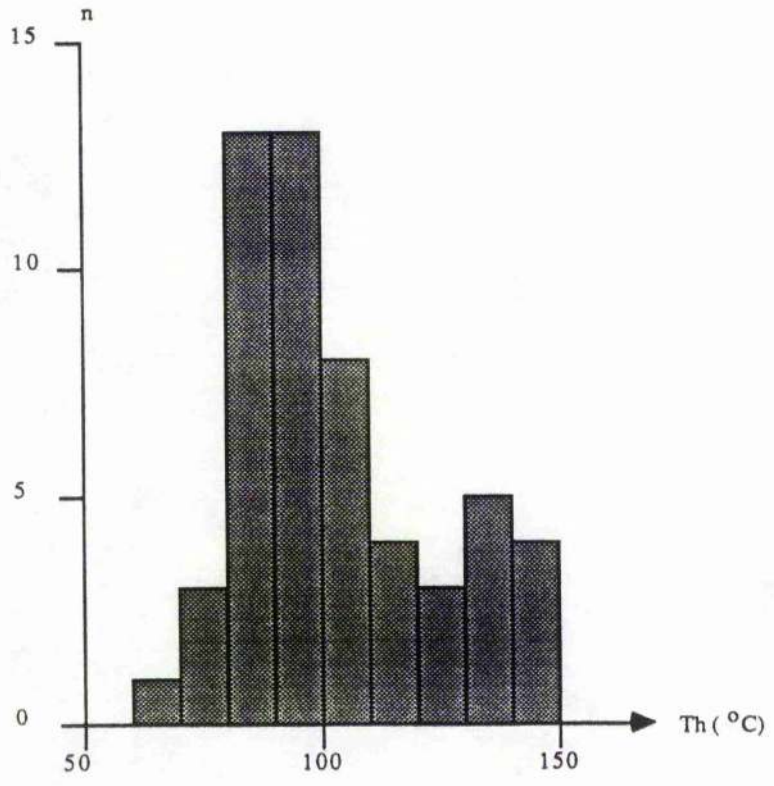

Figure 5.12 Homogenisation temperature histogram for primary, quartz hosted inclusions from Mugdock Quarry, Strathblane

It is noted that the homogenisation temperatures recorded for primary inclusions in quartz are similar to those recorded for secondary inclusions in calcite from Langbank Cutting. Also as noted above, Yermakov (1965) determined the upper formation temperature of liquid filled monophase inclusions (which are found in large numbers in every sample) to be 70 °C. Furthermore, salinities, where recorded, are generally low in these monophase inclusions.

The evidence presented above suggests that the secondary inclusions in calcite (and analcime) do represent later stage, low temperature fluids that were present during burial of the lavas, i.e. that the metadomains were developed prior to burial of the lavas by Dinantian sediments. Thus it is possible to envisage a situation in which early hypersaline, relatively hot

connate fluids are progressively "swamped" by surface derived fluids (possibly seawater, meteoric water, or groundwater at various stages of evolution) as these geothermal systems evolved.

5.5 Integrated Discussion

Multiple generations of fluid inclusions testify to the fact that the metadomains have undergone a protracted period of fluid evolution. The purpose of this section is to compare the fluids which were present during the development of the Clyde Lava metadomains and the physical processes which occurred during hydrothermal activity with those occurring in geothermal and hydrothermal systems worldwide.

5.5.1 Comparison with present day geothermal systems

Perhaps the main difference between the fluids present during metadomain development and those found in modern day geothermal systems lies within salinity variations. Most geothermal systems are characterised by low salinity hydrothermal fluids. For example, at Champagne Pool (Waiotapu, New Zealand) alteration fluids have salinities less than 1 equiv. wt. % NaCl. Salinity will be controlled by three main factors; host rock lithology, origin of the alteration fluid, and processes tending to concentrate or dilute fluids.

In general, fluid salinities within andesitic and silicic volcanic systems are higher than those in basaltic systems (Hedenquist and Henley, 1985), though rarely exceed 2 equiv. wt. % NaCl. Seawater recharged systems are of relatively high salinity (up to 4 equiv. wt. % NaCl). Systems with extremely high salinities (eg. Salton Sea with salinity = 25 equiv. wt. % NaCl, Hedenquist and Henley, 1985) typically contain evaporite sequences reflecting tectonic setting and climate. The situation within the Clyde Lavas is different in that alteration fluids appear to have either originated or interacted with organic and carbonate rich sediments below the lava pile prior to entrapment.

Present day geothermal fluids are commonly neutral to alkaline chloride waters containing a predominance of alkali and alkali earth chlorides (Hedenquist and Henley, 1985 a). Freezing measurements appear to confirm that the latter is the case for fluids present during metadomain development in the Midland Valley.

Temperatures recorded for fluids present during calcite formation are similar to those which are recorded for hot springs and geothermal fluids. For example, the Tauhara and Waiotapu geothermal fields of New Zealand have measured fluid temperatures ranging from 98 to 257 °C and 70 to 225 °C respectively (Hedenquist and Henley, 1985 b). These temperatures are based on measurements of fluid temperatures at the surface and those recorded at depth within these systems.

Fournier (1979) concludes that most geothermal fluids either cool by conduction, boiling or mixing with cooler surface derived waters, during which time partial or total chemical re-equilibration may occur. Fournier (1979) has demonstrated mixing and boiling of geothermal fluids at Cerro Prieto (Mexico), Orakeikorako (New Zealand) and Yellowstone (USA). Fluid inclusion evidence has demonstrated that these processes have also occurred within the metadomains of the Clyde Lavas. However, for all of the present day systems salinity concentration due to boiling is less than 2 equiv.wt.% NaCl. This clearly demonstrates the importance of host rock lithology in controlling salinity.

For most geothermal systems in New Zealand, the temperature of the dilutant fluid of surface origin ranges between 100 to 180 °C (Hedenquist and Henley, 1985 b), which is similar to that found at High Craigton Quarry.

5.5.2 Comparison with other hydrothermal fluids

Figure 5.13 shows the composition of a range of various hydrothermal fluids expressed in terms of temperature and salinity. Also plotted on the diagram is the likely range in compositions for connate brines which constitute part of the metadomain alteration fluids.

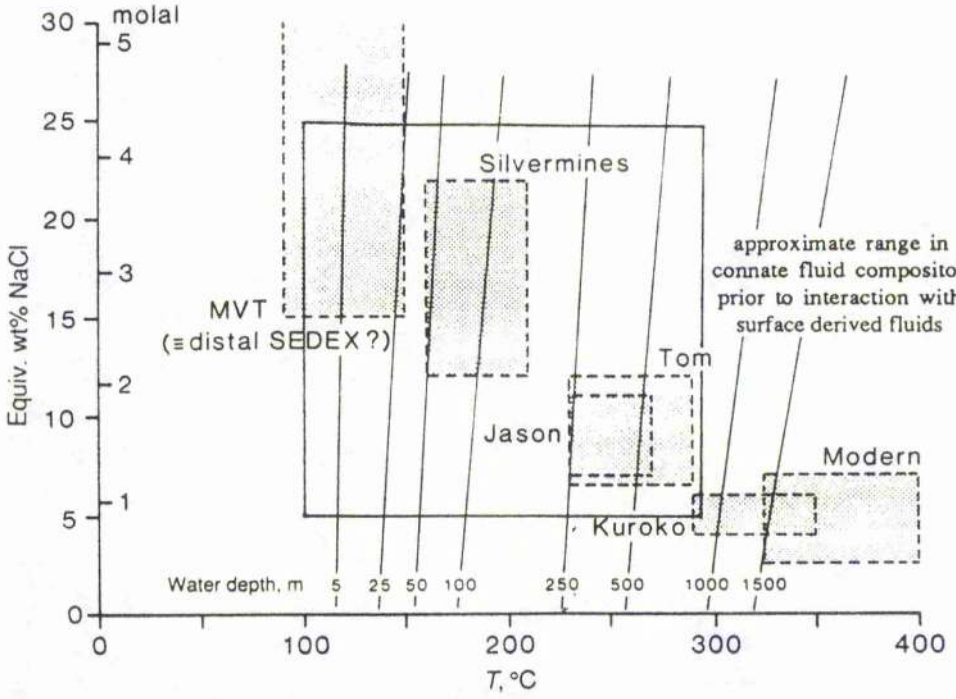

Figure 5.13 Temperature-salinity variations in hydrothermal fluids from a range of environments (Sato, 1972). Also shown in the likely compositional range in connate fluids prior to interaction with surface derived fluids within the Clyde Lava metadomains as determined from fluid inclusion analysis of calcites

It can be seen that these fluids are characteristically of low to intermediate temperature and of high salinity, similar in nature to fluids representing proximal sedex deposits. Sato (1972) described such fluids and suggests that they have densities only slightly lower than seawater. Such fluids are unlikely to mix readily with surface derived fluids owing to density contrasts, and it is perhaps this reason why there is often a marked bimodal distribution in salinities within a given sample.

Large volumes of data from oilfield brines and fluid inclusions from Mississippi Valley-type deposits (Sangster, 1990) demonstrate that such fluids are capable of carrying sufficiently high concentrations of base metals to produce major ore districts. This process has occurred to the south within the Southern Uplands. Samson and Banks (1988) report that the mineralizing fluids in this province were of relatively low temperature (c.150 °C), high salinity, NaCl + $CaCl_2$ dominated modified meteoric fluids on the basis of fluid inclusion and stable isotopic data. These authors propose a Dinantian age for the mineralizing event which

is similar to that which is proposed for the metadomain alteration in the Clyde Lavas. Clearly, the fluids reported in this study share many of the characteristics of the fluids found within the Southern Uplands. Also, brines associated with Pb-Zn-Ba sedex deposits from Silvermines, Ireland reported by Samson and Russell (1987) share many of the characteristics of fluids from the Clyde lavas. These include low eutectics, high salinities (18 to 22 equiv wt. % NaCl) and homogenisation temperatures ranging from 50 to 260 °C. These authors envisage convection and interaction of Carboniferous surface fluids with thick geosynclinal sequences, granitoids, plus a contribution from lower Paleozoic formation waters.

The similarity in fluid compositions between the three provinces is striking, begging the question: why is there not large scale development of base metal mineralisation of Dinantian age within the Clyde area? Minor amounts of native copper are found at Boyleston Quarry. Also, Stephenson and Coats (1983) note minor native copper mineralisation in the Renfrew Hills which ranges from replacement of plant debris by malachite in sandstones belonging to Lower Limestone Group to direct association of native copper with basaltic lavas. These authors also report Ba mineralisation of inferred Upper Carboniferous age within the Misty Law trachytic complex resulting from circulation and mixing of low temperature Ba-rich brines with oxidised, sulphate bearing groundwaters.

Clearly, heat flow within the area is likely to have been enhanced at the time of lava eruption within the Midland Valley providing a heat engine to drive hydrothermal circulation. Strens et al. (1987) demonstrate that hydrothermal systems capable of generating the very largest Pb-Zn deposits requires geothermal gradients ranging between 30 °C km^{-1} (fluid circulation to 10km) to 60 °C km^{-1} (fluid circulation to 6km). There are two possible explainations for the apparent observed lack of large scale base metal deposits within the area. Firstly, there exists the possibility that the metals were not available to the system. Secondly it is possible that there is significant base metal mineralisation at greater depths within the Lower Carboniferous sequence. In classical models of hydrothermal circulation (eg.Craw et al., in press) copper enrichment generally occurs within intermediate levels of the system where significant fluid mixing occurs, whilst other base metals are found at greater depths.

5.5.3 A model for copper mineralisation within the lavas

The occurrence of native copper and its derivatives (eg.cuprite and malachite) at Boyleston Quarry is well known (Bluck, 1973). It is found as small nuggets and streamers within both analcime, prehnite and calcite rich veins, suggesting precipitation was occurring throughout metadomain development. The low concentration of copper at Boyleston renders it an uneconomic reserve.

Johnstone et al. (1990) suggest that transport and deposition of copper within the Sothern Alps hydrothermal system, New Zealand, is controlled by redox conditions. Oxidised Cu enriched meteoric water mixes with upwards moving, reduced metamorphic fluids, the result being the precipitation of a range of copper bearing minerals. A similar model can be used to account for the precipitation of native copper at Boyleston Quarry.

It has been suggested previously, on the basis of fluid inclusion evidence, that mixing of surface derived fluids and deeper connate brines occurred at Boyleston. It is likely that the connate brine was relatively reduced, especially if there are significant quantities of organic material present within the sequence. Thus this locality represents a redox interface where precipitation of native copper occurred as surface derived solutions which were enriched in copper chloride and hydroxide complexes mixed with reduced brines. Pollard et al. (1990) show that native copper is stable at Eh ranging from 0.0 to 0.2 volts (corresponding to a very slightly oxidising environment) and over a pH range of approximately 4 to 8.

As the surface derived fluid descended through the lavas and was heated it would have become progressively enriched in copper, which was removed from the host basalt. Jolly (1974) suggests that basalt is a potential source of copper within low grade hydrothermal systems. Furthermore, Seyfried and Bischoff (1977) have shown that at 260 °C seawater reacted with basaltic glass under water dominated conditions effectively leaches and maintains copper in solution.

The reason why high grades of copper mineralisation are not seen at Boyleston, or elsewhere is probably twofold. Firstly, the volume of basalt through which fluid would have

been transported in the Clyde Lavas is much lower than that for classic mineralised flood basalt provinces such as the Keweenawan Basalts of Michigan which reach thicknesses of up to 8 000 metres. This factor also probably explains why copper is not found at High Craigton Quarry, where mixing is also thought to have occurred; fluid inclusion evidence indicates that this area was a near surface system. Secondly, copper solubility is favoured by high Cl^- cncentrations (Johnstone et al., 1990); fluid inclusion evidence indicates that surface derived fluids were relatively dilute.

5.6 Fluid extraction analysis

5.6.1 Introduction

In order to establish the nature of the volatile phase present within inclusions use has been made of the fluid extraction facility at St. Andrews University. Such volumetric methods of inclusion-gas analysis involves cryogenically separating the various gases into discrete groups based upon freezing point variations and measuring the pressure of these gases in known volumes. From this it is possible to calculate the standard volumes of the gases and thus obtain a semi-quantitative analysis in a relatively short period of time. The method differs from normal fluid inclusion analysis in that it is destructive because gases for analysis are released by stepwise heating and decrepitation of inclusions within a sample thus releasing the volatile phase.

5.6.2 Method

A sample of known weight (correct to 4 significant digits) is transferred on the line and heated to 110 °C for approximately 30 minutes in order to remove any labile water. Following this, the sample is heated to 450 °C +/-10 °C for approximately 10 minutes during which time decrepitation of inclusions occurs and the contents are released into the line. Above 480 °C carbonate begins to decompose (Behar and Pineau, 1979) therefore care was taken to ensure the temperature was maintained well below this value. Once the gases are released from the sample they are passed through a cold trap containing liquid nitrogen (at ~195 °C). At this temperature gases including H_2O, CO_2, NH_3 are frozen down during which time the pressure of the non-condensable gases (CH_4, N_2) is measured. Following this, the cold trap is removed and the gas pressure within the line is taken after 45 seconds during which time any frozen CO_2 present will have vapourised. The line is then gradually warmed in order to vapourise H_2O and the maximum transient pressure recorded. From these three

readings it is then possible to calculate the relative abundance of non-condensible gases (CH_4, N_2), CO_2 and H_2O. Since sample weight is accurately measured results are expressed as moles per gramme of sample (mol g^{-1}).

In addition the extraction line at St. Andrews is coupled to a gas chromatograph which is able to receive and analyse the non-aqueous condensible and non-condensible phases. Full details of this instrument are given in Appendix 5.2. Analysis of the output from several G.C. runs showed that CO_2 constituted >99 % of the fraction released from the freezing loop after 45 seconds. Also detected were N_2 and traces of CO within the non-condensible fractions. The former may either represent the major component of the non-condensible phases or possible leakage of atmospheric air into the G.C. system. Also, it is likely that CO is not a primary gas but may be generated via the thermal degradation of organic matter trapped within the calcite samples during each heating run.

5.6.3 Results and discussion

Samples of calcite were taken from metadomain localities at Boyleston Quarry, Langbank Cutting and High Craigton Quarry (details are given in Appendix 6.1). The overall aim of the study was twofold:

1. To establish the relative abundance of the three main components constituting the inclusion fluids across the Clyde Lavas, i.e. non-condensible gases, CO_2 and H_2O and to compare the values obtained from this study with those from active geothermal systems.
2. To assess if it is possible to use the technique in order to discriminate between fluids which are boiling and those below their critical curve; it has already been suggested that localities which contain populations of inclusions with varying phase ratios might represent boiling assemblages. Such an assemblage might be expected to possess high CO_2 concentrations because this phase is strongly partitioned into the vapour phase.

Given below in Figure 5.14 are the results of 20 analyses performed upon calcite samples collected from the Clyde Lavas (see Appendix 6.1 for details).

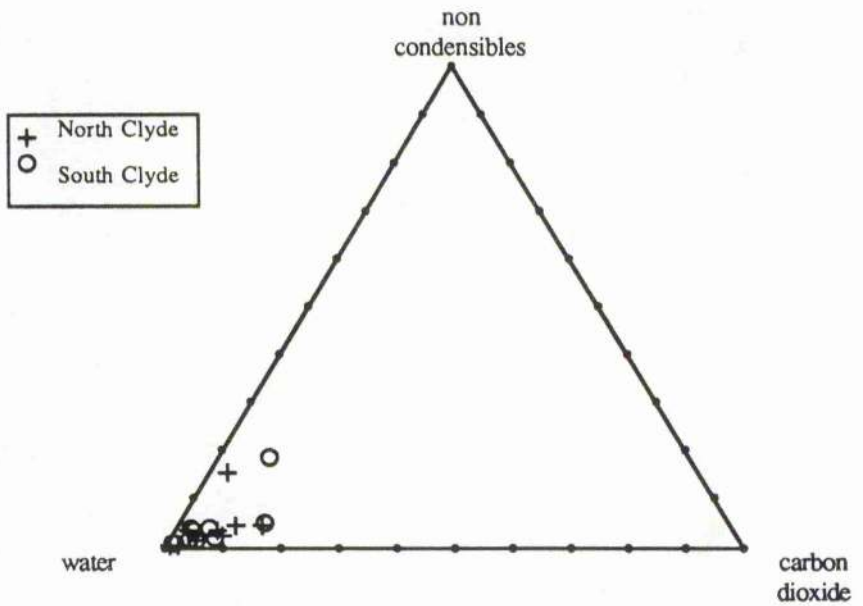

Figure 5.14 Triangular diagram illustrating the proportions of phases within fluids extracted from metadomain calcites by thermal decrepitation

The relative proportions of the three main phases (water, carbon dioxide and non-condensables) are shown in this diagram. Full analyses as expressed both as moles per gram of calcite and relative percentages can be found in Appendix 5.2.

It can be seen from the diagram that the fluids present during the precipitation of calcite within the metadomains appear to be fairly uniform in composition as expressed in terms of the relative proportions of H_2O, CO_2 and non condensibles. Furthermore, all of the samples analysed are water rich with the relative proprtion of H_2O ranging from approximately 70 to >95 %. However, some samples from widely spaced localities appear to contain significant quantities of non-condensible gases which may reflect input from organic matter within the sedimentary succession which was undergoing thermal maturation.

Using the data obtained from fluid extraction analysis it is possible to express CO_2 concentrations within the fluid in terms of moles CO_2 per kg of water. Several studies includng that of Arnorsson et al. (1983) have proposed gas thermometers on the basis that gas concentrations in geothermal fluids are controlled by temperature dependent equilibria with alteration minerals present within the reservoir rock. In Table 5.2 below compositional data is recalculated and expressed as moles CO_2 per kg of water is presented for each analysis.

Fluid inclusion evidence presented above indicates that fluid temperatures ranged from approximately 50 °C up to 300 °C. Therefore, it is possible to express fluids present during calcite precipitation in terms of compositional and temperature variations as shown in Figure 5.15.

Sample No.	log molCO_2/kg H_2O	Sample No.	log molCO_2/kg H_2O
Mg1C	1.07	4A	-0.04
C3	0.32	2A	1.07
2A	0.68	3B	-0.17
3A	0.54	B5	0.43
C1	0.90	C6	0.33
4B	0.84	C7	1.14
X3	0.99	X1	0.73
Mug 2	0.81	Mg1A	0.24
Mug 3	1.10	HC5	0.12
HC 10	0.88	HC_{mise} 2	0.47

Table 5.2. Fluid compositions from metadomain calcites expressed as mol CO_2/kg H_2O

Unfortunately, paired temperature-composition data was not available so only the range is shown. Also shown is data from Arnorsson and Gunnlaugsson (1985) which shows concentrations of CO_2 in geothermal reservoir waters. It can be seen that the CO_2 contents of fluids present during the precipitation of calcite within the metadomains are significantly higher than those predicted using the data of Arnorsson and Gunnlaugsson (1985), often by a factor of up to 10^2. This suggests that CO_2 concentrations within the geothermal fluid were not controlled by fluid-mineral equilibria but that an additional source of CO_2 was available. This might include CO_2 generated during the thermal maturation of organic matter within the sediments underlying the lavas.

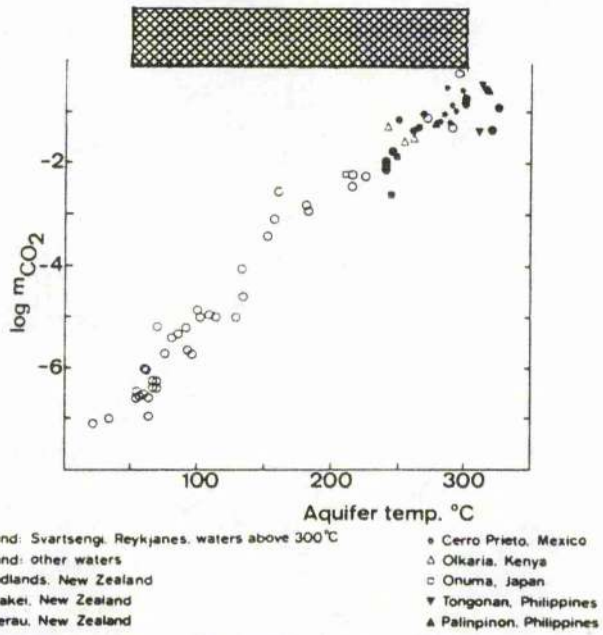

Figure 5.15 Temperature-CO_2 relationships in hydrothermal waters from a range in environments (Arnorsson and Gunnlaugsson, 1985) Also shown is the approximate temperature-compositional range of metadomain fluids (stippled area) as determined from combined fluid inclusion-extraction analysis of calcites.

Figure 5.16 shows how the ratio between CO_2 and non condensibles varies within fluids present at the time of calcite precipitation.

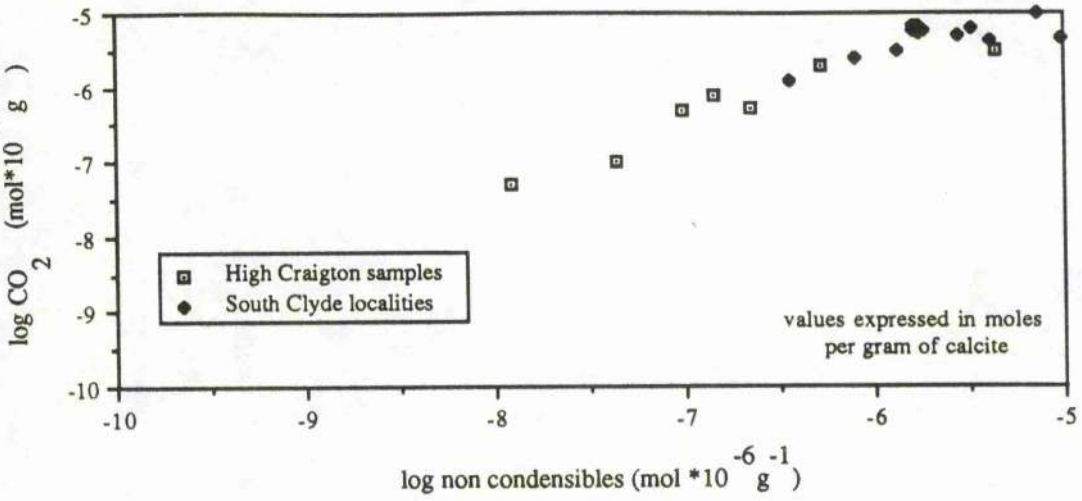

Figure 5.16 Compositional variation in the gas content of metadomain fluids present at time of calcite precipitation

It can be seen that at even at widely spaced localities the ratio CO_2 / non-condensible gases remains relatively constant. It is also apparent that the absolute concentration of both of these

parameters differs markedly in that samples from High Craigton Quarry are more depleted in both CO_2 and non-condensible gases than samples collected south of the Clyde. It was stated earlier in this Chapter that fluid boiling is thought to have occurred at High Craigton Quarry on the basis of fluid inclusion evidence. Such a process would lead to an overall decrease in the concentration of dissolved gases in the residual fluid because of partitioning of gases into the escaping vapour phase as discussed by Giggenbach (1981). Such a process would also lead to calcite precipitation as discussed in Chapter 2 and also provides a possible explanation for observed variations in the absolute concentration of gaseous phases within metadomain fluids.

5.7 Conclusions

a. Analcime

Fluids present during the formation of analcime are typically of very low salinity and show a restricted range in temperature (180 to 220 °C). Mean homogenisation temperature is relatively high (203 °C). This fluid is unusual in that it appears to have transported significant quantites of hydrocarbon rich material, inferring that it came into contact with organic rich sediments during its history. If metadomains developed prior to burial, then a possible source rock may be the Ballagan Formation of the Inverclyde Group. Within the Campsie Fells these beds reach a maximum thickness of 500 metres (Francis, 1983). Upon heating the hydrocarbon material begins to change colour at approximately 230°C, which is similar to results obtained by Hall et al.(1989). This probably represents a maximum trapping temperature for the hydrocarbons. If the fluid did interact with the Ballagan Formation it would be expected that salinity would be markedly higher than that which is observed. This might not be the case if fluid residence time within the sediments was short.

b. Calcite

Fluids present during deposition of calcite within the metadomains across the lava field typically apear to be Ca^{2+}, Na^{+}, Cl^{-} dominated brines which showing a very wide range of salinites (ranging from approximately 0 to 25 equiv. wt. % NaCl). These brines also show a wide range in temperatures, ranging from approximately 50 °C up to 300 °C. It appears that these brines are actually a hybrid formed during the interaction and various degrees of mixing between two "end-member" fluids. One fluid appears to have been a connate brine at high temperature whilst the other appears to have been a low salinity, surface derived fluid which was progressively heated during advection through the lavas. The situation is further complicated since it appears that as well as mixing there have been various degrees of boiling of the hybrid, possibly followed by further mixing. Such processes are found to occur throughout the shallow parts of geothermal systems worldwide. Following initial precipitation of calcite during metadomain activity there appears to have been a later fluid event, possibly related to burial of the lavas. This fluid is characteristically of low salinity and low temperature (estimates range from 80 to 110 °C).

Fluid extraction analysis provides a means of determining the absolute concentrations of gaseous components within fluids trapped at the time of calcite precipitation. CO_2 concentrations within fluids present during calcite precipitation are higher than predicted using information from Arnorsson and Gunnlaugsson (1985) by up to a factor of 10^2. This suggests that CO_2 concentrations were not controlled by mineral-fluid equilibria but that an independent reservoir was involved. One possible source may have organic matter undergoing thermal decomposition within the underlying sediments which also appear to have supplied hydrocarbon material to the metadomain fluid. It also appears that physical processes such as fluid boiling also exert an influence on absolute gas concentrations within the hydrothermal fluid.

CHAPTER 6 STABLE ISOTOPIC ANALYSIS

6.1 Introduction

Stable isotopes were analysed to determine the nature and origin of the fluid phase(s) which were present during metadomain activity. Craig (1956) demonstrated that most hot fluids (>95%) from geothermal systems world-wide are ordinary surface derived fluids. However, Hall et al. (1989) recognised two distinct alteration fluids present at Boyleston Quarry on the basis of a combined fluid inclusion and stable isotopic study. These fluids consisted of a relatively high temperature (>100 °C) surface fluid which appeared to have exchanged oxygen isotopes with hot igneous rock, and a lower temperature (c. 85 °C) surface derived fluid. Also, carbon isotopic data testified to the presence of organic derived CO_2 within these fluids, which was consistent with the concept that the fluids had interacted with sediment hosted organic matter at some stage in their evolution (also advocated in this study). However, evidence suggesting that inorganic carbon (eg. from limestone or seawater bicarbonate) was an important source during calcite formation was not found. This is unusual since carbonate rich sequences occur both above and below the lavas and Francis (1983) suggests that the area was subject to periodic marine incursion during the Dinantian.

Stable isotopic analysis, when combined with fluid inclusion data provides a powerful way of assessing fluid origins and history in hydrothermal environments. The aims of this study were:

1. To study the isotopic composition of carbonates which were found throughout the lavas. This could be used to examine critically the existence of two distinctive fluids at Boyleston Quarry. Is it possible that the findings of Hall et al. (1989) were real, or apparent because of a sampling bias? Analysis of material from other localities could be used to elucidate the nature of the fluid phase present during metadomain alteration across the lava field. Also, carbon isotopic results could be used to identify posible sources of carbonate carbon within the lavas.
2. To study paragenetically early analcime of hydrothermal origin recorded from metadomains within the Clyde Lavas. Recent studies by Karlsson and Clayton (1990) suggests that the partitioning of oxygen isotopes between analcime and water are similar to those of calcite-water. Hence, estimates of fluid composition from analcime $\delta^{18}O$ values could be derived from the

calcite-water fractionation curve, given estimates of formation temperature from fluid inclusion studies.

3. To estimate the isotopic composition of the fluids found at differing times during metadomain development (analcime is always the first phase to form). Having established the nature of the fluid(s) responsible for the formation of each species, it then becomes possible to assess how fluid compositions may have evolved during metadomain development.

6.2 Theoretical Basis

During water-rock interaction the final isotopic composition of a particular fluid is controlled by four fundamental factors:

1. The temperature of interaction.
2. The initial isotopic composition of the rock.
3. The isotopic composition of the hydrothermal fluid.
4. The water-rock ratio; the relative numbers of atoms involved in the exchange process; essentially a measure of hydrothermal intensity.

These factors are discused in detail below. The following section deals briefly with the notation used in the measurement and interpretation of isotopic data and the basic principles of isotopic fractionation.

6.2.1 Notation and basic principles

The variations in the ratios (R) of heavy to light isotopes in minerals are measured on released gases by mass spectrometer. The relative variation in isotopic ratio can be measured more accurately and precisely than the absolute ratio, and is therefore measured relative to an arbitary standard. For isotopes of oxygen the ratio is expressed relative to Standard Mean Ocean Water (SMOW) (Craig, 1961); for carbon the ratio is expressed relative to a belemnite from the Cretaceous Peedee Formation (PDB) (eg. Field and Fifareck, 1986).

Differences in ratio of the sample (R_x) with respect to that of the standard (R_y) are expressed as deviations from the standard by del (δ) values in parts per thousand (per mil or ‰) as given by :

$$\delta\,^{18}O\ (‰) = ((R_x / R_y) - 1)/1\,000$$

The fractionation factor (α) quantifies the partitioning of isotopes between two species, where the species may be either minerals, waters or gases. The fractionation factor for two species is given by

$$\alpha_{ab} = (R_a / R_b)$$

Thus, it follows:

$$1\,000 \ln \alpha_{ab} \sim \delta_a - \delta_b$$

This approximation holds well for values < 10. It is common to find $\delta_a - \delta_b$ referred to as $\Delta_{a\text{-}b}$.

The extent to which an isotopic species fractionates between for example, a mineral and a fluid is dependent upon the vibrational frequencies of the species concerned. These in turn are controlled by the temperature at which interaction occurs. The various equilibrium fractionation factors between minerals and waters have been determined from theoretical considerations or empirical studies. Equilibrium fractionation equations for isotopic reaction pairs of geologically important compounds are readily available in the literature (for example, Friedman and O'Neil, 1977). These equations take the general form:

$$1\,000 \ln \alpha = a\,(10^6\,T^{-2}) + b$$

where a and b are coefficients characteristic of the reaction pair and T is the temperature in degrees Kelvin. Thus, given a knowledge of the temperature of interaction, it is possible to determine the isotopic composition of the fluid by measuring the isotopic composition of the mineral with which it equilibrated.

6.2.2 Isotopic composition of natural waters

Before discussion of isotopic interaction between minerals and fluid within the metadomains it is appropriate to define the isotopic composition of selected fluids which might be expected to occur within the context of the Clyde Lavas.

Figure 6.1 shows the range in isotopic composition of selected natural fluids and common rock types as defined by their hydrogen and oxygen isotopic signatures. Attention is

drawn to the following fluids which are shown on the diagram.

1. Meteoric waters

Present day meteoric waters have δD and $\delta^{18}O$ values which vary systematically (Craig,1963). The $\delta^{18}O$ values of most surface waters are linearly correlated with δD such that :

$$\delta D = 8\,\delta^{18}O + 10$$

Most meteoric waters which have not undergone extensive evaporation plot within a band up to +/-1 per mil of this line (Sheppard, 1986). The values are dependent on geographic location. In general, meteoric waters become isotopically lighter with increased distance from the equator.

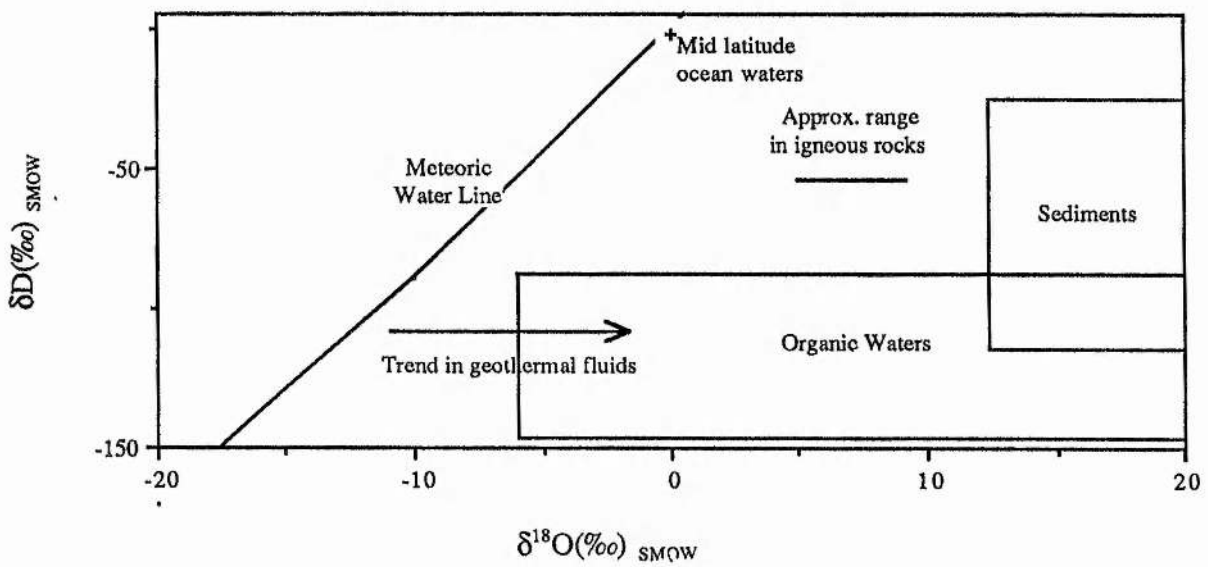

Figure 6.1 Stable isotopic composition of some natural fluids and common rock types (from Sheppard, 1986)

Meteoric water can enter rocks as groundwater whose isotopic composition is similar to the local precipitation. This may not be the case in arid regions where its composition may be modified by evaporation processes. Fallick (pers.comm.) has suggested that the local $\delta^{18}O$ value for Carboniferous meteoric water was approximately 0‰. This is consitent with a sub-equatorial palaeo-latitude for the Midland Valley during the Lower Carboniferous as suggested by Francis (1983).

2. Oceanic waters

These are defined by Sheppard (1986) as waters of the open oceans and seas having direct contact with the oceans, thus excluding intracontinental seas. It is thought that the most profound control on overall isotopic composition is the volume of isotopically light water held within the polar ice caps. On Figure 6.1 SMOW (Standard Mean Ocean Water) is defined as having both a hydrogen and oxygen isotopic composition of 0 ‰.

3. Formation (connate)waters

Sheppard (1986) defines formation waters as those found within interstices and pores within sediments implying no connection with their age or origin. Taylor (1974) notes that waters initially termed connate i.e. waters trapped within sediments at the time of their formation, frequently contain large quantities of meteoric water which have been flushed through palaeo-aquifers. These waters are frequently of high salinity because of evaporite solution during transport.

The range in $\delta^{18}O$ values of fluids recovered from sedimentary basins is very large (-20 to 10 ‰). Ohmoto (1986) points out that low salinity, low temperature brines have the lowest $\delta^{18}O$ values, whilst the reverse is true for higher temperature, high salinity fluids. The final $\delta^{18}O$ value will be controlled to a large extent by the type of sediment encountered by the fluid, as well as fluid temperatures. For example there is a large potential for exchange within a reactive carbonate-rich sequence, whilst the potential for exchange with silica-rich sediments will be limited, especially at lower temperatures.

4.Organic waters

Sheppard (1986) also distinguishes organic waters as those whose δD value is controlled by transformation and maturation of sedimentary organic matter. The $\delta^{18}O$ values of such fluids are controlled by the O-isotopic composition of the host rocks and temperatures of exchange.

6.2.3 Geothermal fluid compositions : Oxygen isotopic exchange

Sheppard (1986) points out that water from most geothermal systems is of surficial, rather than deep seated origin. However, the composition of many of these fluids is modified due to interaction with host rocks, usually at elevated temperatures. Craig et al. (1956) showed that the δD values of these fluids were in most cases identical to those of the local surface waters. This is

interpreted as being due to the fact that even though hydrogen isotope exchange is occurring, the system as a whole is buffered by the isotopic composition of the fluid phase. This is because the amount of hydrogen in rocks is much less than that in water.

In contrast the $\delta^{18}O$ values of geothermal waters are often significantly higher than that of the local meteroic water. This increase in $\delta^{18}O$ value of the fluid is termed O^{18} exchange, reflecting isotopic interaction between heated surface waters and ^{18}O enriched rocks. Generally, the largest shifts occur in the hottest, most saline fluids, though the magnitude of the exchange is highly variable. Figure 6.2 illustrates the magnitude of this exchange for a range of geothermal systems. It can be seen that at Wairakei (New Zealand) there is a general lack of exchange which is attributed to high water-rock ratios. The pronounced shift at Niland (Salton Sea geothermal area) is thought to be due to high temperature (c.300°C), rapid fluid exchange with fine grained carbonates. Similarly, fluids from Lanzarote show a shift of approximately +15 ‰.

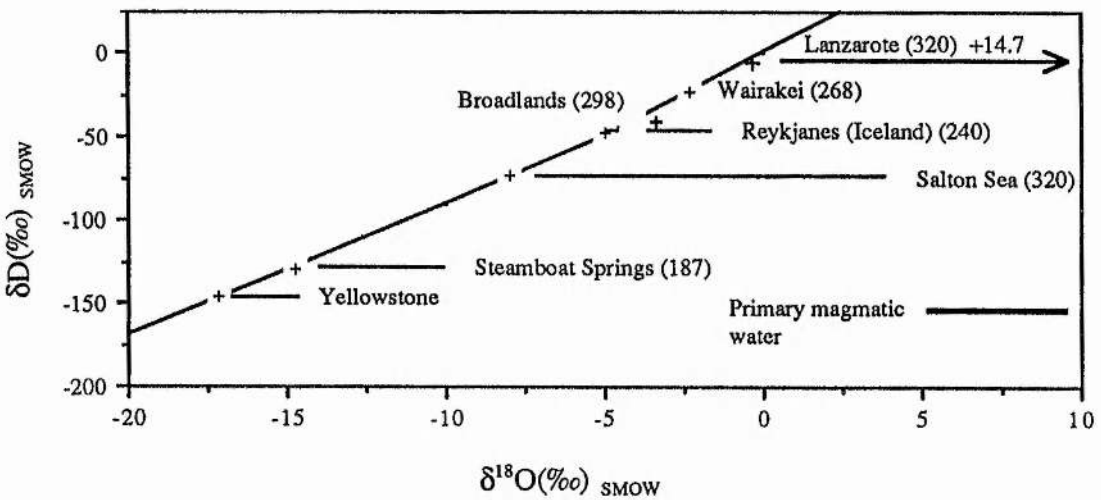

Figure 6.2. Isotopic composition of geothermal waters compared with the composition of local meteoric waters (marked+). Figures in brackets indicate temperatures in °C (Sheppard, 1985).

It is often found that rocks in many active and extinct geothermal systems are highly depleted in ^{18}O relative to normal rocks. For example, although unaltered igneous rocks worldwide display a restricted range in oxygen isotopic composition (typically +5.5 to +10.0‰), within the Scottish Tertiary volcanic centres the average depletion in ^{18}O is approximately 6-7 ‰ within rocks that have undergone exchange with meteoric groundwaters (Taylor and Forester, 1971). This is because any

^{18}O enrichment within the circulating geothermal fluid is offset by a corresponding depletion in ^{18}O within the country rocks.

Isotopic compositions of acidic hot springs such as those found at Yellowstone often display lighter δD signatures than their local meteoric equivalents. This is due to kinetic effects associated with boiling and evaporation. Truesdell and Nathenson (1977) calculaled that single steam separation from 250 °C to 95 °C i.e. the vapour phase remains in contact with the liquid over this temperature range, results in increases in Cl, $10^3 \ln \alpha^{18}O$ and $10^3 \ln \alpha D$ of 1.44 times, 1.75 ‰ and 9.1 ‰ respectively. These latter two values are much reduced for continuous steam separation which involves continuous removal of each steam fraction as it forms.

6.3 Carbon isotope systematics

6.3.1 Causes of isotopic variation

Variations in the isotopic composition of carbon bearing species found within nature are principally due to redox reactions. The major carbon bearing compounds within the geological environment are wide ranging, being both organic and inorganic in origin. Within such compounds carbon occupies a number of valency states, such as C^{4-} within organic compounds to C^{4+} in carbonate minerals. A large number of physiochemical and biological mechanisms control the oxidation state of the carbon and large kinetic isotope effects are associated with these processes, especially reduction which results in large Δ values between the oxidised and reduced species. For example, Hoefs (1980) in Ohmoto (1986) suggests that the bacterial reduction of seawater bicarbonate to form methane results in a depletion of approximately 110 ‰ within the reduced species. There is a tendency for preferential enrichment of the heavier isotope within the compounds possessing carbon in a high oxidation state. Therefore, under equilibrium conditions

$$\delta^{13}C \text{ carbonate} > \delta^{13}C \text{ graphite} > \delta^{13}C \text{ methane}.$$

Attention is drawn to the following types. Further details are given in Ohmoto (1986).

6.3.2 Isotopic variations within carbon bearing species

Attention is drawn to Figure 6.5 which shows the isotopic compositions of the main carbon bearing compounds within the near surface geological environment together with the values determind for carbonates from the Midland Valley following a number of independent studies. Dissolved carbonate within the oceans (mostly as HCO_3^-) has $\delta^{13}C$ values near 0‰ whilst $\delta^{13}C$ of modern marine limestone ranges from approximately -1 to +2‰. Phanerozoic marine limestones show a slightly greater range in $\delta^{13}C$ from -2 to +4‰. The similarity in $\delta^{13}C$ between dissolved carbonate and limestone suggests isotopic equilibrium between the two and the cluster of values around 0‰ is to be expected since the carbon standard (Peedee Belemnite) is of marine derivation. Freshwater limestones are generally characterised by slightly lighter $\delta^{13}C$ values because of a larger contribution from CO_2 generated by the oxidation of organic matter within the environment.

Fluids may acquire carbon from dissolution or decarbonisation of carbonate rich rocks. Ohmoto (1986) concludes that the carbon isotopic composition of the fluid will depend upon : 1) The $\delta^{13}C$ value of the rock. 2) The relative proportions of the aqueous carbonate species. 3) The degree of isotopic fractionation between carbon bearing species within the fluid and carbonate minerals.

4) The extent to which the carbonate minerals decompose. If equilibrium between the aqueous species and the carbonate minerals is not established dissolution or decarbonisation may proceed without any isotopic effect upon the fluid.

Fractionation which results from the uptake of hydrospheric and atmospheric inorganic carbon via photosynthesis to form organic carbon leads to a marked depletion in the isotopic composition of both marine and land plants. The $\delta^{13}C$ value of marine organic carbon varies between -30 and -10 ‰ with a mean value of approximately -22 ‰. Mean $\delta^{13}C$ for terrestrial organic matter is slightly lower at -26 ‰ (Ohmoto, 1986). Reduction of HCO_3^- to CH_4 by bacteria at the sediment-water interface can lead to extreme depletions producing $\delta^{13}C$ values ranging between -55 to -110 ‰.

Hunt (1979) indicates that the production of thermogenic CO_2 from sedimentary organic matter commences at approximately 50 °C. It is thought (Ohmoto, 1986) that the $\delta^{13}C$ value of CO_2 produced in this manner is very similar to that of the parental organic matter. However, CH_4 generated primarily by thermal cracking of aliphatic groups above 100 °C (Hunt, 1979) shows depletion in the heavier isotope with $\delta^{13}C$ values ranging between -35 to -55 ‰. Therefore, as diagenesis continues the net effect is to produce residual organic matter which becomes progressively enriched in ^{13}C.

6.3.3 Carbon bearing species in the hydrothermal environment

Field and Fifarek (1985) show that carbon bearing species within hydrothermal environments show a relatively restricted range in $\delta^{13}C$ values ranging from approximately -20 to +2 ‰ (PDB). Calcites recovered from geothermal areas show a slightly narrower range from -15 to +1 ‰ as shown in Figure 6.5. Variations in the isotopic composition of oxidised carbon bearing species can often be attributed to variations in the relative contributions of multiple sources. For example, calcites recovered from drillcores within the Yellowstone geothermal area exhibit a restricted range in carbon isotopic composition from -4 to -1 ‰ (Keith and Muehlenbachs, 1990). This is attributed to equilibration with fluids having dissolved bicarbonate ranging from -2 to 0 ‰. However, Sternfield (1981) suggests that the wide variation in isotopic composition of individual oxidised carbon species within the Geysers geothermal system (for example calcites with $\delta^{13}C$ values ranging from -15 to +1 ‰) is due to input from biogenic, marine and magmatic carbon in igneous and sedimentary host rocks at differing times during geothermal development. Extreme depletions in the $\delta^{13}C$ values of carbon bearing species is often attributed to interaction between hydrothermal fluid and organic matter hosted within sediments. For example, Kesler et al.(1981) report $\delta^{13}C$ values as low as -25 ‰ (PDB) for carbonaceous material recovered from a volcaniclastic horizon within the extinct Pueblo Viejo hydrothermal system.

Ohmoto (1986) suggests that the exchange of carbon isotopes between species occupying the same valency state (eg. HCO_3^- and CO_2) is sufficiently rapid to allow equilibrium to be established. Sturchio et al. (1990) suggest that calcite will exchange carbon isotopes with

hydrothermal fluid relatively rapidly at temperatures as low as approximately 120 °C. However, several studies such as that by Welhan (1988) suggest that within most hydrothermal systems equilibrium between species in which carbon occupies differing valency states (eg. CH_4 and CO_2) is not attained. Data reported by Ohmoto (1986) for several independent studies of active hydrothermal systems worldwide all show that $\Delta\ (CO_2\text{-}CH_4)_{observed} < \Delta\ (CO_2\text{-}CH_4)_{predicted}$ for systems where fluid temperatures are less than 300 °C confirming that equilibrium is not attained. If exchange rates are extremely slow then the carbon bearing species will retain its isotopic signature during transport from source to site of deposition. Therefore, wide variations in the carbon iotopic composition of carbon bearing species within hydrothermal systems where fluid temperatures can be demonstrated to be less than 300 °C are likely to be due to variation in the source of carbon. For example, McKeag et al. (1989) suggest that carbonates with $\delta^{13}C$ values ranging from approximately -1 to -12 ‰ (PDB) found within graphitic schists at the Macraes hydrothermal system, New Zealand periodically received varying quantities of carbon from the surrounding schists.

Given the $\delta^{13}C$ value of a particular carbonate mineral it is possible to determine the composition of the fluid with which the carbonate equilibrated based on fractionation factors between the mineral and dissolved carbon bearing species (such as bicarbonate). This is because fractionation temperatures are a function of temperature. Thus the following approximation is made, based on the assumption of equilibria amongst species of equal valencies:

$$\delta^{13}C_{\Sigma\ CO2} = \delta^{13}C_{carb.\ min.} - \Delta_{carb.\ min. - H2CO3} \qquad \text{(Ohmoto, 1985)}$$

This type of approach is adopted in Section 6.5 below. Alternatively, if it can be demonstrated that equilibrium between carbon species with varying valency states has not been achieved (a reasonable assumption at fluid temperatures below 250 °C) $\delta^{13}C_{\Sigma\ CO2}$ values can be used directly to estimate the source of carbonate carbon using the criteria outlined in Section 6.3.2.

6.4 Sample preparation and experimental techniques

Mineral samples were selected from metadomains across the Clyde Lavas (full details

are given in Appendix 6.1). Selection criteria were based mainly on mineral availability, the majority of the samples coming from Boyleston Quarry where analcime mineralisation is widespread. However, within this locality care was taken to collect samples from a wide range of representative vein and amygdale localities. For calcite, analysis of CO_2 released following reaction with phosphoric acid was carried out whilst for analcime, oxygen isotopic analysis was performed on framework oxygen. Full details are discussed below.

1. Calcite

Samples were selected and handpicked from metadomains across the lavas, particular interest being paid to those samples which were found in close proximity to analcime. Samples were powdered to approximately 50 μm and purity was checked using XRD analysis. Of particular concern was the possibility of a discrete dolomitic component being present. Therefore, following the method described by Hutchison (1973) the position of the main calcite (001) peak was accurately measured. This was carried out by "spiking" each sample with Analar NaCl whose peak position was accurately known. The location of the carbonate peak on the XRD trace is a function of the degree of contamination by magnesium. For this study it was found that replacement of calcite by dolomite was extremely low (<2%).

Isotopic assay on calcite was carried out on CO_2 released following reaction for a minimum of 3 hours with phosphoric acid at 25 °C. Machine conditions are the same as those quoted for oxygen analysis. All carbon isotopic ratios are reported relative to PDB.

2. Analcime

Mineral separates were handpicked from veins and amygdales within metadomain basalts. Care was taken to remove any traces of carbonate material. Initially, samples were left overnight in 0.1 M HCl in order to remove any traces of carbonate. However, it was found that this procedure caused gelatinisation of the analcime and shifting of the characteristic XRD peaks to higher angles. Therefore, it was decided not to use this method. Prior to final crushing to less than 75 μm (<200 mesh) purity was confirmed using XRD analysis.

Karlsson and Clayton (1990a) demonstrate that only framework isotopic ratios may be used to constrain analcime formation temperatures and fluid compositions. In an accompanying paper Karlsson and Clayton (1990b) show that channel waters are inherited from the meteoric waters at the site of collection, since these waters plot near the meteoric water line and vary systematically with the latitude of the sample site. Therefore, in order to analyse the isotopic

composition of the analcime framewok oxygen it first necessary to remove all channel waters from the sample by dehydration.

Karlsson and Clayton (1990b) suggest that optimum dehydration conditions are those which allow complete dehydration at the lowest possible temperature over a reasonable length of time. They suggest dehydration under vacuum (~10^{-5} torr) lasting for 1to 5 hours to a maximum of 450 °C, with a heating rate of 2-4 °C min $^{-1}$. A pilot study was carried out at St. Andrews using fluid extraction apparatus in order to confirm total removal of channel water at 500 °C. This consisted of heating approximately 20 mg of powdered sample at a rate of approximately 5 °C min $^{-1}$ under vacuum and recording pressure readings at 1 minute intervals. The results of this run are illustrated on Figure 6.3 below and confirm that dehydration is complete at approximately 500 °C. Dehydration is always carried out outside the fluorination line, since the walls of the reaction vessels are coated in hygroscopic fluoride compounds which readily absorb water. Typically 10 mg of powdered sample was dehydrated under vacuum to 450 °C for a minimum of 2 hours. Prior to dehydration the samples were degassed under high vacuum overnight.

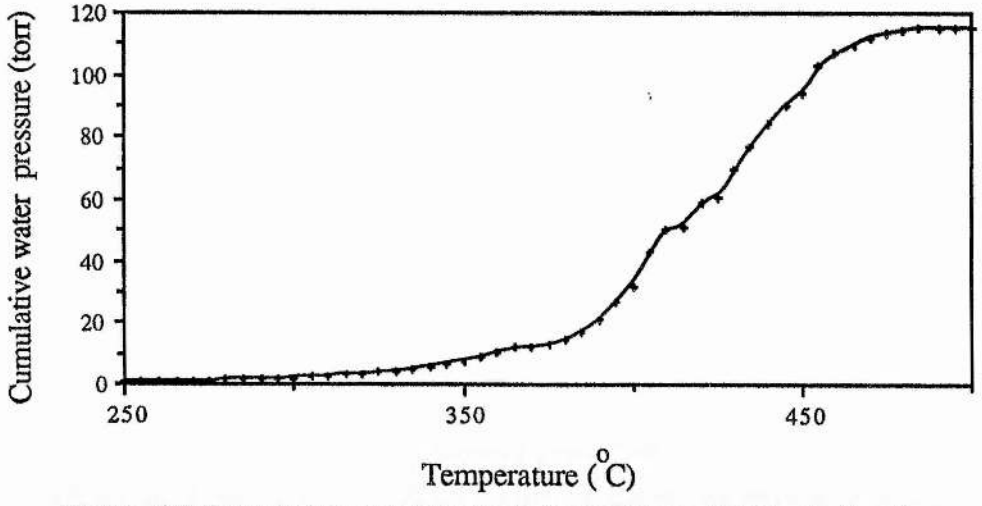

Figure 6.3 Cumulative water pressure-temperature plot illustrating the dehydration behavour of analcime from the Clyde Lavas

Stable isotopic analysis of silicates and carbonates was carried out at the Isotope Geology Unit, SURRC under the supervision of Dr A.E. Fallick. Oxygen was extracted from the dehydrated analcimes using the fluorination technique of Borthwick and Harmon (1982). This involves reaction with ClF_3 at 670 °C for 12 hours. Prior to fluorination samples were heated under vacuum to 200 °C and pre-fluorinated to remove any remaining moisture. Following gas collection, isotopic analysis was carried out using a VG SIRA 10 mass spectrometer calibrated

against NBS 28 ($\delta^{18}O$ = +9.60 ‰ relative to SMOW). All results are quoted relative to SMOW.

6.5 Results and Discussion

6.5.1 Calcite isotopic compositions

Combined carbon and oxygen isotopic analysis for 53 calcites are presented in Table 6.1 below. All analyses are given in per mil. Sample locations are given in detail in Appendix 6.2.

Sample	Yield ($\mu M\ mg^{-1}$)	$\delta^{18}O_{(SMOW)}$	$\delta^{13}C_{(PDB)}$	Sample	Yield ($\mu M\ mg^{-1}$)	$\delta^{18}O_{(SMOW)}$	$\delta^{13}C_{(PDB)}$
OL	8.33	+18.56	-6.93	WF5	4.79	+20.85	-12.59
WF8	6.02	+20.14	-12.08	WF2	7.34	+18.98	-7.43
S5	6.14	+20.86	-11.05	S3	6.64	+19.37	-6.60
B2	7.05	+21.35	-10.75	WF4	7.55	+26.35	-8.03
O2	7.06	+22.01	-7.77	B1	7.76	+18.68	-10.21
S7	5.44	+20.50	-10.85	E2	9.24	+21.07	-12.68
C5	18.87	+22.74	-10.35	S1	7.23	+22.12	+0.22
OM	7.93	+20.96	-10.47	O3	------	+22.56	-10.19
S6	6.99	+21.88	-10.66	$WF4_1$	7.32	+21.15	-11.16
$WF4_2$	5.16	+21.34	-8.21	$O2_1$	5.21	+20.89	-8.94
WF6	5.20	+23.82	-2.34	$CV86_4$	7.35	+21.40	-10.98
MQ	6.75	+17.99	-14.01	HC10	6.45	+16.42	-1.31
Mg1B	7.14	+17.49	-15.54	CPL1	6.56	+18.24	0.31
$CV86_1$	7.25	+22.91	-10.83	HC_{ms3}	7.94	+16.87	-10.87
HC_{msB}	8.11	+18.68	-10.51	HC9	6.89	+15.99	-10.32
HC5	8.13	+17.94	-10.47	MQ1	7.39	+15.67	-2.48
HC1	7.26	+21.94	-10.79	Mug2	5.84	+19.29	+1.18
AP3	9.11	+17.71	-19.63	HCN_2	7.84	+17.59	-10.51
HC_{ms2}	8.00	+17.93	-10.67	HC_{ms4}	7.46	+17.87	-11.03
CV86	7.68	+21.36	-10.86	Mug3	8.23	+15.61	-17.98
HCN5	8.10	+11.36	-3.99	HC_{msA}	7.74	+12.24	-11.53
HCN1	7.44	+16.65	-10.79	Mg1A	7.78	+18.17	-12.08
HC_{ms5}	7.64	+18.08	-10.69	HC8	6.51	+20.03	-10.25
LI2A	7.58	+22.83	-12.21	LI2B	7.54	+19.09	-11.53
$LBC2_5$	4.33	+20.07	-10.79	LC5	7.44	+21.86	-10.93
LB6	6.75	+23.09	-10.68	LC8	4.84	+19.08	-11.06
				LB1	6.38	+22.03	-11.31

Table 6.1 Carbon and Oxygen isotopic data for calcites from the Clyde Lavas

Mean yield is 7.26 μM CO_2 per mg of calcite (with a standard deviation of 1.97) which is less than the ideal 9.99. There is no correlation between either carbon or oxygen isotopic composition and yield. Also there is no relationship between mineralogical description and isotopic composition. Precision is controlled by isotope heterogeneity within individual samples and can be checked by duplicating analyses. This approach gives an estimate of σ_n = +/- 0.9 ‰ for oxygen isotopic analysis.

6.5.2 Discussion of carbonate isotopic analysis

1. Combined carbon and oxygen results

Figure 6.4 is a plot of $\delta^{18}O$ (‰ SMOW) against $\delta^{13}C$ (‰ PDB) for carbonates from this study and also that of Hall et al. (1989) and Evans (1987). From the diagram it appears that except for the study of Hall there is no correlation between the two variables for each individual group. However, for certain groups including samples from Langbank (Port Glasgow), Boyleston Quarry (excluding Hall's investigation) and High Craigton Quarry, there is a much narrower range in carbon isotopic values relative to oxygen.

2. Carbon isotopes

The carbonate $\delta^{13}C$ data reported in this and other studies of Clyde Lava carbonates are generally low in comparison to geothermal carbonates worldwide (for example Hall et al., 1989 record $\delta^{13}C$ as low as -42 ‰ for samples from Boyleston Quarry). Samples collected from localities north of the Clyde (High Craigton Quarries, Campsie Glen) range from +0.3 to -19.6 ‰, whilst localities south of the Clyde (Boyleston Quarry, Langbank Cutting) range from -0.2 to -12.6 ‰. These data are summarised in Figure 6.5 together with data obtained from several independent isotopic studies of carbonates from the Midland Valley.

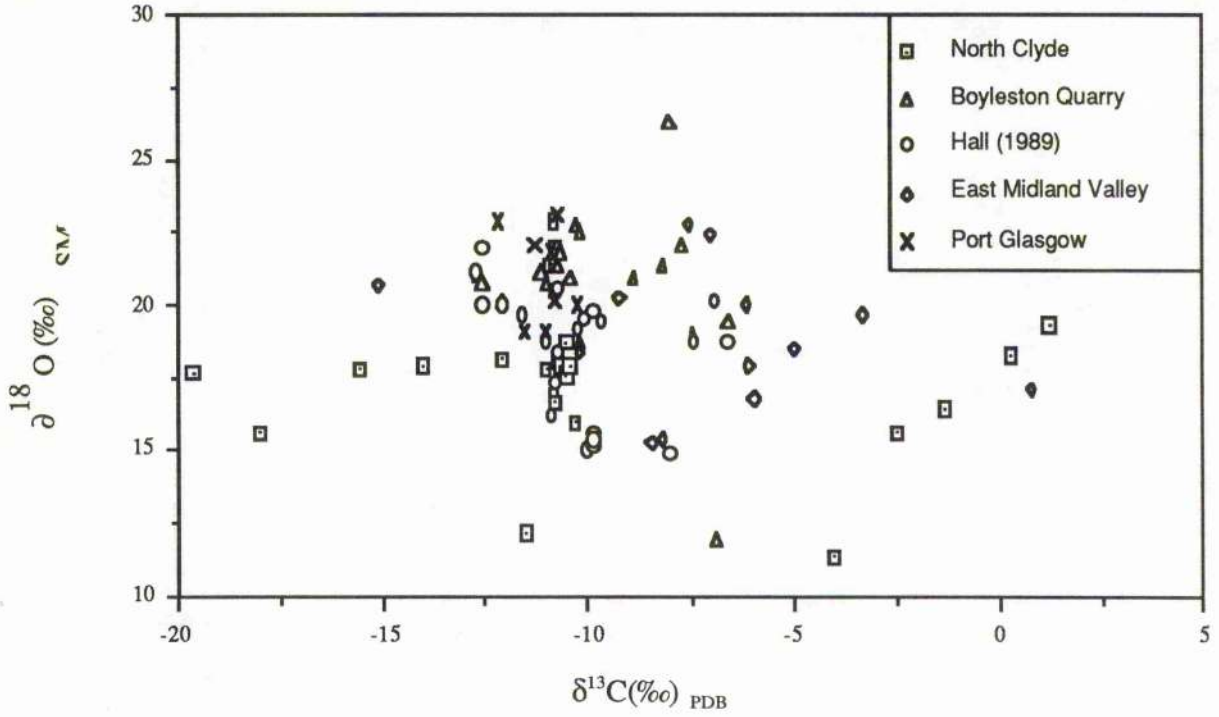

Figure 6.4 Range in carbon and oxygen isotopic compositions of hydrothermal calcites from the Midland Valley Lavas. (East Midland Valley data from Evans, 1987)

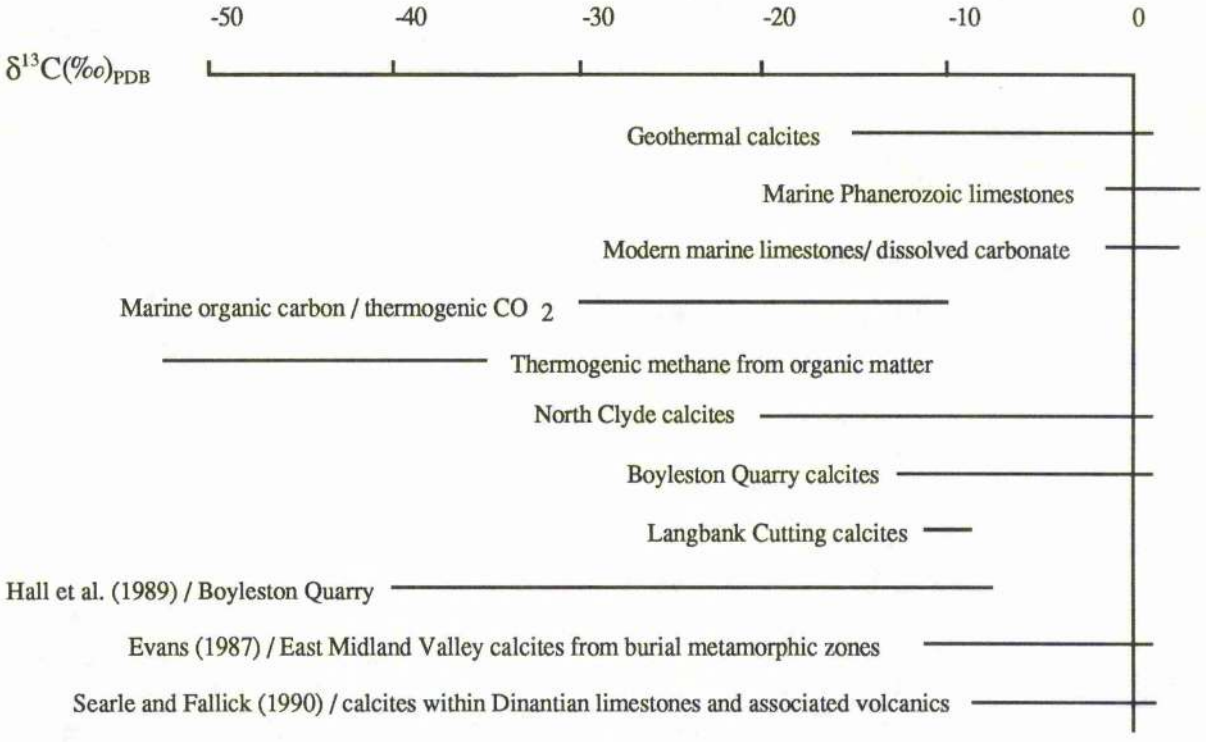

Figure 6.5. Variation in carbon isotopic compositions of Midland Valley calcites. Also shown is the isotopic composition of carbon bearing species in the near surface environment (Field and Fifarek, 1986, Ohmoto, 1985)

Hall et al. record values of $\delta^{13}C$ ranging from -9.7 to -42.7 ‰ for calcites from Boyleston. Evans (1987) reports $\delta^{13}C$ values for calcites from burial metamorphic zones in eastern Midland Valley volcanics ranging from approximately -12 to +1 ‰, with a mode of approximately -8 ‰. Searle and Fallick (1990) report values of $\delta^{13}C$ for calcite cements within Dinantian limestones from East Fife which range from approximately +1 to -6 ‰, with a modal value of approximately -1 ‰. They also report $\delta^{13}C$ values of between -5 and -9 ‰ for calcite viens within Dinantian volcanic vents from the same localities.

The diagram above fails to illustrate fully the variation in the distribution of data points within one individual population of calcites. In order to address this problem data can be grouped on the basis geographical location allowing a comparison to be made of carbon isotopic population distributions across the Midland Valley Lavas. It is possible to sub-divide into the following groups as shown in Figure 6.6:

1.North Clyde Group; includes samples from High Craigton, Mugdock Quarry and Campsie Glen.

2. South Clyde Group; includes samples from Boyleston Quarry (from this study and that of Hall et al., 1989) and Langbank Cutting.

3. East Midland Valley Group; includes those reported by Evans (1987) comprising calcites from burial metamorphic zones in eastern Midland Valley volcanics.

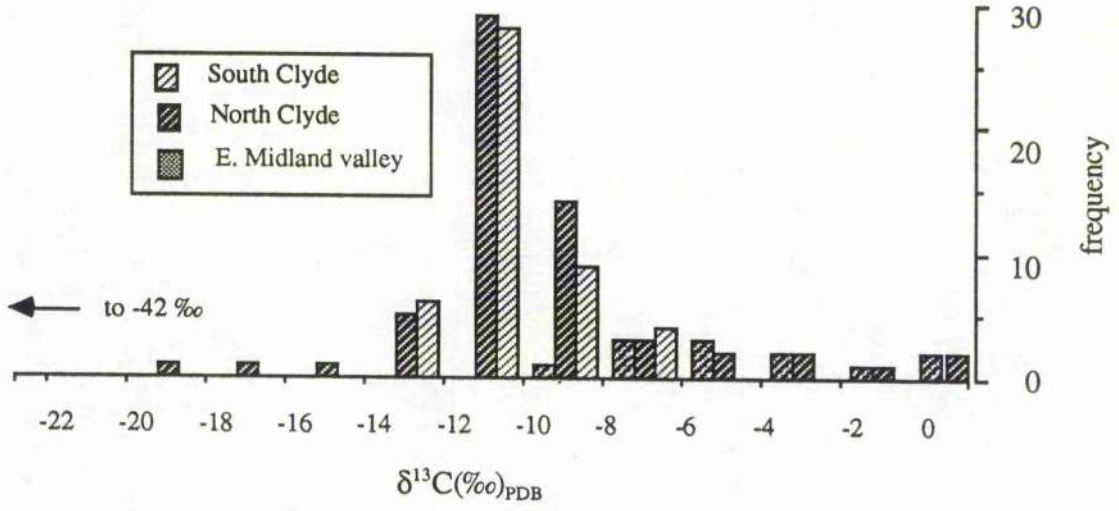

Figure 6.6. Histogram showing the distribution of carbon isotopes within calcites from the Midland Valley.

It is clear from the above diagram that across the Cyde Lavas there is an overall uniformity in the carbon isotopic composition of hydrothermal metadomain calcites; populations from widely spaced outcrops both north and south of the Clyde have very strong modal values at approximately -10 to -11 ‰ (PDB). However, data from Evans (1987) presented above shows that calcites from burial metamorphic zones from the East Midland Valley are characterised by slightly heavier carbon isotopic compositions. It is also noteworthy that samples from the Clyde Lavas which possess heavier isotopic signatures are generally collected from outside the metadomains.

When addressing the question of possible carbon reservoirs in the local geological column it is important to assess the degree to which equilibrium has been achieved amongst differing carbon bearing species present within the hydrothermal fluid. It was stated in section 6.3 that within low temperature hydrothermal systems, such as those within the Clyde Lavas (c.<250 °C), equilibrium between carbon bearing species (particularly those pairs in which carbon possesses differing valencies such as CO_2 and CH_4) is thought not to have been attained. This is because measured fractionation factors between CO_2 and CH_4 within geothermal systems where temperatures have been accurately measured are less than those expected from theoretical considerations. Ohmoto (1986) suggests that where measured fluid temperatures are less than 250 °C then the geothermal fluid can be considered as a non-equilibrium system with respect to carbon isotopes and therefore $\delta^{13}C$ co_2 can be used directly to estimate the source of carbonate carbon. This is because the carbon bearing species will have preserved its original isotopic signature during transport from source to site of deposition due to low fluid temperatures. A possible test is to compare the isotopic composition of metadomain calcites (whose formation temperature has been estimated using primary fluid inclusions) with calculated $\delta^{13}C$ values for calcite in equilibrium with dissolved bicarbonate assuming a realistic range of $\delta^{13}C$ values. This approach is adopted in Figure 6.7, the $\delta^{13}C$ values of dissolved bicarbonate ranging from +2 to -2 ‰, consistent with a sedimentary marine carbonate source. These values were calculated according to the combined $HCO_3^-(aq)$-$CO_2(g)$ (Mook et al., 1974) and $CO_2(g)$-calcite (Bottinga, 1968) fractionation factors as given by Sturchio (1990). Thus;

$$10^3 \ln \alpha_{bicarb.-calcite} = -2.99(10^6 T^{-2})-1.89(10^3 T^{-1})+21.6$$

It can be seen that there is disparency between the calculated calcite $\delta^{13}C$ values and those which are observed, suggesting that calcite was not in equilibrium with dissolved sedimentary bicarbonate within the metadomains. This is in marked contrast to many other studies, including that of Sturicho (1990) who found that calcites from Yellowstone drillholes are generally near isotopic equilibrium with dissolved inorganic sedimentary carbonates over similar temperature ranges to those obtained from fluid inclusion studies within the Clyde Lava metadomains.

Figure 6.7 shows that over the temperature range of calcite formation deduced from fluid inclusions (c. 50 to 200 °C), most calcites from the Clyde Lava metadomains were not in equilibrium with dissolved sedimentary bicarbonate within the metadomains. However, some samples, especially those from outside metadomain localities, and those from the East Midland Valley burial metamorphic zones are characterised by heavier carbon isotopic signatues, ranging from approximately -9.5 to +0.5 ‰.

Figure 6.7 shows the range in formation temperature and carbon isotopic composition of samples from Eastern Midland Valley burial metamorphic zones (Evans,1987) and indicates that they may well have been approaching equilibrium with sedimentary bicarbonate over this temperature interval. If, as was implied in Chapter 5, metadomain development preceded burial metamorphism it can be concluded that the carbon reservoir which was active during geothermal activity had become less active during burial, and had ceased to be an important source of carbon for calcite formation. During burial, carbon was supplied either from inorganic sedimentary or seawater carbonate.

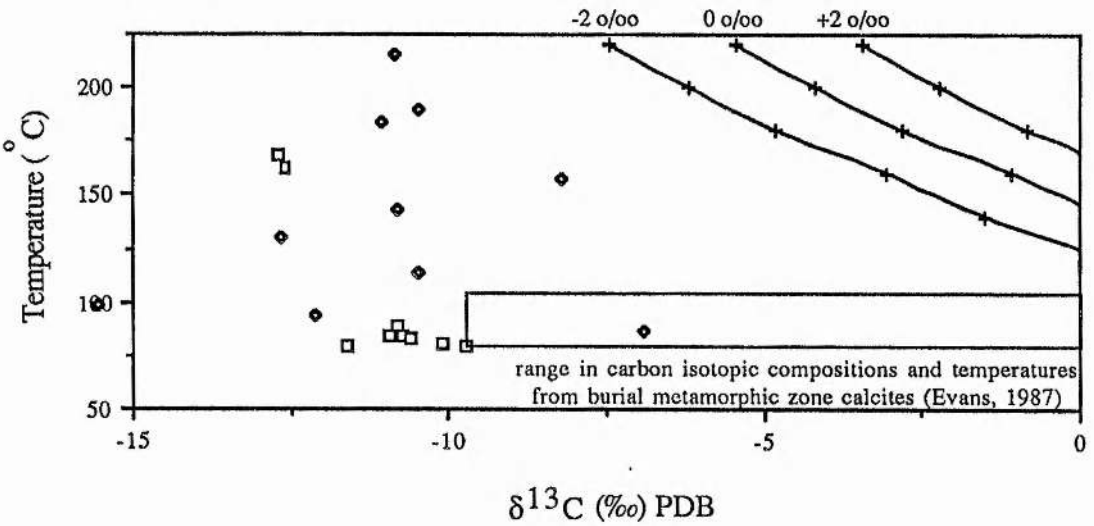

Figure 6.7 Isotopic composition of calcites vs. formation temperatures from fluid inclusions (diamonds for this study, squares from Hall et al., 1989). Solid lines define isotopic composition of calcites in equilibrium with dissolved bicarbonate having constant isotopic composition

The similarity in the distribution of carbon isotopic signatures from metadomains across the Clyde Lavas suggests a single, relatively homogeneous carbon reservoir during metadomain acitvity. Strong modal values between -12 and -10 ‰ (PDB), together with lighter values up to -19 ‰ testify to the importance of organic derived carbon dioxide as a source of carbonate carbon for most of the calcites studied. Also, Hall et al. report values of -42.7 ‰ for calcites from Boyleston Quarry indicating that thermogenic, organic derived methane has acted as a source. However, values as low as this have not been observed in this study. A possible source of organic carbon within the local succession may be the Ballagan Formation which forms part of the Inverclyde Group beneath the lavas, and reaches a thickness of 500 metres in the Campsie Fells (Francis, 1983).

The relative uniformity of carbon isotopic compositions could be explained if it is assumed that the carbon reservoir had been active prior to calcite formation, especially since hydrocarbons are found within earlier formed analcimes from Boyleston Quarry. If CO_2 generation was occurring prior to calcite formation (this seems likely since the thermal decomposition of organic matter commences at approximately 50 °C (Hunt, 1979)) then early formed CO_2 would have a lighter isotopic signature than that which existed at the time of calcite precipitation because progressive maturation of organic matter causes the residual kerogen to become preferentially enriched in ^{13}C (Ohmoto, 1986). This also may explain why the data trend towards the heavier end of the organic carbon field, given that mean $\delta^{13}C$ values for marine and terrestrial organic matter prior to thermal maturation are -22 and -26 ‰ respectively (Ohmoto, 1986). It should be noted that this approach excludes the possibility that the carbon bearing species produced at differing times during maturation of organic matter differ both in their composition and isotopic signature.

3. Oxygen isotopes

Calcite oxygen isotopic ratios for calcites from the Clyde Lavas range from +11.4 to +26.3 ‰ (SMOW), with a mean $\delta^{18}O$ of +19.56 ‰ (standard deviation = +/-2.77 ‰). There is no correlation between temperature of formation and isotopic composition for those samples which also have fluid inclusion material available. This is also the case for the study of Hall et. al. (1989)

Evans (1987) reports oxygen isotopic values ranging from approximately +22 ‰ to

+17 ‰ for volcanic hosted calcites from the Midland Valley and suggests that composition is depth (temperature) controlled since $\delta^{18}O$ values decrease with depth in the volcanic succession. Schmidt (1990), also notes a decrease in calcite $\delta^{18}O$ values ranging from +25 to +5 ‰ over the transition from zeolite to lower greenschist facies within olivine tholeiites of the Keweenawan Plateau Lava Province, Minnesota.

Oxygen isotopic variability results from differing host rock isotopic compositions, differing hydrothermal fluid isotopic compositions and differing temperatures of interaction (Field and Fifarek,1986). Common marine sedimentary rocks are generally enriched in ^{18}O and also have a wide range in isotopic composition relative to igneous rocks as shown in Figure 6.1 (~+10 to +40 ‰ compared to ~+5 to +12 ‰ $_{SMOW}$). Therefore, minerals precipitated in sediment hosted geothermal systems commonly show enrichment in ^{18}O whilst those precipitated in volcanic hosted systems have "lighter" isotopic signatures. For example, hydrothermal calcites from carbonate hosted rocks within the Salton Sea geothermal system have $\delta^{18}O$ values greater than +20 ‰ (Williams and Elders, 1984), whilst those found within the volcanic hosted Broadlands geothermal system (New Zealand) have $\delta^{18}O$ values ranging from approximately -5 to -10 ‰ SMOW (Clayton and Steiner, 1975). Clearly calcites from the Clyde Lavas have oxygen isotopic signatures which suggest a sedimentary source yet they are hosted within volcanic rocks. Therefore, it appears that they have precipitated from a fluid which has interacted with a sediment during its history. This question is addressed more rigorously in the following section.

At Langbank Cutting there is a reasonable correlation between calcite oxygen isotopic composition and distance from the top of the flow boundary (Pearson's r = 0.74) as illustrated in Figure 6.8 below.

Calcite oxygen isotopic compositon ranges from +19.0 ‰ immediately below the flow horizon where there is a significant degree of alteration, to +23.0 ‰ within relatively fresh basalt at a distance of 15 metres from the flow top. It has been shown in Chapter 4 that the degree of alteration decreases with increased distance from the flow boundary as evidenced by changes in basalt chemistry. M^{c} Keag et al. (1989) also note increased calcite oxygen isotopic ratios with distance from mineralized zones within the schist-hosted Au-W deposits of East Otago, New Zealand.

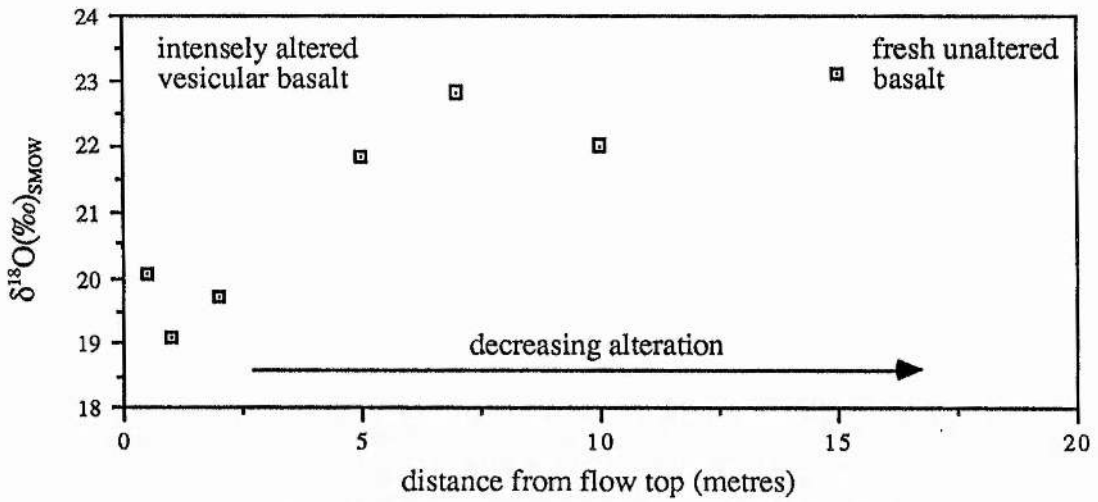

Figure 6.8 Variation in calcite isotopic composition with distance from flow boundary at Langbank Cutting (Port Glasgow).

Within this system isotopic variation is attributed to a progressive decrease in fluid temperature with increased distance from the mineralized zone. A range in oxygen isotopic composition of 4 ‰ at Langbank due to changes in fluid temperature is clearly possible since fluid temperature estimates based on fluid inclusion studies (see Chapter 5) range from 80 to 180 °C. Based on calcite-water fractionation data from Friedman and O'Neil (1977) a systematic temperature decrease from 180 to 80 °C is capable of producing a fractionation of approximately 6 ‰.

6.5.3 Analcime isotopic analysis

Oxygen isotopic analysis for 21 analcimes are presented in Table 6.2 below. Sample locations are given in detail in Appendix 6.1. Repeat analysis of sample OL gave a result of +20.94‰ giving an estimate for precision of approximately +/- 0.4‰.

Sample No.	$\delta^{18}O$ ‰ SMOW
S4	+22.84
S1	+18.91
WF6	+20.70
OM	+20.08
OL	+20.57
CV86	+24.40
WF3	+19.99
WF2	+19.50
HCA	+19.93
S6	+20.11
E1	+22.46
HCB	+29.01
S41	+24.12

WF4	+19.56
Z1	+20.65
S2	+19.93
S61	+27.61
OL1	+22.62
E3	+22.00
WF31	+30.80
WF11	+22.80
*USMN-R967	+17.7
**UCB-16658	+20.4

* from Karlsson and Clayton (1990)b; massive analcime from Old Kilpatrick, Dumbarton.

** from Luhr and Kyser (1998); veinlet forming analcime from Kilpatrick Hills.

Table 6.2 Oxygen isotopic data for analcimes from the Clyde Lavas

Yields range from 2.37 to 13.99 μmol O_2 mg^{-1} dehydrated analcime, with a mean of 6.25 and standard deviation of 2.79. Calculation indicates that this value should be 14.84 μmol mg^{-1}using the formula $NaAlSi_2O_6$ for dehydrated analcime. It is noted that yields quoted for dehydrated analcime carried out by Karlsson and Clayton (1990b) always approach the ideal O_2 yield of 14.84. These authors do not report pre-fluorinating their samples prior to oxygen extraction, though all other experimental details are similar. Therefore, it appears that pre-fluorination may cause partial loss of framework oxygen, since dehydration does not affect the framework oxygen isotopic composition of analcime (Karlsson and Clayton, 1990b). However, since there is no correlation between yield and isotopic composition, and because the range in isotopic compositions reported in this study is similar to that reported for hydrothermal analcimes worldwide (reported by Karlsson and Clayton, 1990b), it appears that pre-fluorination in the experiments reported here does not significantly affect the isotopic composition of the analcime.

6.5.4 Discussion

Oxygen isotopic compositions range from +18.91 to +30.80 ‰ (SMOW). There is a moderately tight cluster between +19 and +23 ‰ (SMOW). Mean isotopic composition is +22.3 ‰, with a standard deviation of 3.2 ‰ . This population is illustrated in Figure 6.9. Two samples (from Boyleston and High Craigton Quarries) give the highest $\delta^{18}O$ value for analcime framework oxygen thus far reported at 30.80 and 29.01 ‰ (SMOW). Also shown on the diagram are two

independent analyses which are reported above in Table 6.2.

Karlsson et al. (1985) first suggested that there is a negative correlation between $\delta^{18}O$ of the analcime framework oxygen and the temperature at which it formed. Subsequent studies by Karlsson and Clayton (1990a) and Karlsson and Clayton (1990b) reinforce this concept. They show that analcimes formed at lower temperatures have high $\delta^{18}O$, whilst those formed at higher temperatures have low $\delta^{18}O$. Low temperature analcimes they term "sedimentary" and have $\delta^{18}O$ ranging from +16.6 to +24.5 ‰ (SMOW); high temperature analcimes are termed "igneous" and have $\delta^{18}O$ ranging from +8.7 to +14.3 ‰ (SMOW). Analcimes which possess intermediate values (actually +4.4 to +26.6 ‰ (SMOW)) are thought to owe their origin to hydrothermal processes. Framework oxygen isotopic ratios should not be regarded as unequivocal evidence of an igneous, hydrothermal or sedimentary origin since there is a degree of overlap between the $\delta^{18}O$ values of each group.

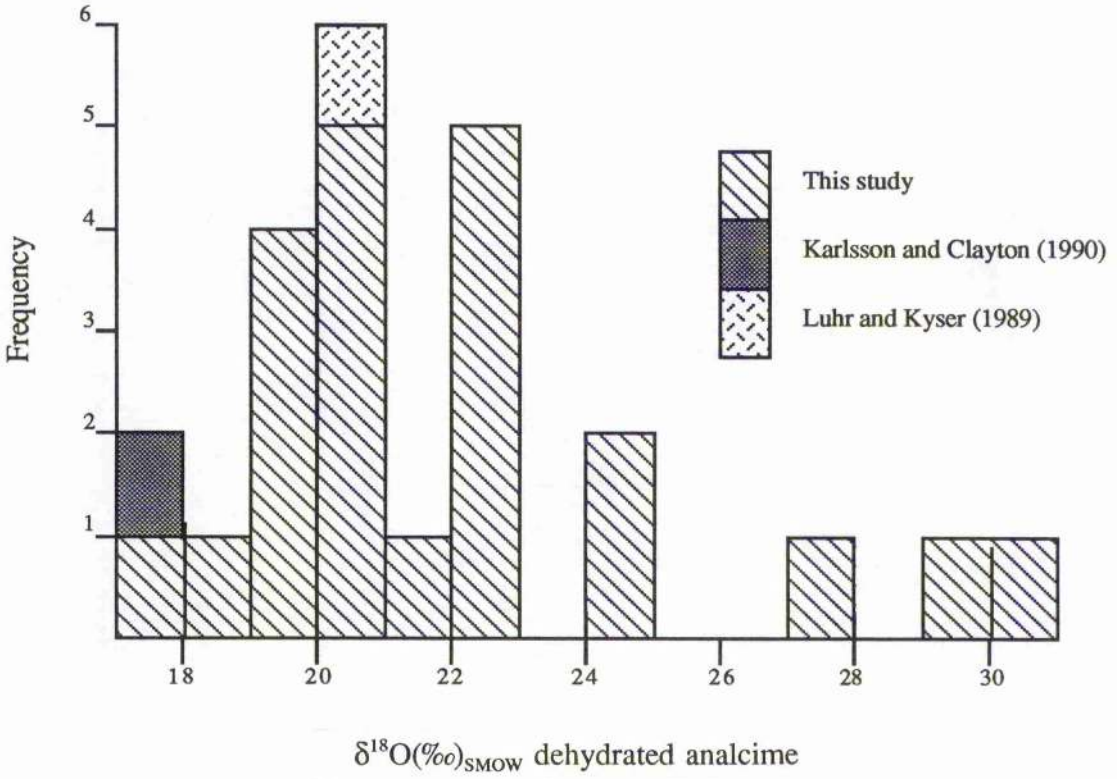

Figure 6.9 Range in isotopic composition of dehydrated analcimes from the Clyde Lavas

It can be seen from Figure 6.9 that analcimes from the Clyde Lavas have $\delta^{18}O$ values ranging from approximately +17 to +30 ‰ (SMOW). Clearly the majority of these samples satisfy hydrothermal criteria as outlined above. However, several samples have $\delta^{18}O$ values greater than +23‰ (SMOW) implying a lower temperature ("sedimentary") origin. Unfortunately however it has proved impossible to obtain an independent estimate of individual sample formation temperatures because of a lack of suitable fluid inclusion material. It is noteworthy that samples collected within close proximity to one another (of the order of metres) possess wide ranges in $\delta^{18}O$ values suggesting that analcime did form over a considerable temperature range.

Sedimentary analcimes used in the study of Karlsson and Clayton (1990b) were collected from Tertiary saline lakes in California, Wyoming and Arizona where it is thought that they formed as low temperature replacement products of pre-existing alkali zeolites such as phillipsite and clinoptilolite. Fluid inclusion evidence from the present study indicates that analcime formed over temperatures ranging from approximately 180 to 220 °C, whilst the study by Hall et al. (1989) indicates a mean formation temperature of approximately 145 °C. This rules out a low temperature, and therefore heavy $\delta^{18}O$ signature for the Clyde Lava analcimes. The two alkali zeolites (phillipsite and clinoptilolite) are characterised by having a high $\delta^{18}O$ framework oxygen signature (>25 ‰), as shown by Karlsson and Clayton (1990b). However, there is no evidence, petrographic or otherwise, to suggest that analcimes developed by replacement of pre-cursor phases within the Clyde Lavas. Therefore, it appears that these zeolites may have formed from a fluid which was enriched in ^{18}O, such as those found in sedimentary basins. This suggestion is addressed towards the end of this chapter.

Hydrothermal analcimes recovered from Icelandic basalts which were analysed by Karlsson and Clayton (1990b) have $\delta^{18}O$ values ranging from +9.2 to +12.2 ‰. Also formation temperature and fluid $\delta^{18}O$ values are well constrained for these samples (~145 °C and 0.0 ‰ respectively). This indicates a mean isotopic fractionation of 10.7 ‰ between analcime and seawater at 145 °C, assuming equilibrium. Karlsson and Clayton (1990a), following an experimental investigation found that isotopic equilibrium between analcimes and hydrothermal fluids is achieved very rapidly at elevated temperatures (within a few days). Therefore, given that 145 °C represents a

lower limit for analcime formation within the Clyde Lavas, and also that mean $\delta^{18}O$ framework values are higher than those for the Icelandic samples, it can be concluded that the fluid which was present during analcime formation showed a considerable enrichment in ^{18}O, thereby ruling out a purely surface derived origin as suggested by Hall et al. (1989). This finding is addressed more quantitatively towards the end of the chapter.

6.5.5. Discussion of metadomain fluid sources: stable isotopic evidence

Given the temperature interval over which hydrothermal fluid was trapped, i.e. the temperature of mineral precipitation (as deduced from primary fluid inclusions), together with a knowledge of the isotopic composition of the mineral, and the appropriate fractionation equation, it is possible to determine the isotopic composition of the fluid which was present at the time of mineral formation. This approach is adopted below for both calcite and analcime. Recent studies by Karlsson and Clayton (1990a) suggests that analcime which forms in geothermal systems rapidly reaches isotopic equilibrium with the ambient fluid; also the partitioning of oxygen isotopes between analcime framework and water is similar to that of calcite-water (the latter being well documented). Therefore, it is possible to assess how the isotopic composition of the metadomain fluid evolved with time since calcite is always paragenetically later than analcime.

1. Oxygen isotopic ratios of associated analcime-calcite pairs.

Table 6.3 presents the isotopic composition of associated analcime-calcite pairs. Locations are given in Appendix 6.1.

Sample	Analcime $\delta^{18}O$(‰)SMOW	Calcite $\delta^{18}O$(‰)SMOW	$\Delta\ ^{18}O_{cal\text{-}anal}$ (‰)
S3	+22.8	+19.4	-3.4
S1	+18.9	+22.1	+3.2
WF6	+20.7	+23.8	+3.1
OM	+20.1	+20.9	+0.8
OL	+20.6	+18.6	-2.0
WF4	+24.4	+21.3	-3.1
WF5	+19.9	+20.8	+0.9
S6	+20.1	+21.9	+1.8
E2	+22.5	+21.1	-1.4
WF3	+24.4	+20.9	-3.2
WF4	*+19.6*	*+21.3*	*+1.7*
S3	+19.9	+19.4	-0.5
WF41	+22.8	+21.3	-1.5
WF42	+19.9	+26.3	+6.4

O2	+22.6	+22.0	-0.6
E2	+22.0	+21.1	-0.9

(For $\Delta\ ^{18}O_{cal\text{-}anal}$, x = 0.08‰ and 1σ = 2.61‰)

Table 6.3 Isotopic composition of associated analcime-calcite pairs from Clyde Lava metadomains

The results of these analyses are displayed in Figure 6.10 below which is a δA-δB plot, comparing the oxygen isotopic composition of co-existing calcite-analcime pairs. If, as shown by Karlsson and Clayton (1990a) fractionation of oxygen isotopes between analcime and water is similar to that between calcite and water, then pairs which co-crystallized in isotopic equilibrium and formed at the same temperature will plot about a straight line with a slope of approximately 1. It can be seen that analyses from the Clyde Lavas plot on either side of such a line labelled Δ = 0 which extends to the origin.

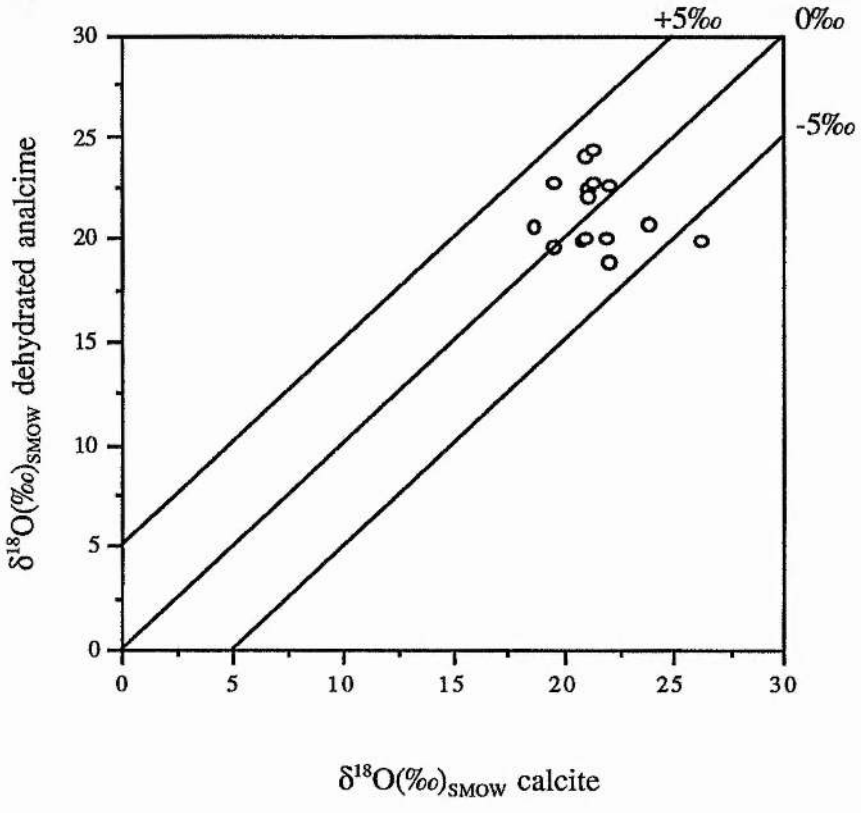

Figure 6.10. $\delta^{18}O$(‰) values for associated calcite-analcime pairs

(* diagonal lines are drawn for integral Δ values where $\Delta = \delta^{18}O(\text{calcite}) - \delta^{18}O(\text{analcime})$)

Except for sample WF42 it can be seen that the difference in oxygen isotopic composition between

co-existing analcime and calcite is small (<4‰). Karlsson and Clayton (1990b) found the difference to be less than 5 ‰ for hydrothermal analcime-calcite pairs worldwide. Thus, results from this study seem to reinforce the suggestions of these authors that analcime-water fractionation is similar to that of calcite-water. Therefore, it is possible to determine the oxygen isotopic composition of the fluid present at the time of analcime formation using the calcite-water fractionation equation of Friedman and O'Neil (1977).

Karlsson and Clayton (1990b) noted that for associated analcime-calcite pairs, the mineral which crystallised first tends to have a lower $\delta^{18}O$ value than the mineral which crystallises second. In this study earlier analcime has both higher and lower $\delta^{18}O$ values than asssociated calcite. Also, analcime has a higher mean formation temperature than calcite (203 °C compared to 140 °C respectively) as deduced from primary fluid inclusion temperatures. Therefore, it can be concluded that analcime was formed from a fluid which possessed an unusually high $\delta^{18}O$ value. Using the calcite-water fractionation factor of Friedman and O'Neil (1977), and a mean formation temperature of 203 °C gives a $\Delta_{\text{analcime-water}}$ value of +9.4 ‰. Taking upper and lower limits for framework analcime isotope ratios of +24.4 ‰ and +18.9 ‰ (samples WF4 and S1 respectively) gives a fluid oxygen isotopic ratio ranging between +15.0‰ and +9.5 ‰. If it is assumed that the fluid phase present during analcime precipitation was ultimately of surface origin (and therfore possessed a $\delta^{18}O$ value ~ 0‰, consistent with Lower Carboniferous palaeolatitude) then then this would have involved an isotopic shift in the water of approximately +9.5 to +15 ‰. Extreme compositional shifts are normally only seen in higher temperature, high salinity geothermal systems which have not necessarily exchanged with sediments. Examples include the Salton Sea and Lanzarote geothermal systems (c.320 °C) which record shifts of approximately 15 and 18 ‰ respectively (Sheppard, 1986). One possible mechanism for oxygen isotopic enrichment is exchange with ^{18}O-rich sedimentary minerals, particularly carbonates whose compositional field is shown in Figure 6.1. A possible local source of sedimentary carbonate may be the Dinantian Ballagan Formation forming part of the Inverclyde Group beneath the lavas, and consisting of alternating carbonate and mudstone rich layers. Although no oxygen isotopic data are available for this particular formation Searle and Fallick (1990) report oxygen isotopic values ranging between approximately +21 to +26 ‰ (SMOW) for carbonate cements from equivalent Dinantian dolomites from East Fife.

Isotopic exchange and interaction with the Ballagan Formation might also explain the presence of abundant hydrocarbon material found in analcime fluid inclusion material (see Chapter 5). Sheppard and Charef (1986) suggest the term "organic water" for waters which have interacted with sedimentary organic matter (which controls fluid δD ratios) and whose $\delta^{18}O$ value is controlled by the sediments with which they interact.

2. Isotopic composition of fluid phase present during calcite formation

Given calcite isotopic composition and an estimate of formation temperature based on fluid inclusion data, the isotopic composition of the fluid may be determined using the calcite-water fractionation equation given by Friedman and O'Neil (1977). This is given by:

$$1\,000 \ln \Delta = 2.78\,(10^6\,T^{-2}) - 2.89.$$

The results of this approach are presented below in Table 6.4. and illustrated in Figure 6.11 which shows the variation in calcite oxygen isotope ratio with formation temperature as deduced from fluid inclusions. Also shown are the theoretical $\delta^{18}O$ values calculated for calcite in equilibrium with waters having constant $\delta^{18}O$ values as indicated.

Sample no.	$\delta^{18}O$ calcite (‰) (SMOW)	Temerature (°C)	$\delta^{18}O$ fluid (calc.)(‰) (SMOW)
S5	+20.9	184	+10.5
OM	+20.9	114	+5.3
E2	+21.1	130	+6.9
OL	+18.6	87	0.0
S7	+20.5	215	+11.7
WF4	+21.3	158	+9.2
HC5	+17.9	189	+7.8
HCN	+16.6	144	+3.5
Mg2	+17.5	98	+0.2
Mg3	+18.2	94	+0.4
CV86	+21.4	115	+5.8

Table 6.4 Stable isotope and fluid inclusion data for calcites from metadomain localities

It can be seen that there is a spread in data points which suggest that calcites equlilibrated with fluids whose isotopic composition varied between approximately 0 and +10‰ (SMOW). Also, it appears that the distribution of data points is not uniform, but is bimodal with modes at approximately 0 and

10 ‰ (SMOW) suggesting the existence of two discrete fluids. Therefore, it appears that two independent studies confirm the existence of two discrete populations of calcite from the Clyde Lava metadomians. A $\delta^{18}O$ value of approximately 0‰ is consistent with a surface derived, mid latitude fluid.

The concept that the higher temperature fluid with $\delta^{18}O$ approximately 10 ‰ is formed from surface fluids which interacted with hot igneous rock as advocated by Hall et al. (1989) is questioned because fluids analysed from volcanic hosted geothermal systems which interact over similar temperature intervals (eg. the Helka and Reykjanes fields of Iceland) show identical isotopic signatures to the local meteoric waters. It is perhaps more likely that these metadomain fluids, whilst being ultimately of surface origin, interacted with the same organic rich Lower Carboniferous sediments that produced the fluid which is recorded from earlier analcimes.

Reference to Figure 6.11 shows that fluids of intermediate composition were also present during metadomain activity. These may represent a hybrid fluid produced during mixing of the surface derived and "sedimentary" end members, implying that these fluids were present at the same time during metadomain activity.

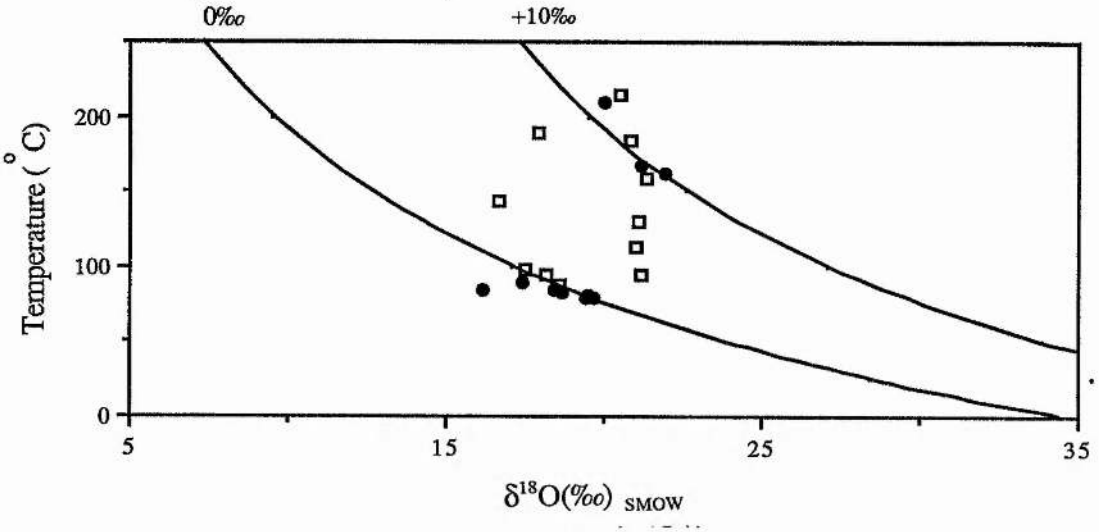

Figure 6.11 Oxygen isotopic composition of calcites against formation temperature, estimated from primary fluid inclusions.Solid lines define calculated composition of calcite in equilibrium with fluid of isotopic composition as indicated calculated using data from Friedman and O' Neil(1977). Squares from this study, filled circles from Hall et al. (1989).

This situation seems unlikely because fluid inclusion evidence (see Chapter 5) indicates that major

ion compositions and salinities of metadomain fluids are relatively uniform across the lava pile implying a similar evolutionary pathway for the two fluids. It is difficult to imagine a situation in which this relic isotopic bimodality would be preserved whilst major ion compositions and salinities became uniform.

Alternatively, there exists the possibility that fluids of intermediate temperature and composition present during calcite formation represent a progressive sequence of cooling within the lavas, which ultimately ended with the widespead circulation and swamping by relatively cool, surface derived fluids in the waning stages of geothermal activity. This stage is represented within fluid inclusion material which shows the widespread occurrence of multiple generations of low temperature, secondary inclusions within both calcite and analcime. If this is the case then analcime and calcite provide a record of fluid evolution within the metadomains.

6.6 Conclusions

1.Isotopic analysis of analcime-calcite pairs seems to support the view expressed by Karlsson and Clayton (1990b) that partitioning of oxygen isotopes between analcime and water is similar to that of calcite-water.

2. Using the calcite-water fractionation equation of Friedman and O'Neil (1977), and given a mean formation temperature of ~ 200 °C (from fluid inclusions) it has been possible to determine the range in isotopic composition of the fluid with which analcime equilibrated. This value varies between approximately +9 to +15 ‰. Assuming that this fluid was ultimately of surface origin then there has been an overall shift in fluid composition of between +9 to +15 ‰. Comparison with modern day systems shows that such shifts are only seen in higher temperature (c. 320 °C), high salinity systems where sediment comprises a significant component of the local geological succession. Therefore, it is suggested that the metadomain fluid has interacted with a "reactive" sedimentary sequence, possibly carbonates from the underlying Inverclyde Group. This may also account for the presence of hydrocarbon inclusions within analcime.

3. Oxygen isotopic analysis of calcite, coupled with estimates of formation temperatures from fluid inclusions has allowed the calculation of the composition of the fluids present during calcite formation. This independent study has strengthened the views expressed by Hall et al. (1989) that there were two fluids present during calcite formation, not only at Boyleston Quarry, but also at

other metadomain localities across the Clyde Lavas. These fluids were of relatively low to intermediate temperature (c. 90 to 200 °C), ranging in composition from approximately 0 to +10 ‰. These compositions correspond to end members of ; a) exclusive surface origin and; b) that which also has interacted with sedimentary material.

4. Carbon isotopic ratios across the Clyde Lava metadomains are remarkably uniform, and testify to the existence of a relatively homogeneous carbon reservoir during metadomain activity. Strong modal values between -12 and -10 ‰ (PDB) highlight the importance of organic derived carbon dioxide as a source of carbonate carbon for most of the calcites studied. A possible source of organic carbon within the local succession may be the Ballagan Formation. This is consistent with oxygen isotopic data presented above. The uniformity of carbon isotopic compositions, coupled with the fact that hydrocarbons are found within the earlier analcimes suggests that the carbon reservoir was activated well before calcite precipitation commenced. Furthermore, calcites precipitated from surface derived fluids also possess carbon isotopic values which indicate an organic source, clearly indicating that the underlying sediments were still active carbon source throughout metadomain activity.

5. It is suggested that analcime and calcite provide a unique view of fluid evolution within the metadomains. Early, high temperature fluids which were present during analcime formation possessed high $\delta^{18}O$ values because of interaction with underlying sediment. As calcite formation commenced fluids were still of relatively high temperature and still possessed heavy to intermediate $\delta^{18}O$ ratios. However, in the waning stages of metadomain history whilst calcite precipitation still continued fluid temperature had decreased and fluid was dominantly surficial in origin. This situation is summarised in Figure7 .1 .

CHAPTER 7 CONCLUSIONS

7.1 Introduction

The purpose of the following chapter is to summarise the data which have been gathered during the present study and to conclude with an integrated model for metadomain alteration. The chapter finishes with some recommendations for possible further work.

7.2 Summary of relevant conclusions from present work

7.2.1 Characteristics of metadomain alteration

Fieldwork has revealed that the main control on metadomain development is the permeability contrasts which exist within the lavas. Of the metadomains studied, such contrasts have included flow horizons such as Boyleston Quarry, Langbank Cutting and Campsie Glen, and lithological and structural controls such as High Craigton.

Using a combination of fieldwork and routine petrographic work it has been possible to identify a range of features which are recognised in both active and fossilised geothermal areas. With regard to the former this has included the localised nature of the metadomain alteration, and associated intense hydrofracturing combined with veining best seen at Boyleston Quarry. Also, petrography has revealed phases which are commonly found in both active and fossilised geothermal environments.

Detailed petrographic analysis has allowed for the development of a temporal model which provides a link between metadomain development and burial metamorphism of the lavas as discussed by Evans (1987). Three separate stages have been identified:

1. Early widespread alteration involving replacement of primary igneous phases (notably plagioclase) by a number of secondary mineralogies including phyllosilicates,albite, analcime,

calcite and epidote.

2. Metadomain development which is most strikingly seen as hydrobrecciation and veining of the basalts on all scales. Characteristic alteration mineralogies include analcime, prehnite and calcite. Also, combined, detailed XRD and microprobe analysis has shown that there is a fundamental change in the nature of the phyllosilicate phases within the metadomains compared to those found outside. This is manifest by the development of more evolved phyllosilicate phases (such as chlorite) within the metadomains. It is possible that metadomain alteration may simply be an expression of a particularly intense form of widespread hydrothermal alteration, the latter affecting the whole lava pile.

3. Burial metamorphism, manifest by the development of a range of zeolites, which has received fuller appraisal by Evans (1987). Petrographic evidence in the form of index zeolite minerals developing upon metadomain minerals provides clear evidence that burial metamorphism occurred after metadomain development.

Comparison of alteration minerals developed within the metadomains with those reported in active geothermal areas suggest that fluid temperatures ranged between approximately 150 °C to 250 °C. This is consistent with estimates based upon compositional data from phyllosilicates which yield temperature estimates up to 220 °C. Again it is possible to see the extent to which permeability controls development of secondary mineralogies as the distribution and composition of the phyllosilicates is ultimately controlled by variations in this parameter.

Chemical analysis performed upon samples of basalt collected from inside and outside metadomain localities demonstrates mobility of most elements during hydrothermal alteration. It has been demonstrated that all of the major oxides excluding Fe_2O_3 and SiO_2 exhibit substantial changes in concentration during metadomain alteration. Also K_2O, Sr, Rb, Cu and Zn exhibit extreme mobility whilst alteration is always associated with an increase in the overall volatile content of the basalts. Comparison of previous studies on basalt-seawater interaction also reveal similar patterns elemental mobility during hydrothermal alteration.

7.2.2 Metadomain fluid characteristics

Combined fluid inclusion and stable isotopic techniques have provided particularly powerful methods for determining the physical nature of the alteration fluids, their composition, origin and evolution. Development of a temporal model of fluid evolution has been made possible by studying both analcime and paragenetically later calcite which are characteristic metadomain minerals. Figure 7.1 illustrates the salient points emerging from this study.

Fluids present during the formation of analcime have been shown to be typically of very low salinity, the dominant ionic species being Na^+ and of relatively high temperature (mean T_h=203 °C).

The presence of hydrocarbon material trapped within grains of analcime testifies to the involvement of organic matter in the metadomain systems. Upon heating the hydrocarbon material begins to change colour at approximately 230°C, probably representing a maximum transportation temperature for the hydrocarbons. Within the local geological succession the Ballagan Formation underlying the lavas may represent a possible source for the hydrocarbons since they contain significant quantities of organic rich shaley material. Because salinities are low it is unlikely that the fluid transporting the hydrocarbons was exclusively derived from the sediments. It is more likely that the fluid was ultimately of surface origin.

In contrast to the fluids present during analcime formation those present during precipitation of paragenetically later calcite show a very wide range of salinities and appear to be dominated by ionic species such as Ca^{2+}, Na^+ and Cl^-. These brines also show wide ranges in temperature ranging from approximately 50 °C up to a maximum of 300 °C. These wide variations in both composition and temperature are indicative of a hybrid fluid generated by the mixing of a high temperature connate brine and a low salinity, low temperature fluid, ultimately of surface origin which has been progressively heated during advection through the lavas. Also, physical processes such as boiling and mixing which are often characteristic of geothermal fluids are shown to have an effect on fluid compositions.

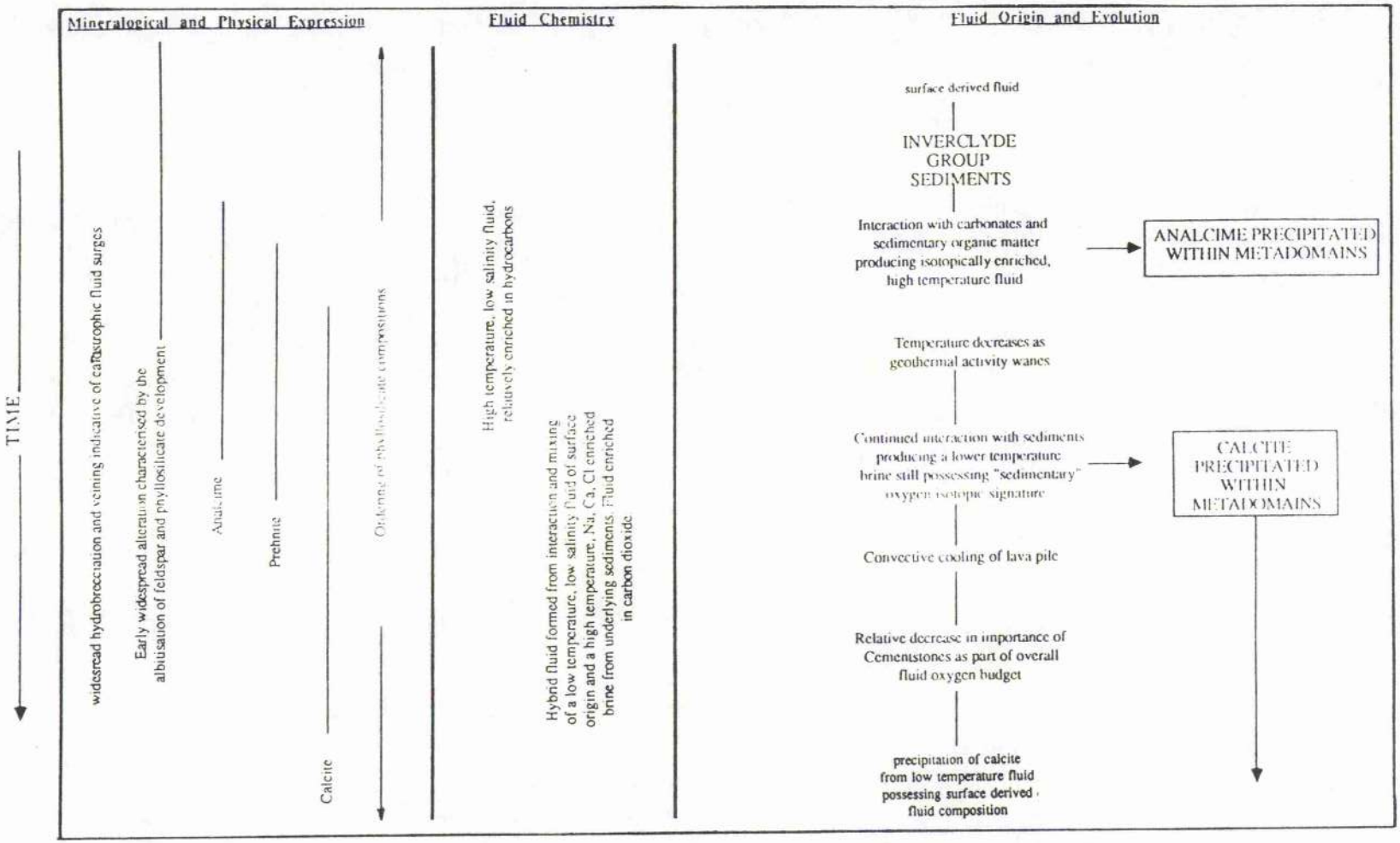

Figure 7.1 Summary diagram showing the evolution of metadomains from the Clyde Lavas

Following metadomain activity it has also been possible to recognise a lower temperature (c. 80 °C to 110 °C) event possibly related to burial of the lavas from fluid inclusion results from quartz, a characteristic burial metamorphic index mineral.

Analysis of fluids from metadomain calcites by GC analysis testifies to the dominance of CO_2 as the volatile phase within the metadomain fluids. However, levels of CO_2 present within these fluids are too high to have been buffered by fluid-mineral equilibria, again indicative of involvement of gas prone sediments underlying the lavas.

Stable isotopic analysis of dehydrated analcime has complemented the study of Karlsson and Clayton (1990) supporting the view that partitioning of oxygen isotopes between analcime and hydrothermal fluids is similar to that between calcite and water. Therefore, it is possible to use calcite-water fractionation data to predict the isotopic composition of waters in equilibrium with metadomain analcime. This represents a novel approach when considering the isotopic composition of fluids in low temperature environments.

Integrated oxygen isotopic and fluid temperature data for analcime suggests equilibration with a fluid of isotopic composition ranging from +9 to +15‰ (SMOW). If the fluid was ultimately of surface origin, as is suggested from fluid inclusion work, then this would represent an overall shift in isotopic composition of +9 to +15‰ (SMOW). Such large shifts in present day and fossilised systems are only seen in high temperature, high salinity systems where sediment composes a significant proportion of the local geological column. This supports the view that these fluids have interacted with reactive carbonate rich sequences within the Inverclyde Group succession beneath the lavas.

Combined oxygen isotopic and fluid inclusion data for metadomain calcites has allowed for the calculation of the isotopic composition of the fluids with which calcite equilibrated. This independent study supports the views expressed by Hall et al. (1989) that two distinctive fluids can be recognised across the whole of the Clyde Lavas. These fluids were of relatively low to intermediate temperatures, as deduced from fluid inclusion studies, ranging in composition from 0‰ to +10‰ (SMOW), corresponding to end members of; a) exclusively surficial origin and; b) fluids which have interacted with reactive sedimentary

sequences.

Carbon isotopic ratios from metadomain calcites across the Clyde Lavas are remarkably uniform with strong modal values between -10‰ and -12‰ (PDB) highlighting the importance of sedimentary organic matter as a source of carbonate carbon. Furthermore, calcites precipitated from surface derived fluids also possess carbon isotopic compositions indicative of an organic source indicating that the underlying sediments were active throughout metadomain activity.

7.3 A model for metadomain development within the Clyde Lavas

Metadomain localities from widely spaced outcrops within the Clyde Lavas represent the roots of narrowly confined zones which it is thought acted as feeders to geothermal activity at higher levels within the lavas. As such they represent an integral part of the overall plumbing system within the lavas during geothermal activity. They are manifest in the field as narrowly confined zones (often only a few metres in lateral extent) within which there was intense, periodically catastrophic, upwards directed fluid advection often evidenced by intense hydraulic fracturing of host basalt. Development of a zone would have proceeded wherever permeability contrasts within the host basalts existed and were subsequently exploited by convecting geothermal fluids. The likely surface expression of this fluid circulation would have been the existence of hot springs currently seen in active geothermal areas worldwide. Figure 7.2 shows a possible scenario for metdomain development within the Clyde Lavas.

As the lava pile continued to cool convectively then fluid advection and mineral deposition within these metadomains would have effectively ceased, ultimately leading to the "shutting down" of each individual system prior to burial metamorphism of the Midland Valley Lavas.

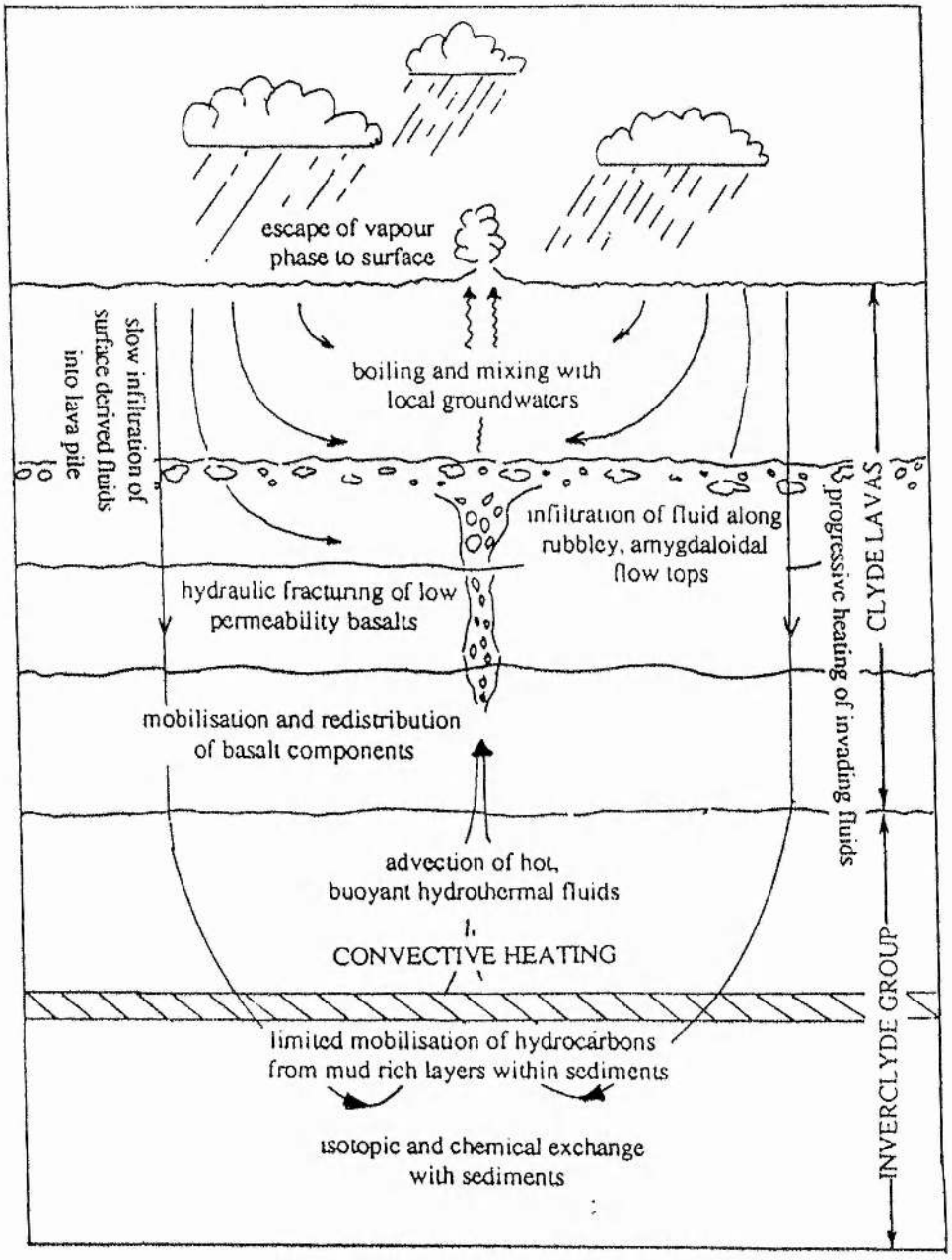

Figure 7.2 A cartoon illustrating the salient features of metadomain development

7.4 Concluding remarks

The original aims of this project have always been focused and well defined; "to investigate the metadomains (plumes) in detail.....and to demonstrate the sources of the fluids

and hydrothermal processes involved in the alteration of the Clyde Plateau Basalts". Combined fluid inclusion and stable isotopic analysis have proved to be powerful techniques and have, to a large extent, demonstrated the main processes and fluid types which have been involved in metadomain alteration.

Following independent studies by Evans (1987) and Hall et al.(1989) this work has contributed significantly to many of the issues identified by these authors. For example, the latter authors identified two different fluids on the basis of a combined carbonate $\delta^{18}O$ and fluid inclusion data. This study has confirmed this hypothesis and shown that such fluids participated in hydrothermal activity across the Clyde Lavas, as well as identifying inorganic carbonate as an important source of carbonate carbon. Also, an investigation of temporal relationships has shown that metadomain activity occurred prior to burial metamorphism and also that fluid compositions, and by inference sources, fluctuated during the evolution of these systems.

There appear to have been processes operating within the hydrothermal fluids which are recognised within geothermal systems which are active today such as fluid mixing and boiling. It is perhaps fluid origins within the Clyde Lava metadomains which differ from those reported in other geothermal areas (active and fossilised). This factor is largely controlled by the local stratigraphic succession and hydrogeology.

One possible area of further study could involve an integrated geochemical study of the Inverclyde Group sediments which underlie the lavas with the aim of establishing the precise diagenetic history of this succession in relation to the geothermal and burial metamorphic history of the lavas. This could involve an attempt to recognise any signs of interaction with the fluids recorded within the metadomains and might also include an assessment of the potential of organic material within the sediments to generate hydrocarbons which are recorded within the metadomain fluids.

A further problem which arises as a consequence of this study is the precise relationship between early geothermal activity and metadomain activity. Is the latter simply an intense form of regional geothermal activity which is recorded as replacement of

plagioclase feldspar by albite and phyllosilicates? Clearly, a stable isotopic investigation of the main phyllosilicate phases would help elucidate this relationship, though are likely to be impeded by practical considerations of mineral separation.

Finally, Summer and Verosub (1988) point out that many economically important hydrocarbon accumulations can be associated with volcanism. Geothermal fluids can play a part in the maturation of source rocks and subsequent transport of evolved hydrocarbons to reservoirs. This study has clearly demonstrated that hydrothermal fluids can interact with sedimentary sequences over a large area and shows that fluid-rock interaction could be come important where lateral aquifers facilitate distribution of magmatic heat over hydrocarbon prone sediments.

LIST OF APPENDICES

APPENDIX 2.1 SAMPLE LOCALITIES

This appendix presents location maps of localities at Boyleston Quarry and High Craigton Quarry where samples were selected for thin section analysis. Sample localities for Campsie Glen are given in Appendix 3.2. The section numbers which are given here are also those used for XRD, XRF, fluid inclusion and stable isotope samples.

1. Boyleston Quarry (495 597)

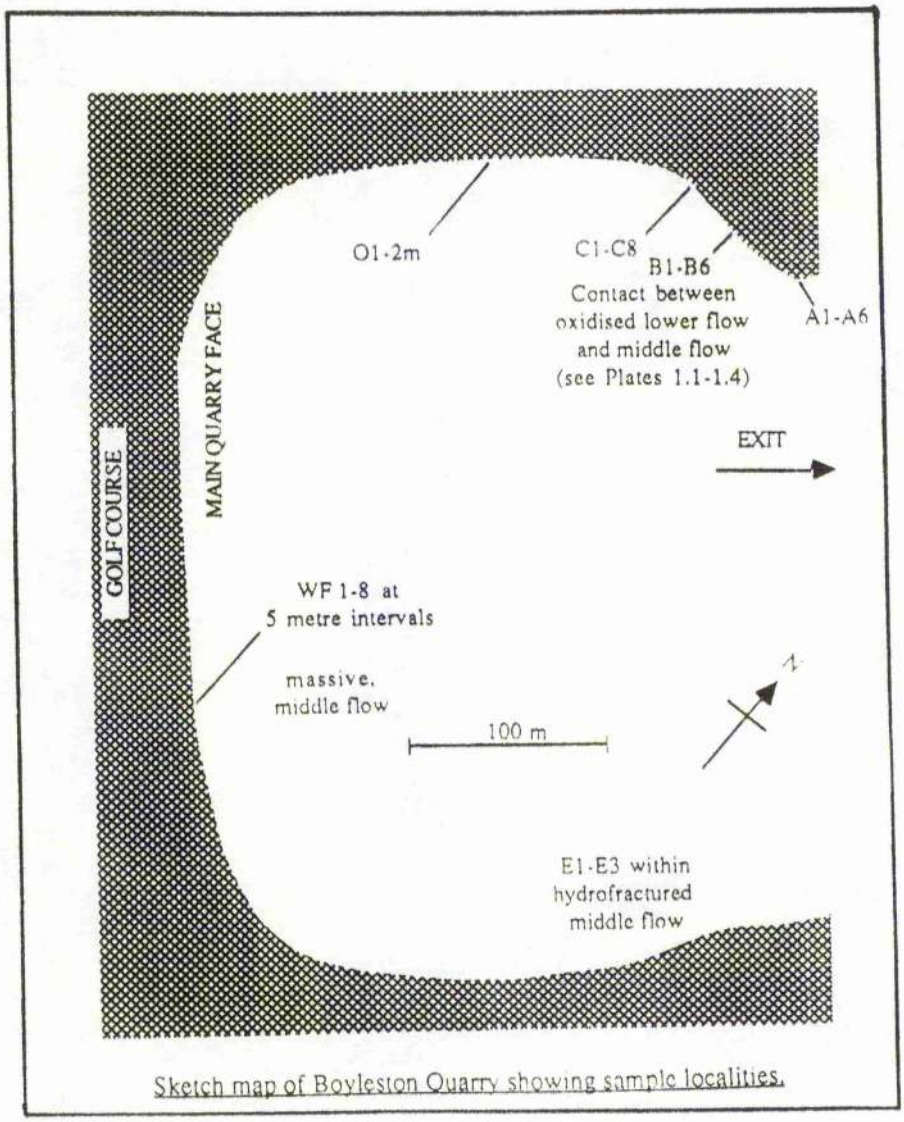

Sketch map of Boyleston Quarry showing sample localities.

2.High Craigton Quarry (526 796)

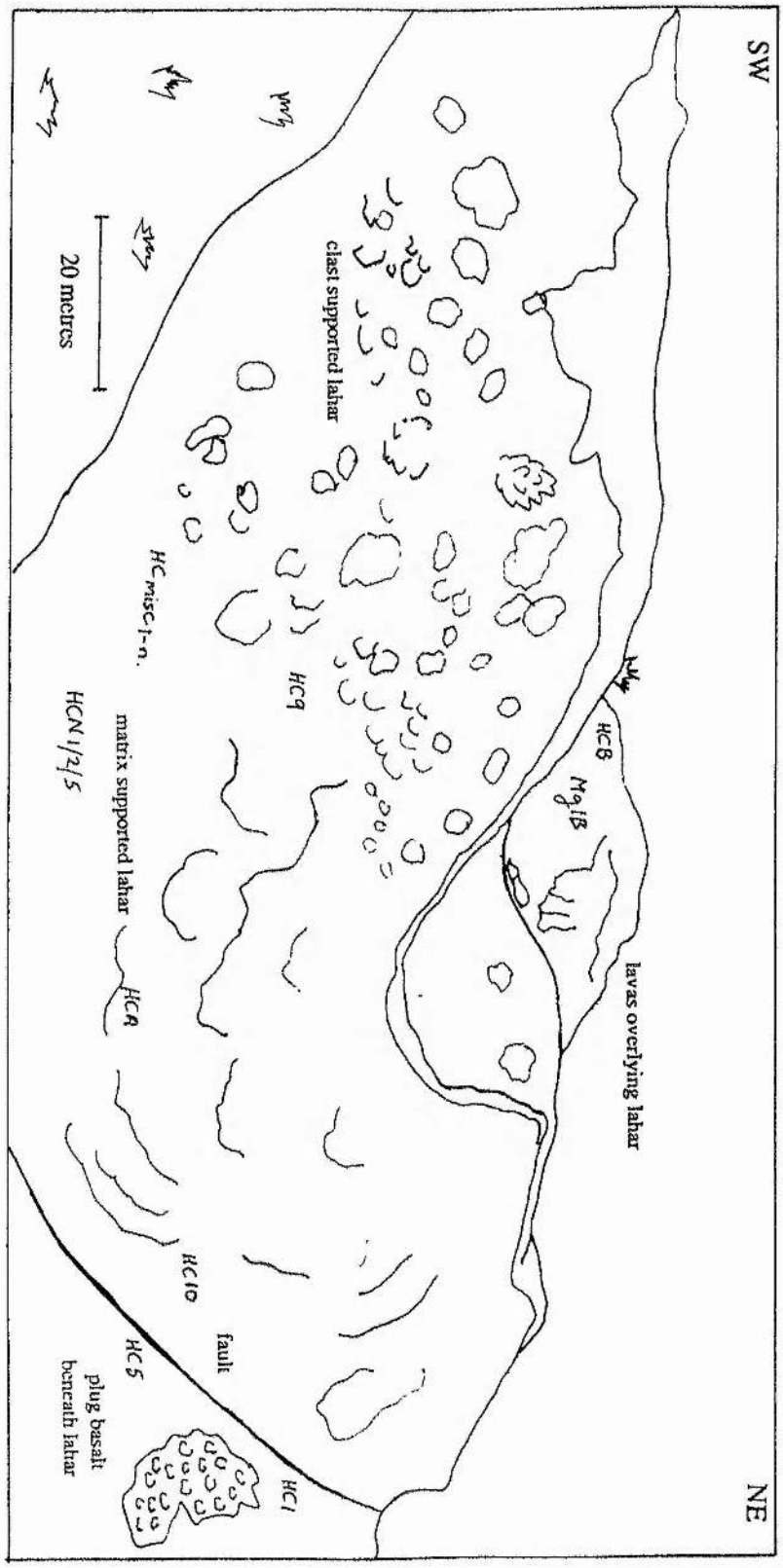

Sketch section showing metadomain locality along the western face of the quarry at High Craigton.

3. Langbank Cutting (NS 369 735)

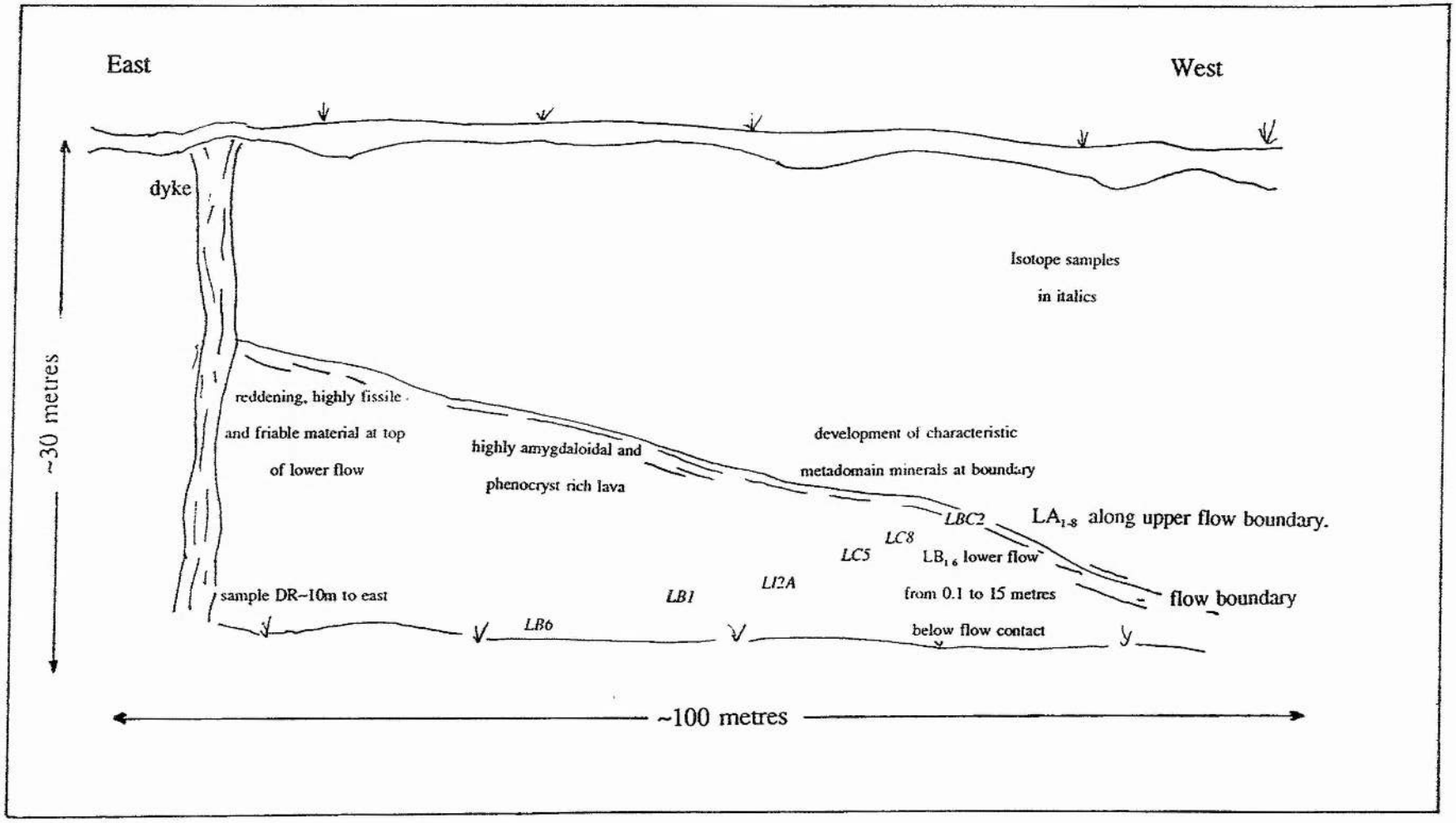

APPENDIX 3.1 : XRD ANALYSIS

Methodology

1. Sample preparation

Fist sized samples were collected from a range of environments, both within and outside metadomains. Initial treatment involved scrubbing and removal of weathered areas. After drying, samples where powdered in a Tema mill producing a coarse powder, and further disaggregated for a further 20 minutes in an ultrasound bath. Following this, samples were transferred to a centrifuge were the appropriate size fraction (< 2μm) was separated. For appropriate centrifuge settings and time intervals the reader is referred to Thomas (1986). Finally, the residual paste was pipetted to a glass slide and dried in air prior to analysis.

2. Machine specifications ; Philips PW 1010 X-Ray generator : Philips PW 1049 Diffractometer

Source : Cu-Kα radiation

Divergence slit : 1°

Receiving slit : 0.2mm

Operating conditions : 40 KV, 20 mA

Range : 5-35 ° at 1 ° / minute stepped or 0.02 ° / second.

3. Treatments for clay mineral identification

a. *Glycolation* ; Walker (1949); this is a simple method which is used to test for the presence of smectites and mixed-layer clays. The air dried sample is placed in a desiccator containing ethylene glycol at 60 ° C and left to stand overnight. If a swelling clay is present, then there is a characteristic shift (expansion) in the d-spacings of the new reflections following treatment.

b. *Heating* ; this method is based on the principal that dehydration of various clay mineral species occurs at specific temperatures and thus each species produces characteristic reflections following treatment. Premounted, glycolated samples are heated to 550 ° C for approximately 1 hour.

c. *HCl treatment* ; this test is used primarily to identify kaolinite which is not affected following treatment (unlike, for example, chlorite). Following the method of Biscaye (1964), an aliquot of powdered sample is heated to 80 ° C with 2M HCl for approximately 8 hours prior to analysis.

XRD Analysis Results

Location : Boyleston Quarry Sample details ; all slides < 2μ ; orientated

(see Appendix 2.1 for sample locations)

Ref.: O.S. Landranger 1 : 50 000 Sheet 64 (NS 492 598)

Sample No.	Lithology	Ch.	Ill.	Kao.	R.C.S.	I.C.S.	R.C.V.	I.C.V.	Comments
A1	Metadom.Basalt	*	-	-	-	*	-	-	
A2	"	-	-	-	-	*	-	-	
A3	"	-	-	-	-	*	-	-	
A4	"	*	-	-	-	*	-	-	
A5	"	-	*	-	-	*	-	-	
A6	*	-	*	-	-	-	-	-	
B1	Metadom. basalt	-	-	-	-	*	-	-	All showing
B2	"	-	-	-	-	*	-	-	one main peak at
B3	"	-	-	-	-	*	-	-	14.2-13.1 Å
B4	"	-	-	-	-	*	-	-	expanding to ~
B5	"	-	-	-	-	*	-	-	15.5.Å
B6	"	-	-	-	-	*	-	-	upon glycolation
C1	"	*	*	-	-	*	-	-	sharpening of
C2	"	-	*	-	-	*	-	-	illite 001 after
C3	"	-	*	-	-	*	-	-	heating = I_V
C4	"	-	*	-	-	*	-	-	
C5	"	-	-	-	-	*	-	-	
C6	"	-	-	-	-	*	-	-	poor trace
C7	"	-	-	-	-	*	-	-	
C8	"	-	-	-	-	*	-	-	
BQ1	*	-	-	-	-	*	-	-	
BS	Volcaniclastic sediment	-	-	-	-	*	-	-	< 2 μ and < 5 μ

*Basalt taken from outside of metadomain areas

Location : Campsie Glen (Jamie Wright's Well) Sample details ; all slides < 2μ ; orientated

(see location map below)

Ref.: O.S. Landranger 1 : 50 000 Sheet 64 (NS 616 803)

Sample No.	Lithology	Ch.	Ill.	Kao.	R.C.S.	I.C.S.	R.C.V.	I.C.V.	Comments
AP1	altered	*	-	*	-	-	-	*	002 chlorite on 001 kaol
AP1X	plagiophyre	*	-	*	-	-	-	*	V. strong kaol. peaks
AP2	"	*	-	*	-	-	-	*	
AP3	"	*	-	*	-	-	-	*	
CDX	carbonated	-	-	*	-	-	-	*	

	dyke							
Vertical Traverse through Campsie Glen								
CG3	basaltic lava	-	-	-	-	*	-	-
CG4	"	-	-	-	-	*	-	-
CG5	"	-	-	-	-	*	-	-
CG6	"	-	-	-	-	*	-	-
CG7	"	-	-	-	-	*	-	-
CG10	"	-	-	-	-	*	-	-
CG11	plagiophyre	-	-	-	-	*	-	-
CG13	basaltic lava	-	-	-	-	*	-	-
CG15	"	-	-	-	-	*	-	-
CG16	oxidised trachyte	-	-	-	-	*	-	-
CP1	Essexite	-	-	-	-	*	-	-

Location : Langbank Cutting Sample details ; all slides < 2μ ; orientated

Ref.: O.S. Landranger 1 : 50 000 Sheet 63 (NS 369 735)

Sample No.	Lithology	Ch.	Ill.	Kao.	R.C.S.	I.C.S.	R.C.V.	I.C.V.	Comments
LB2	metadom basalt	*	*	-	-	-	-	-	Illite with I_M behavour
LB1	"	*	*	-	*	-	-	-	
LA2	"	*	-	-	*	-	-	-	
LB3	"	-	*	-	*	-	-	-	
LB4	"	*	-	-	*	-	-	-	
LA1	"	-	-	-	-	*	-	-	
LB5	"	-	-	-	-	*	-	-	
LA4	dyke	*	-	-	*	-	-	-	
LA6	metadom basalt	*	*	-	*	-	-	-	
LA3	"	*	*	-	-	*	-	-	
LB6	"	-	-	-	-	*	-	-	
LA7	"	-	*	-	-	-	*	-	
LA5	"	-	*	-	-	-	*	-	
LA8	"	*	*	-	-	*	-	-	
CMV	"	-	-	-	*	-	-	-	
DR+		*	-	-	*	*	-	-	

+ basalt taken from outside of metadomain area as shown in field sketch in Appendix 2.1.

Location : High Craigton Quarry Sample details ; all slides < 2μ ; orientated

Ref.: O.S. Landranger 1 : 50 000 Sheet 64 (NS 525 779)

Sample No.	Lithology	Ch.	Ill.	Kao.	R.C.S.	I.C.S.	R.C.V.	I.C.V.	Comments
Mg3	altered lava	*	-	-	*	-	-	-	
HC22	"	*	-	-	-	-	-	*	
HC3	"	-	-	-	-	*	-	-	
HC9	"	-	-	-	-	*	-	-	
Mg1	"	-	-	-	-	*	-	-	
HC7	"	-	-	-	-	*	-	-	

HC7	"	-	-	-	-	*	-	-
Mg3	"	-	-	-	*	-	-	-
CPU	"	-	-	-	-	*	-	-
HC8	"	-	-	-	-	*	-	-
HC7$_1$	"	-	-	-	-	*	-	-
Z	"	-	-	-	-	*	-	-
HC2	"	-	-	-	-	*	-	-
Mugdock Quarry (556 776)								
Mug7	basaltic lava	-	-	-	-	*	-	-

Ch. = chlorite; Ill. = Illite; Kao. = Kaolinite; R.C.S. = Regular chlorite-smectite; I.C.S. = Irregular chlorite-smectite; R.C.V. = Regular chlorite-vermiculite; I.C.V. = Irregular chlorite-vermiculite.

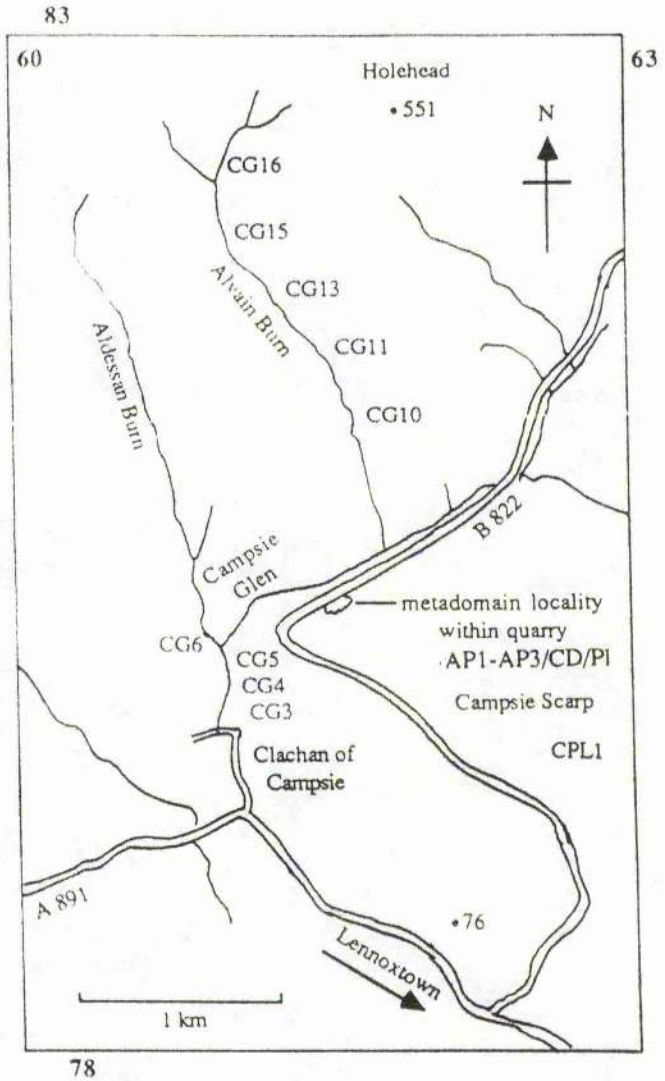

Sketch map of Campsie Glen showing sample localities

APPENDIX 3.2 MICROPROBE ANALYSES OF PHYLLOSILICATES PRESENT WITHIN BASALTS AT CAMPSIE GLEN

1. JEOL JCXA-733 SUPERPROBE: Machine specifications

Acc. voltage	15kV
Beam current	15nA
Beam diameter	~1μm

Standards

Ca	wollastonite
Si	"
Ti	rutile
Al	corundum
Fe	metal
Mn	metal
Mg	periclase
Na	jadeite
K	orthoclase

Results of analyses are presented in full over the page.

A map of sample locations is given in Appendix 3.1.

Sample CG 13

SiO_2	31.50	31.63	29.28	30.40	32.13	30.98
TiO_2	0.00	0.07	0.03	0.15	0.05	0.01
Al_2O_3	17.85	13.67	13.64	14.03	15.28	13.93
FeO	25.68	26.28	26.99	30.56	23.01	27.57
MnO	0.23	0.24	0.15	0.16	0.14	0.18
MgO	13.19	15.09	14.15	13.28	15.52	13.54
CaO	0.66	0.18	0.38	0.10	0.45	0.60
Na_2O	0.80	0.00	0.16	0.00	0.00	0.13
K_2O	0.26	0.04	0.06	0.04	0.04	0.04
Total	89.45	85.67	87.19	87.59	83.85	89.55
Si	6.44	6.51	6.72	6.35	6.60	6.64
Al^{IV}	1.55	1.48	1.28	1.65	1.40	1.31
Al^{VI}	2.75	2.00	2.13	1.93	2.24	2.36
Fe	4.39	4.76	4.79	5.54	4.18	4.76
Mn	0.04	0.04	0.03	0.03	0.03	0.03
Mg	4.02	4.87	4.48	4.28	5.02	4.17
Ca	0.14	0.04	0.08	0.02	0.14	0.05
Na	0.03	0.00	0.07	0.00	0.00	0.05
K	0.06	0.01	0.02	0.01	0.01	0.02
SiO_2	30.99	31.89	32.52	31.52	32.16	31.64
TiO_2	0.05	0.00	0.00	0.00	0.02	0.01
Al_2O_3	13.93	14.89	17.39	16.18	16.64	14.12
FeO	27.44	27.26	24.87	25.26	25.23	29.50
MnO	0.21	0.23	0.29	0.27	0.22	0.12
MgO	12.98	14.75	13.39	14.36	13.21	12.53
CaO	0.53	0.48	0.76	0.67	0.74	0.19
Na_2O	0.00	0.06	0.07	0.67	0.11	0.06
K_2O	0.08	0.07	0.16	0.13	0.18	0.27
Total	86.19	89.67	89.48	88.51	88.53	88.67
Si	6.69	6.58	6.61	6.52	6.63	6.69
Al^{IV}	1.31	1.42	1.39	1.48	1.36	1.31
Al^{VI}	2.22	2.20	2.77	2.46	2.68	2.21
Fe	4.95	4.70	4.17	4.37	4.35	5.22
Mn	0.21	0.04	0.05	0.05	0.04	0.02
Mg	4.17	4.54	4.23	4.43	4.06	3.95
Ca	0.12	0.11	0.16	0.15	0.16	0.04
Na	0.00	0.03	0.03	0.03	0.04	0.09
K	0.02	0.02	0.04	0.04	0.05	0.07

SiO_2	29.40	31.07
TiO_2	0.08	0.06
Al_2O_3	14.07	15.46
FeO	30.39	26.04
MnO	0.18	0.23
MgO	12.29	12.28
CaO	0.15	0.85
Na_2O	0.07	0.10
K_2O	0.06	0.28
Total	86.70	86.37
Si	6.43	6.64
Al^{IV}	1.57	1.36
Al^{VI}	2.06	2.52
Fe	5.56	4.65
Mn	0.03	0.04
Mg	4.01	3.91
Ca	0.04	0.20
Na	0.03	0.04
K	0.02	0.08

Sample Pl 1

SiO_2	30.55	29.12	28.50	28.11	25.39	27.43
TiO_2	0.03	0.02	0.21	0.27	0.61	0.15
Al_2O_3	20.55	20.62	17.33	17.48	17.90	18.61
FeO	28.38	26.21	29.84	29.73	29.31	29.90
MnO	0.05	0.01	0.04	0.09	0.05	0.01
MgO	8.33	9.03	11.44	11.11	10.45	9.76
CaO	0.70	0.14	0.20	0.17	0.10	0.16
Na_2O	0.95	0.22	0.31	0.17	0.10	0.06
K_2O	0.26	0.55	0.19	0.22	0.08	0.19
Total	89.86	85.96	87.94	87.22	83.96	86.29
Si	6.31	6.23	6.11	6.08	5.74	6.00
Al^{IV}	1.70	1.77	1.89	1.92	2.26	2.00
Al^{VI}	3.30	3.42	2.48	2.52	2.51	2.80
Fe	4.90	4.68	5.35	5.37	5.54	5.47
Mn	0.01	0.00	0.01	0.02	0.01	0.00
Mg	2.56	2.84	3.65	3.58	3.52	3.18
Ca	0.15	0.03	0.04	0.03	0.02	0.03
Na	0.38	0.09	0.01	0.02	0.01	0.02
K	0.06	0.15	0.05	0.06	0.02	0.05

SiO_2	32.11	31.20
TiO_2	2.12	0.19
Al_2O_3	19.14	20.24
FeO	26.79	26.53
MnO	0.04	0.09
MgO	10.15	9.53
CaO	0.26	0.15
Na_2O	0.03	0.27
K_2O	0.72	0.72
Total	91.40	88.94
Si	6.43	6.43
Al^{IV}	1.58	1.56
Al^{VI}	2.94	3.34
Fe	4.49	4.57
Mn	0.01	0.02
Mg	3.03	2.92
Ca	0.05	0.03
Na	0.01	0.10
K	0.18	0.19

Sample CG 5

SiO_2	36.73	36.47	35.22	33.25	32.80	35.02
TiO_2	0.00	0.01	0.02	0.03	0.03	0.03
Al_2O_3	15.19	15.03	14.68	13.96	13.28	14.75
FeO	19.88	22.18	23.29	23.48	23.78	23.02
MnO	0.04	0.07	0.03	0.04	0.03	0.03
MgO	14.78	14.66	15.48	15.89	17.65	15.76
CaO	0.35	0.31	0.42	0.16	0.16	0.32
Na_2O	0.31	0.21	0.22	0.13	0.08	0.27
K_2O	1.22	0.95	0.63	0.45	0.22	0.57
Total	88.53	89.92	90.05	87.83	88.04	90.14
Si	7.32	7.23	7.03	6.86	6.76	6.99
Al^{IV}	0.68	0.75	0.97	0.82	1.24	1.01
Al^{VI}	2.88	2.70	2.48	2.25	1.99	2.34
Fe	3.31	3.67	3.89	4.05	4.10	3.89
Mn	0.01	0.01	0.01	0.00	0.00	0.01
Mg	4.38	4.33	4.61	4.88	5.42	4.69
Ca	0.07	0.06	0.08	0.12	0.03	0.06
Na	0.12	0.07	0.08	0.05	0.03	0.10
K	0.31	0.24	0.16	0.11	0.05	0.14

SiO_2	34.72	33.45	34.50	34.54	34.95	34.54
TiO_2	0.00	0.06	0.03	0.02	0.02	0.00
Al_2O_3	14.78	13.60	13.81	13.94	14.33	14.80
FeO	23.07	24.50	25.38	23.61	22.79	22.77

MnO	0.05	0.05	0.11	0.07	0.00	0.12
MgO	15.46	15.23	14.49	14.41	15.18	15.42
CaO	0.29	0.20	0.29	0.31	0.38	0.25
Na_2O	0.15	0.21	0.27	0.28	0.17	0.19
K_2O	0.63	0.36	0.58	0.82	0.54	0.52
Total	89.17	87.66	89.45	88.97	88.35	88.64
Si	7.00	6.94	7.03	7.09	7.09	6.99
Al^{IV}	1.00	1.06	0.97	0.91	0.91	1.01
Al^{VI}	2.51	2.26	2.34	2.46	2.52	2.52
Fe	3.89	4.25	4.32	4.05	3.87	3.85
Mn	0.01	0.01	0.01	0.01	0.00	0.02
Mg	4.64	4.71	4.40	4.41	4.59	4.65
Ca	0.06	0.04	0.06	0.06	0.08	0.05
Na	0.05	0.08	0.10	0.11	0.06	0.07
K	0.16	0.09	0.15	0.21	0.13	0.13

Sample CG6

SiO_2	39.02	37.95	35.93	35.20	36.17	34.69
TiO_2	0.03	0.06	0.13	0.00	0.02	0.02
Al_2O_3	12.62	14.36	12.91	14.24	13.21	12.05
FeO	24.24	22.40	23.24	22.42	24.04	23.52
MnO	0.06	0.07	0.13	0.10	0.06	0.12
MgO	11.06	10.62	12.10	13.98	11.19	13.89
CaO	0.81	1.29	0.06	0.52	0.76	0.44
Na_2O	0.00	0.02	0.03	0.77	0.00	0.00
K_2O	0.58	0.21	0.16	0.09	0.10	0.06
Total	87.35	86.27	85.95	86.73	84.51	85.39
Si	7.80	7.66	7.53	7.23	7.65	7.20
Al^{IV}	0.21	0.34	0.47	0.77	0.36	0.80
Al^{VI}	3.78	3.48	2.64	2.70	2.86	2.68
Fe	3.62	3.36	4.24	3.85	4.11	3.89
Mn	0.00	0.01	0.01	0.01	0.02	0.01
Mg	3.32	3.19	3.78	4.28	3.53	4.30
Ca	0.17	0.28	0.14	0.11	0.02	0.09
Na	0.02	0.00	0.01	0.01	0.00	0.01
K	0.14	0.05	0.04	0.02	0.02	0.01
SiO_2	35.68	35.97	38.51	34.85	34.49	35.32
TiO_2	0.05	0.05	0.02	0.05	0.05	0.00
Al_2O_3	13.21	12.05	16.81	13.75	13.23	13.03
FeO	24.04	23.52	19.54	22.48	22.99	21.60
MnO	0.10	0.06	0.12	0.08	0.11	0.08
MgO	11.32	13.99	9.70	15.28	15.19	15.30
CaO	0.69	0.63	0.64	0.41	0.40	0.41
Na_2O	0.00	0.00	0.03	0.00	0.00	0.00
K_2O	0.14	0.19	0.40	0.13	0.12	0.09

Total	85.39	86.48	85.81	87.05	86.70	86.08
Si	7.52	7.47	7.77	7.16	7.15	7.30
Al^{IV}	0.48	0.52	0.23	0.84	0.85	0.70
Al^{VI}	2.80	2.84	3.76	2.48	2.38	2.46
Fe	4.23	4.08	3.29	3.86	3.98	3.75
Mn	0.01	0.01	0.01	0.01	0.01	0.01
Mg	3.55	3.90	2.92	4.68	4.69	4.74
Ca	0.15	0.13	0.13	0.09	0.10	0.09
Na	0.00	0.00	0.01	0.00	0.00	0.00
K	0.03	0.03	0.04	0.01	0.03	0.03

SiO_2	37.68
TiO_2	0.05
Al_2O_3	12.62
FeO	22.25
MnO	0.04
MgO	9.63
CaO	1.03
Na_2O	0.09
K_2O	0.40
Total	83.85
Si	7.97
Al^{IV}	0.03
Al^{VI}	3.12
Fe	3.91
Mn	0.01
Mg	3.03
Ca	0.23
Na	0.03
K	0.10

Sample CG7

SiO_2	31.65	32.04	33.04	32.45	31.87	31.78
TiO_2	0.00	0.00	0.25	0.01	0.00	0.00
Al_2O_3	14.08	15.36	15.77	14.95	15.56	14.75
FeO	22.35	23.29	21.25	22.50	24.11	23.19
MnO	0.03	0.01	0.07	0.05	0.06	0.04
MgO	17.14	15.99	16.01	17.11	16.18	17.07
CaO	0.26	0.27	0.23	0.23	0.27	0.27
Na_2O	0.05	0.14	0.16	0.63	0.16	0.16
K_2O	0.09	0.35	0.40	0.17	0.31	0.25
Total	85.65	87.45	87.35	87.53	88.52	87.55
Si	6.67	6.64	6.76	6.67	6.55	6.58

Al^{IV}	1.33	1.35	1.24	1.32	1.58	1.42
Al^{VI}	2.16	2.38	2.56	2.30	2.27	2.18
Fe	3.94	4.04	3.64	3.87	4.14	4.02
Mn	0.01	0.00	0.01	0.01	0.01	0.01
Mg	5.39	4.94	4.88	5.25	4.96	5.27
Ca	0.06	0.06	0.09	0.05	0.06	0.06
Na	0.02	0.06	0.06	0.03	0.02	0.06
K	0.02	0.09	0.10	0.04	0.08	0.07

SiO_2	31.77	32.48	31.97	31.19	32.11	32.19
TiO_2	0.02	0.06	0.00	0.08	0.03	0.00
Al_2O_3	15.13	15.27	15.79	15.78	13.89	15.35
FeO	23.02	23.62	22.80	22.07	23.25	22.28
MnO	0.01	0.01	0.12	0.35	0.00	0.00
MgO	16.73	17.38	15.74	16.31	17.51	16.82
CaO	0.31	0.22	0.27	0.98	0.22	0.21
Na_2O	0.06	0.00	0.10	0.06	0.03	0.13
K_2O	0.29	0.20	0.31	0.15	0.18	0.24
Total	87.38	89.24	87.09	86.99	87.23	87.22

Si	6.58	6.59	6.28	6.49	6.67	6.64
Al^{IV}	1.42	1.41	1.37	1.51	1.33	1.36
Al^{VI}	2.28	2.22	2.49	2.35	2.07	2.37
Fe	3.99	3.65	3.95	3.84	4.04	3.84
Mn	0.00	0.00	0.02	0.06	0.00	0.00
Mg	5.17	5.26	4.86	5.05	5.42	5.17
Ca	0.07	0.05	0.06	0.22	0.05	0.05
Na	0.02	0.00	0.04	0.03	0.01	0.05
K	0.08	0.05	0.08	0.04	0.05	0.06

SiO_2	32.36	31.68	33.48	32.13	32.83	33.01
TiO_2	0.05	0.08	0.01	0.05	0.16	0.04
Al_2O_3	14.22	14.43	15.03	14.69	16.96	14.78
FeO	23.28	22.68	22.83	22.51	21.51	22.67
MnO	0.05	0.02	0.02	0.06	0.18	0.03
MgO	17.96	17.80	17.84	16.80	17.33	17.13
CaO	0.15	0.19	0.33	0.31	0.50	0.24
Na_2O	0.15	0.17	0.15	0.12	0.11	0.05
K_2O	0.15	0.17	0.21	0.13	0.28	0.18
Total	88.23	87.19	89.90	86.79	89.84	88.13

Si	6.64	6.58	6.70	6.68	6.54	6.74
Al^{IV}	1.36	1.42	1.30	1.32	1.46	1.26
Al^{VI}	2.08	2.11	2.25	2.27	2.51	2.29
Fe	3.99	3.94	3.82	3.91	3.58	3.87
Mn	0.01	0.00	0.00	0.01	0.03	0.00
Mg	5.49	5.51	5.32	5.21	5.14	5.21
Ca	0.03	0.04	0.07	0.07	0.11	0.05
Na	0.00	0.03	0.06	0.05	0.04	0.02
K	0.04	0.04	0.05	0.03	0.07	0.05

SiO_2	31.94	32.20	33.94	32.09	31.97
TiO_2	0.07	0.09	0.23	0.13	0.03
Al_2O_3	15.08	13.91	17.35	16.22	15.65
FeO	22.67	23.27	20.91	22.30	22.83
MnO	0.06	0.04	0. 21	0.27	0.12
MgO	17.18	15.95	16.82	15.73	15.31
CaO	0.31	0.32	0.28	0.38	0.23
Na_2O	0.10	0.15	0.08	0.13	0.15
K_2O	0.23	0.31	0.25	0.21	0.43
Total	87.64	86.16	90.08	87.47	86.71
Si	6.58	6.78	6.68	6.61	6.67
Al^{IV}	1.42	1.22	1.32	1.39	1.34
Al^{VI}	2.25	2.23	2.71	2.54	2.51
Fe	3.91	4.08	3.44	3.84	3.98
Mn	0.01	0.01	0.04	0.05	0.02
Mg	5.28	5.01	4.94	4.83	4.76
Ca	0.07	0.07	0.06	0.05	0.05
Na	0.04	0.06	0.03	0.05	0.06
K	0.06	0.08	0.06	0.06	0.12

Sample CG11

SiO_2	37.06	40.97	41.24	42.04	42.13	40.88
TiO_2	0.06	0.08	0.11	0.05	0.00	0.07
Al_2O_3	13.84	17.99	15.74	15.68	15.46	15.32
FeO	22.51	18.43	19.01	19.23	21.03	20.75
MnO	0.01	0.04	0.01	0.05	0.05	0.06
MgO	10.59	8.31	9.70	9.21	9.33	9.01
CaO	0.55	0.63	0.56	0.44	0.60	0.83
Na_2O	0.31	0.33	0.51	0.54	0.43	0.35
K_2O	3.80	3.73	4.11	4.30	4.29	3.69
Total	88.78	90.59	91.00	91.53	93.33	90.98
Si	7.59	7.90	7.98	8.09	8.02	7.98
Al^{IV}	0.41	0.10	0.00	0.00	0.00	0.02
Al^{VI}	2.93	3.98	3.56	3.72	3.48	3.50
Fe	3.85	2.97	3.07	3.09	3.34	3.38
Mn	0.01	0.01	0.00	0.01	0.01	0.01
Mg	3.23	2.39	2.80	2.64	2.65	2.62
Ca	0.12	0.13	0.11	0.08	0.12	0.17
Na	0.12	0.12	0.18	0.20	0.15	0.13
K	0.99	0.91	1.01	1.05	1.04	0.91
SiO_2	41.68	39.58	39.93	38.67	39.38	41.23

TiO_2	0.03	0.07	0.09	0.12	0.15	0.05
Al_2O_3	15.73	14.44	13.86	13.88	14.50	15.78
FeO	20.79	23.38	21.88	22.97	23.79	18.13
MnO	0.05	0.03	0.04	0.05	0.10	0.00
MgO	9.09	9.02	9.70	8.49	9.19	9.20
CaO	0.79	0.59	0.51	0.60	0.56	0.57
Na_2O	0.37	0.36	0.38	0.24	0.43	0.34
K_2O	4.06	3.66	4.50	3.67	4.01	4.32
Total	92.61	91.18	90.88	88.74	92.13	89.63
Si	7.99	7.85	7.92	7.88	7.77	8.07
Al^{IV}	0.02	0.14	0.08	0.12	0.23	
Al^{VI}	3.56	3.22	3.16	3.21	3.14	
Fe	3.33	3.87	3.63	3.91	2.70	2.96
Mn	0.01	0.00	0.00	0.00	0.01	0.00
Mg	2.59	2.66	2.87	2.58	2.70	2.68
Ca	0.16	0.12	0.10	0.13	0.11	0.11
Na	0.13	0.13	0.14	0.09	0.16	0.13
K	0.99	0.92	1.14	0.95	1.01	1.07

Sample AP3

SiO_2	34.68	30.64	29.73
TiO_2	0.00	0.05	0.02
Al_2O_3	23.33	21.35	23.25
FeO	23.22	24.34	27.97
MnO	0.00	0.00	0.07
MgO	6.15	6.10	7.18
CaO	0.13	0.03	0.06
Na_2O	0.12	0.00	0.00
K_2O	2.25	2.11	0.76
Total	89.91	84.63	89.13
Si	6.89	6.60	6.14
Al^{IV}	1.72	1.40	1.16
Al^{VI}	2.17	2.01	1.90
Fe	3.85	4.38	4.83
Mn	0.00	0.00	0.01
Mg	1.82	1.95	2.21
Ca	0.03	0.01	0.01
Na	0.04	0.01	0.00
K	0.56	0.58	0.20

Sample AP2

SiO_2	27.86	28.13	30.07	30.51	28.67	29.34
TiO_2	0.02	0.05	0.08	0.09	0.06	0.01

Al_2O_3	20.52	20.67	19.93	19.21	18.61	20.9
FeO	28.14	29.11	28.76	28.85	25.43	27.59
MnO	0.11	0.07	0.10	0.02	0.00	0.09
MgO	8.76	8.69	8.32	8.09	6.61	8.32
CaO	0.05	0.14	0.18	0.02	0.13	0.14
Na_2O	0.05	0.00	0.08	0.03	0.02	0.06
K_2O	0.69	0.58	1.22	0.57	1.82	1.47
Total	86.21	87.48	88.79	87.32	81.39	88.58
Si	6.03	6.02	6.32	6.49	6.53	6.27
Al^{IV}	0.60	1.98	1.68	1.50	1.46	1.73
Al^{VI}	3.26	3.22	3.26	3.30	3.52	3.42
Fe	5.09	5.21	5.05	5.13	4.84	4.83
Mn	0.09	0.01	0.01	0.00	0.00	0.02
Mg	2.82	2.77	2.60	2.24	2.54	2.43
Ca	0.01	0.02	0.04	0.01	0.03	0.03
Na	0.02	0.00	0.03	0.01	0.01	0.02
K	0.19	0.15	0.32	0.15	0.52	0.38

SiO_2	27.49	28.29
TiO_2	0.00	0.00
Al_2O_3	19.37	19.78
FeO	30.57	32.27
MnO	0.13	0.08
MgO	8.19	7.82
CaO	0.39	0.37
Na_2O	0.13	0.09
K_2O	0.43	0.59
Total	86.69	89.36
Si	6.01	6.03
Al^{IV}	1.98	1.96
Al^{VI}	3.00	3.00
Fe	5.59	5.76
Mn	0.02	0.01
Mg	2.67	2.48
Ca	0.09	0.08
Na	0.05	0.03
K	0.11	0.15

Sample CG10

SiO_2	35.19	35.95	35.68	38.36	35.04
TiO_2	0.01	0.03	0.08	0.18	0.11
Al_2O_3	10.70	10.22	11.85	9.40	11.78
FeO	26.27	25.12	27.01	24.92	25.74
MnO	0.08	0.54	0.04	0.06	0.09
MgO	11.70	15.14	10.24	14.17	9.93
CaO	0.49	0.30	0.52	0.33	0.49
Na_2O	0.18	0.16	0.05	0.35	0.49
K_2O	0.72	0.69	0.36	1.39	0.49
Total	85.43	87.66	85.84	89.16	83.76
Si	7.57	7.48	7.61	7.82	7.64
Al^{IV}	1.57	0.52	1.32	0.01	0.36
Al^{VI}	2.28	1.98	2.58	2.08	2.66
Fe	4.73	4.37	4.80	4.25	4.69
Mn	0.01	0.01	0.01	0.01	0.01
Mg	3.75	4.69	3.27	4.31	3.22
Ca	0.11	0.06	0.11	0.07	0.11
Na	0.07	0.06	0.01	0.13	0.04
K	0.19	0.18	0.09	0.36	0.13

APPENDIX 4.1 XRF ANALYSIS

1.Method of analysis

a) Sample preparation

All samples were prepared by first removing all weathered material using a surface grinder. Samples were then fed into a jaw crusher to reduce the rock to small chips. These were then ground in a Tema swing mill until the powder was less than 200 mesh.

b) Major and minor elements

Major element compositions were determined using a fused bead prepared from 0.5g of rock powder together with 2.5g of Spectroflux 105 and ammonium nitrate as an oxidant. This method is essentially that described by Norrish and Hutton (1969).

Iron was determined as total Fe_2O_3 and the weight loss of the rock sample on fusion was measured and used as an estimate of loss on ignition (F.Loss).

Trace elements were analysed using pressed powder discs prepared using 5g of rock powder and Moviol as a binder.

c) Machine conditions

Analysis was carried out using Philips PW 1450/20 and PW 1212 sequential spectrometers. In all cases a Rh tube was used for primary excitation of elements. Operating conditions were either 50 kV-30 mA (PW 1450/20) or 40 kV-32 mA (PW 1212).

d) Accuracy and Precision

Accuracy is estimated by reference to "accepted" values from well known USGS reference standards. The six standards were ran blind during one analytical session. The maximum difference between reported USGS standard and values obtained at St. Andrews is given in the table below for each major element oxide.

SiO_2	0.62%
TiO_2	0.01%
Al_2O_3	0.27%
Fe_2O_3	0.19%
MgO	0.38%
CaO	0.06%
Na_2O	0.1%
K_2O	>0.1%
P_2O_5	0.02%

Precision estimates for the major oxides are based upon six replicates each on six separate beads. Mean sample compositions and standard deviations are given in the table below.

	Mean composition	Standard deviation
SiO_2	71.65	0.16
TiO_2	0.39	0.00
Al_2O_3	14.52	0.05
Fe_2O_3	2.66	0.01
MnO	0.55	0.00
MgO	0.68	0.05
CaO	1.93	0.00
Na_2O	3.6	0.1
K_2O	3.5	0.0
P_2O_5	0.08	0.01
V	34.4	0.8
Ba	908	9
La	105	1.3
Ce	129.4	2.1
Hf	5.83	0.35
Cr	60.7	0.6
Ni	106	0.7
Cu	34.5	0.7
Zn	62.5	0.8
Nb	27.3	1.18
Zr	216	0.9
Y	26.1	0.9
Sr	324	1.5
Rb	176	1.5
Th	24.4	3.0
Pb	23.8	0.9

e) Results

Given below are the major and trace element compositions of samples collected from Boyleston Quarry, Langbank Cutting and Campsie Glen. Full sample details are given in Appendix 2.1.

Location : Boyleston Quarry
Ref.: O.S. Landranger 1 : 50 000 Sheet 64 (NS 492 598)

Sample	A1	A2	A3	A4	A5	A6*
SiO_2	44.29	47.02	48.37	45.99	52.36	48.22
TiO_2	1.65	1.93	2.01	1.87	1.70	1.97
Al_2O_3	16.02	15.06	15.03	13.96	14.89	16.29
Fe_2O_3	9.67	12.29	13.34	12.18	11.26	13.82
MnO	0.06	0.11	0.10	0.14	0.13	0.34
MgO	1.42	3.44	4.52	6.15	3.86	5.55
CaO	15.30	9.79	4.94	6.79	4.71	5.58
Na_2O	4.4	4.9	6.1	5.1	6.7	3.6
K_2O	0.4	0.7	0.8	1.1	1.9	0.5
P_2O_5	0.25	0.32	0.34	0.29	0.24	0.28
F.Loss	5.4	3.4	3.8	6.4	2.6	3.6
Tot.	98.93	98.96	99.35	99.97	100.35	99.75
Zn	15	75	73	88	71	80
Cu	548	26	13	9	4	5
Ni	22	52	53	51	31	40
Cr	24	30	29	31	22	29
V	354	449	434	447	195	339
Ba	20	187	163	242	384	1219
Hf	6	3	3	3	3	4
Ce	34	63	58	60	60	58
La	16	26	19	20	17	18
Nb	21	28	27	26	26	26
Zr	115	135	153	142	129	87
Y	18	22	23	21	21	21
Sr	258	474	293	334	381	1510
Rb	0	5	4	12	22	42
Th	7	6	4	1	2	0
Pb	2	8	5	9	4	7

Sample	B1	B2	B3	B4	B5
SiO_2	48.70	47.35	40.17	43.35	45.62
TiO_2	1.83	2.21	1.43	1.83	1.86
Al_2O_3	15.29	14.05	15.96	14.73	14.13
Fe^3O_3	12.09	13.70	9.85	11.02	10.70
MnO	0.12	0.14	0.06	0.07	0.08
MgO	4.59	5.81	2.59	2.59	2.85
CaO	5.97	5.30	18.80	12.38	11.6
Na_2O	6.3	5.7	5.4	5.8	5.5
K_2O	0.2	0.3	0.9	0.0	0.1
P_2O_5	0.29	0.35	0.33	0.36	0.32
F.Loss	4.0	4.4	5.4	6.6	6.6
Tot.	98.38	99.10	100.89	98.73	99.36
Zn	89	94	42	47	60
Cu	5	2	84	42	21
Ni	45	65	27	33	46
Cr	32	37	23	20	23
V	493	470	386	366	322
Ba	19	82	7	21	31
Hf	3	3	3	3	3
Ce	38	65	64	50	61

Nb	23	28	20	25	27
Zr	131	150	121	145	148
Y	21	24	24	22	20
Sr	524	706	100	237	265
Rb	3	1	0	0	0
Th	2	3	1	5	3
Pb	2	1	6	5	3

Sample	C1	C2	C3	C4	C5	C6	C7	C8	C9
SiO_2	45.82	49.96	45.84	46.77	45.06	49.04	39.47	45.82	48.65
TiO_2	2.03	2.01	1.76	1.78	1.63	1.76	1.37	2.07	1.96
Al_2O_3	16 15	15.99	14 14	14.58	13 79	14.60	13.38	14.49	15.01
Fe_2O_3	13 02	10.98	11 56	11 89	10 98	11.76	9.12	13.50	12.08
MnO	0.12	0.13	0.15	0.13	0.15	0.15	0.12	0.13	0.16
MgO	4.35	4.12	5.76	3.59	4.87	4.52	3.96	3.99	7.40
CaO	6.89	5.13	6.82	7.93	8.54	6.35	12.50	7.98	5.48
Na_2O	3.9	7.1	6 1	5.2	5.8	6 4	5.7	5.5	4.2
K_2O	2 4	0 9	1 2	2.2	1 3	0.9	1.4	1.2	1.6
P_2O_5	0 27	0 23	0 35	2 18	1.32	0.92	0.22	0.34	0.28
F.Loss	5.0	4.2	6 2	4.2	6.6	4	13.4	5.4	3.8
Tot.	99.95	100.8	99.88	100.5	100.0	100.4	100.6	100.4	100.5
Zn	100	n.d.	113	91	100	93	83	76	105
Cu	27	n.d	165	28	17	8	145	41	6
Ni	28	n d	28	28	28	31	23	36	51
Cr	17	n d	20	17	16	19	12	19	59
V	314	120	182	140	127	104	88	206	657
Ba	400	184	294	426	311	249	350	228	897
Hf	4	3	3	3	3	3	3	4	4
Ce	34	68	40	28	53	53	53	49	65
La	24	17	24	25	23	27	23	19	26
Nb	25	24	25	23	27	23	22	27	30
Zr	106	105	130	131	148	134	116	129	98
Y	20	19	21	21	20	19	20	24	23
Sr	1257	628	284	492	265	415	614	728	1290
Rb	56	11	11	44	0	1	12	27	28
Th	3	0	2	0	3	0	0	0	3
Pb	2	11	11	12	3	0	0	3	7

* denotes composition of sample collected outside of metadomain area.
n.d. ; no data.

Location; Langbank Cutting
Ref. O.S. Landranger 1:50 000 Sheet 63 (NS 369 735)

Sample	LA1	LA2	LA3	LA4	LA5	LA6
SiO_2	43.34	40 86	43.82	43.72	51.62	48.70
TiO_2	3.03	2.15	2 87	2.28	2.05	2.60
Al_2O_3	18.09	17 94	18.71	19.22	17.11	17.90
Fe_2O_3	13.34	9.82	10 82	9.93	9.04	11.07
MnO	0.14	0.18	0.19	0.13	0.13	0.12
MgO	5.81	7.07	8.18	5.89	3.85	3.62
CaO	1.59	6 16	2 17	2.61	1.98	2.44
Na_2O	1.2	4 3	2 7	2.4	3.0	4.9
K_2O	5 3	1 6	2 4	3 1	7.0	3.3
P_2O_5	0.21	0 47	0.44	0.30	0.30	0.40
F.Loss	7.8	10.7	7.0	10.6	3.0	5.6
Tot	99 85	101 25	99.30	99.78	99.08	100.65
Zn	208	n d	239	n d	169	193
Cu	0	n d	0	n.d.	0	0
Ni	19	n d	14	n.d	16	15
Cr	0	n.d.	0	n.d.	16	15
V	41	n.d.	83	n.d.	80	11
Ba	407	n d	316	n.d.	1074	566
Hf	n.d	n d.	n d	n d	n d.	n.d.
Ce	82	n d	96	n.d	31	54
La	43	n.d	47	n.d	22	26
Nb	47	n.d.	39	n.d.	29	32
Zr	238	n d.	204	n.d.	148	174
Y	34	n d	32	n d.	18	23
Sr	172	n d	332	n.d	172	277
Rb	218	n.d	69	n.d	96	82
Th	6	n.d	5	n.d	1	3
Pb	87	n.d.	91	n.d.	17	42

Location: Langbank Cutting
Ref. O.S. Landranger 1:50 000 Sheet 63 (NS 369 735)

Sample	LA7	LA8	LB3	LB4	LB5	LB6	LB1	DR*
SiO_2	47.22	48.77	44.93	47.37	51.65	44.61	48.98	46.85
TiO_2	2.54	2.47	2.46	3.14	1.84	2.37	2.49	3.41
Al_2O_3	17.84	17.56	17.78	15.64	16.71	17.19	17.56	15.95
Fe_2O_3	11.08	10.90	11.81	13.32	8.29	10.63	9.97	11.64
MnO	0.51	0.24	0.22	0.17	0.08	0.11	0.15	0.20
MgO	4.18	4.75	9.27	5.14	1.42	3.38	4.46	6.69
CaO	2.83	4.19	1.36	2.89	4.53	8.51	2.83	4.19
Na_2O	4.2	4.8	3.6	5.8	9.4	3.9	5.2	5.7
K_2O	3.4	2.7	2.1	1.5	0.1	2.1	2.5	0.9
P_2O_5	0.40	0.37	0.34	0.55	0.32	0.36	0.40	0.62
F Loss	5.8	3.2	6.8	4.0	5.0	6.0	6.4	4.8
Tot	98.60	100.0	100.67	99.52	99.34	99.16	100.9	100.9
Zn	203	285	445	250	86	53	236	283
Cu	0	0	0	0	0	0	0	0
Ni	15	14	14	5	9	14	13	7
Cr	0	0	0	0	0	0	0	0
V	115	195	131	198	28	179	107	216
Ba	464	826	292	318	26	411	244	163
Hf	n.d.	n.d.	n.d.	n.d.	n.d.	n.d.	n.d.	n.d.
Ce	66	54	62	89	39	51	58	39
La	24	23	24	33	16	23	29	17
Nb	35	31	35	53	27	30	34	15
Zr	189	206	185	272	141	199	184	319
Y	26	23	24	33	16	23	25	22
Sr	460	1121	243	336	151	1098	325	370
Rb	110	70	62	34	3	47	89	14
Th	5	5	4	5	3	4	5	7
Pb	40	29	53	41	9	0	41	29

* denotes composition of material collected outside of metadomain

Location Campsie Glen
Ref O.S Landranger 1:50 000 Sheet 64 (NS 616 803)

Sample	Pl*	AP1	AP2	AP3	CD
SiO_2	46.88	51.69	41.37	49.33	55.53
TiO_2	3.08	2.02	3.58	2.47	3.68
Al_2O_3	15.72	10.39	18.32	13.08	15.66
Fe_2O_3	15.74	13.86	17.46	15.79	12.28
MnO	0.13	0.23	0.11	0.16	0.31
MgO	1.89	2.23	2.49	2.55	1.64
CaO	5.91	7.84	2.89	4.99	1.07
Na_2O	3.5	0.2	2.9	0.6	2.9
K_2O	0.4	0.9	1.1	0.9	0.7
P_2O_5	0.54	0.29	0.63	0.41	0.51
F.Loss	4.6	9.8	8.6	8.8	6.4
Tot.	98.49	99.45	99.45	99.08	100.68
Zn	53	68	63	n.d.	n.d.
Cu	0	0	0	n.d	n.d.
Ni	9	7	9	n.d	n.d.
Cr	0	0	0	n.d	n.d.
V	0	0	0	n.d.	n.d.
Ba	230	206	215	n.d.	n.d.
Hf	n.d.	n.d.	n.d.	n.d.	n.d.
Ce	64	39	89	n.d	n.d.
La	25	17	37	n.d	n.d.
Nb	32	24	40	n.d	n.d.
Zr	243	173	271	n.d.	n.d.
Y	30	22	36	n.d.	n.d.
Sr	447	49	51	n.d.	n.d.
Rb	9	18	23	n.d.	n.d.
Th	4	4	5	n.d	n.d
Pb	2	3	3	n.d	n.d.

* denotes composition of material collected outside of metadomain

Element	Boyleston Quarry	Langbank Cutting	Campsie Glen
	n=19	n=13	n=3*
SiO_2	3.0	3.2	4.4
TiO_2	0.2	0.4	0.7
Al_2O_3	0.8	1.4	3.3
Fe_2O_3	1.2	1.4	1.5
MnO	<0.1	<0.1	<0.1
MgO	1.4	1.9	0.1
CaO	3.8	1.9	2.0
Na_2O	0.8	1.7	2.0
K_2O	0.7	<0.1	1.2
P_2O_3	0.5	1.5	0.1
F.Loss	2.2	2.3	0.52
Sr	375	52	1
Rb	17	52	2
Cu	125	0	0
Zn	24	99	2.5
Y	1	5	7
Zr	17	37	49

* n=2 for trace elements

Table showing standard deviation for each element as determined using XRF analysis. Gains and losses accompanying metadomain alteration, using the isocon technique, are determined using Figure 4.3(majors in wt.%, traces in ppm)

APPENDIX 5.1 FLUID INCLUSION RESULTS

Mineral : Calcite
Location : Boyleston Quarry

Sample No: OM *associated with ananlcime*

Type	*Tfm ice*	*Tm ice*	*Th*	*F*	*Type*	*Tfm ice*	*Tm ice*	*Th*	*F*
L+V					L+V				
			107	0.90				132	0.90
			165	0.90		-67		67	0.95
		0		0.85			0	115	0.90
	-67	0		0.90					

Sample No: E2 *associated with analcime*

L+V					L+V				
	-50	-9	115	0.90		-45	-2		
		-16		0.90		-64	-10		0.90
	-64	-13		0.90			0	110	0.95
	-55	-14		0.95		-62	-5	126	0.85
	-66	-17	138	0.90				138	0.90
			145	0.85				138	0.90
	-51			0.60					

Sample No: OL *associated with analcime*

L+V					L+V				
	-39	-1	123	0.85		-47	-2	58	0.95
		0	111	0.90		-39	0	58	0.95

Sample No: S1 *associated with prehnite*

L+V					L+V				
	-65			0.90		-65	-23	72	0.95
	-66	-21		0.90		-46	-20	144	0.90
	-66	-21	173	0.90		-66	-20	119	0.95
			138	0.95				58	0.95
			208	0.90				157	0.85
			169	0.85				230	0.90
			210	0.85			0	196	0.80
		0	179	0.95			0	111	0.95
		0	116	0.95			0	190	0.80
		0	177	0.80			0	202	0.90
		0	165	0.85			0	191	0.85
		0	155	0.85					

Sample No: S5 *associated with prehnite*

L+V					L+V				
	-60	-19		0.90		-60	-19		0.90
	-60	-18	142	0.90		-64	-18	129	0.90
			144	0.95			-18	115	0.95
	-64	-20	155	0.95		-64	-19	123	0.90

Sample No: S7 *associated with prehnite*

L+V					L+V				
		0		0.80			0		0.70
		0		0.80			-2		0.80
			222	0.90				185	0.90
			176	0.80				255	0.80

Sample No: WF4 *associated with analcime*

L+V				L+V			
	0	100	0.95		0	165	0.85
	0		0.85			139	0.90
	0		0.80		0	161	0.90
	0	149	0.90		0	206	0.90
		182	0.90	-59	-1		0.95
		149	0.90	-64	-16	181	0.85

Sample No: WF7 *associated with analcime*

L+V				L+V			
-56		137	0.95	-40	-20	136	0.85
-49		102	0.85	-69		100	0.90
-74	-25		0.90			137	0.90
-65	-23	58	0.90			174	0.90
-63		126	0.90			129	0.90
		90	0.90	-49	-24	149	0.85
-49	-19	174	0.80	-48	-13	123	0.90
-67	-7	160	0.90		-13		
-49	-19	174	0.90	-60	-14	134	0.90
-47	-14	203	0.85	-50	-14	136	0.90
-52	-18	173	0.90	-46	-14	114	0.90
-52	-8	210	0.90	-49	-17	138	0.90
-60	-24	93	0.90	-45	-9	188	0.80
-41	-7	172	0.90	-49	-6	186	0.90
-47	-16	211	0.90	-47		134	0.90
-47	-15	98	0.90				

Sample No: S5 *associated with prehnite*

L+V				L+V			
		225	0.80		0	192	0.85
	0		0.80		0	178	0.90
	0		0.80			180	0.90
-57	-28				0	218	0.85
-60	-21	163	0.90		0	194	0.80
-66	-28	176	0.90			241	0.90
-60	-23	164	0.95			111	0.85
-45	-4	179	0.90	-35	-1		0.80
		137	0.90				

Mineral : Calcite

Location: High Craigton Quarry (no prehnite at this locality)

Sample No: X

Type	*Tfm ice*	*Tm ice*	*Th*	*F*	*Type*	*Tfm ice*	*Tm ice*	*Th*	*F*
L+V					L+V				
		-12	61	0.90		-66	-16	81	0.90
		-16	65	0.95			-18	50	0.90
		-16	88	0.90		-60			
		-16	74	0.90			-22	62	0.90
	-60		59	0.95			-12	90	0.95
		-17	90	0.90		-72	-12		
		-14	126	0.90		-60	-16	144	0.85
	-56	-12				-57	-15		
		-19	160	0.95			-19	151	0.95
	-72	-14	172	0.85		-58	-15	147	0.90
	-72	-14							

Sample No: Mg2

L+V				L+V			
	0	128	0.90		0	139	0.90
	0	131	0.95		0	136	0.95
	0	151	0.90		0	145	0.90
	0	133	0.90		0	110	0.95
	0	149	0.90		0	74	0.95
	0	76	0.90		0	76	0.90
	0	125	0.90		0	113	0.90
		86	0.90		0	80	0.90
		85	0.95		0	110	0.90
		121	0.90		0	131	0.90
	0	75	0.95		0	81	0.95
	0	132	0.90		0	132	0.90
	0	69	0.95		0	68	0.95
	0	133	0.90			98	0.95
	0	92	0.90			129	0.95
	0	94	0.95			114	0.90
		87	0.90			89	0.95
		177	0.85				

Sample No: Mg3

L+V				L+V			
		115	0.90			98	0.95
		106	0.90			55	0.95
		94	0.90		0	92	0.90
		111	0.90				

Sample No: HCN

L+V				L+V			
	0	185	0.80		0	123	0.90
	0	135	0.90		0	164	0.80
	0	165	0.80		0	151	0.80
	0	114	0.95	-50	-16	153	0.85
	0	115	0.90	-31	-2	147	0.90
	0	105	0.95		0	105	0.95
	0	108	0.95		0	113	0.95
		115	0.90		0	120	0.90
	-15			-70	-16		
-65	-16	164	0.85	-65	0	107	0.95
-65	-16	167	0.80	-63	-16	99	0.90
-68	-17	120	0.90			117	0.90
	0	115	0.90		0	115	0.90
	0	98	0.90		0	129	0.90
	0	127	0.90				

Sample No: HC5

L+V, V+L				L+V, V+L			
-61	-15			-62	-14	187	0.80
-43(L)				-47	-14		
-53	-16	163	0.75	-60	-17	174	0.80
-66	-13			-66			
		196	0.90			160	0.90
-51	-15	205	0.85	-69	-26	143	0.85
		129	0.90			190	0.85
		162	0.85			135	0.90
		139	0.90			134	0.90
		140	0.90			165	0.90
		159	0.85	-63	-21	309	0.60
-57	-8	309	0.55		-17	240	0.60
		255	0.70		-15	233	0.60

Mineral : Calcite
Location: Langbank Cutting
Sample No: CV86 (Evans, 1987)

Type	*Tfm ice*	*Tm ice*	*Th*	*F*	*Type*	*Tfm ice*	*Tm ice*	*Th*	*F*
L+V(primary)					L+V(primary)				
	-62	-21	85	0.95		-62	-6	110	0.95
	-62	-22	89	0.95		-62	-18	145	0.95
	-63	-20	144	0.95		-62	-19	142	0.95
	-62	-17	123	0.95		-59	-3	133	0.95
	-62	-7	115	0.95		-64	-18	164	0.95
			96	0.95			0	124	0.95
	-62		171	0.85				134	0.90
			107	0.95				114	0.90
	-58		126	0.90		-65		128	0.90
			129	0.90			0	123	0.90
			89	0.95				86	0.95
			130	0.90				143	0.95
		0	133	0.90		-61	-12	134	0.90
		-3	163	0.95		-61		165	0.95
			80	0.90				84	0.90
			97	0.90				98	0.90
			110	0.90			-4	107	0.90
			97	0.90				132	0.90
			142	0.95				133	0.90
		0	94	0.90				118	0.90
			87	0.90				98	0.95
			123	0.90				127	0.90
			126	0.90					
L+V(secondary)									
		0	122	0.95				102	0.95
			91	0.95				71	0.90
			73	0.95			0	115	0.95
		0	107	0.95			0	83	0.90
			116	0.90				97	0.95
			79	0.95					

Mineral : Analcime
Location: Boyleston Quarry
Sample No: WF2

Type	*Tfm ice*	*Tm ice*	*Th*	*F*	*Type*	*Tfm ice*	*Tm ice*	*Th*	*F*
L+V(primary)					L+V(primary)				
	-23	0	108	0.90			-3	149	0.90
		-1	168	0.95		-19		133	0.90
		-1	115	0.90			0	187	0.85
	-21	-1	259	0.90		-25	-1	239	0.75
	-20	-2	289	0.90			0	232	0.85
	-21	0	188	0.90				113	0.90
			113	0.90			0	152	0.90
		0	156	0.80			0	204	0.90
	-24	0				-21	0		
	-21	0				-21	0		
	-24	0	257	0.90		-22	0	251	0.90
	-20	0		0.90		-20	0	253	0.85
	-20	0	257	0.85		-20	0	267	0.90
	-27	0	187	0.80		-20	0	214	0.75
	-24	0	224	0.75		-24	0	243	0.80
	-24	0	255	0.75		-23	0	178	0.80
		0	173	0.90			-1	212	0.85
			200	0.90			0	190	0.85
		0	186	0.90			0	186	0.90

0	185	0.90		-1	181	0.90
0	181	0.90		-1	175	0.90
	175	0.90		0	175	0.90

Mineral : Quartz
Location: Mugdock Quarry
Sample No: MQ1

Type	*Tfm ice*	*Tm ice*	*Th*	*F*	*Type*	*Tfm ice*	*Tm ice*	*Th*	*F*
L+V(primary)					L+V(primary)				
		0	142	0.95		-27	0	147	0.95
		0	82	0.95			0	94	0.95
		0	81	0.95		-36	0	105	0.95
	-31	0	100	0.95				95	0.95
			75	0.95				96	0.95
	-27	0	87	0.95			0	87	0.95
		0	105	0.95				87	0.95
	-29		91	0.95		-28	0	92	0.95
			77	0.95				145	0.95
			133	0.95				101	0.95
			84	0.95				101	0.95
			125	0.95				107	0.95
			96	0.95				66	0.95
			105	0.95				146	0.95
		0	138	0.95				89	0.95
		0	156	0.90		-29	0	95	0.95
			87	0.95			0	72	0.95
			93	0.95				83	0.95
			89	0.95				82	0.95
		0	79	0.95		-28	0	96	0.95
			86	0.95				118	0.95
			122	0.95				97	0.95
			108	0.95			0	121	0.95
			116	0.95				112	0.95
			139	0.95		-29	0	140	0.95
			105	0.95				118	0.95
			107	0.95				133	0.95
			97	0.95					

APPENDIX 5.2 FLUID EXTRACTION DETALS

1. Fluid extraction results

Given below are the results of 20 analyses performed upon calcite samples collected from the Clyde Lavas (see Appendix 6.1 for details). The proportions of water, carbon dioxide and non-condensables determined from analysis are expressed both as moles per gram of calcite and relatative percentages.

Sample No	H_2O ($mol.g^{-1}$)	CO_2 ($mol.g^{-1}$)	Non C. ($mol.g^{-1}$)	H_2O (%)	CO_2 (%)	Non C. (%)
HCmisc 2	$9.2*10^{-6}$	$4.9*10^{-7}$	$9.6*10^{-8}$	93.9	5.0	1.1
HC10	$6.0*10^{-6}$	$5.0*10^{-7}$	$2.2*10^{-7}$	89.3	7.4	3.2
HC5	$1.3*10^{-4}$	$3.0*10^{-6}$	$4.3*10^{-6}$	94.5	2.3	3.2
Mug3	$2.9*10^{-4}$	$1.9*10^{-6}$	$5.2*10^{-7}$	99.0	0.6	0.3
Mg1A	$2.0*10^{-5}$	$7.9*10^{-7}$	$1.4*10^{-7}$	81.5	3.2	15.3
Mug2	$8.3*10^{-7}$	$9.9*10^{-8}$	$4.4*10^{-8}$	85.3	10.1	4.5
Mg1C	$2.6*10^{-6}$	$5.1*10^{-8}$	$1.2*10^{-8}$	97.6	1.9	0.5
X1	$2.5*10^{-5}$	$2.5*10^{-6}$	$7.8*10^{-7}$	88.7	8.6	2.6
X3	$3.1*10^{-5}$	$5.5*10^{-6}$	$1.6*10^{-6}$	81.1	14.5	4.3
B6	$1.9*10^{-4}$	$3.1*10^{-6}$	$1.3*10^{-6}$	97.7	1.6	0.7
A4	$1.5*10^{-4}$	$5.7*10^{-6}$	$1.8*10^{-6}$	95.2	3.6	1.1
C3	$7.9*10^{-5}$	$6.9*10^{-6}$	$1.7*10^{-6}$	90.2	7.8	1.8
A2	$7.5*10^{-5}$	$6.9*10^{-6}$	$1.6*10^{-6}$	90.2	7.9	1.9
B3	$4.9*10^{-4}$	$6.1*10^{-6}$	$3.2*10^{-6}$	98.1	1.2	0.6
A3	$1.6*10^{-4}$	$1.0*10^{-5}$	$7.3*10^{-6}$	90.0	5.7	4.1
B5	$2.3*10^{-5}$	$1.2*10^{-6}$	$3.5*10^{-7}$	93.8	4.7	1.4
C1	$2.9*10^{-5}$	$5.3*10^{-6}$	$1.7*10^{-6}$	80.1	14.9	4.8
C6	$1.1*10^{-4}$	$4.1*10^{-6}$	$4.0*10^{-6}$	92.9	3.5	3.4
B4	$3.7*10^{-5}$	$4.6*10^{-6}$	$9.7*10^{-6}$	72.2	8.9	18.8
C7	$1.1*10^{-4}$	$4.9*10^{-6}$	$2.7*10^{-6}$	93.2	2.3	4.2

N.C.= non condensables.

2. Gas Chromatograph details

For G.C. analysis of the non aqueous condensible phase 0.4 g of sample is used. The non condensible phases are sent directly to a Carlo Erba G.C. fitted with a thermal conductivity detector and 6' * 1/8 " glass column fitted with "Porapack Q" 80-100. Analysis is carried out under a Helium flow of 25 mL min^{-1} with an oven temperature of 100 °C isothermal. The column was calibrated using standard gas mixtures.

3. Accuracy and precision

Accuracy was determined by comparing results obtained from the British Geological Survey on a sample of quartz from Carrock Fell, Cumbria. A total of three runs were carried out, the results of which are tabulated below

	H_2O	CO_2	Non Condensibles
St. Andrews	71.3	1.48	0.35
St. Andrews	72.6	1.5	0.4
St. Andrews	75.3	1.4	0.4
B.G.S.	*74.7*	*1.47*	*0.3*

Precision estimates are based upon repeated analysis of Brazilian Quartz, the results of which are tabulated below.

H2O	CO2	Non Condensibles
5.8	3.9	0.54
5.6	3.8	0.60
5.1	3.8	0.50
5.6	3.8	0.52
5.52+/-0.3	3.82+/-0.05	0.54+/-0.04

All results quoted in $mol*10^{-6}g^{-1}$.

APPENDIX 6.1. LOCATION AND DESCRIPTION OF SAMPLES USED FOR ISOTOPE ANALYSIS

Mineral: Analcime

Boyleston Quarry

Sample No.	Description	Sample No.	Description
OL/OL1	Euhedral, isometric and cloudy within amygdales.	OM	Clear, isometric, massive crystals with some green staining Intensely hydrofractured.
S4	Analcime dominated vein with minor calcite. Massive analcime.	S1/ S41	Analcime rich hydrofractured vein with minor calcite. Cloudy massive analcime.
S6/S61	Analcime rich hydrofractured vein. Minor prehnite and calcite.	WF 11	Hydrofractured massive analcime Cloudy analcime with widescale green staining.
WF2	Minor cloudy analcime in small quartz rich vein.	WF3/WF31	Isometric cloudy analcime dominating fist sized amygdale.
WF4	Cloudy, massive analcime in vein. Also present minor green prehnite and calcite.	WF6	Calcite dominated vein system with minor prehnite and clear to slightly cloudy analcime.
E1	Small iron stained vein network dominated by clear analcime.	E3	Hydofractured, analcime rich vein. Clear analcime.
Z1	Analcime rich vein with minor calcite. Cloudy, massive analcime.		

High Craigton Quarry

HCA	Cloudy analcime from hydrofractured vein dominated by calcite.	HCB	Massive, pink analcime from large amygdale. Also calcite.

Langbank Cutting

CV86	Massive, cloudy analcime in large calcite dominated amygdale.

Mineral: Calcite

Boyleston Quarry

Sample No.	Description	Sample No.	Description
OL	Minor clear cacite rhombs in analcime dominated amygdale.	O2/O21	Clear calcite from amygdale. Green staining around margins.
OM	Intensely hydrofractured analcime dominated vein. Minor clear calcite with green staining.	O3	Clear calcite from fine grained vein.
WF2	Minor, fine grained, clear calcite in small hydrofractured vein network.	WF4/WF41	Minor, clear, massive calcite in prehnite rich vein.
WF5	Minor clear calcite rhombs growing on milky analcime.	WF6	Clear, calcite dominated vuggy amygdale with minor prehnite.
WF8	Minor calcite after clear polycrystalline quartz.	S1	Vuggy clear calcite.
S3	Minor clear calcite from small prehnite vein.	S5	Milky and clear calcite rich hydrofractured vein.
S6	Minor, polycrystalline clear calcite grains on analcime.	S7	Clear calcite from minor prehnite rich vein.

Sample No.	Description	Sample No.	Description
B1	Minor calcite on white analcime amygdale.	C1	Large calcite rhombs on botroydal prehnite. Minor green staining.
E2	Minor, clear calcite within hydrofractured middle flow		
High Craigton Quarry			
HC 10	Cloudy calcite vein within lahar.	HC9	Cloudy calcite vein within lahar.
HC5	Clear calcite vein from Hydrofractured fresh basalt.	HC1	Clear calcite vein from Hydrofractured fresh basalt.
HCN1/2/5	Large amygdale infilled with large calcite rhombs from lahar.	$HC_{misc\ 1\text{-}n}$	Calcite from base of lahar associated with minor analcime mineralisation.
Mg1A	Calcite with masive pink analcime found within amygdale from Upper High Craigton Quarry.	Mg1B	Calcite from lower bole.Host basalt impregnated with analcime and calcite.
Langbank Cutting			
LI2A	Vein calcite from approx. 7 metres below flow boundary	LI2B	Small calcite vein network approximately 5 metres below flow boundary.
LBC2/5	Calcite vein approximately 10 metres below flow boundary.	LC5	Amygdale calcite 5 metres below flow boundary.
LC8	Calcite approximately 2 metres below flow boundary	LB6	Calcite approximately 15 metres below flow boundary within amygdale.
LB1	Amygdale calcite 10 metres below flow boundary.		
$CV86_{1/4/5}$	L. Evans (1987) Langbank Cutting.		
Mugdock Quarry.			
MQ/1	Fibrous vein calcite.	Mug 2	Calcite infilling vesicles in highly altered feldspathic basalt.
Mug 3	Clear vein calcite in fresh basalt.		
Campsie Glen			
AP3	Small calcite vein from highly altered Markle basalt within Flow 18.	CPL1	Vein calcite from vesicular basalt along Campsie Scarp.

REFERENCES

Alt, J.C., Honnorez, J., Laverne, C., Emmermann, R. 1986. Hydrothermal alteration of a 1 km section through the upper oceanic crust, DSDP Hole 504B: Mineralogy, chemistry and evolution of seawater-basalt interactions. Journal of Geophysical Research. Volume 91. pp.10309-10335.

Arnorsson, S, Gunnlaugsson, E. 1985. New gas geothermometers for geothermal exploration-calibration and application. Geochim. et Cosmochim. Acta, Volume 49, pp.1307-1325.

Arnorsson, S, Gunnlaugsson, E., Svavarsson, H. 1983. The chemistry of geothermal waters in Iceland II. Mineral equilibria and independent variables controlling water compositions. Geochim. et Cosmochim. Acta, Volume 47, pp. 547-566.

Bamford, D. 1979. Seismic constraints on the deep geology of the Calidonides of northern Britain. *In Harris, A.L., et al.Calidonides of the British Isles-reviewed. Spec. Publ. Geol. Soc. London, No 8.*

Banks, D. 1987. The Origin of Base Metal Deposits at Tynagh. Unpublished Ph.D. Thesis. University of Strathclyde.

Battey, M.H. 1981. Mineralogy for Students. Second Edition. Longman Inc. New York. 355p.

Behar, Pimeau. 1979. Bull. Mineral., Volume 102,pp.611-621.

Bettison, L.A., Schiffman, P. 1988. Compositional and structural variations of phyllosilicates from the Point Sal ophiolite, California. American Mineralogist, Volume 73, pp.62-76.

Bevins, R.E. 1985. Pumpellyite - dominated metadomain alteration at Builth Wells - evidence for a fossil submarine hydrothermal system. Mineralogical Magazine, Vol. 49 pp.451-456.

Bevins, R.E., Merriman, R.J. 1988. Compositional controls on coexisting prehnite - actinolite and prehnite - pumpellyite facies assemblages in the Tal y Fan metabasic intrusion, North Wales: implications for Caladonian metamorphic field gradients. Journal of Metamorphic Geology, Vol.6, pp.17-39.

Biscaye, P.E. 1964. Distinction between kaolinite and chlorite in recent sediments by X-ray diffraction. Amer. Mineralogist, 49, pp.1281-1289.

Bluck, B.J. (ed.).1973. Excursion Guide to the Geology of the Glasgow District. Geol. Soc. of Glasgow.

Bodnar, R.J., Reynolds, T.J., Kuehn, C.A. 1985. Fluid-inclusion systematics in epithermal systems. *In Berger, B.R., Bethke, P.M. 1985. Geology and Geochemistry of Epithermal Systems. Reviews in Economic Geology, Volume 2. Society of Economc Geologists, pp.73-97.*

Bottinga, Y. 1968. Calculation of fractionation factors for carbon and oxygen exchange in the system calcite-carbon dioxide-water. J. Phys. Chem., Volume 72, pp.800-808.

Borthwick, J., Harmon, R.S. 1982. A note regarding ClF_3 as an alternative to BrF_5 for oxygen isotope analysis. Geochim. et Cosmochim. Acta, Volume 46, pp.1665-1668.

Bowers, T.S., Taylor, H. P. 1987. Some calculations pertaining to an integrated chemical and stable-isotope model of the origin of mid-ocean ridge hydrothermal systems. *In Helgeson (ed.). Chemical Transport in metasomatic Processes, Reidel Publishing Co, pp.633-655.*

Browne, M.A.E. 1980. Stratigraphy of the lower Calciferous Sandstone Measures in Fife. Scottish Journal of Geology, Volume 16, pp.321-328.

Browne, P.R.L., Ellis, A.J. The Ohaki-Broadlands hydrothermal area, New Zealand: Mineralogy and related geochemistry. American Journal of Science, Volume 269, pp.97-131.

Cambell, A.S., Fyfe, W.S. 1965. Analcime - albite equilibria. American Journal of Science, Vol. 263, pp. 807-816.

Cameron, I.B., Stephenson, D. 1985. British Regional Geology. The Midland Valley of Scotland. Third Edition. H.M.S.O.

Cann, J.R. 1979. Metamorphism in the Ocean Crust. Reprint from Deep Drilling Results in the Atlantic Ocean: Ocean Crust: Eds. Taiwani, M., Harrison, C.G., Hayes, D.E. Maurice Ewing Series 2. American Geophysical Union, Washington, Geodynamics Project: Sci. Rep. No. 48, pp.230-238.

Cann, J.R., Strens, M.R. 1982. Black smokers fuelled by freezing magma. Nature, Volume 298, pp. 147-149.

Cathelineau, M., Nieva, D. 1985. A chlorite solid solution geothermometer in the Los Azufres (Mexico) geothermal system. Contributions to Mineralogy and Petrology, Vol. 91, pp.235-244.

Clayton, R.N., Steiner, A. 1975. Oxygen isotope studies of the geothermal system at Wairakei, New Zealand. Geochim. et Cosmochim. Acta, Volume 39, pp.1179-1186.

Clynne, M.A., Potter, R.W. II. 1977. Freezing point depression of synthetic brines. Geol. Soc. Am. Abs. with Programs 9, 930.

Cowan, J., Cann, J.R. 1988. Supercritical two phase separation of hydrothermal fluids in the Troodos ophiolite. Nature, Volume 333, pp.259-261.

Craig, G.Y. (ed.) 1983 Geology of Scotland, 2nd edition. Edinburgh: Scottish Academic Press.

Craig, H., 1961. Isotopic variations in meteoric waters. Science, Volume 133, pp. 1702-1703.

Craig, H., 1963. The isotope geochemistry of water and carbon in geothermal areas. In: Nuclear Geology in Geothermal Areas, E. Tongiorgi, ed., Pisa, Consiglio, Nazionale della Richerche, Spoleto, 17-53.

Craig, H., Gordon, L., Horible, Y. 1963. Isotopic exchange effects in the evaporation of water. Journal of Geophysical Research, Volume 68, pp. 5079-5087.

Craw, D., Johnstone, R.D., Rattenbury, M.S. In press. Tectonic-hydrothermal Au-Cu mineralization in a metamorphic fluid mixing zone, Westland, New Zealand.

Curtis, C.D., Hughes, C.R., Whitman, J.A., Whittle, C.K. 1985. Compositional variation within some sedimentary chlorites and some comments on their origin. Mineralogical Magazine, Volume 49, pp.375-386.

Curtis, C.D., Ireland, B.J., Whiteman, J.A., Mulvaney, R.,Whittle, C.K. 1984. Clay Minerals, 9, pp.471-481.

Deer, W.A., Howie, R.A., Zussman, J. 1966. An introduction to the rock forming minerals. Longman. 528 p.

Evans, L.J. 1987. Low Grade Regional Metamorphism of the Lower Palaeozoic Rocks of the Midland Valley of Scotland. Unpublished Ph.D. Thesis. University of St.Andrews.

Field, C.W., Fifarek, R.H. 1985. Light Stable-Isotope Systematics in the Epithermal Environment. *In Berger, B.R., Bethke, P.M. 1985. Geology and Geochemistry of Epithermal Systems. Reviews in Economic Geology, Volume 2. Society of Economc Geologists, pp. 99-123.*

Fisher, R.V., Schonineke, H.V. 1984. Pyroclastic Rocks. Springer-Verlag.

Fournier, R.O., 1979. Geochemical and hydrologic considerations and the use of enthalpy-chloride diagrams in the prediction of underground conditions in hot-spring systems. Journal of Volcanology and Geothermal Research, 5, pp.1-16.

Fournier, R.O., 1981. Application of water geochemistry to geothermal exploration and reservoir engineering. In Rybach, L., Muffler, L.P.J., (eds.). Geothermal Systems: Principles and Case Histories: John Wiley and Sons, New York, pp.109-143.

Fournier, R.O. 1985. Carbonate transport and deposition in the geothermal environment. *In Berger, B.R., Bethke, P.M. 1985. Geology and Geochemistry of Epithermal Systems. Reviews in Economic Geology, Volume 2. Society of Economc Geologists, pp.63-71.*

Francis, E.H. 1983. Chapter 9; Carboniferous. *In Craig, G.Y. (editor). The Geology of Scotland, Second Edition. Scottish Academic Press.*

Francis, E.H. 1983. Chapter 10; Carboniferous and Permian Igneous Rocks. *In Craig, G.Y. (editor). The Geology of Scotland, Second Edition. Scottish Academic Press.*

Friedman, I., O'Neil, J.R. 1977. Compelation of stable isotope fractionation factors of geochemical interest. I*n Fleischer, M. (ed.). Data of geochemistry, 6th Edition. U.S. Government Printing Office, Washington, D.C.*

Giggenbach,W.F. 1981. Geothermal mineral-equilibria. Geochim. et Cosmochim. Acta, Volume 44, pp.2021-2032.

Grant, J.A. 1986. A simple solution to Gresen's Equation for metasomatic alteration. Economic Geology, Volume 81, pp. 1976-1982.

Gresens, R.L. 1966. Composition-volume relationships of metasomatism. Chemical Geology, Volume 2, pp. 47-65.

Giggenbach, W.F. 1981. Geothermal-mineral equilibria. Geochim. et Cosmochim. Acta, Volume 45, pp.393-410.

Hall, A.J., Banks,D., Fallick, A.E., Hamilton, P.J.1989. An hydrothermal origin for copper impregnated prehnite and analcime from Boyleston Quarry, Barrhead, Scotland. Journal of the Geological Society of London, Volume 146, pp.701-713.

Haas, J.L. 1971. The effect of salinity on the maximum thermal gradient of a hydrothermal system at hydrostatic pressure. Economic Geology, Volume 66, pp.940-946.

Hauff, P.L. 1981. Corrensite: Mineralogical ambiguities and geologic significance. U.S. Geological Survey Open File Report. pp. 81-85.

Heddle, M.F. 1897. On analcime with new forms. "Transactions" Edin. Geological Society, Volume VII., pp.241-243.

Hedenquist, J.W., Henley, R.W. 1985. Effects of CO_2 on freezing-point depression measurements of fluid inclusions - evidence from active systems and application to epithermal studies. Economic Geology, Voume 80, pp. 1379-1406.

Hedenquist, J.W., Henley, R.W. 1985. Hydrothermal eruptions in the Waiotapu Geothermal System, New Zealand: Their origin, associated breccias, and relation to precious metal mineralization. Economic Geology, Voume 80, pp.1640-1668.

Hein, U.F., Luders, V., Dulski, P. 1990. The fluorite vein mineralization of the southern Alps: Combined application of fluid inclusions and rare earth elements (REE) distribution. Mineralogical Magazine, Volume 375, pp. 325-335.

Henley, R.W. 1985. The geothermal framework of epithermal deposits. *In Berger, B.R., Bethke, P.M. 1985. Geology and Geochemistry of Epithermal Systems. Reviews in Economic Geology, Volume 2. Society of Economic Geologists, pp. 1-21.*

Henley, R.W., Browne, K.L. 1985. A practical guide to the thermodynamics of geothermal fluids and hydrothermal ore deposits. *In Berger, B.R., Bethke, P.M. 1985. Geology and Geochemistry of Epithermal Systems. Reviews in Economic Geology, Volume 2. Society of Economic Geologists, pp. 25-43.*

Henley, R.W., Ellis, A.J. 1983. Geothermal systems, ancient and modern. Earth Science Reviews, Vol. 19, pp.1-50.

Hey, M.H. 1954. A new review of the chlorites. Mineralogical Magazine, Volume 30, pp.272-292.

Hoefs, J. 1980. Stable Isotope Geochemistry, Second edition: Springer-Verlag, Berlin-Heidelberg, New York, 208 p.

Hower, J. 1981. X Ray Diffraction Identification of Mixed Layer Clay Minerals. In Longstaffe, F.J. (Ed.) A Short Course Handbook Number 7. Mineralogical Society of Canada. pp. 39-59.

Hutchison, C.S. 1974. Laboratory handbook of Petrographic Techniques. Willey-Interscience. 527 p.

Hunt, J.M.1979. Petroleum Geochemistry and Geology. W.H. Freeman, San Francisco.

Iijima, A. 1978. Geological occurrences of zeolites in marine environments. In Sand, L.B. and Mumpton, F.A. (eds.) Natural Zeolites, occurrence, properties and use. Pergamon Press, Oxford, pp. 175-198.

Iijima, A., Matsumoto, R. 1982. Clays and Clay Minerals, Volume 30, pp.264-274.

Jahren, J.S., Aagaard, P. 1989. Compositional variations in diagenetic chlorites and illites, and relationship with formation water chemistry. Clay Minerals, Volume 24, pp.157-171.

Johnstone, R.D., Craw, D., Rattenbury, M.S. 1990. Southern Alps Cu-Au hydrothermal system, Westland, New Zealand. Mineralium Deposita, Volume 25, pp.118-125.

Jolly, W.T. 1974. Behavour of Cu, Zn and Ni during the prehnite - pumpellyite rank metamorphism of the Keweenawan Basalts, North Michigan. Economic Geology, Volume 69, pp.1118-1125.

Jolly, W.T., Smith, R.E. 1974. Degredation and metamorphic differentiation of the Keweenawan tholeiitic lavas of North Michigan, U.S.A. Journal of Petrology, Volume 13, pp.273-309.

Karlsson, H.R., Clayton, R.N., Mayeda, T.K. 1985. Analcime: A potential geothermometer (abstr.). Geol. Soc. Amer., 17, pp.622-623.

Karlsson, H.R., Clayton, R.N. 1990. Oxygen isotopic fractionation between analcime and water: An experimental study. Geochim. et Cosmochim. Acta, Volume 54, pp.1359-1368.

Karlsson, H.R., Clayton, R.N. 1990. Oxygen and hydrogen isotope geochemistry of zeolites. Geochim. et Cosmochim. Acta, Volume 54, pp.1369-1386.

Kawachi, Y. 1975. Pumpellyite-actinolite and contiguous facies metamorphism in part of the Upper Wakatipu District, South Island, New Zealand. New Zealand Journal of Geology and Geophysics, 18, pp.401-441.

Kelly, D.S., Delany, J.R. 1987. Two phase separation and fracturing in mid ocean ridge gabbros at temperatures greater than 700°C. Earth and Planetary Science Letters, Volume 83, pp.53-66.

Kesler, S.E., Russell, N., Seaward, M., Rivera, J., McCurdy, K., Cumming, G.L., Sutter, J.F. 1981. Geology and geochemistry of the sulphide mineralization underlying the Pueblo Viejo gold-silver oxide deposit, Dominican Republic. Economic Geology, Volume 76, pp. 1096-1117.

Kisch, H.J. 1974. Anthracite and meta-anthracite coal ranks associated with "anchimetamorphism" and "very-low stage" metamorphism. I, II, III. Proc. K. Ned. Akad. Wet., Amsterdam, Ser. B.77 (2), pp.81-118.

Krismannsdottir, H. 1983. Chemical evidence from Icelandic geothermal systems as compared to submarine geothermal systems. *In Rona, P.A., Bostrom, Laubier, L., Smith, K.L., Jr. Hydrothermal Processes at Seafloor Spreading Centres. NATO Conference Series: Series IV : Marine Sciences.*

Liou, J.C., Seki, Y.G.,Saki, H. 1985. Compositions and paragenesis of secondary minerals in the Onikobe geothermal system, Japan. Chemical Geology, 49, pp.1-20.

Liou, J.C., Maruyama, S., Cho, M. 1987. Very low-grade metamorphism of volcanic and volcaniclastic rocks-Mineral assemblages and mineral facies. *In Frey (ed.) Very Low Grade Metamorphism, pp. 59-113. Blackie and Son, Glasgow.*

Luc, C.M.B., Cornelius Maijer, J. Ben H. Hasen. 1989. Premetamorphic metabasites of Rogaland, S.W. Norway. Contributions to Mineralogy and Petrology, Volume 103, pp.306-316.

Luhr, J.F., Kyser, T.K. 1989. Primary igneous analcite: The Colima Minettes. American Mineralogist, Volume 74, pp.216-223.

MacDonald, J.C. 1973. Carbon dioxide metasomatism in the Campsie Lavas. Mineralogical Magazine, Volume 39, pp.119-121.

MacDonald, R. 1975. Petrochemistry of the early Carboniferous (Dinantian) lavas of Scotland. Scottish Journal of Geology, Volume 11, pp.269-314.

MacDonald, R., Thomas, J.E., Rizzello, S.A. 1977. Variations in basalt chemistry with time in the Midland Valley province during the Carboniferous and Permian. Scottish Journal of Geology, Volume 13, pp.11-22.

MacGregor, A.G. 1928. The classification of Scottish Carboniferous olivine-basalts and mugearites. Trans. Geol. Soc. Glasgow, Volume 18, pp.324-360.

McKeag, S.A., Craw, D. 1989. Contrasting fluids in gold bearing quartz vien systems formed progressively in a rising metamorphic belt: Otago Schist, New Zealand. Economic Geology, Volume 84, pp.22-33.

Mottl, M.J. 1983. Hydrothermal processes at seafloor spreading centres: application of basalt-seawater experimental results. *In Rona, P.A., Bostrom, Laubier, L., Smith, K.L., Jr. Hydrothermal Processes at Seafloor Spreading Centres. NATO Conference Series: Series IV : Marine Sciences.*

Mottl, M.J. 1983. Metabasalts, axial hot springs and the structure of hydrothermal systems at mid-ocean ridges. Geological Society of America Bulletin, Volume 94, pp. 161-80.

Mook, W.G., Bommerson, J.C., Staverman, W.H. 1974. Carbon isotopic fractionation between dissolved bicarbonate and gaseous carbon dioxide. Earth and Planetary Science Letters, Volume 22, pp.169-176.

Nakajima, T., Banno, S., Suzuki, T. 1977. Reactions leading to the disappearance of pumpellyite in low-grade metamorphic rocks of the Sambagawa metamorphic belt in Central Shikoku, Japan. Journal of Petrology, 18, pp.263-284.

Nelson, C.E., Giles, D.L. 1985. Hydrothermal eruption mechanisms and hot spring gold deposits. Economic Geology, Volume 80, pp.1633-1639.

Norrish, K., Hutton, J.T. 1969. An accurate X-ray spectrographic method for the analysis of a wide range of geological samples. Geochim. et Cosmochim. Acta, Volume 33, pp.431-453.

Norton, D.L. 1984. Theory of hydrothermal systems. Ann. Rev. Earth Planet. Sci.,Volume 12, pp.155-177.

Ohmoto, H. 1986. Stable Isotope Geochemistry of Ore Deposits. *In : Valley, J.W., Taylor, H.P., O'Neil, J.R. (eds.). Stable Isotopes in High Temperature Geologic Processes. Reviews in Mineralogy, 16, pp. 491-513.*

Paterson, I.B., Hall, I.H.S. 1986. Lithostratigraphy of the Late Devonian and Early Carboniferous rocks in the Midland Valley of Scotland. British Geological Survey Report. Volume 18. Number 3. H.M.S.O.

Pearce, J.A. 1982. Trace element characteristics of lavas from destructive plate boundaries; pp 525-548. *In Thorpe, R.S. (ed.) Andesites. John Wiley and Sons.*

Pearce, J.A, Cann, J.R. 1973. Tectonic setting of basic volcanic rocks determined using trace element analyses. Earth Planet. Sci. Lett., 19, pp.290-300.

Phillips, W.J. 1972. Hydraulic fracturing and mineralisation. Journal of the Geological Society of London, Volume 128, pp.337-357.

Pollard, A.M., Thomas, R.G., Williams, P.A. 1990. Connellite: stability relationships with other secondary copper minerals. Mineralogical Magazine, Volume 54, pp.425-431.

Sams, M.S., Thomas-Betts, A. 1988. Models of convective fluid flow and mineralisation in South-West England. Journal of the Geological Society of London, Volume 145, pp.809-817.

Samson, I.M., Banks, D.B. 1988. Epithermal base-metal mineralisation in the Southern Uplands of Scotland: Nature and origin of the fluids. Mineralium Deposita, Volume 23,pp.1-8.

Samson, I.M., Russell, M.J.1987. Genesis of the Silvermines zinc-lead-barite deposit, Ireland: fluid inclusion and stable isotopic evidence. Economic Geology, Volume 82, pp.371-394.

Sangster, D.F. 1990. Mississippi Valley-type and sedex lead-zinc deposits: a comparative examination. Trans. Instn. Min. Metall. (Sect. B: Earth Sci.), Volume 99, pp. 21-41.

Sato,T. 1972. Behaviour of ore-forming solutions in seawater. Min. Geol., Volume 22, pp.31-42.

Sarkisyan, S.G., Kotelnikov, D.D. 1972. Genesis and thermodynamic stability of dioctahedral and trioctahedral mixed-layer minerals in sedimentary rocks. Proceed. Intern. Clay Conf., Madrid., pp.281-289.

Searl, A, Fallick, A.E. 1990. Dinantian dolomites from East Fife: hydrothermal overprinting of early mixing-zone stable isotopic and Fe/Mn compositions. Jour. Geol. Soc. London, Volume 147, pp.623-638.

Seyfried, W, Bishcoff, J.L. 1977. Hydrothermal transport of heavy metals by seawater: the role of the seawater / basalt ratio. Earth and Planetary Science Letters, Volume 34, pp.71-77.

Seyfried, W., Jr. Mottl, M.J. 1982. Hydrothermal alteration of basalt by seawater under seawater dominated conditions. Geochim. et Cosmochim. Acta, Volume 46, pp.985-1002.

Shepherd,T.J., Rankin, A.H., Alderton, D.H.M. 1985. A Practical Guide to Fluid Inclusion Studies. Blackie. 239 p.

Sheppard, S.M.F. 1986. Characterization and isotopic variations in natural waters. *In : Valley, J.W., Taylor, H.P., O'Neil, J.R. (eds.). Stable Isotopes in High Temperature Geologic Processes. Reviews in Mineralogy, 16, pp. 165-183.*

Sheppard, S.M.F., Charef, A. 1986. Eau Organique: caracterisation isotopique et evidence de son role dans le gisemet Pb-Zn de Fedj-el-Adoum, Tunisie. Compte Rendu de l' Academie des Sciences Paris. t.302, serie II, 19, 1189-1192.

Sibson, R.H., Moore, J., Rankin, A.H. 1975. Seismic pumping-a hydrothermal transport mechanism. J. Geol.Soc.Lond. 131, pp.653-660.

Spooner, E.T.C., Fyfe, W.S. 1973. Sub-sea-floor metamorphism, heat and mass transfer. Contrib. Min. Petrol., Volume 42, pp.287-304.

Staudigel., H, Hart, S.R. 1983. Alteration of basaltic glass. Mechanisms and significance for the oceanic crust-seawater budget. Geochim. Cosmochim Acta 47, pp. 337-350.

Stephenson, D., Coats, J.S. 1983. Baryte and copper mineralisation in the Renfrewshire Hills, central Scotland. Mineral Reconnaissance Programme Rep. Inst. Geol. Sci., No. 68.

Sternfield, J.N. 1981. The hydrothermal petrology and stable isotope geochemistry of two wells in the Geysers geothermal field, Sonoma County, California. Unpublished M.S. Thesis, University of California, Riverside.

Strens, M.R., Cann, D.L., Cann, J.R. 1987. A thermal balance model of the formation of sedimentary-exhalative lead-zinc deposits. Economic Geology, Volume 82, pp. 1192-1203.

Sturchio, N.C., Keith, T.E.C., Muehlenbachs, K. 1990. Oxygen and carbon isotopic ratios of hydrothermal minerals from Yellowstone drill cores. Journal of Volcanology and Geothermal Research, Volume 40, pp. 23-37.

Summmer, N.S., Verosub, K.L. 1988. The role of hydrothermal fluids in the distillation of hydrocarbons. *In Hydrothermal Processes in Volcanic Terrains: Geol. Soc. London, conference program with absracts.*

Taylor, H.P. 1974. The application of oxygen and hydrogen isotope studies to the problems of hydrothermal alteration and ore deposition. Economic Geology, Volume 69, pp.843-883.

Thomas, L.J. 1986. Low Grade Metamorphism and the Stable Isotopic Composition of Alteration Fluids. Lower Palaeozoic Succession. English Lake District. Unpublished Ph.D. Thesis. University of St. Andrews.

Thompson, A.B. 1971. Analcime-albite equilibria at low temperatures. American Journal of Sciences, 271, pp.79-92.

Thompson, G. 1983. Basalt-Seawater Interaction. *In Rona, P.A., Bostrom, Laubier, L., Smith, K.L., Jr. Hydrothermal Processes at Seafloor Spreading Centres. NATO Conference Series: Series IV : Marine Sciences.*

Thorez, J. 1976. Practical Identification of Clay Minerals. A handbook for teachers and students in clay mineralogy.

Institute of Mineralogy. 577 p.

Th. Schmidt, S. 1990. Regional and local control on phyllosilicate paragenesis during burial metamorphism in the North Shore volcanic Group, Minnesota. *In IGCP Project 294: Very Low Grade Metamorphism: Phyllosilicates as indicators of very low grade metamorphism; Conference Program With Abstacts.*

Truesdell, A.H., Fournier, R.O. 1976. Calculation of deep temperatures in geothermal systems from the chemistry of boiling spring waters of mixed origin. *In: Proceedings of the 2nd United Nations Symposium on the Development and use of Geothermal Resources, San Francisco, Volume 1. U.S. Government Printing Office, Washington D.C., pp. 837-844.*

Truesdell, A.H., Nathenson, M. 1977. The effects of subsurface boiling and dilution on the isotopic compositions of Yellowstone thermal waters. Journal of Geophysical Research.Volume 82, No. 26, pp.3694-3704.

Upton, B.G.J., Aspen, P., Chapman, N.A. 1983. The upper mantle and deep crust beneath the British Isles: evidence from inclusions in volcanic rocks. J. Geol. Soc. Lond. 140, pp.105-122.

Velde, B. 1977. A proposed phase diagram for illite, expanding chlorite, corrensite and illite-montmorillonite mixed layer minerals. Clays and Clay Minerals, Volume 25, pp.264-270.

Viereck, L.G., Griffin, B.J., Schmincke, H-U., Pritchard, R.G. 1982. Volcaniclastic rocks of the Reydarfjordur Drill Hole, Eastern Iceland. 2. Alteration. Journal of Geophysical Research, Volume 87, pp. 6459-6476.

Walker, G.F. 1949. Distinction of vermiculite, chlorite and montmorillonite in clays. Nature., Lond. 164, pp.577-578.

Walsh, J.J. 1983. Secondary element mobility within the Støren Greenstones, Norway. Norsk Geologisk Tidskrift, Volume 63, pp.27-37.

Welhan, J.A. 1988. Origins of methane in hydrothermal systems. Chemical Geology, 71, pp.183-198.

Whitford, D.J., Mc Pherson, W.P.A., Wallace, D.B. 1989. Geochemistry of the host rocks of the volcanogenic massive sulphide deposit at Que River, Tasmania. Economic Geology Volume 84, Number 1, pp.1-21.

Whyte, F., MacDonald, J.C. 1974. Lower Carboniferous vulcanicity in the northern part of the Clyde Plateau. Scottish Journal of Geology, Volume 10, pp. 187-198.

Williams, A.E., Elders, W.A. 1984. Stable isotope systematics of oxygen and carbon in rocks and minerals from the Cerro Prieto geothermal anomaly, Baja, California, Mexico. Geothermics, Volume 13, pp.49-63.

Wilson, M.J., Bain, D.C. 1970. The clay mineralogy of the Scottish Dalradian Meta-Limestones. Contributions to

Mineralogy and Petrology, Volume 26, pp.285-295.

Winchester, J.A., Floyd, P.A. 1977. Geochemical discrimination of different magma series and their differentiation products using immobile elements. Chemical Geology, Volume 20, pp.325-343.

Wood, D.A., Gibson, I.L., Thompson, R.N. 1976. Element mobility during zeolite facies metamorphism of Tertiary basalts in Eastern Iceland. Contributions to Mineralogy and Petrology, Volume 55, pp.241-254.

Yermakov, N.P. 1965. Research on the nature of mineral-forming solutions. International Series of Monographs in Earth Sciences 22, p.473. Pergamon.

Zheng, Y.-F. 1990. Carbon-oxygen isotopic covariation in hydrothermal calcite during degassing of CO_2. Mineralium Deposita, Volume 25, pp.246-250.